ACTA UNIVERSITATIS SZEGEDIENSIS

ACTA MINERALOGICA-PETROGRAPHICA

TOMUS XXIV, Fasc. 1.

SZEGED, HUNGARIA
1979

ACTA UNIVERSITATIS SZEGEDIENSIS

ACTA MINERALOGICA-PETROGRAPHICA

TOMUS XXIV, Fasc. 1.

SZEGED, HUNGARIA
1979

HU ISSN 0365—8066

Adjuvantibus

BÉLA MOLNÁR et TIBOR SZEDERKÉNYI

Redigit

GYULA GRASSELLY

Edit

Institutum Mineralogicum, Geochimicum et Petrographicum
Universitatis Szegediensis de Attila József nominatae
Egyetem u. 2—6., H-6722 Szeged, Hungary

Nota
Acta Miner. Petr., Szeged

Szerkeszti
GRASSELLY GYULA

a szerkesztő bizottság tagjai
MOLNÁR BÉLA és SZEDERKÉNYI TIBOR

Kiadja

a József Attila Tudományegyetem Ásványtani, Geokémiai és Kőzettani Tanszéke
H-6722 Szeged, Egyetem u. 2—6.

Kiadványunk címének rövidítése
Acta Miner. Petr., Szeged

Felelős Kiadó: Grasselly Gyula
79-4422 — Szegedi Nyomda — Felelős vezető: Dobó József igazgató
Készült: Monószedéssel, ívés magasnyomással, 16,5 A/5 ív terjedelemben,
az MSZ 5601—59 és 5602—55 szabvány szerint
Példányszám: 625

CONTENTS

Acta Mineralogica-Petrographica, Szeged, XXIV/1, 5—18, 1979

PETROLOGICAL REVIEW OF THE ÓFALU SERPENTINITE, MECSEK MOUNTAINS, HUNGARY

M. F. GHONEIM and T. SZEDERKÉNYI

SUMMARY

The Ófalu serpentinite as a 10 m thick sill-like body lies in the metamorphites of the Ófalu Group. It consists of two varieties petrographically: 1. massive serpentinite, 2. sheared serpentinite due to the powerful tectonism of the "Mecsekalja Tectonic Belt" including the Ófalu Group. Main minerals of the serpentinite are lizardite, clinochrysotile, antigorite and chlorite with disseminated ore grains among them, such as chromite, magnetite, pentlandite, heazlewoodite and subordinate sulphide minerals. Based on data of the chemical analyses and Ni/Co ratio this rock belongs to so called "Alpine-type" serpentinites. The Ni and Cr content as well as MgO/SiO_2 ratio suggest an ultramafic- more accurately harzburgite-lherzolite origin. Process of serpentinization took place at 450—500 °C temperature and 0,5—1 Kb pressure. The serpentinite mass together with parent rocks of metamorphites of the Ófalu Group suffered a low grade regional metamorphism at the circumstances of the greenschist-amphibolite transitional facies.

INTRODUCTION

A few kilometers southeast of Ófalu village (Mecsek Mountains) a sill-like serpentinite mass crops out surrounded by low grade metamorphites. The short geological description of this serpentinite was made formerly by GHANEM and RAVASZ-BARANYAI, [1969] and T. SZEDERKÉNYI, [1974]. The scope of the present study has been focussed on the brief description of lithostratigraphic building up, petrography, mineralogy, ore-mineralogy and petrochemistry in order to throw more light on the origin, serpentinization and regional metamorphism of the Ófalu serpentinite.

GEOLOGICAL SETTING

The Ófalu serpentinite crops out in the form of sill-like body of about 10 m thickness. It trends in NNE-SSW direction in strict parallelism with regional trend of the enveloping eugeosynclinal metasedimentary and metavolcanic rocks of the Ófalu Group, M. F. GHONEIM—T. SZEDERKÉNYI, [1977]. The place of the Ófalu serpentinite within the SE Transdanubian Crystalline Mass is presented by *Fig. 1.*

It seems to be a part of the "Mecsekalja Tectonic Belt" together with metamorphites of the Ófalu Group, T. SZEDERKÉNYI, [1974]. Site of the Ófalu serpentinite within metamorphites of the Ófalu Group is marked by geological sketch-map of the area Ófalu by M. GHONEIM, [1977], *Fig. 2.*

Producing an artificial outcrop of the serpentinite body, its real size can be seen as well as relations with the host metasedimentary rocks, *(Fig. 3.)*

The adjacent host rocks are represented by carbonate bearing phyllitic tuffs, more exactly serizite-phyllite and siliceous shale with definite tectonic zones on both side of the serpentinite body. These tectonic zones are full of traces of hydro-

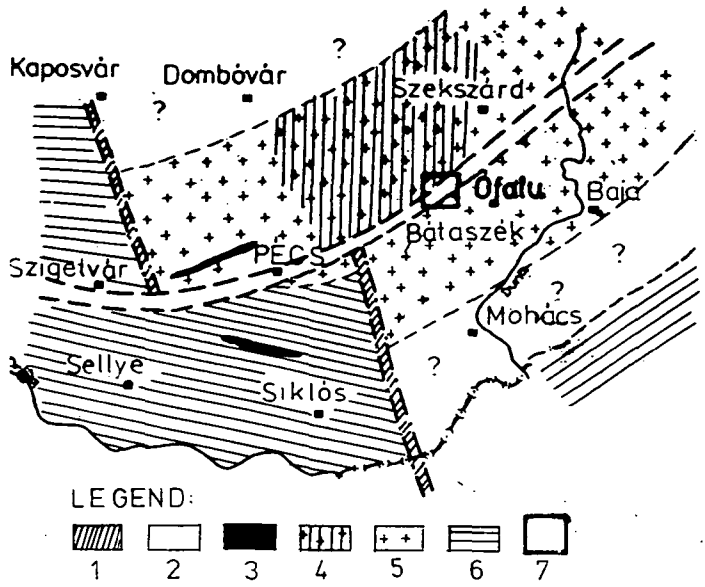

Fig. 1. Geological-tectonic sketch of South-East Transdanubia at the beginning of Late Paleozoic, by T. SZEDERKÉNYI, [1970]. Legend: 1. Precambrian (?) tectonic belt. 2. Variscan tectonic belt with Ófalu Group. 3. Ultramafic bodies. 4. Silurian rocks underlying with granites. 5. Granites, migmatites. 6. Crystalline schists with effective strikes. 7. Site of the Ófalu Group

thermal effects, such as dolomitic and quartz veins, high arsenic and chalcophile element content, etc., but groundmass of the serpentinite body is also crossed by veinlets as well as clusters of carbonates (mainly dolomite). No relict mineral of the original parent rock has been recorded. The serpentinite is represented by two rock types: 1. massive serpentinite having a light grey colour with black spots and „mesh" texture, 2. sheared serpentinite giving a major portion of the rock, accompanied to the tectonic borders of the mass. This latter rock type is full of bright red patches due to oxidation of rather high FeO content and exhibits the following characteristics: lack of the "mesh" texture, abundant of carbonate granules, high undulose extinction of serpentinite minerals, as well as common occurrences of antigorite.

MAIN MINERALS OF THE SERPENTINITE

Some representative samples of the Ófalu serpentinite were investigated by DTA method. Detection of serpentinite minerals from the DTA curves was carried out in accordance with G. T. FAUST and FAHEY J. J. [1962].

Sample №. 215. contains a mixture of lizardite, chrysotile and antigorite admixed with chlorite and dolomite *(Fig. 4a)*. The above-mentioned serpentine minerals give a large endothermic peak at 765 °C on the DTA curve, while the chlorite is indicated by a relatively small endothermic deflection at 663 °C. Decomposition reaction of dolomite and chlorite is represented by an endothermic peak at 875 °C.

Sample №. 216. consists of chrysotile + lizardite as indicated by major endothermic peak at 675 °C followed by an exothermic one at 805 °C *(Fig. 4b)*.

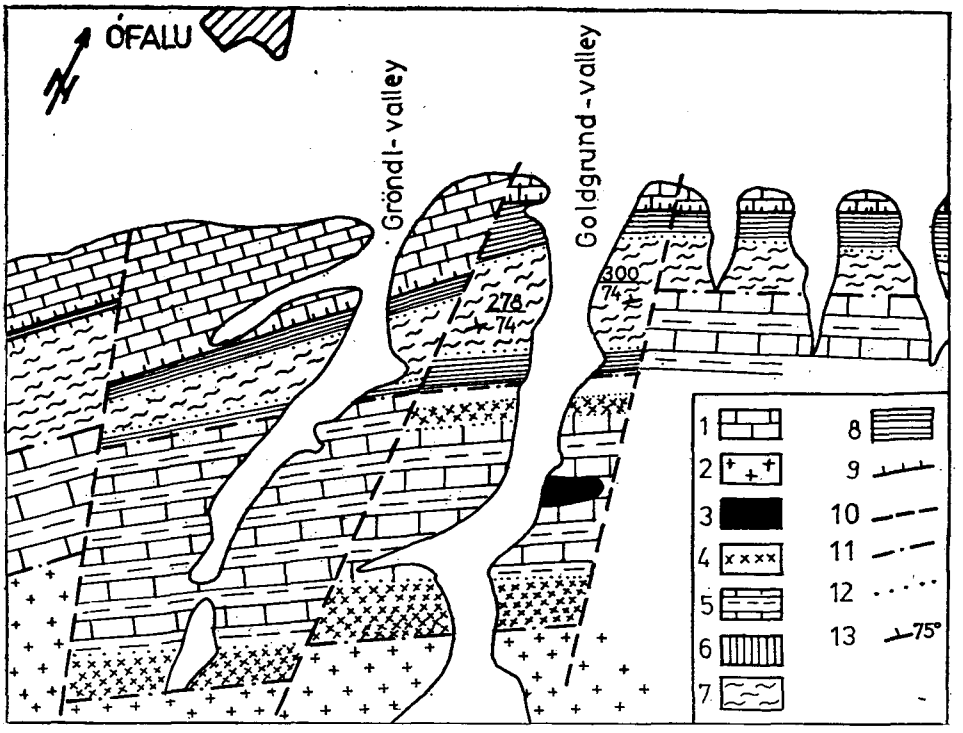

Fig. 2. Geological sketch-map of the area Ófalu, by M. GHONEIM, [1977]. Scale: 1 : 25 000. Legend: 1. Jurassic limestone, 2. Anatectic granite, 3. Serpentinite and associated rocks, 4. Albite porphyry, 5. Marble and phyllitic tuffs, 6. Amphibolite, 7. Mica schist, 8. Andesitic basalt and its metasomatized varieties, 9. Intra-Pannonian overthrusting zone, 10. Faults, 11. Approximate formation contact, 12. Gradational contact, 13. Strike and dip.

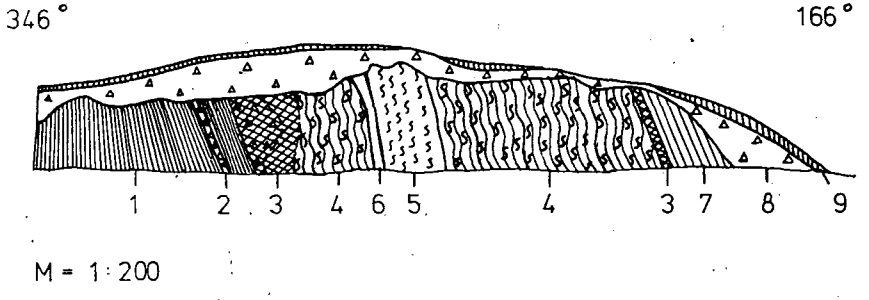

Fig. 3. Profile of the opencast Ófalu serpentinite mass. Scale: 1 : 200. Legend: 1. Serizite-phyllite, 2. Serizite-phyllite breccia, 3. Tectonic zone, 4. Sheared serpentinite, 5. Massive serpentinite, 6. Chlorite schist, 7. Siliceous shale, 8. Talus, 9. Loess

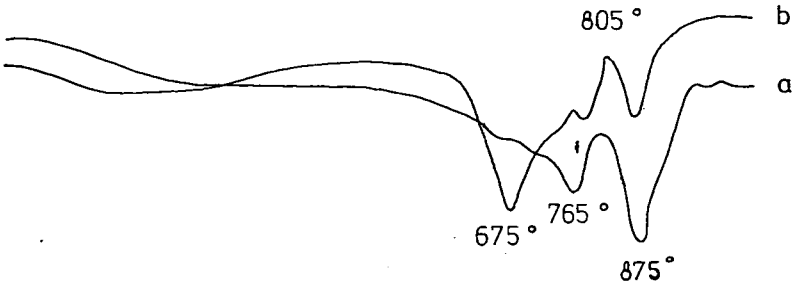

Fig. 4. DTA curves for Ófalu serpentinite. *a)* Sample №. 215, sheared serpentinite consists of antigorite, chlorite and dolomite. *b)* Sample №. 216, massive serpentinite consists of chrysotile+lizardite and dolomite+chlorite

Based on X-ray diffraction the Ófalu serpentinite consists of the following mineral association:

(a) Lizardite: characterized by the (202) peak at 2.501 Å and pair peaks (of relatively low intensity) (060) and (208) at 1.534 Å as well as 1.504 Å. Other characteristic indices are somewhat weaker and overlapped by else constituents.

(b) Clinochrysotile: is indicated by moderately high (202) peak at 2.460 Å.

(c) Antigorite: shows a (202) peak which lies at 2.528 Å, this is the strongest peak and characteristic of antigorite. Other reflections for antigorite are masked by (060) reflection of lizardite which is included in the rock.

(d) Chlorite of the Ófalu serpentinite is IIb monoclinic polytypic modification. The (001) reflection is equal to 14.254 Å and the octahedral aluminum content is (=1.05). The present chlorite is close to clinochlorite according to M. H. HEY's classification.

OPAQUE MINERALS

Ore mineralogical study of the Ófalu serpentinite was decided as an important tool to elucidate the real nature and genesis of these rocks. The polished sections were investigated under reflected light microscope, using oil immersion and high power magnification. Electronprobe microanalysis was carried out on JEOL JXA 5 type electronprobe microanalyser. The standards employed were synthetic CrK_α, FeK_α, etc. Refinement of data and computer programming were made by utilizing P. DUNCUMB and E. M. JONES, [1969], and G. NAGY, [1970]. Generally, the ore minerals of the present serpentinite are represented mainly by chromite (together with its alteration derivatives) and lesser amounts of magnetite and sulphides.

(a) *Chromite* crystals examined in reflected light occur as euhedral to rounded grains rimmed by single or double zones of relatively higher reflectivity, *(Fig. 5)*. The cores of the crystals are relatively fresh and exhibit a characteristic greyish colour and low reflectivity, especially under oil immersion. The chromite is generally isotropic, inner reflections are seldom met with. It presents usually fractured and cracked structure. The chromite with its decoloration band usually forms a myrmekite-like intergrowth (1 mm across) with the gangue groundmass.

As determined by electronprobe microanalysis, the inner zone of the chromite crystals are enriched in Cr_2O_3, Al_2O_3 and MgO (Table 1). The molecular composition

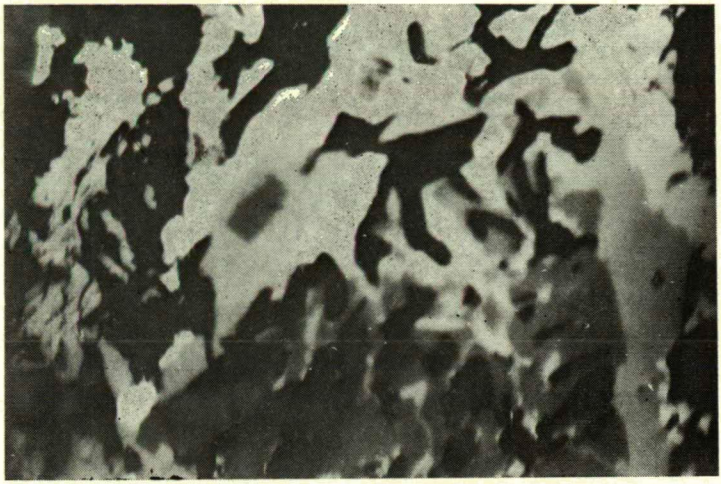

Fig. 5. Photomicrograph of the Ófalu serpentinite showing myrmekitic intergrowth of opaque minerals with the groundmass of gangue (silicate minerals) and double zoning of chromite formed of deep grey colour at the core surrounded by middle grey inner zone and light grey outer one
Reflected light, oil immersion. Mag. 320×

of the inner zone was calculated on the basis of 32 oxygen atoms, the chemical analyses were recalculated to 100% and FeO and Fe_2O_3 were computed assuming a perfect spinel stoichiometry. The chemical formula is then simplified, so the approximate composition accordingly is close to

$$(Mg_{0,35}Fe^{2+}_{0,65}) \cdot (Cr_{1,3}Fe^{2+}_{0,4})O_4$$

The outer zone has higher reflectivity than the inner one and progressively merges into magnetite which sometimes is martitized along (111) and the (001) directions. The outer zone is distinguished by an abrupt deficiency of Cr_2O_3, Al_2O_3 and MgO (Table 1). The molecular composition of the outer zone is

$$(Mg_{0,05}Fe^{2+}_{0,95}) \cdot (Cr_{0,03}Fe^{2+}_{1,95}Al_{0,02})O_4$$

TABLE 1

Oxides	1	2	3	4	5
Al_2O_3	3,03	0,50	0,01	8,40	1,70
Cr_2O_3	45,84	3,17	0,03	53,58	3,50
MgO	6,45	1,05	0,86	4,02	1,06
FeO	22,23	28,59	24,71	17,48	34,00
Fe_2O_3	21,78	65,69	69,34	16,58	59,50
TiO_2	0,50	0,53	0,06	—	—
Total	99,83%	99,53%	95,01%	100,06%	100,30%

The analyses were carried out at the Geochemical Research Laboratory of Hungarian Academy of Science.

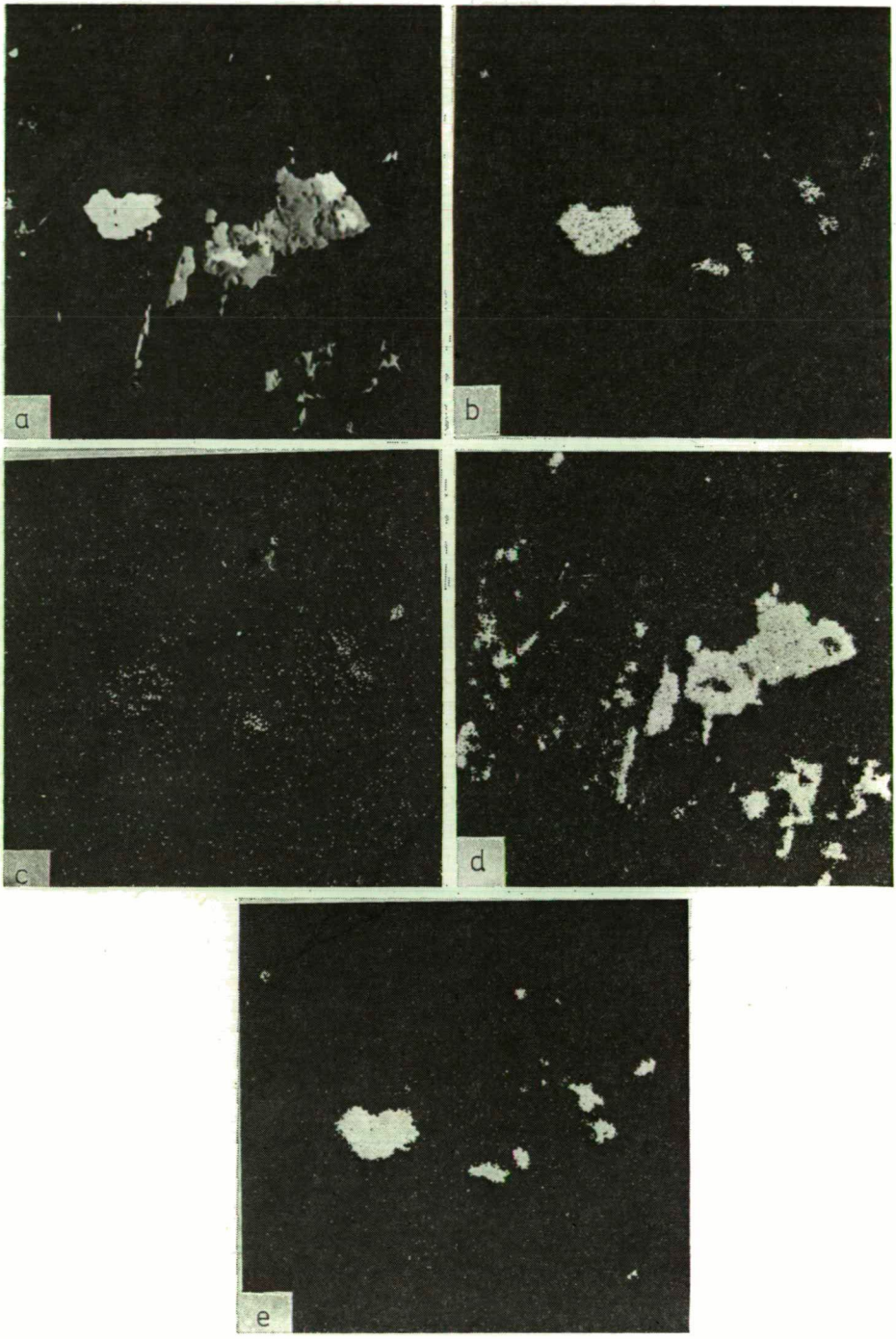
a
b
c
d
e

1. Chromite. Core crystal from the zoned chromite, central Manitoba. [N. W. BLISS and W. H. MACLEAN, 1975]
2. Magnetite as outer zone of ferrite-chromite [N. W. BLISS and W. H. MACLEAN 1975]
3. Magnetite as discrete grain in serpentinite [N. W. BLISS and MACLEAN W. H. 1975]
4. Zone I (inner zone) of alteration of chromite, Ófalu serpentinite
5. Zone II (outer zone) of alteration of chromite, Ófalu serpentinite

(b) *Magnetite* crystals are less abundant than chromite. They occur in different forms and different generations. 1. Shells or crust surrounding an early ferrit-chromite which seems to be of secondary origin. 2. Disseminated grains in the form of fine rounded octahedral grains of about 0.06 mm diameter, as well as stringers or trains of grains concentrated to form partial or complete "veils" around serpentinite clusters. The latter represents the margins of the original olivine grains. There are subordinate forms of magnetite, such as brecciated and fractured grains. The magnetite sometimes altered to sulphide minerals, in which the alteration started from outer parts and extended to inner ones.

(c) *Sulphides*. Sulphide minerals represent less than 10% of the total opaques and they occur as highy disseminated anhedral to subhedral grains of 0.01 mm in diameter, as well as a complex intergrowth of ore minerals including a chromite core surrounded by a ferrit-chromite rim and the latter is partly replaced by sulphide, mainly pentlandite. In addition, the sulphide and chromite form grains in juxtaposition. The contact between the minerals is always rectilinear.

— P e n t l a n d i t e: represents the main sulphide mineral in the Ófalu serpentinite. It occurs very commonly as traces and replacement relict in magnetite. It is light cream in colour and distinguished by an isotropic character differing it from pyrrhotite. The latter is anisotropic with very characteristic yellow colour shades.
— H e a z l e w o o d i t e. Electron-probe distribution of Ni, Co, Fe and S in heazlewoodite are shown in Plate I. Analysis of the Ófalu heazlewoodite yielded a sulphur content of 30%, Fe content of 1%, Co ranging from 0.6 to 0.7% and Ni attaining 55%. The latter element is relatively poorer than in other natural heazlewoodites. Pyrrhotite is commonly associated with pentlandite and heazlewoodite as an alteration product.
— C h a l c o p y r i t e and some p y r i t e grains are also encountered in few cases as triads and anhedral grains.

PETROCHEMISTRY

Eleven chemical analyses of the Ófalu serpentinite are listed in Table 2. They are plotted in AFM diagram *(Fig. 6.)* It is expedient to notice that P. J. WYLLIE, [1967] and T. P. THAYER, [1967b] used the AFM diagrams to illustrate the chemical behaviour of their ultramafic rocks. O. R. BOWES *et al.* [1966] used similar diagram to compare the chemical trends of Alpine-type ultrabasic rocks with other types ultramafic and mafic gneisses in the Lewisian. P. J. WYLLIE, [1967] and T. P. THAYER, [1967b] re-

Explanation of Plate I
a) Black-scattered electron picture of heazlewoodite crystal. Reflected light $V_{acc} = 20$ KV
b) NiK_α X-ray picture
c) CoK_α X-ray picture
d) FeK_α X-ray picture
e) SK_α X-ray picture

Mag. 320 x

TABLE 2

Chemical analyses of the Ófalu serpentinites and associated rocks

Wt%	Numbers of the samples 216	215	21.L	29/2	243/3	6E	7E	ÁGK—136	ÁGK—138	ÁGK—139	ÁGK—141
SiO_2	29.65	22.81	35.55	42.73	37.17	30.33	32.91	30.29	34.57	41.14	30.62
TiO_2	0.02	tr.	N.D.	N.D.	N.D.	0.03	0.02	tr.	tr.	tr.	tr.
Al_2O_3	1.55	1.62	N.D.	1.53	2.30	3.00	1.70	1.73	1.88	2.04	2.00
Fe_2O_3	7.19	7.09	5.86	5.45	6.41	6.00	5.45	7.46	8.35	9.04	5.28
FeO	1.67	3.06	2.49	2.65	2.46	1.56	1.53	1.50	1.27	0.60	2.70
MnO	0.17	0.19	N.D.	0.13	0.08	0.11	0.10	0.15	0.07	0.17	0.21
MgO	32.58	18.74	20.72	24.70	34.88	32.66	32.01	28.93	32.35	23.68	32.45
CaO	7.04	17.33	12.13	7.63	3.17	7.02	7.13	8.82	4.90	6.44	6.30
Na_2O	0.07	0.07	N.D.	0.10	0.05	0.03	—	0.14	0.16	0.11	0.17
K_2O	0.02	0.03	N.D.	0.15	0.03	0.09	0.08	tr.	tr.	0.15	tr.
P_2O_5	0.03	tr.	N.D.	—	0.03	0.04	0.02	0.20	0.14	0.20	0.18
H_2O^-	0.27	0.15	N.D.	0.08	0.18	0.75	0.66	0.07	0.23	0.16	0.14
H_2O^+	9.35	3.64	N.D.	5.66	10.69	8.70	8.96	7.47	10.32	7.16	9.79
CO_2	10.08	23.76	15.25	9.09	3.01	9.76	9.31	12.69	4.69	7.86	8.75
Cr_2O_3	0.74	0.98	0.53	—	—	—	—	—	—	—	—
NiO	0.21	tr.	N.D.	—	—	—	—	—	—	—	—
SO_3	0.03	0.08	N.D.	—	—	—	—	0.08	0.07	0.08	0.14
Total	100.67	99.45	99.53	99.90	100.46	100.00	99.88	99.53	99.00	98.83	98.74
L.O.I. %	19.73	27.55	15.25	14.83	13.91	19.25	18.93	17.12	19.24	14.57	19.33
Cr ppm	5068	6700	3630	—	—	2500	—	3000	5000	5000	5000
Ni	1654	1650	—	—	—	—	—	1500	2000	2000	1000
Co	80	100	—	—	—	—	—	100	100	100	—
Mn	1318	698	—	1007	620	1300	1290	400	200	200	800
Ti	119	N.D.	—	—	—	180	119	—	—	—	—
Ni/Co	20.67	16.50	—	—	—	—	—	15.00	20.00	20.00	—
MgO/SiO_2	1.09	0.82	0.60	0.60	1.94	1.07	0.97	0.95	0.93	0.57	1.06

Chemical analysis made by MRS. SOHA I. and MRS. BIRÓ J.
Trace element analysis made by G. RISCHÁK and M. KÁDAS
N.D. = not detected
— = not analyzed

ported that the rocks of the Alpine mafic stem (ultramafites, gabbro, dolerite, basalt and granophyric rocks) chemically differ from stratiform gabbroic complexes in that the former follows a typical calc-alkaline plutonic trend [H. H. HESS, 1955] rather than the Skaergaard rock trend.

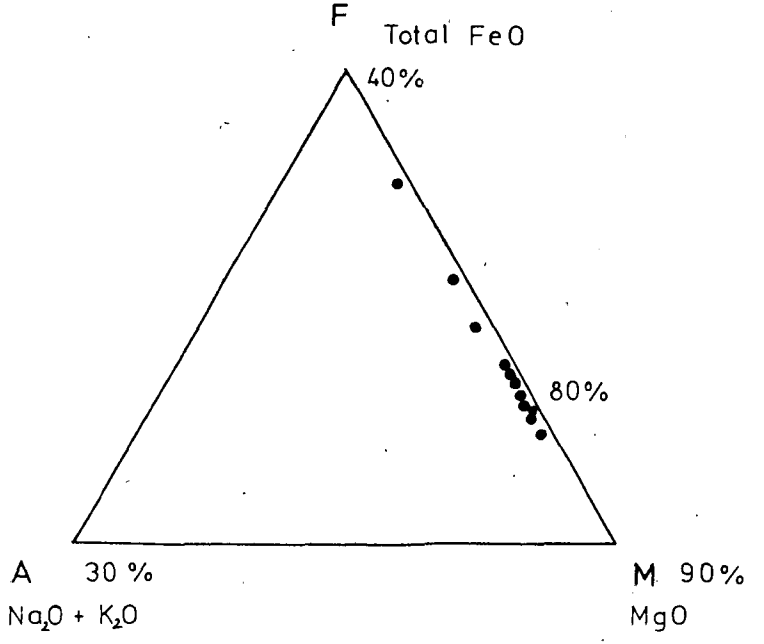

Fig. 6. AFM diagram of the Ófalu serpentinite

It is clear from the AFM diagram that the Ófalu serpentinite rocks are rich in iron content and have deficiency in Mg, which reflect the intense serpentinization as well as regional metamorphism of these rocks. The chemical analyses of the Ófalu metavolcanics [M. GHONEIM and T. SZEDERKÉNYI, 1977] and the Ófalu serpentinite as well as some basic xenolites and enclaves collected from granitoid mass of Mecsek mountains, were calculated in anhydrous form, (Table 3) and plotted in AFM diagram *(Fig. 7)* in which the magmatic trend of these rocks is nearly similar to the "Alpine" intrusion chemical trend rather than being stratiform layered complex (e.g. Skaergaard rock trend).

The high value of Ni/Co ratio was used by L. N. KOGARKO, [1973] to characterize the rocks derived from the early stages of magma differentiation. The Ni/Co ratio is also used as a possible source of genetic information [O. F. GÜLACAR and M. DELALAYE, 1976]. The numbers of Ni/Co ratio (8.07 and 20.97) were taken as values characteristic for the dunite and peridotites of the Bushveld complex (layered part) and for those of Alpine type serpentinite, respectively. As it is evident from Table 2 the Ni/Co ratio for the Ófalu serpentinite rocks moves between 15.00 and 20.67, which reflect their early stage of differentiation as well as similarities to Alpine-type serpentinite described by O. F. GÜLACAR and M. DELALAYE, [1976].

Values of loss on ignition (LOI) were used as a measure for the degree of serpentinization [I. A. MALAKHOV, 1965]. The values of LOI give the limits of serpentinization, namely 2.13% is slightly, 6.05% moderately and 11.67% intensively ser-

TABLE 3

Chemical analysis of the supposed ophiolitic rocks calculated in anhydrous form (volatile-free basis)

	Ófalu serpentinite											Ófalu metavolcanics								
	215	216	21L	29/2	242/3	6E	7E	ÁGK 136	ÁGK 138	ÁGK 139	ÁGK 141	Sc 17	226	26	88/1	203	13	401753	2	S_{A-5}
SiO_2	31.48	36.78	42.55	50.17	43.15	37.55	40.62	38.16	41.13	49.36	38.27	51.70	52.88	51.52	52.00	53.22	48.35	67.38	52.25	55.99
TiO_2	—	0.03	—	—	—	0.41	0.02	tr.	tr.	tr.	tr.	1.90	2.50	2.45	1.56	2.12	1.70	1.04	2.61	1.33
Al_2O_3	2.24	1.92	2.29	1.60	2.67	3.71	2.10	2.17	2.23	2.44	2.50	13.48	14.31	15.66	13.49	17.52	20.05	16.08	19.46	19.66
Fe_2O_3	9.78	8.92	6.77	6.40	7.44	4.43	6.73	9.39	9.93	10.84	6.65	3.45	3.42	4.26	3.96	2.99	4.01	1.28	2.50	2.12
FeO	4.22	2.07	2.98	3.11	2.86	1.93	1.89	1.89	1.51	0.72	3.37	10.78	8.29	8.31	6.90	4.28	5.71	3.58	8.30	4.70
MnO	0.12	—	—	0.15	0.09	0.14	0.12	0.18	0.08	0.20	0.26	0.18	0.18	0.23	0.19	0.11	0.16	0.06	0.22	0.06
MgO	25.86	40.40	24.80	29.00	40.50	40.43	39.50	36.45	38.49	28.41	40.56	8.20	5.94	4.95	6.51	6.95	7.27	2.74	6.43	4.96
CaO	23.92	8.73	14.52	9.00	3.68	8.69	8.79	11.11	5.83	7.72	7.87	6.84	7.71	9.85	10.43	5.68	6.53	1.87	6.49	2.93
Na_2O	0.10	0.09	—	0.12	0.06	0.04	0.05	0.17	0.19	0.13	0.21	2.49	4.36	2.91	4.13	4.34	6.12	4.26	4.10	5.06
K_2O	0.04	0.08	—	0.18	0.04	0.11	0.14	tr.	tr.	0.18	tr.	0.99	0.53	0.34	0.48	3.48	2.67	2.72	0.62	3.26
LOI.	27.55	19.73	15.25	14.83	13.91	19.25	18.93	18.85	19.11	14.75	14.70	14.32	2.87	3.07	3.93	5.25	3.70	3.71	3.87	5.14
FeOΣ	15.02	10.00	9.25	8.86	9.55	8.61	7.94	8.20	8.78	8.72	7.45	13.61	11.37	12.34	10.46	6.97	9.32	4.71	10.35	6.60

	Basic enclaves in Mecsek granite							
	47.L.	221	200	52/15	33/143/2	35/13/2	43/127/1	24/114/1
SiO_2	53.28	53.28	54.95	54.00	53.88	53.10	52.16	46.40
TiO_2	1.09	0.67	1.58	1.73	1.36	1.23	1.73	1.04
Al_2O_3	14.96	10.68	16.34	12.20	12.74	13.64	14.06	12.37
Fe_2O_3	2.84	1.17	1.95	2.85	1.96	2.08	1.64	8.42
FeO	5.71	5.50	5.11	5.38	6.32	6.65	5.63	4.15
MnO	0.13	0.13	0.12	0.44	0.07	0.20	0.17	0.44
MgO	7.42	15.02	6.12	9.17	9.60	9.24	9.83	11.21
CaO	6.62	8.69	6.32	6.79	8.13	8.08	7.23	8.83
Na_2O	1.77	1.34	2.14	1.55	1.46	1.98	1.06	1.41
K_2O	5.79	3.61	4.14	4.94	4.23	4.97	6.64	4.53
LOI.	1.92	3.64	2.91	5.32	1.97	5.82	4.22	5.44
FeOΣ	8.27	6.55	6.96	7.44	8.08	8.52	7.12	11.72

Source of samples: No. 215, 216, 21.L, 29/2, 242/3, 6E, 7E, Sc.17, 226, 26, 88/1, 203, 13, 401,753, 2, S_{A-5} GHONEIM, M.—SZEDERKÉNYI, T. [1977], ÁGK 136, ÁGK 138, ÁGK 139 ÁGK 141, SZEDERKÉNYI, T. [1978], 47.L basic stock of Üveghuta GHANEM, M. A. E. and RAVASZ—BARANYAI L. [1969], 200 from, Üveghuta near curch, 221 inside Mórágy granite quarry, 52/15, 33/143/2, 35/13/2, 43/127/1 and 24/144/1 basic enclaves inside the anatectic granite JANTSKY, B. [1974]

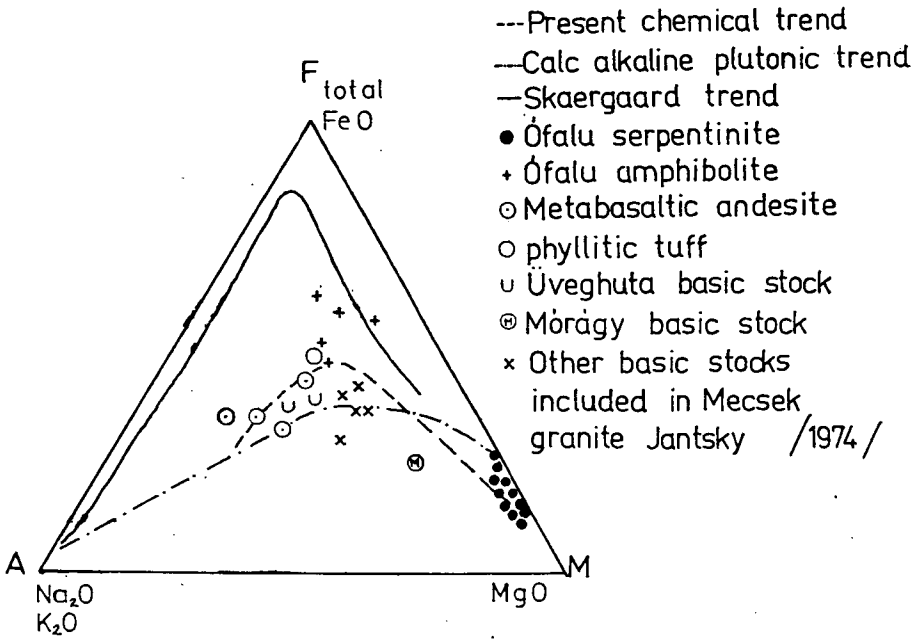

Fig. 7. AFM diagram shows the chemical trend of the rocks of the Ófalu area. The chemical analyses are calculated in anhydrous form

pentinized rock. Consequently the Ófalu serpentinite belongs to intensively serpentinized category (Table 2).

The Ni and Cr content of the Ófalu serpentinite suggested the peridotite parent rock origin. According to G. T. FAUST, K. J. MURATA and J. J. FAHEY, [1956] the sedimentary origin is marked by less than 0.002% Ni and 0.01% Cr content in the serpentinites. Higher concentration indicates igneous ultrabasic origin. The peridotite magmatic origin of the Ófalu serpentinite is in complete harmony with COLEMAN's work on the origin of serpentinite rocks. R. G. COLEMAN, [1971] calculated the MgO/SiO_2 ratio for brucite-bearing serpentinite derived from dunite and other serpentinite originated from harzburgite and lherzolite. The serpentinite derived from dunite has a MgO/SiO_2 ratio equal to 1.23, for harzburgite and its serpentinite derivatives the ratio was 1.11, while the lherzolite-derived serpentinite had a MgO/SiO_2 ratio equalling 0.89. In addition, R. G. COLEMAN, [1971] claimed that the presence of brucite in the serpentinite rocks favoured the dunite ultramafic origin. The Ófalu serpentinite has MgO/SiO_2 ratio ranges from 0.6 to 1.07 (Table 2) and brucite is absent in the mineral assemblage. Both evidences indicate the harzburgite and lherzolite origin of the present rocks.

As it was obvious from the field and laboratory, the Ófalu serpentinites undergone moderate degree of CO_2 metasomatism due to hydrothermal phenomena within the tectonic borders of the serpentinite body. The CO_2 metasomatism can be also illustrated from $MgO—CaO—Al_2O_3$ diagram *(Fig. 8)*, in which the plots show a general trend almost directly away from the MgO corner toward the CaO apex.

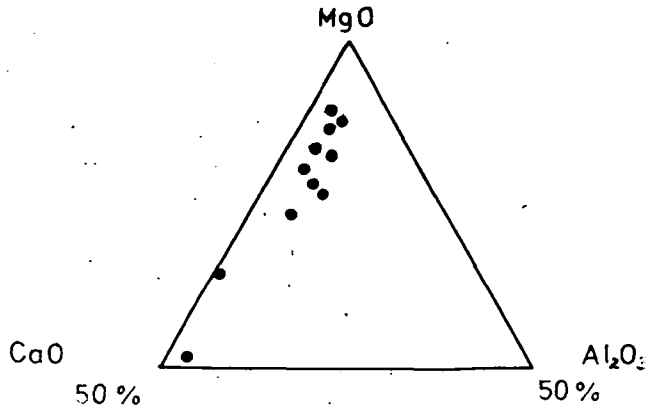

Fig. 8. MgO—CaO—Al_2O_3 diagram of Ófalu serpentinite. The chemical analyses are calculated in volatile-free basis

SERPENTINIZATION

It can be concluded that the Ófalu serpentinite remained constant in composition during the early stage of serpentinization, followed by partial removal of MgO, FeO and Al_2O_3 during the late stage of regional metamorphism. The above-mentioned conclusions were supported by the following:

— Lack of evidences for considerable Si or Mg metasomatism in surrounding rocks.
— The volume increase (due to constant composition) during serpentinization assists in the intrusion of the serpentinite along a zone of structural weakness.
— Absence of brucite in the Ófalu serpentinite may indicate constant composition serpentinization, since the presence of brucite is due to Mg production during serpentinization [R. G. COLEMAN, 1971].

The regional metamorphism promotes open system conditions under which partial change in chemical composition took place. The latter changes are well-documented in chromite grains, i.e. the chromite forms zoned crystals and the electron probe microanalysis shows that the outer zone is depleted in Al, Mg, and Cr as compared to unaltered relict chromite in the core of the crystal.

The presence of chromite, magnetite, pentlandite, pyrrhotite and heazlewoodite minerals and the absence of an awaruite (Ni_3Fe) intermetallic compound and sulphides low in sulphur indicate moderate O_2 and S_2 availability during the serpentinization process. Accordingly, the Ófalu serpentinite belongs to zone 2 of intermediate O_2 and S_2 availability of O. R. ECKSTRAND, [1975], and the temperature of hydration reaction of the Ófalu serpentinite lies in the range of 450—500 °C and pressure of 0.5 to 1 Kb according to data of J. B. MOODY, [1976].

As evident from the field works, the intrusion of the Ófalu serpentinite seems to be at temperatures low enough to satisfy the field requirements of absence of the thermal effect on the country rocks. Bearing in mind the "crystal mush" hypothesis [F. J. TURNER and J. VERHOOGEN, 1960] which is now widely accepted, it is belived that the Ófalu serpentinites were emplaced as an ultramafic body in a largely crystalline cold condition lubricated by interstitial liquids of magmatic source, which imparted the necessary degree of mobility. The instrusion of the Ófalu serpentinite along zones of major dislocation would be accompanied by external water, which normally streaming upwards along the same path of minimum resistance, must have provided facilities for further mobility and complete serpentinization.

REGIONAL METAMORPHISM

It was elucidated that, the Ófalu serpentinite underwent regional metamorphism together with the host eugeosynclinal metasedimentary and metavolcanic rocks of the Ófalu Group reaching up to the greenschist-amphibolite facies. This conclusion has been supported by the next statements:

— The close association of the Ófalu serpentinite with the enveloping country rocks in such a case that the former shows the same regional trend as the latter (the country rocks regionally metamorphosed up to greenschist-amphibolite facies.
— The presence of antigorite mineral in Ófalu serpentinite undoubtedly indicates higher PT conditions, rather than those rocks containing chrysotile and lizardite only.
— Chromite grains in the Ófalu serpentinite are surrounded by zones of ferrite-chromite which is intermediate in composition between relict chromite and secondary magnetite. According to up-to-date interpretations by R. K. SPRINGER, [1974], H. W. BLISS and W. H. MACLEAN, [1975], P. M. ASHLEY, [1975], B. W. EVANS and B. R. FROST, [1975], J. B. MOODY, [1976], the latter phenomena indicate a metamorphic event (greenschist-amphibolite transition facies) of temperature-pressure higher than necessary for the formation of lizardite-chrysotile serpentinite in which chromite grains are surrounded directly by a magnetite rim.

ACKNOWLEDGEMENTS

Thanks to geologists of Transdanubian Geological Service of the Hungarian Geological Survey for their help at field works and to M. EMSZT, GY. PANTÓ, G. NAGY and MRS. M. FÖLDVÁRY for their constant help in chemical analyses and electron-microprobe and DTA analyses.

REFERENCES

ASHLEY, P. M. [1975]: Opaque mineral assemblage formed during serpentinization in the Coolac Ultramafic Belt, New South Wales. J. Geol. Soc. Aust., Vol. **22,** 91—102.

BENSON, N. N. [1926]: The tectonic conditions accompanying the intrusion of basic and ultrabasic igneous rocks. Meth. Acad. Sci. Mem., Vol. **19,** 20 p.

BLISS, N. W. and MACLEAN, W. H. [1975]: The paragenesis of zoned chromite from Central Manitoba. Geochim. Cosmochim. Acta Vol. **39,** 973—990.

BOWES, O. R., WRIGHT, A. E. and PARK, R. G. [1966]: Origin of ultrabasic and basic masses in the Lewisian. Geol. Mag., Vol. **103,** 281 p.

CARMICHAEL, I. S. E., TURNER, F. J. and VERHOOGEN, J. [1974]: Igneous Petrology. International series in the earth and planetary sciences. McGraw-Hill Inc. New York.

COLEMAN, R. G. [1971]: Petrologic and geophysical nature of serpentinites. Geol. Survey of Amer. Bull., Vol. **82.** 897—918.

DUNCUMB, P. and JONES, E. M. [1969]: Electron-probe microanalysis. An easy-to-use computer program for correcting quantitative data. Tube investments. Res. lab. Report.

ECKSTRAND, O. R. [1975]: The Dumont serpentinite. A model for control of nickeliferous opaque mineral assemblages by alteration reaction in ultramafic rocks. Econ. Geol., Vol. **70.** 183—201.

EDEL'STEIN, I. I. [1963]: in WYLLIE, P. J. (ed.): Ultramafic and Related Rocks. John Wiley and Sons Inc., 1967, New York, 358—359.

EWANS, B. W. and FROST, B. R. [1975]: Chrome-spinel in progressive metamorphism -a preliminary analysis. Geochim. Cosmochim. Acta Vol. **39.** 959—972.

FAUST, G. T., MURATA, K. J. and FAHEY, J. J. [1956]: Relation of minor elements of serpentinites to their geologic origin. Geochim. Cosmochim. Acta Vol. **10,** 316—320.

FAUST, G. T. and FAHEY, J. J. [1962]: The serpentinite-group minerals. U. S. Geol. Surv. Prof. Pap., №. **384-A,** 1—92.

GHANEM, M. A. E. and RAVASZ-BARANYAI, L. [1969]: Petrographic study of crystalline basement rocks of Mecsek Mountains, Hungary. Acta Geol. Sci. Hung., Vol. **13,** 191—219.

GHONEIM M. F. and SZEDERKÉNYI T. [1977]: Preliminary petrological and geochemical studies on the area Ófalu, Mecsek Mountains, Hungary. Acta Miner. Petr. Univ. Szeged Vol. **XXIII, 1.** 15—28.

GÜLACAR, O. F. and DELALAYE, M. [1976]: Geochemistry of nickel, cobalt and copper in Alpine-type ultramafic rocks. Chem. Geol., Vol. **17,** 269—280.

HESS, H. H. [1955]: Serpentinites, orogeny and epeirogeny. Geol. Soc. Amer. Special Paper №. **62.** 391—408.

HEY, M. H. [1954]: A new review of the chlorite. Min. Mag., Vol. **30,** 277. pp.

KOGARKO, L. N. [1973]: The Ni—Co ratio as an indicator of the mantle origin of magmas. Geochem. Int., Vol. **10/5,** 1081—1086.

MALAKHOV, I. A. [1965]: Criteria of degree of serpentinization of ultramafic rocks. Geochem. Int., Vol. **2/4,** 678. pp. (Abstract)

MOODY, J. B. [1976]: Serpentinization: a review. Lithos Vol. **9.** 125—138.

MOORES, E. and VINE, F. [1971]: The Troodos massif, Cyprus and other ophiolites as oceanic crust: evaluation and implications. Phil. Trans. Roy. Soc. London, Vol. **268,** 443—466.

NAGY, G. [1970]: Mennyiségi elemzés elektron-mikroszondával. (Quantitative analysis by electron-microprobe.) Földt. Kutatás Vol. **XII,** №. 2, 27—38.

SPANGENBERG, K. [1943]: Die Chromitlagerstätte von Tampedal in Zobten. Z. Prakt. Geol., Vol. **51,** 13—35.

SPRINGER, R. K. [1974]: Contact metamorphosed ultramafic rocks in the Western Sierra Nevada foothills. Calif. J. Petr., Vol. **15,** 160—195.

SZEDERKÉNYI, T. [1974]: A délkeletdunántúli ópaleozóos képződmények ritkaelem kutatása. (Rare-element investigation of Old-Paleozoic formations of SE Transdanubia.) Cand. Sc. Diss. MTA Library.

SZEDERKÉNYI, T. [1977]: A mecseki ópaleozóos-prekambriumi alapszelvények komplex földtani feldolgozása. (Complex geological preparation of Old-Paleozoic and Precambrian basis-profiles of Mecsek Mountains.) Manuscript, Hung. Geol. Survey Library.

THAYER, T. P. [1960]: Some critical differences between alpine-type and stratiform peridotite-gabbro complex. 21-st Inter. Geol. Congress, Copenhagen, 1960, Report. pt. **XIII,** 247—259.

THAYER, T. P. [1967a]: Serpentinization considered as constant volume metasomatic process, a reply. Amer. Miner., Vol. **52,** 549—553.

THAYER, T. P. [1967b]: Chemical and structural relations of ultramafic rocks in alpine industrive complexes. In WYLLIE, P. J. (ed.): Ultramafic and related rocks. John Wiley and Sons, Inc., 1967, New York, 222—239.

TURNER, F. J. and VERHOOGEN, J. [1960]: Igneous and Metamorphic Petrology. McGraw-Hill, New York.

Manuscript received, July 20, 1979

DR. MOHAMED AHMED GHONEIM
Tanta University, Faculty of Science,
Geol. Dept. Tanta, Egypt

DR. TIBOR SZEDERKÉNYI
Institute of Mineralogy, Geochemistry
and Petrography
Attila József University
H-6722 Szeged, Egyetem u. 2—6.
Hungary

Acta Mineralogica-Petrographica, Szeged, XXIV/1, 19—27, 1979

MINERALOGICAL STUDY OF KAERSUTITE IN THE VOLCANIC NODULE AT EIFEL, W. GERMANY

SACHINATH MITRA

ABSTRACT

Some lapilli and bombs occurring in the ash ejecta around Eifel in Germany were investigated by the author and one such contained pitch-black shining crystal-aggregates, which on detailed study were found to contain kaersutite, having a chemical formula obtained by wet chemistry as: $(Si_{5.7}\ Al_{2.3})\ (Al_{0.2}\ Ti_{0.4}\ Fe^{3+}{}_{0.5}\ Mn_{0.01}\ Mg_{3.2})\ (Ca_{2.0}\ Na_{0.5}\ K_{0.4}\ P_{0.01})\ (O, OH, F)_{32} \cdot Fe^{2+}$ and Fe^{3+} contents determined by MÖSSBAUER were different from chemical data and are in the ratio of 73 : 27.

High content of Al_2O_3 (3.87—10.84 wt.%) with Tschermak's component ranging from 5.9 to 18.4 mol. p.c. in clino-pyroxenes in the wehrlite and clinopyroxenite inclusions in the volcanics of Eifel region suggest the parent magmas to be alkali-basalt in composition. The chemistry of kaersutite suggests that the crystallization took place in hydrous condition in the lowest part of the crust.

INTRODUCTION

Eifel region in W. Germany is one of the major oft-visited places for geologists, interested in Germany's geology, volcanism or upper mantle studies. The lapilli and nodules ejected out by volcanism at Eifel have become the subject of intensive studies of many groups of workers [AOKI and KUSHIRO, 1968; FRECHEN, 1948, 1963; ROSS *et al.*, 1954; WHITE, 1963] involved in the studies on the mineralogy and geochemistry of the upper mantle.

Studies on the ultramafic inclusions in volcanic effusives, collected from continental, circum-oceanic and oceanic regions indicated that they are broadly of two groups occurring in two types of rocks assemblages: one with extremely silica-undersaturated alkali-basalts such as olivine-nephelinite, nepheline-basanite, and the other are moderately undersaturated alkali-basalt such as olivine-basalt, hawaiite and ankaramite [WHITE, 1966]. Inclusions in the former are generally of lherzolite group and those in the other are of dunite, wehrlite, clinopyroxenite and feldspathic peridotite, likely to be formed by crystal accumulation from alkali-basalt magma. Those of lherzolite may be xenolithic fragments of heterogeneous upper mantle materials, which are not capable of generating basalt magmas [AOKI and KUSHIRO, 1968; WHITE, 1966]. Both the two groups of inclusions have been reported from the tuff from Eifel, W. Germany.

While searching for such nodules in the ash ejecta around a volcanic cone at Eifel (Laachersee) in a team of geoscientists in the summer of 1968 *(Fig. 1)* the author found a nodule (with about 12 cm as major axis and 8 cm minor axis) containing pitch-black mineral with strong shining cleavages. A part of the bomb has been investigated by the present author and the rest was left at the Mineralogical Institute, Heidelberg.

Fig. 1. Geoscientists searching (September, 1968) for volcanic inclusions in the loose tuffs of Eifel. The low angle stratification of ash is conspicuously seen in a nearly vertical exposure

Mineralogical studies of the black minerals is presented in this paper but details of mineralogy and chemistry of the associated ash and other inclusions in the volcanics of the area have not been dealt with by the author except citing some relevant references to other workers' observations. It should be noted here that the Laachersee volcanic province is distinctly different from West Eifel, while both being notable for richness in ultrabasic nodules the former is more abundant in felsic volcanics.

MINERALOGY

With a brown coconut-like shell of ash the nodule contains inside pitch-black large (almost as large as the length of the nodule) crystals of hornblende with angular interpenetrating grain boundaries between subhedral crystals. The chemical composition of a clean cleaved block, of this mineral, crushed to 100 mesh and separated from ore minerals by Franz Isodynamic Magnetic Separator, is shown in Table 1. In this analysis the sample was fused with bisulfate before wet chemical treatment. On the basis of 24 oxygens (with F and OH replacing oxygens) the formula was calculated as:

$(Si_{5.7}Al_{2.3})\ (Al_{0.2}Ti_{0.4}Fe^{3+}_{0.5}\ Mn_{0.01}Mg_{3.2})\ (Ca_{2.0}K_{0.4}Na_{0.5}P_{0.01})\ (O, OH, F)_{24}$

A comparison of this composition with a hornblende from hornblende-clinopyroxene and kaersutite from a cognate xenolith in trachyte, Japan is also presented in Table 1. Optical study shows dark brown equal absorption along Y and Z direction changing to lighter brown colour in X direction.

$$N_x = 1.660$$
$$N_y = 1.703$$
$$N_z = 1.722$$

$N_z - N_x = 0.062$ and $2V = 68°$ (determined by A. Roy). The Fe^{3+} ratio with Fe^{2+} per formula unit in Eifel sample is three times more than in the Hastings country sample. Mössbauer studies discussed latter give this $Fe^{2+}:Fe^{3+}$ ratio as 73:27 (Table 2), which is more conformable with Scoon's 79:21 and Aoki's 71:29 ratios (from Table 1).

TABLE 1

Chemical composition (wt%) of volcanic kaersutite (I) from Eifel and its comparison with hornblende (II) from hornblende clinopyroxenite from the same volcanic suites (AOKI and KUSHIRO, 1968) and kaersutite (III) from cognate xenolith in trachyte, Japan

Oxides	I		II		III	
SiO_2	38.79		42.40		39.68	
Al_2O_3	14.73		12.78		12.81	
TiO_2	4.02		2.59		7.12	
Fe_2O_3	4.55		3.41		4.04	
Cr_2O_3	...		0.42			
FeO	5.15		5.42		8.79	
MnO	0.06		0.14		0.16	
MgO	14.52		15.53		11.22	
CaO	12.51		10.70		11.06	
Na_2O	1.71		2.53		3.37	
K_2O	2.32		1.58		1.04	
P_2O_5	0.016					
H_2O^+	1.82		2.29		0.78	
H_2O^-	nil		0.05		0.15	
Others (F, etc.)	—				0.33	
Total	100.196		99.84		100.55	
	Number of ions on the basis of 24 (O, OH, F, Cl)					
Si	5.65	8.00	6.13	8.00	5.937	8.00
Al	2.35		1.87		0.063	
Al	0.18	4.907	0.31	5.04	0.197	5.07
Ti	0.44		0.28		0.801	
Fe^{3+}	0.50		0.37		0.454	
Fe^{2+}	0.63		0.66		1.000	
Mg	3.15		3.35		2.501	
Mn	0.007		0.02		0.020	
Cr^{3+}	n.d.		0.05			
Ca	1.95	2.88	1.66	2.66	1.773	2.95
Na	0.48		0.71		0.976	
K	0.44		0.29		0.198	
P	0.01		...			
OH			1.81		0.778	0.93
F			...		0.156	
Analyst	B. P. GUPTA		K. AOKI and I. KUSHIRO		K. AOKI	

TABLE 2

^{57}Fe hyperfine parameters of volcanic hornblende (kaersutite) from Eifel (χ^2 of the fit being 0.65 with 400 degrees of freedom)

Oxidation state	Quadrupole splitting (mm/s)	Isomer shift* (mm/s)	fwhm (mm/s)	% of Total Fe
Fe^{2+}	2.37±0.11	1.24±0.12	0.75±0.13	73
Fe^{3+}	0.67±0.17	0.30±0.19	0.53±0.16	27

* With respect to 99.999% pure Fe-metal.

Thin bar-like inclusions of ilmenite of nearly equal length and with translucent to transparent patches (rutile or leucoxene phases?) occur in an orderly fashion *(Figs. 2* and *3)* aligned parallel to certain crystallographic phases and running along another plane. In some sections two sets of exsolution lamellae align themselves to make acute angles (30°—45°) *(Figs. 2* and *3a)*. Exsolution lamellae reported from Iki Island, Japan, lie parallel mainly to the *c*-axis and sometimes to *a*-axis in (010) [AOKI, 1970].

However, the Ti content in this kaersutite (0.4 Ti per formula unit or TiO_2=4.02%) falls slightly shorter than as stipulated earlier to be around 5% TiO_2 (i.e. 0.5 to 1.0 atoms per formula units) *(ibid)*.

The Fe^{3+}:Fe^{2+} ratio per formula unit in Eifel sample is 5:6 but ^{57}Fe Mössbauer studies as discussed later give this ratio as 73:27 (Table 2), which is more conform-

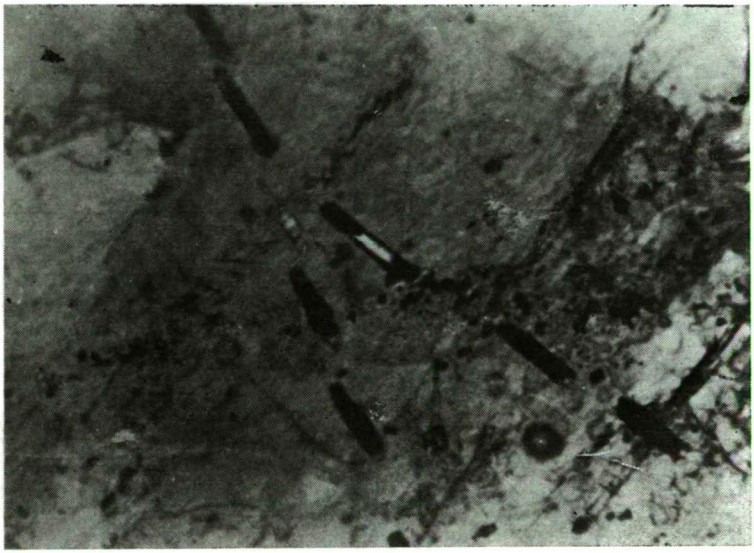

Fig. 2. A microphotograph of volcanic hornblende with Fe—Ti-oxide exsolution laths, some being partly or fully translucent

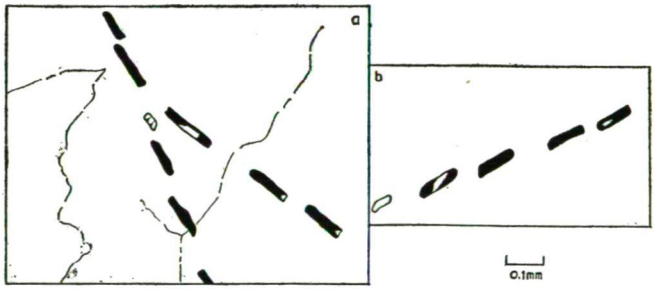

Fig. 3. Sketch showing the nature of ilmenite exsolution along some crystallographic planes. In some sections (a) the bifurcation of the alignment of laths are predominantly seen, cutting across some kaersutite zones showing different absorption characteristics. In some sections (b) only one set of exsolutions

able with AOKI's 71:29 ratios obtained from cognate xenolith in trachyte, Japan (Table 1).

The high $Fe^{3+}:Fe^{2+}$ ratio observed in silicate mineral analyses by wet chemistry is primarily due to two reasons: *(1)* oxidation of the minerals in post crystallization stage, during subaerial or submarine placement and *(2)* oxidation after collection of the sample and during treatment for wet chemical analysis.

$Fe^{3+}:Fe^{2+}$ ratios in kaersutites emplaced in subaerial volcanic rocks are higher than those in the submarine lavas etc. and often they are oxidized to oxykaersutites. But this sample is less oxidized to be called an oxykaersutite, which needs to have the ratio of about 2 [AOKI, 1970]. However, no clue for estimating the original $Fe^{3+}:Fe^{2+}$ ratio at the time of crystallization was available to the author.

For the sample as collected, the author is inclined to accept the Mössbauer data for the Fe^{2+} and Fe^{3+} contents in preference to wet chemical analyses. No warranted chemical method of Fe^{2+}, Fe^{3+} determination in silicates exists because some part of Fe^{2+} in the sample gets oxidized to Fe^{3+} during grinding in atmospheric air, fusion, dissolution and even during titration or later treatment. Mostly we obtain Fe^{3+} values at the cost of Fe^{2+}. By Mössbauer studies this problem is solved to a great extent (although Fe^{2+} oxidation while grinding and during sample preparation cannot be totally ruled out) and the distribution of Fe^{2+} and Fe^{3+} at M_1, M_2, M_3 and M_4 sites has been determined with a discussion on the structural characteristics of this mineral. The structural description of the amphibole group of minerals as relevant for understanding the stereochemistry of this mineral is discussed below [BURNS, 1970, p. 99].

There are three sets of six-fold co-ordination designed as M_1, M_2 and M_3 and one of six to eight-fold co-ordination, designed as M_4. Cations in the two M_1 and one M_3 positions are each co-ordinated to four oxygen ions and two hydroxyl ions. The OH-groups are in *cis* arrangement in the M_1 sites and *trans* in the M_3 site. Cations in the M_2 positions are surrounded by six oxygen ions and oxygen ions surrounding the M_1, M_2, M_3 sites are linked to one silicon atom. Cations in M_4 positions are preferentially filled by Ca, Na etc. and are surrounded by four oxygen ions each linked to one silicon atom and two to four oxygen atoms which are each shared by two silicon atoms. The octahedra about M_1, M_2 and M_3 positions are almost regular and the cation sites are centrosymmetric, whereas the M_4 co-ordination site is very distorted and has C_{2v} symmetry and cations here do not lie at the centre of symmetry of the site. This M_4 site and orthopyroxene M_2 sites resemble one another in the nature of oxygen ligands and the distortion of co-ordination sites. This is linked with the Crystal Field Stabilization Energies (CFSE) of Fe^{2+} at these sites.

The amount of Fe entering in some eight-fold co-ordinated M(4) site and the Si I and Si II tetrahedral sites are negligible. Normally, electrical neutrality is maintained by substituting Si in the tetrahedral site. Fe^{3+} may, however, proxy for Al^{3+} when in sufficient amount. The Mössbauer spectra *(Fig. 4)* suggests that Fe^{3+} is occurring in octahedral sites. HUCKENHOLZ [1971] have shown that significant Fe^{3+} can enter into tetrahedral sites in the related diopside structure. It is possible that even when Al is present in excess of what are required for filling Si I and Si II sites, randomisation of Al and Fe^{3+} among M_2 and tetrahedral sites could occur at high temperature in the volcanic condition.

^{57}Fe Mössbauer spectrum [for details of the instrumental set-up etc. MITRA and BANSAL, 1975] of the sample obtained with a 512 multichannel analyser at room temperature is shown in *Fig. 4*. Since the line-width of the low velocity peak is much

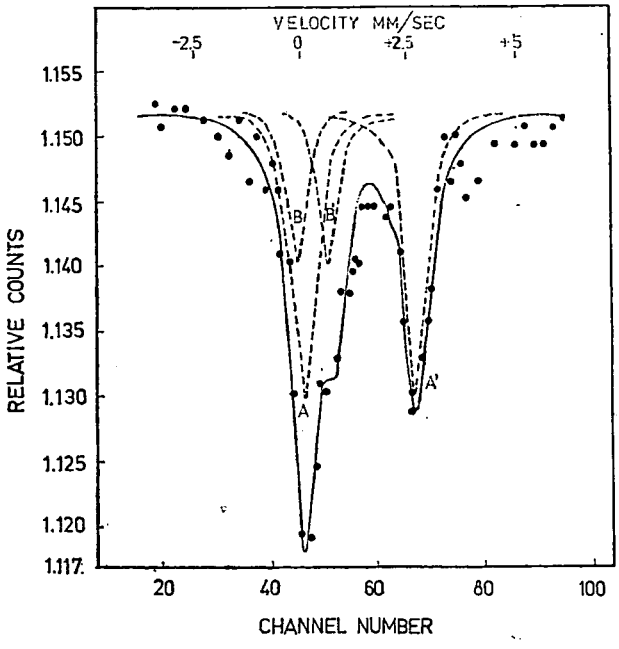

Fig. 4. Mössbauer spectrum of ^{57}Fe in volcanic hornblende from Eifel, W. Germany

higher than usual the spectrum was least-square fitted to two pairs of Lorentzian lines *AA'* and *BB'*, with constrains that the widths and intensities of the individual lines of a doublet are equal. A χ^2 value of 0.65 was obtained for this fit with 400 degrees of freedom.* Since enough Ca, Na and K (totalling to 2.9 per formula unit) are present to fill the M_4 site, most of the iron is assumed to fill up the remaining M_1, M_2 and M_3 sites [SEMET, 1973]. Since the environment at these three sites are nearly identical the hyperfine parameters are nearly the same and it becomes difficult to resolve the contributions due to individual sites. Although some workers [GREAVES *et al.*, 1971] have resolved these in some cases of actinolites with χ^2 values above 500 (Table 3), the three sites in the sample investigated are considered to give rise to an apparent single pair of lines for both Fe^{2+} and Fe^{3+}. The line-widths obtained are larger than those expected for individual sites, which again shows that there is overlap of two or three sites with nearly equal isomer shifts and quadrupole splittings. Thus the doublets AA' and BB' have been assigned to Fe^{2+} and Fe^{3+} at the M_1, M_2, M_3 sites. The isomer shifts and quadrupole splittings are listed in Table 2 along with errors. The percentage of each iron species are rough estimates calculated by assuming

* The χ^2 values obtained in Mössbauer spectroscopy are frequently higher than one would expect because the function (Lorentzian) used is not absolutely correct. Peaks may deviate from Lorentzian shapes by order-disorder phenomena where they may be distorted by a number of small variations in the electronic state of the absorbing atoms due to environmental fluctuations. Other factors which affect the χ^2 value include instrumental drift, counting geometry, cosine effects, and the proportion of the spectrum computed as being in zero-absorption base-line.

TABLE 3

^{57}Fe *hyperfine parameters in other amphiboles*

Species	Oxidation state	Sites	Quadrupole splitting (mm/s)	Isomer shift (mm/s)	Ref.
Actinolite	Fe^{2+}	M_2	1.89—2.03	1.13—1.16	BANCROFT *et al.* [1967]
		M_1, M_3	2.81—2.82	1.15—1.16	
Actinolite	Fe^{2+}	M_1	2.89	1.14	Sp. No. In GREAVES
		M_2	1.91	1.14	14.785 *et al.* [1971]
		M_3	2.57	1.12	
	Fe^{3+}	(M_1, M_2, M_3)	0.53	0.28	
Actinolite	Fe^{2+}	M_1	2.89	1.15	Sp. No. In GREAVES
		M_2	1.91	1.14	44.973 *et al.* [1971]
		M_3	2.57	1.12	
	Fe^{3+}	(M_1, M_2, M_3)	0.57	0.40	
Cummingtonite	Fe^{2+}	(M_1, M_2, M_3)	2.72—2.90	1.14—1.18	BANCROFT *et al.* [1967]
		M_4	1.50—1.68	1.05—1.11	
Anthophyllite	Fe^{2+}	(M_1, M_2, M_3)	2.58—2.61	1.12—1.13	BANCROFT *et al.* [1967]
		M_4	1.80—1.81	1.09—1.11	
Crocidolite	Fe^{2+}	M_1	2.82	1.25	BANCROFT and BURNS
		M_3, M_2	2.39	1.25	[1969]
	Fe^{3+}	(M_1, M_2, M_3)	0.41	0.46	
Glaucophane	Fe^{2+}	M_1	2.82	1.22	BANCROFT and BURNS
		M_3, M_2	2.33	0.33	[1969]
	Fe^{3+}	(M_1, M_2, M_3)	0.48	0.45	

that the fraction f^* of Fe^{57} nuclei absorbing the γ-ray resonantly without recoil, to be the same for both Fe^{2+} and Fe^{3+} at M_1, M_2, M_3 sites.

It is presumed that Fe in Fe—Ti-oxide mineral inclusions have contributed counts only in the background part of the spectrum and significantly none in the peaks. Thus the Mössbauer analysis eliminates the Fe from minor oxide impurities whereas the chemical analysis (Table 1) might incorporate the unliberated magnetic fragments after crushing and magnetic separation. For comparison, hyperfine parameters of those reported from other amphiboles are presented in Table 3. It is seen that the I.S. of alkali amphiboles are generally above the value of 1.20 and larger compared to those of other amphiboles (Tables 2 and 3).

DISCUSSION

Kaersutites defined as titaniferous pargasite-ferropargasite series amphiboles have part of Mg replaced by Fe^{2+} and the general formula of type sample is shown as $(Na, K, Ca)_{2-3}$ $(Mg, Fe^{2+})Ti$ $Al_2^{IV}Si_6O_{23}(OH)$ by WILKINSON [1961]. Table 1 shows that Eifel kaersutite gives Si as 5.7 per formula unit having (O, OH, F)=24, which is slightly less than 6. Kaersutites from monzonite, teschenite and trachyte have Si content slightly higher than 6 and often have insufficient Al^{3+} to fill the Z group, while those crystallized in volcanic rocks have high Al^{3+} in the Z group

* f' is defined as $\approx 1-K^2<\chi^2>$ for an Einstein solid with $3N$ vibrational modes where N is, the number of atoms in the solid and $K=2\pi/\lambda=E/nc$, $<\chi^2>$ is the component of mean square vibrational amplitude of the emitting nucleus in the direction of the gamma ray. It is therefore dependent on temperature and on the vibrational spectrum at each of the M sites.

[AOKI, 1963]. The Al^{3+} content (3.8 per formula unit) in the present sample is high and Al^{3+} fills up the Z group with Si^{4+} and one-third of the total Al^{3+} goes into Y group. This is higher than reported earlier from normal or oxidized kaersutites which have $Al \approx 2$ per formula unit *(ibid)*.

The high content of Al_2O_3 (3.87–10.84 wt.%) with Tschermak's component ranging from 5.9 to 18.4 mol. p.c. in clinopyroxenes in the wehrlite and clinopyroxenite inclusions in the volcanics of Eifel region suggest the parent magmas to be alkali-basalt in composition and was located at relatively deep sites in the continental crust.

The calciferous amphiboles are supposed to have 1.8 to 2.1 Ca ions per formula unit [BOYD, 1959) and in this kaersutite having Ca to an amount of 2 show a pronounced substitution for Mg as common in calciferous amphiboles. (Na+K) of this sample is 0.9 with a ratio of 5:4 indicating fair availability of equivalent amount of these alkalies in the crsytallizing magma.

Crystallization of kaersutite-hornblende is presumed to be effected at high pressure temperature condition with hydrous environment. It is known that hornblende breaks down to garnet+ pyroxene at pressures above 12 Kb and temp. below 950 °C and brown hornblende is stable at total pressures of at least 13 Kb (corresponding to a depth of 40 km) at 900 °C when $P_{total} = P_{H_2O}$ [NISHIKAWA and KUSHIRO, 1967; LOVERING and WHITE, 1969]. At the same pressure and temp. conditions, it appears that amphibole crystallizes at an earlier stage of fractionation from a silica-undersaturated magma than from an oversaturated magma [AOKI, 1970]. Kaersutites of plutonic xenoliths from Tristan da Cuñha is supposed to have crystallized at water pressure below 1.4 Kb [LE MAITRE, 1969] i.e. below 5 km depth. Studies on the kaersutite-bearing inclusions in Iki Island, Japan by AOKI [1970] suggest that alkali-basalt magma crystallized phenocrysts of olivine, rare-aluminous orthopyroxene, aluminous clinopyroxene, kaersutite, plagioclase and titano-magnetite successively under hydrous conditions at depth of 25 to 30 km in the lowest part of the crust. On the basis of Al-content in the associated olivine-clinopyroxene nodules in the tuffs of Eifel, it may be presumed that identical high P—T hydrous condition must have controlled the crystallization of kaersutite below the crust in the Eifel region of W. Germany.

ACKNOWLEDGEMENT

Thanks are due to MR. C. BANSAL, Nuclear Spectroscopy Division, Tata Institute of Fundamental Research, Bombay for valuable discussions and co-operation in the Mössbauer studies of this sample. Sincere thanks are expressed to PROF. G. C. AMSTUTZ, Direktor, Mineralogisches Institut der Universitat Heidelberg for the financial support and other facilities to do field work in the volcanic regions in W. Germany.

REFERENCES

AOKI, K. [1965]: The kaersutites and oxykaersutites from alkalic rocks of Japan and surrounding areas. Journ. Petrol., **4**, 198.

AOKI, K. [1970]: Petrology of kaersutite-bearing ultramafic and mafic inclusions in Iki Island, Japan. Contrib. Mineral. and Petrol., **25**, 270—283.

AOKI, K. and KUSHIRO, I. [1968]: Some clinopyroxenes from ultramafic inclusions in Dreiser, Weiher, Eifel. Contr. Mineral and Petrol., **18**, 241—256.

BANCROFT, G. M. and R. G. BURNS [1969]: Mössbauer and absorption spectral study of alkali amphiboles. Miner. Soc. Amer. Spec. Pap., **2**, 137—148.

BANCROFT, G. M. A. G. MADDOCK and R. G. BURNS [1967]: Applications of the Mössbauer effect to silicate mineralogy. Part I. Iron silicates of known crystal structures. Geochim. Cosmochim. Acta **31,** 2219—2246.
BOYD, F. R. [1959]: Hydrothermal investigations of amphiboles, Researches in Geochemistry, Wiley & Sons, N. Y. 377—96.
BURNS, R. G. [1970]: Mineralogical Applications of Crystal Field Theory. Cambridge University Press, 224. p.
FRECHEN, J. [1948]: Die Genese der Olivinausscheidungen vom Dreiser Weiher (Eifel) and Finkenberg (Siebengebirge). Neues Jahrb. Miner. Abh., **79A,** 317—406.
FRECHEN, J. [1963]: Kristallisation, Mineralbestand, Mineralchemismus und Forderfolge der Mafinite vom Dreiser Weiher in der Eifel. Neues Jahrb. Mineral. Monatsh., 205—225.
GHOSE, S. [1965]: A scheme of cation distribution in the amphiboles. Amer. Mineral., **54,** 1399—1408.
GREAVES, C., R. G. BURNS and G. M. BANCROFT [1971]: Resolution of actinolite Mössbauer spectra into three ferrous doublets. Nature (Phys. Sci.) **233,** 60—61.
HAFNER, S. S. and H. G. HUCKENHOLZ [1971]: Mössbauer spectrum of synthetic ferri-diopside. Nature (Phys. Sci.) **233,** 9—10.
HUCKENHOLZ, H. G., J. F. SHAIRER and H. S. YODER [1969]: Synthesis and stability of ferri-diopside. Mineral. Soc. Amer. Spec. Pap., **2,** 163—177.
LOVERING, J. F. and WHITE, A. R. J. [1969]: Granulite and eclogite inclusions from basic pipes at Delegate, Australia. Contrib. Mineral. and Petrol., **21,** 9—52.
MAITRE, R. W. LE [1969]: Kaersuite-bearing plutonic xenoliths from Tristan da Cuñha. Min. Mag., **37,** (286), 185—197.
MITRA, S. and BANSAL, C. [1975]: ^{57}Fe Mössbauer study of volcanic hornblende. Chem. Phys. Letters **30** (3), 403—405.
NISHIKAWA, M. and KUSHIRO, I. [1967]: Breakdown of hornblende under high temperature and pressure. Bull. Volcanol. Soc. Japan **12,** 153 (Japan. abstr.).
ROSS, C. S., M. D. FOSTER and A. T. MYERS [1954]: Origin of dunites and olivine-rich inclusions in basaltic rocks. Am. Miner., **39,** 639—737.
SEMET, M. P. [1973]: A crystal-chemical study of magnesiohastingsite. Am. Mineral., **58,** 480—494.
WHITE, R. W. [1966]: Ultramafic inclusions in basaltic rocks from Hawaii. Contr. Mineral. and Petrol., **12,** 245—314.
WILKINSON, J. F. G. [1961]: Some aspects of the calciferous amphiboles, oxyhornblende, kaersutite and barkevikite. Am. Mineral., **46,** 340—354.

Manuscript received, March 1, 1979

DR. S. MITRA
Reader in Geology
Department of Geological Sciences
Jadavpur University
Calcutta-32, India

Acta Mineralogica-Petrographica, Szeged, XXIV/1, 29—40, 1979.

PETROCHEMISTRY AND PETROGENESIS OF SOME POST-TRAP ALKALINE GRANITE OF GABAL HUFASH, SURDUD AREA, YEMEN ARAB REPUBLIC

MAHMOUD L. KABESH, MONIR M. ALY
and
MOHAMED Y. ATTAWIYA

ABSTRACT

The paper deals with the chemistry of the alkaline granites of Surdud area, Yemen Arab Republic. The chemical analyses of ten samples are presented for the first time. The chemical data are processed and utilized in the chemical evaluation of these granites applying several parameters. The examined granites are aegirine-riebeckite bearing and form a suite of post-trap granitic intrusions so widely distributed in Yemen.

INTRODUCTION

The present paper deals with the essential petrochemical characters of some post-trap granites of Surdud area, Yemen Arab Republic.

Broadly, post-trap granites are poorly represented among the basement rocks of Yemen.

Same as the crystalline basement rocks, the post-trap granites of Yemen are ill-defined and scarcely studied. GEUKENS' map of the Yemen Arab Republic [1966] represents, however, the only comprehensive work on the geology of Yemen Arab Republic. This map forms part of the geological map of the Arabian Peninsula published by the U. S. Geological Survey in 1972. Studies on the basement rocks of Yemen are almost lacking. However, recently the petrochemistry and petrogenesis of some Precambrian granitic rocks in Yemen have been undertaken by KABESH *et al.* [1979]. Moreover, the investigation of biotites of some Precambrian granitic rocks has been carried out by KABESH and ALY [1979].

The post-trap granites have been scarcely trated. However, the chemistry of arfvedsonites and riebeckites from post-trap alkali granites of Gabal Sabir, Taiz area, Yemen Arab Public has been recently studied. [REFAAT and KABESH, 1979].

According to GEUKENS, [1966], the post-trap granites defined as recent granites *(op.cit.)* protrude locally above the general topography carved in the volcanic trap series.

These granites form intrusive masses deforming the trap series on their flanks and thus they are dated as post-trap. GEUKENS further described some of these intrusions reaching 10 kms in length and few kms in width while others appear as letnicular dykes from 0.1—1.5 m wide.

Post-trap granites form very few and minor outcrops among the basement of Yemen. The general distribution of these granites is shown in *Fig. 1.*

The two major outcrops are represented by Gabal Sabir (Taiz area), and Gabal Hufash (Surdud area).

The present paper is intended to deal with the petrochemistry and petrogenesis of the post-trap alkaline granites of Gabal Hufash, Surdud area.

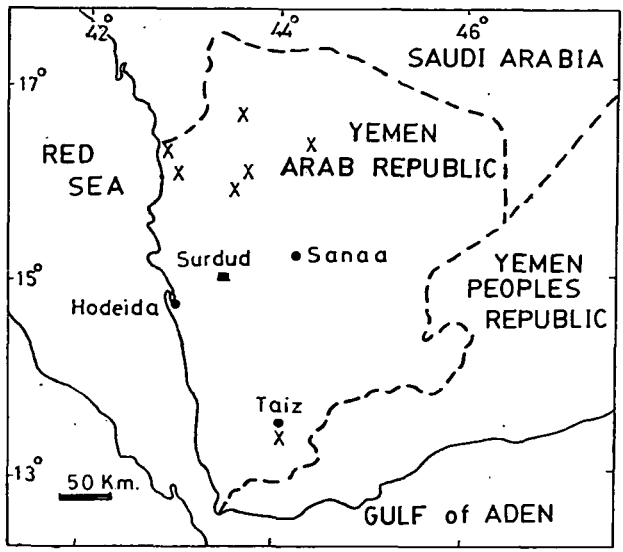

Fig. 1. Key map showing distribution of post trap granites in Yemen Arab Republic: ■ Examined area; X Other post trap granites

ANALYTICAL METHODS

The rock samples collected from Gabal Surdud area were selected for chemical analysis for major elements. SiO_2 was determined gravimetrically. Total iron oxides, P_2O_5, MnO and TiO_2 were determined colorimetrically. Al_2O_3, CaO and MgO were estimated by visual titration against standard EDTA solution. The value of FeO was obtained by titration against a standard solution of potassium permanganate and, by subtraction of FeO from total iron oxides, Fe_2O_3 was estimated. Na_2O and K_2O were determined by flame photometry.

PETROGRAPHY

Petrographic studies showed that the mineralogical composition of the Surdud granites comprises essentially quartz, orthoclase perthite, plagioclase, riebeckite, aegirine in addition to zircon, apatite, epidote and iron ores as accessories.

The quartz forms irregular clear grains occupying the interstices of the feldspars and mafics.

Plagioclase shows normal zoning with occasional alteration through sericitization and saussuritization.

Perthites are mostly due to the process of exsolution at high temperature and partly to replacement at relatively low temperature.

Alkali feldspars are represented by orthoclase which is largely kaolinized.

Riebeckite and aegirine form the dominant mafics in Surdud granites. The riebeckite is strongly pleochroic with x=green, y=greyish green and z=dark indigo blue.

Some samples are porphyritic in which megacrysts of plagioclase and alkali amphiboles are set in a groundmass of quartz and feldspars.

TABLE 1

Chemical data for the investigated granites

S.No.	1	2	3	4	5	6	7	8	9	10
SiO_2	71.05	72.53	71.06	71.45	70.88	71.26	72.15	70.64	71.92	70.78
Al_2O_3	11.55	11.65	11.75	11.05	12.00	11.55	11.75	12.11	11.22	11.94
Fe_2O_3	1.14	1.21	1.96	1.18	1.21	1.00	1.12	0.66	1.16	1.18
FeO	1.56	1.68	1.38	1.22	1.39	1.51	1.43	1.42	1.90	1.66
MnO	0.19	0.20	0.19	0.05	0.06	0.13	0.08	0.15	0.14	0.18
MgO	0.64	0.71	0.66	0.49	0.52	0.71	0.64	1.01	0.49	0.82
CaO	1.21	0.99	1.14	1.48	1.95	1.68	1.71	1.32	1.68	1.62
Na_2O	5.06	4.22	4.91	5.16	4.25	5.32	4.68	5.55	4.21	4.65
K_2O	5.32	5.03	5.21	4.22	4.97	4.72	4.94	5.38	4.86	5.08
TiO_2	0.39	0.33	0.41	0.68	0.41	0.37	0.33	0.40	0.60	0.51
P_2O_5	0.07	0.09	0.09	0.07	0.09	0.09	0.11	0.11	0.06	0.06
H_2O^-	0.32	0.41	0.22	0.50	0.38	0.38	0.28	0.39	0.40	0.35
H_2O^+	1.09	0.84	1.11	1.14	1.21	0.74	0.84	1.06	0.99	0.74
Total	99.59	99.88	100.08	99.19	99.92	99.46	100.11	100.20	99.63	99.57
Calculated alkalinity ratio	9.72	6.47	8.67	8.46	5.76	7.95	6.01	9.74	5.74	6.08
Agpaitic coefficient	1.22	1.06	1.17	1.26	1.11	1.20	1.11	1.24	1.09	1.10

PETROCHEMISTRY

The chemical characters of the granitic rocks under investigation have been reached through complete analysis of 10 selected samples, the data is presented in Table 1. The calculated Niggli-values and the CIPW Norms are given in Tables 2 and 3 respectively.

The data of the chemical analyses were plotted on histograms *(Fig. 2)* to illustrate their distribution. The plots show that the analyses are not strongly variable indicating the homogeneity of the rocks.

The relative abundance of K_2O+Na_2O, $FeO+Fe_2O_3$ and MgO are plotted on an AFM diagram *(Fig. 3)*. The diagram shows that these granites are enriched in alkalies and impoverished in magnesium and iron.

The plot of Mol Na_2O vs. Mol K_2O *(Fig. 4)* shows that the investigated granites are mostly potassic with rarely sodic tendencies according to RAGUIN's, [1965] suggestions.

The analyses have been plotted on the triangular diagram K_2O—Na_2O—CaO *(Fig. 5)*. The plot shows that the investigated granites lie near the mid point of K_2O-Na_2O line with some calcium present in minerals other than feldspars as indicated from the petrography.

The Niggli-value *fm* has been plotted *vs* the *al* value *(Fig. 6)* which indicate that the investigated granites are salic.

The *alk-al* plot is presented in *Fig. 7* which reveal that the investigated salic magma is peralkalic to relatively alkalic rich [BURRI, 1964]. WRIGHT [1969] has proposed a ratio given by

$$\frac{Al_2O_3+CaO+\text{total alkalies}}{Al_2O_3+CaO-\text{total alkalies}}$$

TABLE 2

Niggli-values for the investigated granites

S.No.	1	2	3	4	5	6	7	8	9	10
al	34.59	36.60	34.62	34.35	35.48	34.10	35.43	34.51	34.98	34.88
fm	16.65	18.89	18.87	14.14	14.54	15.95	15.85	16.04	17.51	18.10
c	6.59	5.60	6.11	8.36	10.48	9.02	9.38	6.84	9.52	8.60
alk	42.17	38.91	40.41	43.14	39.49	40.93	39.34	42.61	37.99	38.41
si	361.08	386.70	355.29	376.94	355.65	357.08	369.23	341.63	380.48	350.93
ti	1.49	1.32	1.50	2.70	1.55	1.39	1.27	1.45	2.39	1.90
p	0.15	0.20	0.19	0.16	0.19	0.19	0.24	0.23	0.13	0.13
h	23.90	22.23	22.18	28.86	26.61	18.72	19.12	23.39	24.53	18.03
mg	0.29	0.30	0.26	0.27	0.27	0.33	0.31	0.45	0.22	0.33
k	0.41	0.44	0.41	0.33	0.40	0.37	0.41	0.39	0.43	0.42
qz	115.15	137.98	111.03	130.74	109.72	113.84	123.59	95.48	137.57	107.87

TABLE 3

Norm values for the investigated granites

S.No.	1	2	3	4	5	6	7	8	9	10
ap	0.15	0.19	0.19	0.15	0.19	0.19	0.23	0.23	0.13	0.13
il	0.55	0.47	0.57	0.97	0.58	0.52	0.47	0.56	0.86	0.72
or	31.95	30.33	31.22	35.47	29.87	28.25	29.54	31.87	29.49	30.52
ab	32.14	34.57	33.83	36.15	36.76	35.62	35.38	34.41	33.41	35.75
na	3.00	—	1.19	3.47	0.97	2.77	0.91	3.98	0.38	0.76
ac	3.23	3.28	5.54	3.36	3.43	2.82	3.30	1.85	3.32	3.35
mt	—	0.06	—	—	—	—	—	20.78	—	—
ht	—	—	—	—	—	—	—	—	—	—
an	—	—	—	—	—	—	—	—	—	—
cor	—	—	—	—	—	—	—	—	—	—
wo	—	—	—	0.39	0.53	—	—	—	—	—
di	4.51	3.49	4.11	4.85	6.33	6.28	6.29	4.68	6.53	6.22
en	0.78	1.22	0.84	—	—	0.44	0.27	1.40	0.19	0.70
fs	0.96	1.50	0.86	—	—	0.46	0.28	0.94	0.33	0.67
q	25.92	24.88	23.74	26.45	22.62	23.69	24.57	20.78	26.62	22.44
or %	49.85	46.73	47.99	41.34	44.83	44.23	45.51	48.09	46.88	46.05
ab %	50.15	53.27	52.01	58.66	55.17	55.77	54.49	51.91	53.12	53.95
vn %	—	—	—	—	—	—	—	—	—	—
D.I.	90.01	89.78	88.79	88.07	89.25	87.56	89.49	87.06	89.52	88.71

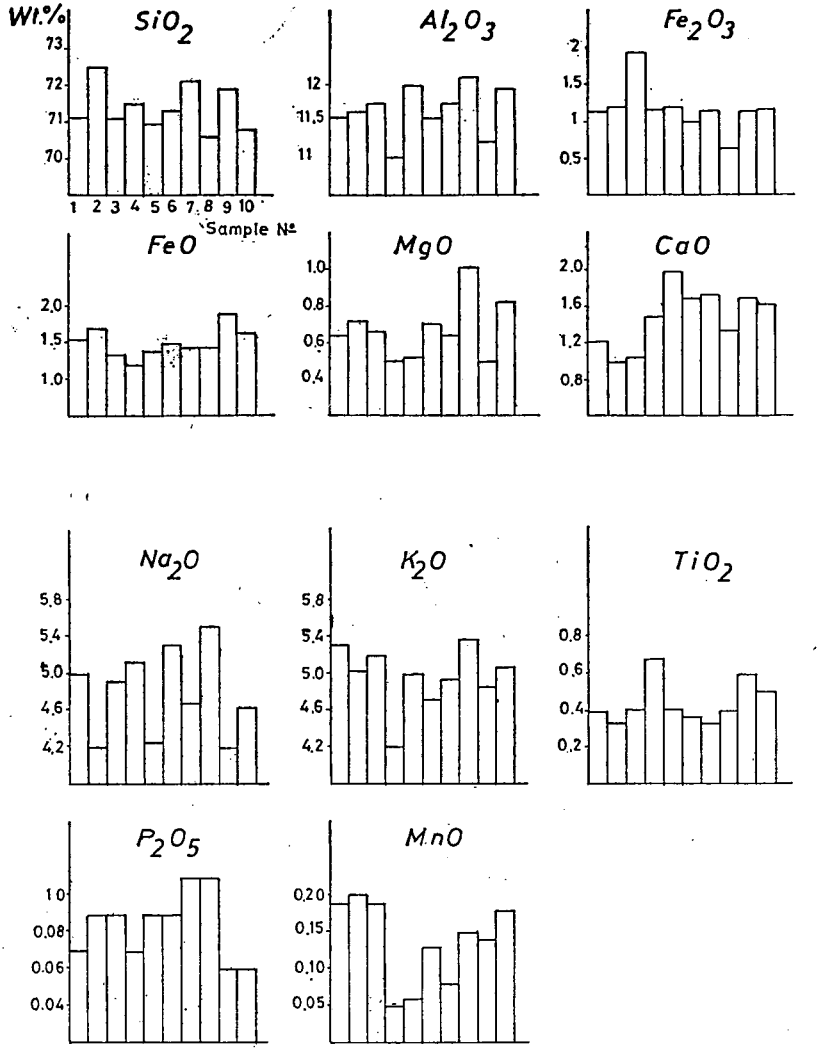

Fig. 2. Histograms showing distribution of the major oxides in the granites investigated

(all in weight percent) as a parameter for the alkalinity ratio. If silica exceeds 50% and K_2O/Na_2O is $>1<2.5$, 2 Na_2O is used in place of total alkalies. In the present work K_2O:Na_2O is not always 1 and so the alkalinity ratio is calculated as given above. The ratio has been tested on some well documented igneous suites in the form of variation diagram by plotting it versus SiO_2 on semilog scale.

The alkalinity ratios for the investigated granite samples have been calculated (Table 1), and plotted against silica *(Fig. 8)*. The diagram indicates the alkaline to peralkaline nature of the investigated granites. The alkalinity ratio ranges from 5.74 to 9.72.

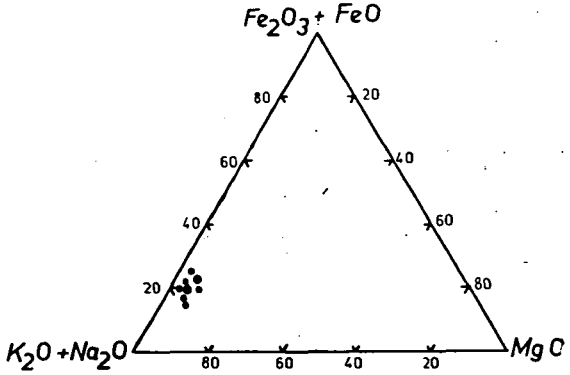

Fig. 3. AFM diagram for the investigated granites

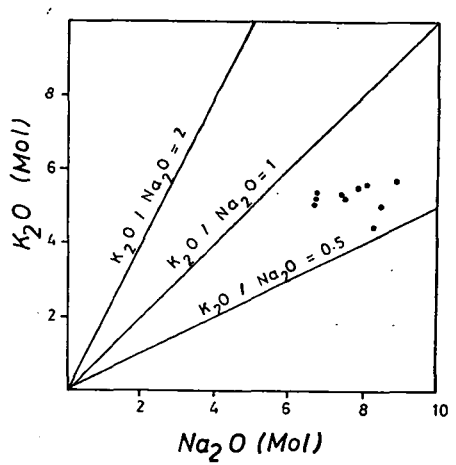

Fig. 4. Mol Na_2O *vs* Mol K_2O for the investigated granites

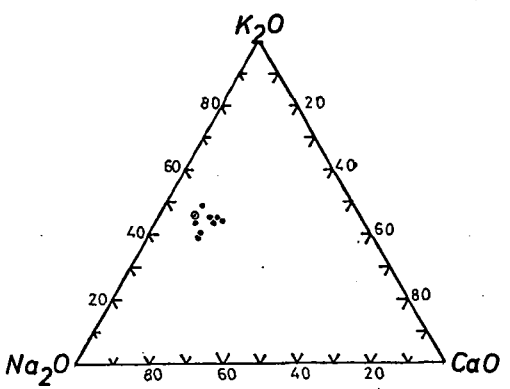

Fig. 5. K_2O—Na_2O—CaO diagram

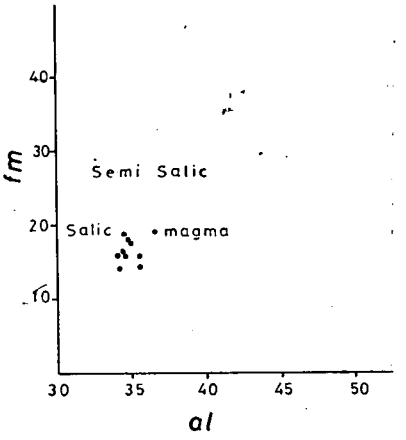

Fig. 6. fm vs al diagram of NIGGLI

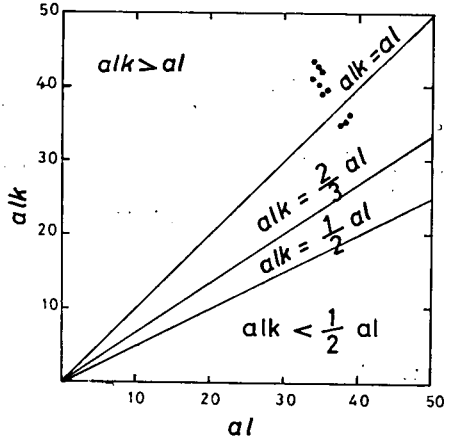

Fig. 7. alk—al diagram of NIGGLI. Classification principles of magmas after BURRI [1964]:

$alk > al$	peralkalic
$alk > \frac{2}{3} al$	relatively alkalic rich
$alk > \frac{1}{2} al$	intermediate alkali
$alk < \frac{1}{2} al$	relatively alkali poor

The peralkalinity index, the agpaitic coefficient from Zavaritski-parameters (*c.f.* BAILEY and MACDONALD, 1970) is plotted against SiO_2 to illustrate the peralkalinity nature of the post-trap granites. Accordingly the studied granites may be classified into two main groups: the agpaitic and the miaskitic types with agpaitic coefficient more or less than 1 respectively. It is clear that nearly all the studied samples are classified as an agpaitic type i.e. Mol ratio of Na_2O+K_2O/Al_2O_3 exceeds unity *(Fig. 9)*, and the excess of the strong bases has to combine with trivalent ions other than Al (e.g. Fe^{+++}) in order to form minerals like aegirine or riebeckite. RAGUIN [1965] stated that amongst the alkaline granites, the hyperalkaline granites contain less Al_2O_3 molecules than (Na_2O+K_2O) molecules, which results in the appearance of alkaline amphiboles or pyroxenes in the rock.

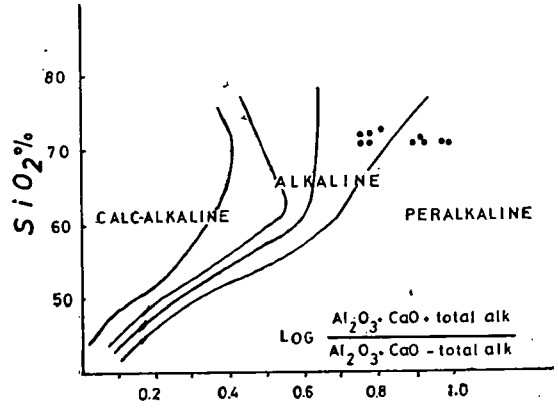

Fig. 8. Plots of calculated alkalinity rations of the investigated granites on the alkalinity variation diagram of WRIGHT [1969]

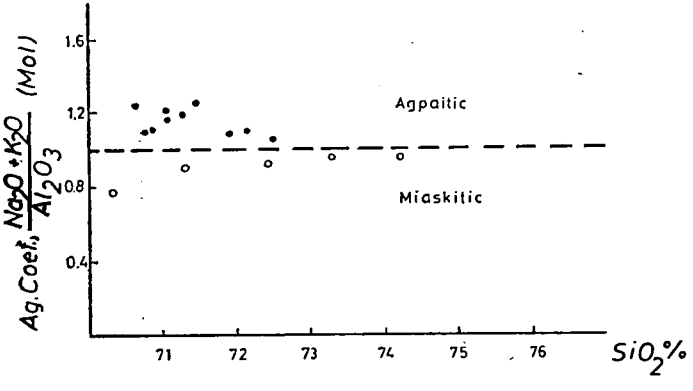

Fig. 9. The agpaitic index — silica diagram:
· Investigated granites
o Precambrian granites of Yemen

The previous observation has been confirmed by thin section study of the examined granites.

For the sake of comparison, one sample from each of five previously investigated Precambrian granitic rocks of Yemen are included in the plot *(Fig. 9)* which show the miaskitic nature of these granitic rocks.

The *T*-value is suggested by RITTMANN [1967] and GOTTINI [1968] as a solid indicator for the distribution of simatic and sialic material, where *T* is given by:

$$T = \frac{Al_2O_3 - Na_2O}{TiO_2}$$

The plot *T* value *vs.* SiO_2 *(Fig. 10)* show that nearly all the investigated granites fall in the sialic field.

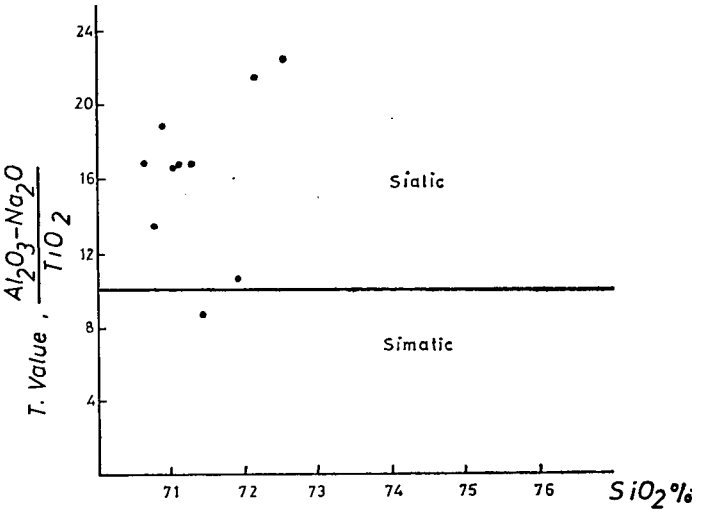

Fig. 10. *T* value *vs* SiO_2 for the investigated granites

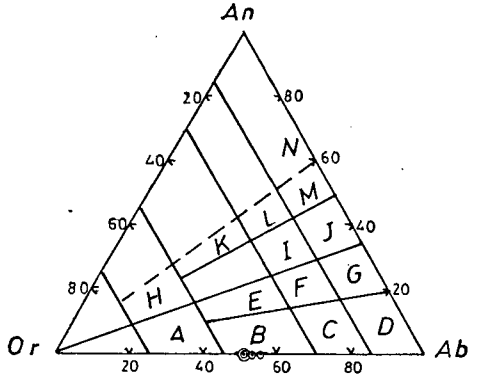

Fig. 11. Triangular diagram for *An, Ab,* and *Or* normative ratio in the investigated granites [HIETANEN, 1963].

CHEMICAL CALSSIFICATION

HIETANEN, [1963] suggested a scheme of chemical classification based on the relative abundance of the feldspars *(Fig. 11)* where *An, Or* and *Ab* are plotted in a trilinear relation.

According to this diagram the investigated granites fall within the field of granite with *Or—Ab* feldspars and *An* is almost absent.

PETROGENESIS

When plotting the ionic weight percentages of Ca, Na and K of the granites in a trilinear diagram including the suggested field for magmatic rocks [RAJU and RAO, 1974] *(Fig. 12)*, nearly all the analyses fall in the field representing granites of magmatic origin.

The normative quartz, orthoclase and albite proportions of the granitic rocks (Table 3) are plotted and the results compared with the experimental data of TUTTLE and BOWEN, [1958] *(Fig. 13)*. It is observed from *Fig. 13* that all the investigated granites have their compositions close to minimum melting point at high water vapour pressures in the $NaAlSi_3O_8-KalSi_3O_8-SiO_2-H_2O$ system.

The normative orthoclase, albite and anorthite proportions of the investigated granites (Table 3) have been plotted in a ternary diagram *(Fig. 14)*. All the plots fall around the plagioclase field, mostly close to the isobaric univariant curve, indicating the crystalliquid equilibrium was the dominant mechanism involved in the genesis of these granites [JAMES and HAMILTON, 1972].

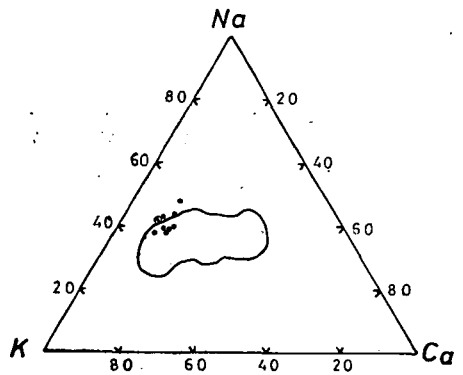

Fig. 12. Plots of Ca, Na and K proportions of the granites. The field representing granitic rocks of magmatic origin suggested by RAJU and RAO [1974] is included

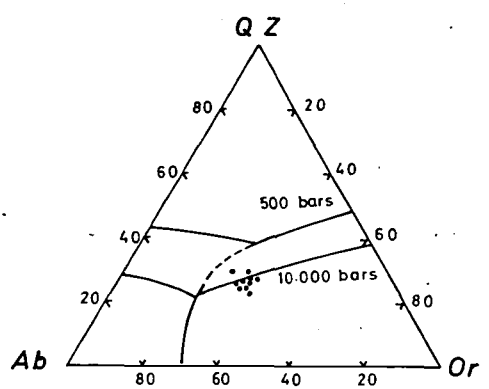

Fig. 13. Normative albite — orthoclase — quartz of the investigated granites, plotted in the system $NaAlSi_3O_8$—$KAlSi_3O_8$—SiO_2—H_2O. Field boundaries at 0.5 and 10 Kbars are shown. Dotted line represents the trace of the isobaric minimum or eutectic point at intermediate water pressures [after LUTH *et al.*, 1964]

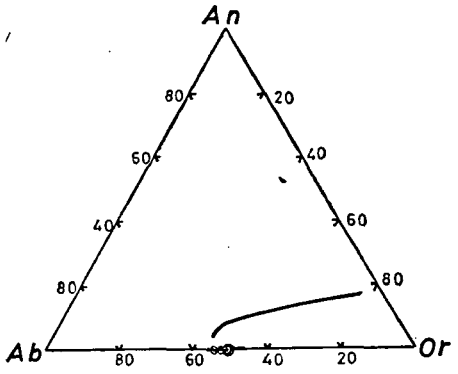

Fig. 14. Normative *Or—Ab—An* proportions for the investigated granites. The solid line represents the two feldspar boundary curve for the quartz saturated ternary feldspar system at 100 bars water pressure [JAMES and HAMILTON, 1969]

CONCLUSION

The alkaline granites of Gabal Hufash-Surdud area Yemen Arab Republic are chemically characterized. They belong to the post-trap lacolithic intrusions widely distributed in Yemen.

They are alkaline to peralkaline aegirine-riebeckite bearing and represent sialic material of magmatic origin. It is argued that crystallization proceeded under relatively high pressure conditions.

REFERENCES

BAILEY, D. K. and MACDONALD, R. [1970]: Petrochemical variations among mildly peralkaline (comendite) obsidians from the oceans and continents. Contr. Mineral. and Petrol., V. **28,** p. 340—351.

BROWN, G. F. [1972]: Arabian Peninsula Series-Map AP-2 U. S. Geological Survey.

BURRI, C. [1964]: Petrochemical Calculations. Basele (Birkhäuser Verlag), pp. 304.

GEUKENS, F. [1966]: Geology of Arabian Peninsula-Yemen. Geol. Surv. Prof. Paper **560-B**

GOTTINI, V. [1968]: The TiO_2 frequency in volcanic rocks. Geol. Rdsch., **57,** 930—935.

HIETANEN, A. [1963]: Idaho batholith near Pierce and Bungalow. U. S. Geol. Surv. Paper **344-D**

JAMES, R. S. and HAMILTON, D. L. [1972]: Phase relations in the system $NaAlSi_3O_8$—$KAlSi_3O_8$—$CaAl_2Si_2O_8$ at 1 Kilobar water pressure. Contr. Mineral. Petrol., **21,** 111—141.

KABESH, M. L. and ALY, M. M. [1979]: The chemistry of biotites as a guide to petrogenesis of some Precambrian granitic rocks, Yemen Arab Republic. Chemie der Erde (In-Press).

KABESH, M. L., ALI, M. A. and HEIKAL, M. A. [1979]: Remarks on the petrochemistry of some Precambrian granitic rocks. Yemen Arab Republic. Chemie der Erde **38,** 147—159.

LUTH, W. C., JAHNS, R. H. and TUTTLE, O. F. [1964]: The granitic system at pressures of 4 to 10 Kilobars. J. Geophys. Res., **69,** pp. 759—773.

RAGUIN, E. [1965]: Geology of granite. Interscience Publ.

REFAAT, A. M. and M. L. KABESH [1979]: The chemistry of arfvedsonites & riebeckites from Sabir alkali granites, Taiz Area, Yemen Arab Republic. Chemie der Erde **38.**

RAJU, R. D. and RAO, J. R. [1974]: Chemical distinction between replacement and magmatic granitic rocks. Contr. Mineral. Petrol., **35,** 169—172.

RITTMANN, A. [1967]: Die Bimodalität des Vulkanismus und die Herkunft der Magmen. Geol. Rdsch., **57,** 277—295.

THORNTON, C. P. and TUTTLE, O. F. [1960]: Chemistry of Igneous Rocks. I-differentiation index. Amer. J. Sci., **258**, 664—684.
TUTTLE, O. F. and BOWEN, N. L. [1958]: Origin of granite in the light of experimental studies in the system $NaAlSi_3O_8$—$KAlSi_3O_8$—SiO_2—H_2O. Geol. Soc. Amer. Mem., **74**.

Manuscript received, June 10, 1979

PROF. DR. MAHMOUD L. KABESH
National Research Center, Dokki,
Cairo, Egypt
DR. MONIR M. ALY and
DR. MOHAMED Y. ATTAWIYA
Nuclear Raw Materials Authority,
Cairo, Egypt

Acta Mineralogica-Petrographica, Szeged, XXIV/1, 41—62, 1979

PETROGRAPHY AND CHEMISTRY OF THE GRANITIC ROCKS AND THE OVERLYING NUBIAN SANDSTONES IN BIR UM HIBAL AREA, SOUTHEAST OF ASWAN, EASTERN DESERT, EGYPT

M. EZZELDIN HILMY, HAFEZ S. ABDEL WAHAB and A. A. EL-SOKKARY

ABSTRACT

The present work deals with detailed petrographic and chemical studies on the granitic rocks and the overlying Nubian Sandstones in Bir Um Hibal area, South Eastern Desert of Egypt.

Fort the first time, it is concluded that the porphyritic Aswan type granites are not only restricted to Aswan Province, but they extend further south, at least, till Bir Um Hibal area. The overlying Nubian Sandstones are proved to be "sublitharenites". They contain considerable amounts of rock fragments from different types; the most common of which are the granite, granodiorite and gneiss fragments. These Nubian Sandstones were most probably deposited in a fresh water environment. The detailed petrographical and chemical studies showed that the Nubian Sandstones of Bir Um Hibal area are submature (subgreywacke type) and were mostly derived from the pre-existing underlying basement rocks.

INTRODUCTION

Bir Um Hibal area lies in the South Eastern Desert of Egypt — latitude 23° 46′ N and longitude 33° 15′ E; being situated almost 60 km southeast of Aswan town *(Fig. 1)*.

This area was chosen for the present work because it can serve as a model to illustrate the relationship between the Nubian Sandstones, which occur in different types, and the underlying basement rocks.

As far as the authors are aware, no petrographical or chemical studies were carried out either on the Nubian Sandstones or on the underlying basement rocks, which are mainly granitic, in Bir Um Hibal area. Relatively few works on the geology of the Nubian Sandstones in the Eastern Desert of Egypt were carried out by some authors, i.e., ANDREW [1937], SHUKRI and SAID [1944], SHUKRI and EL-AYOUTI [1953], ABDEL WAHAB [1972], EL-HINNAWI *et al.* [1973] and EL-BADRY [1974].

ANDREW [1937], gave a detailed description on the Nubian Sandstones occurring in the Eastern Desert of Egypt. He pointed out that all the sandstones interposed between the fossiliferous carbonate rocks and the Precambrian are of upper Cretaceous age, in the region south of latitude 28° 40′ N. ANDREW attributed these sandstones to be either of local origin or derived from a southern source. Aswan area and the surroundings were considered by ANDREW as type localities where the relationship between the Nubian Sandstones and the underlying basement rocks can be illustrated. The Nubian Sandstones are generally underlain by a conglomeratic and irregular surface of the older rocks. A peculiar phenomenon pertaining to many of these Nubian Sandstones is the rare occurrence of pebbles of the underlying basement rocks, even in the lowermost layers of the sandstones.

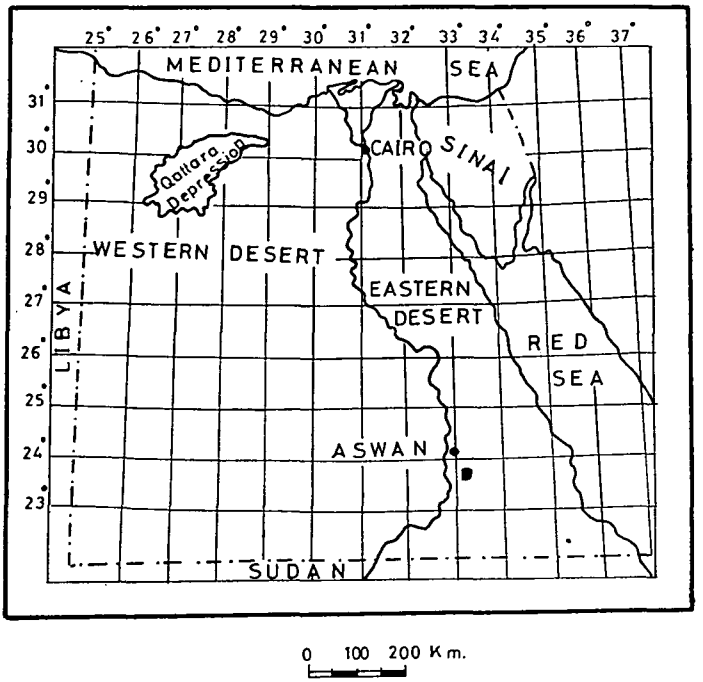

Fig. 1. Location map of the area investigated

The problem of the mode of deposition and origin of the Nubian Sandstones in Egypt has been a matter of discussion since about a century. POMEYROL [1968] has summarized most of the published views in this concern.

Regarding the basement rocks underlying the Nubian Sandstones in the investigated area, they are mainly represented by granites. As already mentioned before, no petrological or chemical studies were carried out on the granites in Bir Um Hibal area. Only some works on the regional geology, geochronology, geochemistry, and petrology of the basement rocks in Aswan province and surroundings were carried out by some workers, the most important are those of BARTHOUX [1922], HUME and HARWOOD [1925], GINDY [1954], ATTIA [1955], HIGAZY and WASFY [1956], EL-SHAZLY [1964], Hunting geology and geophysics [1967], EL-SOKKARY [1970], HASHAD *et.al.* [1972] and EL-GABY [1975].

The present paper mainly deals with the petrography and chemistry of the granitic rocks and the overlying Nubian Sandstones in Bir Um Hibal area. Also, the relationship between the two rock types is treated.

SAMPLING AND METHODS OF STUDY

Thirty two representative Nubian Sandstone samples from the different varieties were carefully collected together with sixteen granitic samples from the underlying basement rocks. It should be noted that the Nubian Sandstone samples are collected from the immediate contact with the underlying granites.

Two chips were removed from each sample, one for a thin section and the second to be stained with sodium cobalti nitrite for the determination of potash feldspar/plagioclase feldspar ratio. Of these thirty two Nubian Sandstone samples and those sixteen granitic ones, six samples from each were crushed and split for rapid rock analysis of major elements, direct-reader spectrometric analysis of trace elements and X-ray diffraction analysis of major minerals. Rapid rock analyses were performed in the Department of Mineralogy of Eötvös Loránd University, Budapest, Hungary; using the single solution wet chemical method described by SHAPIRO [1967]. Direct-reader spectrometric analyses were performed in the Department of Petrology and Geochemistry of the same University using spectrograph ISP-28 (Soviet, medium disp. with quartz optics). X-ray diffraction was carried out using Siemens Crystalloflex−4 type diffractometer with CuK_{α} radiation.

PETROGRAPHY OF THE GRANITIC ROCKS

Microscopic examination of thin sections of the granitic rocks revealed that the investigated samples are nearly of the same mineralogical composition, though of variable proportions of minerals.

Petrographical description revealed that these granitic samples are holocrystalline, generally coarse-grained and subhedral. These samples are essentially composed of potash feldspars, plagioclase feldspars, quartz, biotite and sphene. The potash feldspars include microcline, microcline-microperthite and a few orthoclase. The microcline shows a characteristic cross-hatching twinning *(Fig. 2)*. The microperthites are of the film-type and they consist of small and thin streaks of plagioclase within the potash feldspar matrix. Some orthoclase is present showing simple twinning. The microcline is cracked with occasional quartz inclusions, and it sometimes contains small patches of earlier plagioclases which are in optical continuity with each other.

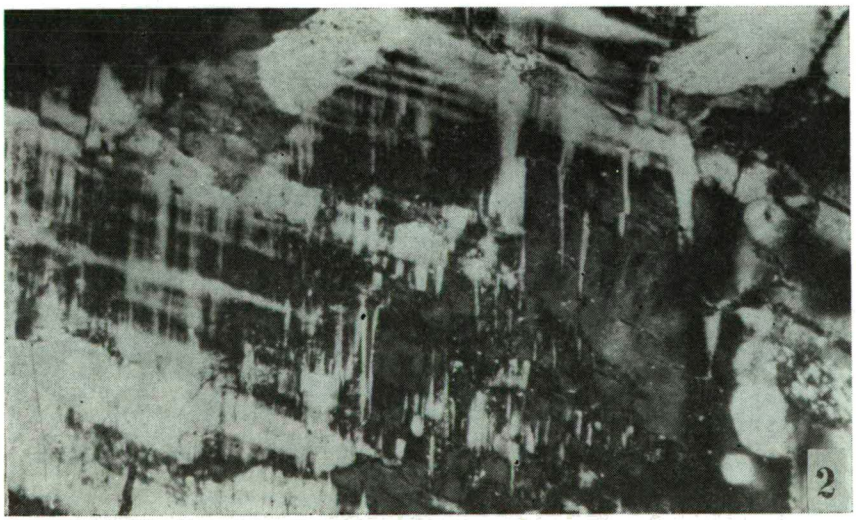

Fig. 2. Photomicrograph showing well-developed cross-hatched microcline. Crossed nicols, × 80

Plagioclase grains are mostly turbid, cracked, highly weathered and sericitized *(Fig. 3)*. It is observed that the degree of weathering in the plagioclase grains is more conspicuous at their interior parts, thus giving a sort of zoning of highly and slightly weathered bands in the plagioclase grains. Lamellar twinning is very clear, especially at the margins of the plagioclase grains and the twin lamellae are thin. The plagioclase may exhibit patchy extinction, which may indicate strain in such grains. Mostly, the plagioclase is an oligoclase. It is to be mentione that the invesigated granitic rocks are characterized by the occasional occurrence of myrmekitic exture *(Fig. 4)*.

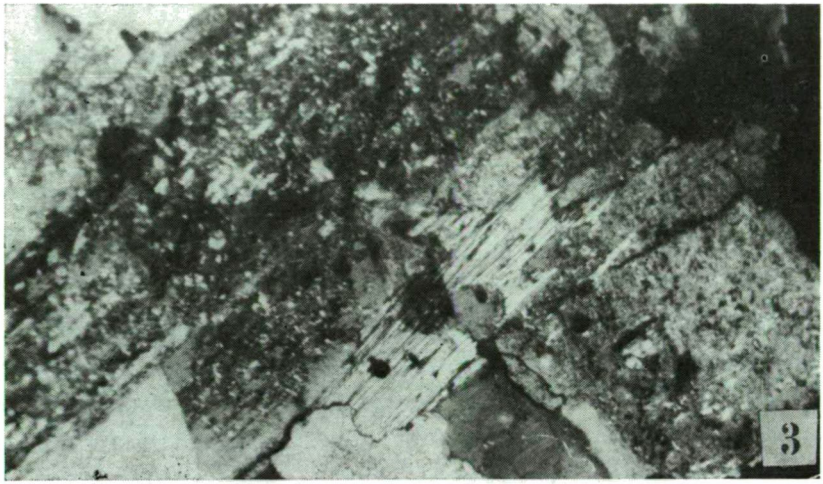

Fig. 3. Photomicrograph of intensively weathered plagioclase. The cores are more weathered. Crossed nicols, × 70

Fig. 4. Photomicrograph showing myrmekitic texture. Crossed nicols, × 54

Quartz is usually anhedral and occasionally shows strong undulose extinction. Biotite is relatively abundant and shows distinct pleochroism from yellowish brown to deep brown. Some of the biotites are partially chloritized and bent *(Fig. 5)*.

Hornblende is occasionally found in some thin sections, exhibiting its characteristic cleavage in granite *(Fig. 6)*. Accessory minerals include opaque minerals (mostly brown iron oxides), sphene with the characteristic wedge-shaped crystals, while zircon and apatite are found but to a less extent.

Modal analysis of selected six granitic samples, aided by the stained chips with sodium cobalti nitrite was carried out. The data are given in Table 1 and are illus-

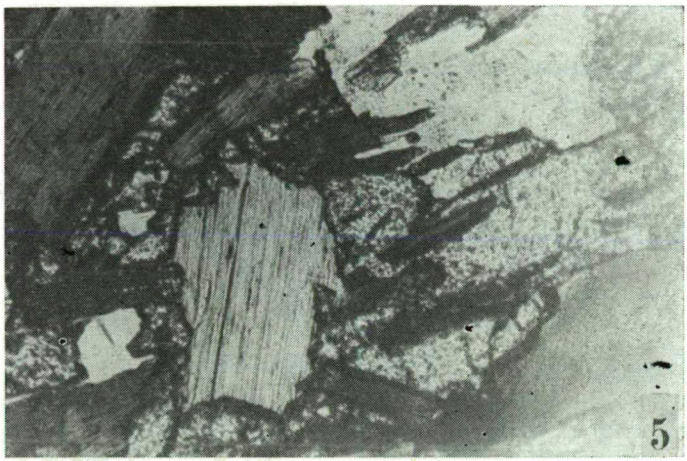

Fig. 5. Photomicrograph showing biotite flakes partially chloritized and bent.
Crossed nicols, × 54

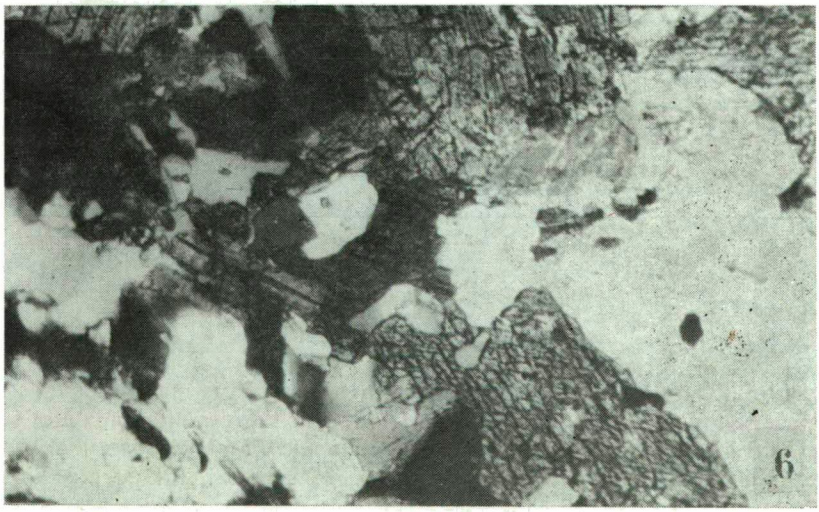

Fig. 6. Photomicrograph showing hornblende crystals with the characteristic cleavage in granite
Crossed nicols, × 80

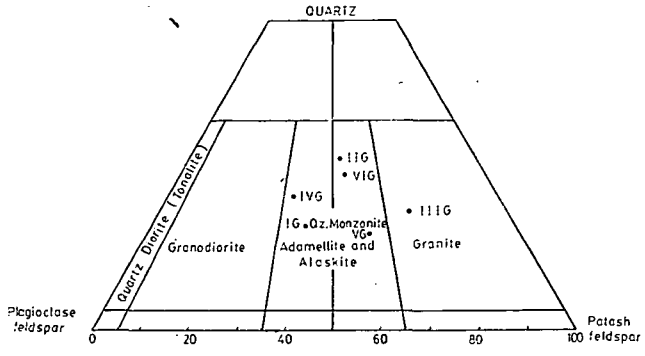

Fig. 7. Modal analysis of the studied granitic samples plotted quartz — plagioclase feldspar — potash feldspar ternary diagram

trated on quartz-plagioclase feldspar-potash feldspar ternary diagram *(Fig. 7)*. It is shown that samples I G, II G, IV G, V G and VI G fall in the adamellite field, though samples I G and IV G have granodioritic tendencies. Sample III G is of granitic composition.

It should be mentioned that the petrography of the studied granitic rocks given here is very similar to the petrography of the typical Aswan coarse granites as given by EL-SOKKARY [1970].

TABLE 1

Modal composition of the studied granitic samples

Constituent \ Sample No.	I G	II G	III G	IV G	V G	VI G
Quartz	21.83	36.56	22.22	28.13	20.96	32.94
Potash feldspar	27.71	28.04	41.62	23.18	40.13	30.15
Plagioclase feldspar	36.84	25.46	15.79	37.51	26.96	25.12
Biotite	9.50	9.80	7.00	11.00	8.02	9.40
Hornblende	—	—	10.37	—	—	—
Opaque minerals	1.24	—	—	—	—	—
Others (apatite, zircon)	0.20	0.14	0.11	0.18	1.0	0.14
Chlorite	2.20	—	2.89	—	2.93	2.25
Sericite	0.48	—	—	—	—	—

CHEMISTRY OF THE GRANITIC ROCKS

Major Elements

Table 2 illustrates the data of chemical analyses of the major elements for the six granitic samples. The data are compared with the corresponding data of the low-calcium and high-calcium granites given by TUREKIAN and WEDEPOHL [1961]. Also the data are compared with the average analysis of a typical pink porphyritic granite from Aswan [EL-SOKKARY, 1970].

It is shown that samples I G, II G, IV G, V G, and VI G are not precisely identical either with the low-calcium or with the high-calcium granites. Thus these

Chemical analysis of the studied granitic samples TABLE 2

Oxide	I G	II G	III G	IV G	V G	VI G	A	B	C
SiO_2*	71.18	71.55	61.18	73.01	70.99	70.05	74.29	67.23	70.29
Al_2O_3	12.80	13.14	18.84	11.99	12.83	13.85	13.61	15.50	13.79
Fe_2O_3	1.65	1.99	2.15	1.05	1.83	1.00	2.03	4.23	0.43
FeO	2.59	3.15	4.00	0.63	2.19	3.09	—	—	2.00
MgO	0.63	0.83	1.20	0.93	0.73	0.93	0.27	1.56	1.10
CaO	2.15	1.00	1.75	2.00	1.95	2.13	0.71	3.54	1.24
Na_2O	3.05	2.40	4.05	3.69	3.43	3.68	3.48	3.83	3.00
K_2O	4.65	5.05	5.53	4.08	5.00	4.85	5.06	3.04	6.00
TiO_2	0.63	0.43	0.70	0.87	0.67	0.46	0.20	0.57	0.60
MnO	0.05	0.06	0.03	nil	0.01	0.03	0.05	0.07	0.06
P_2O_5	0.25	0.34	0.35	0.45	0.65	0.45	0.14	0.21	0.15
Total	99.63	99.94	99.78	98.70	100.28	100.53	99.64	99.36	98.66

*: Analyst, HAFEZ S. ABDEL WAHAB
**: Represents total iron.
A: Low-calcium granite (TUREKIAN and WEDEPOHL, 1961].
B: High-calcium granite [TUREKIAN and WEDEPOHL, 1961].
C: Average pink porphyritic granite of Aswan [EL-SOKKARY, 1970].

five samples have SiO_2, MgO and CaO contents which are intermediate between the two reference granites of TUREKIAN and WEDEPOHL. K_2O and MnO are distributed according to the low-calcium granite, while Fe_2O_3, TiO_2 and P_2O_5 are distributed according to the high-calcium granite. By comparing the data of the five samples with the average analysis of the pink porphyritic Aswan granites [EL-SOKKARY, 1970], it is found that the two sets are generally in a close accordance.

Sample III G is generally conformable in chemical composition with the high-calcium granite. However, SiO_2 content is notably lower than the high-calcium granite and K_2O is much higher.

The modal analysis of sample III G indicates a high potash feldspar/plagioclase feldspar ratio, and allocates it in the granite field *(Fig. 7)*. The X-ray diffraction pattern showed this sample with a potash feldspar/plagioclase feldspar ratio less than one. This may be tentatively attributed to the micro- or cryptoperthitic nature of the potash feldspars in sample III G.

The authors are of the opinion that the potash feldspar/plagioclase feldspar ratio as given by X-ray diffraction is more reliable and more conformable with the chemical analysis. The modal analysis of sample III G with a high potash feldspar content can be interpreted on the basis that white micas and clay minerals (as intensive alteration product of plagioclase) may absorb sodium cobalti nitrite stain, thus giving rise to a false-high potash feldspar content [DEER *et.al.*, 1963]. Moreover, the high sericitization of the plagioclase in this sample may be responsible for the fixation of extraneous K_2O and consequently increase of K_2O content in sample III G.

Generally, the chemical composition of the investigated granitic samples are correlated with Aswan coarse granites and it is revealed that most of them are similar in chemical composition.

Trace Elements

Table 3 illustrates the contents of 14 trace elements (in ppm) in the six granitic samples. The data are compared with the corresponding data of the low and high-calcium granites given by TUREKIAN and WEDEPOHL [1961]. Also the data are compared with the coarse pink porphyritic granites of Aswan [EL-SOKKARY, 1970].

From trace elements point of view, the investigated granites do not follow either the low or high-calcium granites. It is found that the elements Ba, Cr, Ni, V and Cu are distributed according to the low-calcium granite, while Co and Zn are distributed according to the high-calcium granite. B and Sr take intermediate distributions between the two reference granites. This adds to the peculiar character of these granitic rocks as already revealed from the elemental distribution of both major and minor elements.

Sample III G shows enrichment in B, Zn and Sb, a matter which may be attributed to the concentration of these elements, particularly B and Zn in amphiboles which are notably abundant in this sample [see GOLDSCHMIDT, 1962].

The distribution of trace elements in the investigated granitic samples shows some similarities with those of Aswan granites, especially in the distribution of Sr, Ga, Ni, V and Cu. This again assures that the studied granites from Bir Um Hibal area are similar to the typical pink Aswan granites.

TABLE 3

Trace elements (ppm) in the investigated granites

Sample No.	B	Ba	Sr	Ga	Be	Co	Cr	Ni	V	Cu	Pb	Zn	Sb	W
I G	10	790	160	20	<10	<10	9	<10	42	10	<10	60	<160	<100
II G	12	680	180	22	<10	10	6	11	17	15	<10	130	<160	200
III G	19	750	210	15	<10	13	6	<10	15	13	<10	160	160	<100
IV G	<10	470	110	19	10	<10	5	12	40	16	30	50	<160	<100
V G	14	900	180	60	<10	10	8	<10	30	19	44	80	<160	<100
VI G	<10	600	100	25	<10	10	<3	<10	16	10	41	40	<160	<100
L.D.	10	100	100	1	10	10	3	10	10	10	10	40	160	100
A	10	840	100	17	3	1	4	5	44	10	19	39	0.2	2.2
B	9	420	440	17	2	7	22	15	88	30	15	60	0.2	1.3
C	—	1350	209	21	4	3	1	3	25	8	19	—	—	—

L.D.: Limit of detection (ppm).
—: Not detected.
A: Low-calcium granite [TUREKIAN and WEDEPOHL, 1961].
B: High-calcium granite [TUREKIAN and WEDEPOHL, 1961].
C: Average coarse pink porphyritic granites of Aswan [EL-SOKKARY, 1970].

The Nubian Sandstones in Bir Um Hibal area are generally semi-friable and friable, however, compact beds are occasionally found. These sandstones have different shades of colours; yellow, buff, grey and brown. When the thin weathered layers are removed, the sandstones appear yellowish in colour.

The Nubian Sandstones in the investigated area exhibit a number of primary structures. The most important is stratification; following the terminology of McKee and Wier [1953], the main type encountered is the tabular planar and to less extent are the dipping tabular planar and the truncated wedge cross strata types. Also, graded bedding and the asymmetrical ripple marks are recorded in some exposures.

Microscopic examination of 32 thin sections revealed that the Nubian Sandstones of Bir Um Hibal area consist mainly of quartz. Beside the quartz grains, rock fragments, feldspars, hematite, calcite, dolomite, gypsum, micas and clay minerals are found.

The roundness of the quartz grains vary from subangular to rounded. Well rounded grains are next in abundance, while angular and very angular grains are very subordinate in amount. This may be attributed to the fact that the Nubian Sandstones near the basement complex (our investigated area) represent a shoreline type of sandstone, where the sand grains were subjected to strong effects of back and forth rolling and rounding.

Generally, these sandstones are moderately well sorted and they mostly have sizes between 0.20 and 1.0 mm.

The *quartz* grains are mostly polycrystalline "composite" and to less extent monocrystalline "single". Both types may have undulose extinction *(Fig. 8)* and

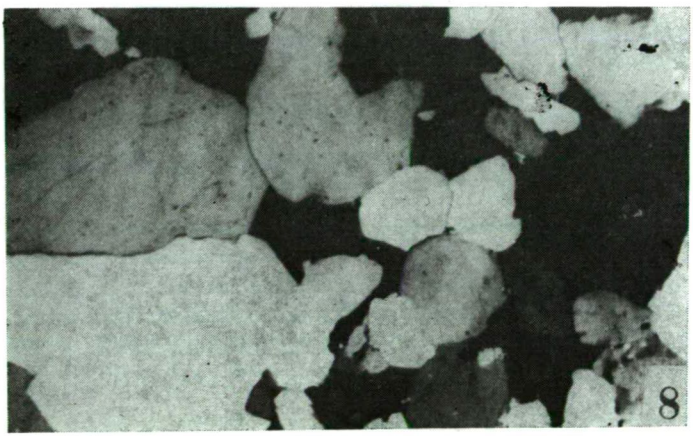

Fig. 8. Photomicrograph showing polycrystalline quartz grains with clear sutures and undulose extinction. Crossed nicols, × 56

may show overgrowths *(Fig. 9)*. The pore spaces between the quartz grains are partially and/or completely filled with a variety of matrices and cements. The most frequent are hematite, kaolinite, calcite, chert, gypsum, opal and chalcedony.

The quartz grains are mostly cemented by *iron oxides* (hematite). The irregular contact between the quartz grains and the hematitic cement indicates that the depo-

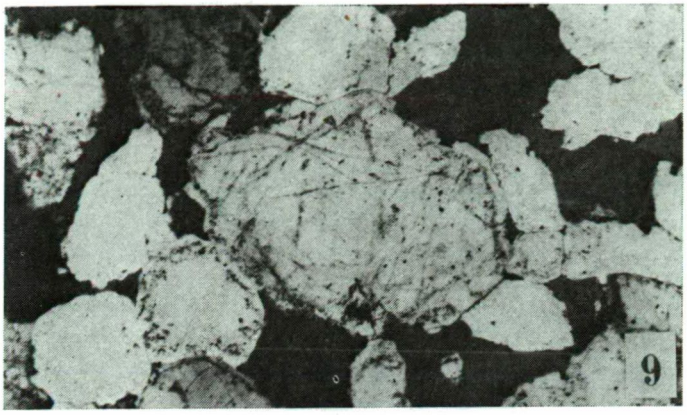

Fig. 9. Photomicrograph of silica cemented Nubian Sandstone. Quartz grains show overgrowth. Crossed nicols, × 16

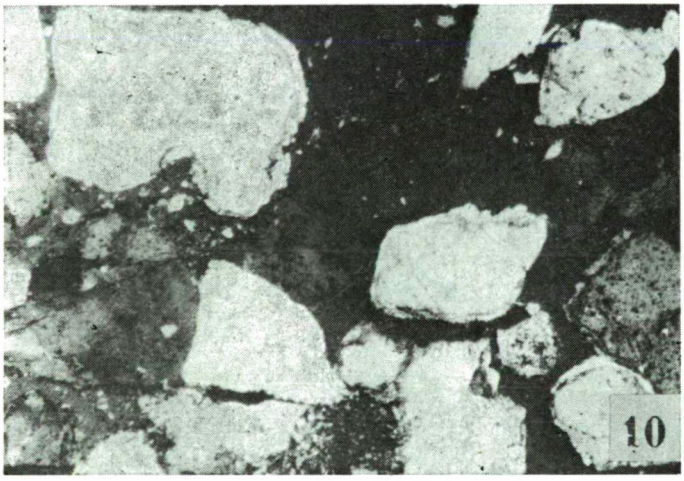

Fig. 10. Photomicrograph of Nubian Sandstone cemented by hematite. Note the irregular contact between the quartz grains and the hematitic cement. Crossed nicols, × 16

sition of the cementing material took place syngenetic or just later *(Fig. 10)*. The main source of ferric oxides in the Nubian Sandstones was in-place alteration of iron rich minerals.

Clay minerals as a matrix is mainly kaolinite (as revealed from the X-ray diffraction). The abundance of kaolinite indicates humid tropical weathering conditions in the source area [DAPPLES, 1967]. It is observed that kaolinite is usually associated with chert in the matrix between the quartz grains *(Fig. 11)*.

Carbonate cement is common in many of the studied sandstones, thus calcite and dolomite (as revealed microscopically and from X-ray diffraction) are abundant cementing materials *(Fig. 12)*.

Chert is also precipitated in the matrix thus giving rise to a cherty sandstone *(Fig. 13)*. Precipitation of chert in the matrix is an early locomorphic process [DAPPLES, 1967]. *Gypsum* has been observed partly filling the interspaces between the

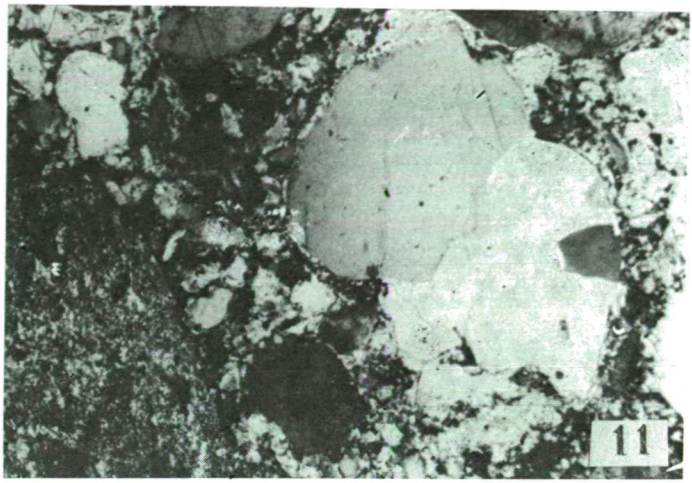

Fig. 11. Photomicrograph showing polycrystalline quartz grain together with single ones set in a hematite-kaolinite matrix. Crossed nicols, × 56

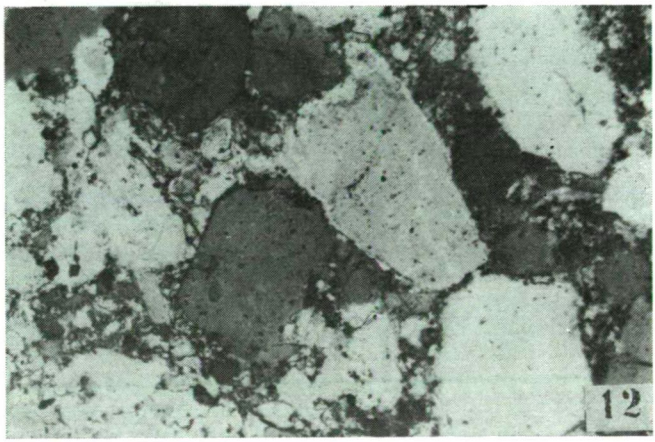

Fig. 12. Photomicrograph showing subrounded detrital quartz cemented by carbonate (calcite and dolomite) and partly by chert-kaolinite matrix. Note the sprinkled dolomite rhombs within the calcite cement. Crossed nicols, × 56

quartz grains *(Fig. 14)*. The occurrence of gypsum is to be related to evaporite conditions at the time of sedimentation or to the movement of hypersaline pore waters from an overlying evaporite formation [see, for example, MURRAY, 1964].

Opal and *chalcedony* are also observed to fill the pore spaces between quartz grains. Quartz is only found adjacent to chalcedony which always separates quartz from opal *(Fig. 14)*.

The Nubian Sandstones of Bir Um Hibal area are characterized by abundance of rock fragments (9%), mainly granite, gneiss, schist, granodiorite, chert, siltstone and quartzite *(Figs. 16* and *17)*.

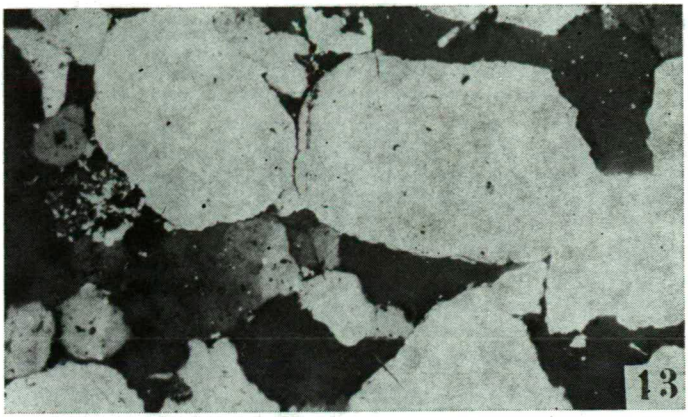

Fig. 13. Photomicrograph showing chert filling the pore spaces between the quartz grains. Crossed nicols, × 80

Fig. 14. Photomicrograph showing scattered gypsum between the quartz grains. Crossed nicols, × 24

It is found that the granitic fragments sprinkled within the lowermost horizons of the Nubian Sandstone beds are largely correlated with the underlying granitic rocks of Bir Um Hibal area. This may be taken as a proof for the derivation of these Nubian Sandstones from the pre-existing underlying basement rocks.

PARAGENETIC RELATIONS OF CEMENTING MATERIALS

It is agreed that the diagenetic modification of sands following deposition occur as progressive stages. *Redoxomorphic* (oxidation-reduction) *reactions* involving iron in particular characterize early burial. *Locomorphic changes* (cementation and mineral replacement) involving primarily silica and carbonates are typical of lithification. The *phyllomorphic stage* (authigenesis of micas and feldspars) is a late burial feature.

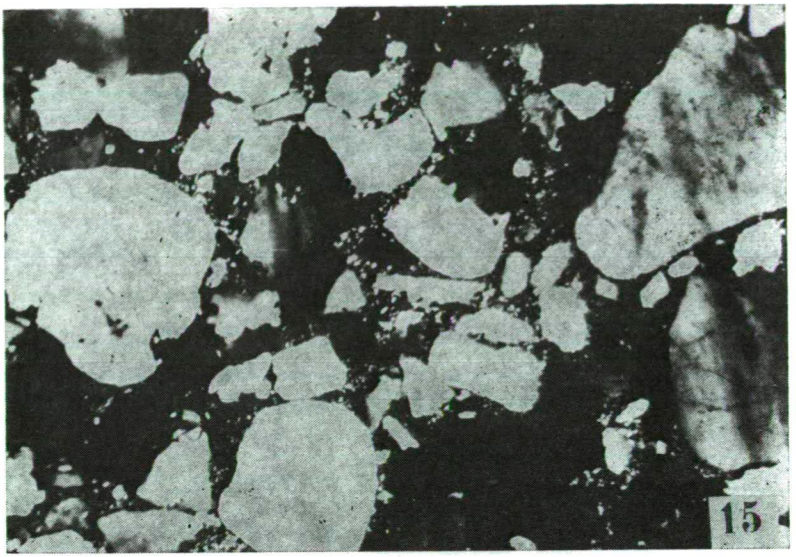

Fig. 15. Photomicrograph showing chalcedony filling the pore spaces between quartz grains; the latter are separated from opal by chalcedony. Crossed nicols, × 16

Fig. 16. Photomicrograph of Nubian Sandstone with rock fragments mainly of granite and chert. Crossed nicols, × 16

Chemical reactions which occur during each of the three stages of diagenesis result in equilibrium mineral assemblages which are considered to identify the pH and Eh of the interstitial fluids.

Petrographical studies of the Nubian Sandstones of Bir Um Hibal area showed the latter to contain different diagenetic features. The paragenetic sequence of them can be explained as in the following.

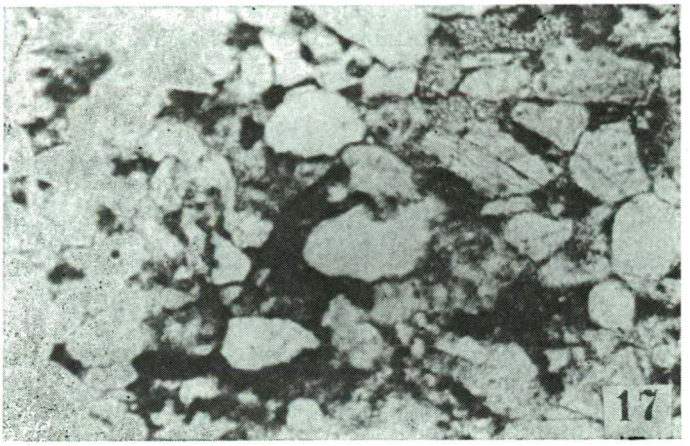

Fig. 17. Photomicrograph showing Nubian Sandstone with granodioritic rock fragments; note the occurrence of feldspars with traces of cleavage. Crossed nicols, × 16

Redoxomorphic Changes

As described in the petrographical discussion, the quartz grains are seen to be isolated or "floating" in the hematitic cement *(Fig. 10)*. This texture only originates as a result of pore filling by hematite. This situation may exist during which the burial environment is oxygenated by contact with atmosphere and iron oxides arrive as part of the detritus. In the burial environment oxygen gathers electrons principally donated by iron to form hematite and related ferric oxides or hydrates, which along with those having arrived as part of the detritus, remain stable [DAPPLES, 1967]. In some thin sections, it is observed that the matrix is composed of mixtures of clay minerals (kaolinite, as revealed from X-ray diffraction) and hematite *(Fig. 11)*, such a mixture is modified only a result of differential compaction between the sand and clay sizes.

According to DAPPLES [1967], the nature of the clay-cemented sandstones is primarily a surface film phenomenon and attains its greatest tensile strength when clay dries. Ideally, cementation of this type does not involve precipitation of mineral matter.

The source of clays in the investigated Nubian Sandstones is mostly resulted from the decomposition of feldspars in the sediment, as it is observed that some kaolinitic grains preserve the outline of the original detrital feldspar grain.

Locomorphic Changes

The reaction tendencies of the locomorphic stage can be classified as one of three types; namely: *(1)* transition from a metastable mineral phase into a more stable form primarily as a function of time; *(2)* solution of one mineral and precipitation of another as a result of change in solubilities with change in pH or temperature of permeating waters; and *(3)* shift in an equilibrium assemblage with change in pH, temperature and oxidation potential.

The unidirectional reaction: opal → chalcedony → quartz is a very good illustration of the first type. The disordered opal lattice becomes increasingly ordered in

time and is replaced by either fibrous chalcedony or chert. Once the chert is formed, the silica has achieved a relatively stable condition which is not perceptibly altered by moderate increase in pressure or temperature due to deep burial. Precipitation of chert in the matrix normally is an early locomorphic process.

Replacement of interstitial clay by chert can be taken as an event of the locomorphic stage. This may be explained by the fact that silica may be released and reprecipitated in the form of chert. Such chert is accommodated in the interstitial space by crowding or engulfing the detrital clay minerals present.

Precipitation of secondary quartz as overgrowths and filling the interstitial spaces *(Fig. 9)* can be currently attributed to the so called zones of quartz enlargement or "case hardening" of outcrop surfaces. This precipitation appears to be favoured by supersaturation of solutions bearing silica, such as develop from surface or underground waters leaching silicate rocks [see, KELLER and REESMAN, 1963].

Calcite is one of the dominant cement among the investigated Nubian Sandstones. The precipitation of calcite is directly associated with the instability of chert and quartz. Some years ago, the antipathetic reaction between quartz and calcite was attributed by CORRENS [1950] to the inverse relation in solubility with change in pH. Calcite decreases in solubility and silica becomes more soluble as the pH is elevated. The occurrence of replacement of quartz by calcite in the Nubian Sandstones of Bir Um Hibal area suggest that shift in pH is very important in this locomorphic process despite the very small differences in solubility. Also, the local changes in the partial pressure of CO_2 resulting from temperature differences near the outcrop are considered to be the direct cause of change in pH values.

In some thin sections, it is observed that the clay matrix may be replaced by calcite *(Fig. 12)*. The mechanism of such replacement is not fully understood, but it appears that the clay mineral kaolinite is flocculated by Ca-ion and occupies less interstitial pore space allowing the remainder to be filled with the precipitated calcite [see EDES and GRIM, 1960]. Within the calcite cement, it is observed that few rhombs of dolomite are sprinkled *(Fig. 12)*. It seems that the amount of available magnesium tends to be insufficient to permit the crystallization of large amounts of dolomite; and the common occurrence is in the form of individual rhombs within masses of calcite. This occurrence suggests that the dolomite may possibly represent some exsolution phenomenon rather than the result of introduction of magnesium from some outside source.

MODAL ANALYSIS

The last two decades witnessed a flow of papers on sandstone classification. Nearly 50 schemes of sandstone classifications have been proposed by different authors; a review of these schemes is given by HUCKENHOLTZ [1963], KLEIN [1963], SHUTOV [1965], OKADA [1971] and PETTIJOHN *et al.* [1973]. Most of the methods depend upon the percentage of quartz, feldspars and rock fragments in the sandstone.

The average modal analysis of the Nubian Sandstones of Bir Um Hibal area was calculated from counts made on several thin sections. The number of counts was sufficiently high to give a reasonable accuracy [see EL-HINNAWI, 1966].

The average results obtained are given in the following:

Quartz	*Feldspars*	*Rock fragments*
86%	5%	9%

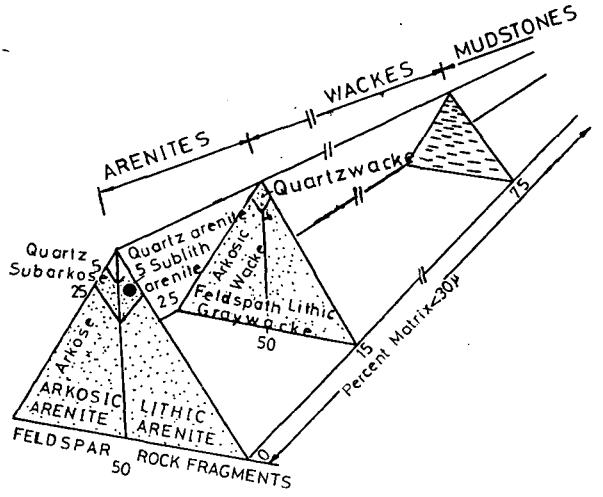

Fig. 18. Classification of terrigenous sandstones (after PETTIJOHN *et. al.*, [1973]).
● represents the Nubian Sandstones of Bir Um Hibal area

It should be noted that chert is grouped with rock fragments and not with quartz as recommended by OKADA [1971].

Applying these data to the schematic classification proposed by PETTIJOHN *et al.* [1973], the Nubian Sandstones of Bir Um Hibal area are accordingly classified as "sublitharenites" *(Fig. 18)*.

CHEMISTRY OF THE NUBIAN SANDSTONES

Major Elements

The bulk chemical composition of a sandstone is normally a function of the composition of the source rocks, the nature and maturity of the weathering processes, the effectiveness of the winnowing or washing out of the finest weathering products, the quantity and nature of the introduced cements and other changes during diagenesis and the presence or absence of biochemical or other contaminants.

In the present work, six representative Nubian Sandstone samples were chemically analysed. The results of chemical analyses are given in Table 4.

The most important chemical characteristics of the investigated Nubian Sandstones can be outlined in the following.

1. Silica percentage varies from 77.83 to 81.03. The abundance of silica content is practically valueless for any indication of the pre-diagenetic history of sandstones, as silica may be introduced during the diagenetic processes.
2. Alumina percentage varies from 7.95 to 9.18. The comparatively high content of Al_2O_3 is mainly attributed to the presence of clay minerals, micas and feldspars.
3. The presence of iron has no valuable importance as its presence is not only controlled by its provenance but largely affected by the diagenetic phases.
4. It is observed that MgO exceeds CaO in all studied samples. However, the pet-

TABLE 4

*Chemical analyses of the studied Nubian Sandstones**

Oxide	I S	II S	III S	IV S	V S	VI S
SiO_2	79.13	80.00	77.83	78.72	79.14	81.03
Al_2O_3	8.35	8.21	9.03	9.18	8.14	7.98
Fe_2O_3**	2.19	2.03	3.01	2.31	3.10	2.05
MgO	3.40	3.18	3.33	3.18	2.11	3.00
CaO	2.18	2.05	1.38	1.98	2.00	1.64
Na_2O	0.41	0.51	0.63	0.61	0.40	0.26
K_2O	0.60	0.71	0.42	0.84	0.63	0.49
H_2O^+	0.50	0.73	0.82	0.89	0.86	0.54
TiO_2	0.54	0.47	0.99	0.77	0.99	0.80
P_2O_5	0.03	0.09	0.10	0.08	0.02	0.04
MnO	0.01	nil	nil	0.01	nil	nil
CO_2	2.14	2.05	2.60	1.58	2.00	2.54
Total	99.48	100.03	100.14	100.15	99.39	100.37

* Analyst, HAFEZ S. ABDEL WAHAB.
** Represents total iron.

rographical studies revealed that calcite is the main carbonate cementing material, while dolomite is very subordinate and found only as scattered rhombs within calcite. Therefore, the abundance of Mg is not only attributed to the presence of dolomite, but largely to the alteration of ferromagnesian minerals present in these sandstones.

5. The alkali elements Na and K are mainly found in the feldspars, the Na_2O/K_2O ratio (less than 1 except sample №. III S) means that the albitization in the feldspars — if any — is of a very limited extent. This indicates that these Nubian Sandstones were not affected by later solutions bearing sodium.
6. Titanium is mainly found in clays, and in some recorded heavy minerals.

Chemically speaking, these Nubian Sandstones are generally homogeneous in chemical composition and that they are related to the "sublitharenite" [PETTIJOHN *et.al.*, 1973], after making some allowance for diagenetic effects.

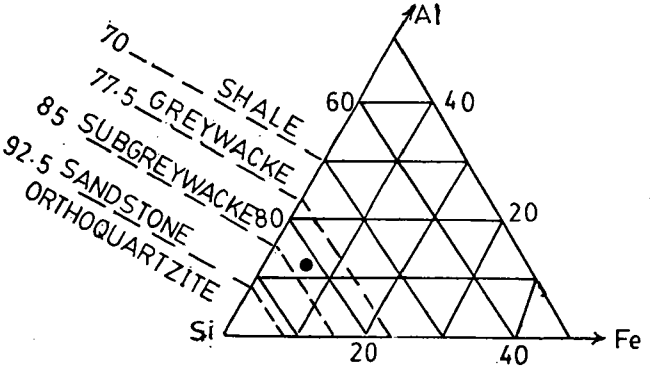

Fig. 19. Ternary plot of atomic Si—Al—Fe ratios of Nubian Sandstones of Bir Um Hibal area. ● represents the average

Fig. 19 illustrates the ternary plot of the atomic percentages of Si—Al—Fr ratios of the Nubian Sandstones in Bir Um Hibal area. From this figure it is cleae that these sandstones are submature and are of "subgreywacke" type [according to the terminology given by MOORE and DENNEN, 1970].

Is is found that the Nubian Sandstones are similar in chemical composition to those of Kalabsha area, southwest of Aswan [ABDEL WAHAB, 1976]. The slight variation in the chemical composition between them is mainly attributed to the local diagenetic processes.

Trace Elements

Table 5 gives the abundance of 14 trace elements (ppm) in the investigated Nubian Sandstones. Admittedly, trace elements data of Nubian Sandstones are quite meagre, and as such data accumulate, better understanding of this huge formation will be achieved.

Out of the reported fourteen trace elements, eleven of them, namely: B, Be, Co, Ga, Pb, Sb, Sr, V, W, Zn, and Ni are almost always below detection limit. Only Ba, Cr and Cu show variable quantities above the detection limit. It is possible to say that the studied Nubian Sandstones are depleted with respect to many trace elements.

Boron content in the investigated Nubian Sandstones is below 10 ppm which reflects a real impoverishment in this element. The source of boron may be in tourmaline grains or it may be associated with kaolinite. If it is assumed that boron is wholly attributed to the clay fraction in the present sandstones, its dropping quantities may indicate a fresh water environment of deposition [KEITH and DEGENS, 1959].

The general depletion of Ba and Sr in the present sandstones reflects the fact that they are feldspar-poor sandstones. The variable dropping quantities of Cr may be due to the presence of rare grains of chromite or it may be associated with the clay mineral (kaolinite) in these sandstones. The trace element Cu indicates that these sandstones were derived from a non-mineralized source province. The range of Cu in the Nubian Sandstones (10—21 ppm) is very close to the range of Cu content in the underlying granites (10—19 ppm).

THE RELATION BETWEEN THE NUBIAN SANDSTONES AND THE UNDERLYING GRANITES

At Bir Um Hibal area, the Nubian Sandstone lies on an irregular surface of Precambrian granitic rocks. The top part of these granitic rocks is highly weathered into kaolin, the latter is overlain by a nearly horizontal conglomeratic bed. This indicates that the granitic rocks were subjected to intensive weathering prior to the deposition of the overlying Nubian Sandstone.

The conglomeratic bed occurring at the contact between the Nubian Sandstone and the underlying granitic rocks is mainly composed of pebbles of quartz, quartzite and grit. The present authors record the occurrence of pebbles of granite, schist, gnei ss andgranodiorite disseminated within the conglomeratic bed. Also, these types of igneous and metamorphic pebbles are rarely seen to be scattered in the lowermost horizons of the Nubian Sandstone beds. The occurrence of these pebbles with this type of distribution is a very good indication to postulate that the Nubian Sandstones in Bir Um Hibal area which are submature in nature were most probably derived from the pre-existing underlying basement rocks.

TABLE 5

Trace elements (ppm) in the investigated Nubian Sandstones

Sample No.	B	Ba	Sr	Ga	Be	Co	Cr	Ni	V	Cu	Pb	Zn	Sb	W
I S	< 10	100	< 100	< 1	< 10	< 10	4	< 10	< 10	10	< 10	< 40	< 160	< 100
II S	< 10	100	< 100	< 1	< 10	< 10	7	< 10	< 10	21	24	< 40	< 160	< 100
III S	< 10	150	< 100	< 1	< 10	< 10	9	10	< 10	15	< 10	< 40	< 160	< 100
IV S	< 10	180	< 100	< 1	< 10	< 10	6	10	< 10	12	< 10	< 40	< 160	< 100
V S	< 10	100	< 100	< 1	< 10	< 10	6	< 10	< 10	10	< 10	< 40	< 160	< 100
VI S	< 10	130	< 100	< 1	< 10	< 10	6	< 10	< 10	13	< 10	< 40	< 160	< 100
L.D.	10	100	100	1	10	10	3	10	10	10	10	40	160	100

L.D.: Limit of detection.

DISCUSSION AND CONCLUSIONS

The present studies showed that the granitic rocks of Bir Um Hibal area are mainly of adamellitic composition and they are similar in the petrography to the porphyritic Aswan granites, which are considered to be an independent granitic province. The chemical analyses of both major and trace elements showed that the investigated granitic rocks have intermediate composition between the high and low-calcium granites. At the same time, they are correlated with the porphyritic Aswan granites. This led the present authors to postulate that the porphyritic Aswan granites are not only restricted to Aswan province, but they extend further south, at least, till Bir Um Hibal area.

The Nubian Sandstone beds overlying the granitic rocks are generally medium in size, moderately well-sorted and submature sandstones. The petrographical modal analysis as well as the chemical analysis allowed the classification of these sandstones as "sublitharenites". These "sublitharenites" are characterized by the presence of different types of rock fragments, mainly granite, gneiss, granodiorite, chert, siltstone and quartzite. The granitic fragments disseminated in the Nubian Sandstones are correlated with the underlying granitic rocks. This may be taken as indication for the derivation of the Nubian Sandstones from the underlying basement rocks.

The copper content in the Nubian Sandstones proves that they were derived from a non-mineralized source province. Indeed, the Cu content in the underlying granites is very close to that in Nubian Sandstones.

Concerning the possible environment of deposition of the investigated Nubian Sandstones, it is found that the dropping boron content may indicate a fresh water environment of deposition for these sandstones.

In summary, the field relations between the Nubian Sandstones and the underlying granitic rocks in Bir Um Hibal area as well as the petrographical and chemical studies of both the two rock types favour the idea that the Nubian Sandstones represent derivation products from the underlying basement rocks, similar to the Nubian Sandstones of the nearly Aswan area.

REFERENCES

ABDEL WAHAB, H. S. [1972]: The geology and mineralogy of Nubian Sandstones from Wadi Natash and Kom Ombo Districts. — Unpublished Ph. D. thesis, Fac. Sci., Ain Shams Univ, 148., p.

ABDEL WAHAB, H. S. [1976]: Chemical composition and geochemical evaluation of Nubian Sandstones of Kalabsha area, Egypt. — Acta Geologica, Hung. Ac. Sci. (in print).

ANDREW, G. [1937]: On the Nubian Sandstone of the Eastern Desert of Egypt. — Bull. Instit. Egypt, **XIX**, 93.

ATTIA, M. I. [1955]: Topography, geology and iron-ore deposits of the district east of Aswan. — Geol. Surv. Egypt. Cairo, p. 262.

BARTHOUX, J. [1922]: Chronologie et description des roches ignées du Desert Arabique. — Mem. Instit. d'Egypte, TOME **V**, pp. 200—230.

CORRENS, C. W. [1950]: Zur Geochemie der Diagenese. — Geochim. Cosmochim. Acta **17**, 53—107.

DAPPLES, E. C. [1967]: Diagenesis of sandstones. In "Diagenesis of sediments" by CHILINGAR, G. V. *et al.*, Elsevier Publ. Co., Amsterdam.

DEER, W. A., R. A. HOWIE and J. ZUSSMAN [1963]: Rock-forming minerals, Framework silicates, vol. **4**, John Willey and Sons, Inc.

EDES, J. L. and GRIM, R. E. [1960]: The reaction of hydrated lime with pure clay minerals in soil stabilization. In. "R. E. GRIM (editor), Applied Clay Mineralogy. — McGraw-Hill, New York, N. Y., p. 268.

EL-BADRY, O. M. [1974]: Sedimentology and mineralogy of the sedimentary rocks along Qena-Safaga and Qena-Quesseir roads, Eastern Desert, Egypt. — Unpublished Ph. D. thesis, Fac. Sci., Ain Shams Univ., p. 150.

EL-GABY, S. [1975]: Petrochemistry and geochemistry of some granites from Egypt. — N. Jb. Miner. Abh., **124**, 2, 147—189.
EL-HINNAWI, E. E. [1966]: Methods in chemical and mineral microscopy. — Elsevier Publ. Co., Amsterdam, p. 222.
EL-HINNAWI, E. E., KABESH, M. L. and I. ZAHRAN [1973]: Mineralogy and chemistry of Nubian Sandstones from the central Eastern Desert of Egypt. — N. Jb. Miner. Abh., **118**, 3, 211—234.
EL-SHAZLY, E. M. [1964]: On the classification of the Precambrian and other rocks of magmatic affiliation in Egypt. — Intern. Geol. Congr. India, Section 10.
EL-SOKKARY, A. A. [1970]: Geochemical studies of some granites in Egypt, U. A. R. — Unpublished Ph. D. thesis, Fac. Sci., Alexandria Univ., p. 230.
GINDY, A. R. [1954]: The plutonic history of the Aswan area, Egypt. — Geol. Mag., **91**, 484—497.
GOLDSCHMIDT, V. M. [1962]: Geochemistry. — Oxford, Clarendon Press.
HASHAD, A. H., SAYYAH, T. A., EL-KHOLY, S. and YOSSEF, A. [1972]: Rb/Sr isotopic age determination of some Egyptian granites. — J. Geol. Egypt **16**, 255.
HIGAZY, R. A. and WASFY, H. M. [1956]: Petrogenesis of granitic rocks in the neighborhood of Aswan, Egypt. — Bull. Instit. Désert d'Egypte, Tome VI, No. 1. pp. 209.
HUCKENHOLTZ, H. G. [1963]: Der gegenwärtige Stand in der Sandstein Klassifikation. — Fortschr. Miner., **40**, 151.
HUME, W. F. and HARWOOD, H. F. [1925]: Notes on some analysis of Egyptian igneous and metamorphic rocks. — Geol. Magazine, vol. **LXII**, No. 727.
Hunting geology and geophysics [1967]: Assessment of the mineral potential of the Aswan region, U.A.R.
KEITH, L. L. and DEGENS, E. T. [1959]: Geochemical indicators of marine and fresh water sediments; in "Researches in geochemistry", edited by PHILIP H. ABELSON, John Wiley and Sons. Inc.
KELLER, W. D. and REESMAN, A. L. [1963]: Dissolved products of artificial silicate minerals and rocks. — J. Sediment. Petrol., **33**, 426—438.
KLEIN, G. DEVRIES [1963]: Analysis and review of sandstone classification in north American geological literature, 1940—1960. — Geol. Soc. America Bull., **74**, 555.
MCKEE, E. D. and WEIR, G. W. [1953]: Terminology for stratification and cross-stratification. — Geol. Soc. America Bull., **64**, 381.
MOORE, B. R. and DENNEN, W. H. [1970]: A geochemical trend in silicon—aluminium—iron ratios and the classification of clastic sediments. — Jour. Sed. Petrology **40**, 1147.
MURRAY, R. C. [1964]: The origin and diagenesis of gypsum and anhydrite. — Jour. Sed. Petrology **34**, 512.
OKADA, H. [1971]: Classification of sandstone; analysis and proposal. — J. Geol., **79**, p. 509.
PETTIJOHN, F. J., POTTER, P. E. and SIEVER, R. [1973]: Sand and sandstone. — New York; Springer—Verlag, 618 p.
POMEYROL, R. [1968]: "Nubian Sandstone". — Am. Assoc. Petroleum Geologists Bull., **52**, 589.
SHAPIRO, LEONARD [1967]: Rapid analysis of rocks and minerals by a single — solution method. — U.S. Geol. Survey Prof. Paper **575-B**, p. B 187-B 191.
SHUKRI, N. M. and R. SAID [1944]: Contribution to the geology of the Nubian Sandstone. Part I: Field observations and mechanical analysis. — Bull. Fac. Sci., Cairo Univ., **25**, 149.
SHUKRI, N. M. and M. K. EL-AYOUTI [1953]: The mineralogy of the Nubian Sandstone in Aswan. — Bull. Instit. Desert, Egypt, **III**, 65.
SHUTOV, V. D. [1965]: Review and analysis of mineralogical classification of arenaceous rocks (in Russian). — Litologyia i Poleznie Iskopaemie, n. **1**, p. 95.
TUREKIAN, K. K. and WEDEPOHL, K. H. [1961]: Distribution of the elements in some major units of the earth's crust. — Geol. Soc. Amer. Bull., **72**, 175—192.
Manuscript received, March 1, 1979

M. EZZELDIN HILMY,
HAFEZ S. ABDEL WAHAB
Department of Geology,
Faculty of Science,
Ain Shams University

A. A. EL-SOKKARY
Department of Geology,
Nuclear Raw Materials Establishment,
Cairo

Acta Mineralogica-Petrographica, Szeged, XXIV/1, 63—90, 1979

SYNTHESIS OF Mn, Fe, Ni, Co OXIDE-HYDROXIDE PHASES ON MANGANESE OXIDES: ON A MODEL FOR TRANSITION METAL ORE FORMATION IN RECENT BASINS

I. M. VARENTSOV, N. V. BAKOVA, YU. P. DIKOV, T. S. GENDLER, and R. GIOVANOLI

ABSTRACT

Experimental data are presented on the sorption dynamics of the dissolved forms of Ni, Co, Mn, Fe from seawater by manganese oxides (Mn_3O_4). The study of the initial sorbent and final products by scanning microscopy, X-ray photoelectron spectroscopy, X-ray analysis has revealed that these components accumulate in the form of a newly-formed sorbed layer. The process is of a multistage nature. The initial stages are characterized by the development of ion-exchange and hydrolytic reactions, and the later ones by the interface autocatalytic oxidation of the components accumulated. The composition of the newly-formed compounds is controlled by the kinetics of the two basic stages, viz.: a) sorption proper; b) interface catalytic oxidation.

The highest oxidized forms of the metals accumulated are observed at the relatively lower sorption rates, when the blocking effect of the first stage does not inhibit the development of the second stage. For instance, during the final experimental runs, at the relatively lower sorption rates, the external parts of the newly-formed layer show fairly large amounts of oxidized forms (%): $Mn^{4+}=60$, $Ni^{3+}=30$, $Co^{3+}=30$. Iron, as evidenced by MÖSSBAUER spectroscopy, is present within the sorbed layer as $FeOOH \cdot H_2O$.

The specific feature of the sorption of metals by hydrous manganese oxides is a partial interaction of Ni and Co with structural Mn^{2+} and Mn^{3+}. As a results of this interaction, Mn is displaced from the substrate into the solution in an amount equivalent to 16.14% of the sorbed Co or 17.96% of the sorbed Ni.

The results presented together with a survey of the existing situation in the experimental field relating to the problem under study support the validity of an earlier model describing formation of the transition metal ore accumulations in recent basins. According to this model, the process is a multistage chemisorption interaction in which the main role is the interface autocatalytic oxidation of the sorbed metals.

INTRODUCTION

There are two principal and widely occurring types of ores in the World Ocean, viz. ferromanganese nodules and metalliferous sediments. The ferromanganese nodules of certain oceanic regions are presently regarded as high-grade ores of Mn, Ni, Co, Cu and other metals.

Notwithstanding the sharply differing views as to the genesis of Fe—Mn nodules, the data available enable the majority of investigators to believe that their formation is associated with the process of the extraction of metals from the component-bearing solutions [ANDRUSCHENKO and SKORNYAKOVA, 1967; BEZRUKOV *et al.*, 1976; VARENTSOV, 1972, 1976; VARENTSOV *et al.*, 1978; VERNADSKY, 1954; PRONINA and VARENTSOV, 1973; PRONINA *et al.*, 1973; SKORNYAKOVA, ANDRUSCHENKO, 1970; STRAKHOV, 1976; BURNS, 1976; BURNS, BURNS, 1975, 1977; GLASBY, 1974; GOLDBERG, 1954, 1961; GOLDBERG, ARRHENIUS, 1958; LALOU *et al.*, 1973, 1976; MICHARD,

1969; MURRAY, 1974, 1975 *a, b;* RENARD *et al.,* 1976; VAN DER WEIJDEN, 1976 *a, b;* VARENTSOV and PRONINA, 1973, 1976].

For the large deposits of Fe—Mn nodules, such a metal-bearing solution is seawater, usually bottom water, where the trace amounts of transition metals are present in a solute form [ROBERTSON, 1968, 1970; SCHUTZ and TUREKIAN, 1965; BREWER, SPENCER, 1974; MURRAY and BREWER, 1977; SLOWEY and HOOD, 1971; SPENCER and BREWER, 1969; SPENCER *et al.,* 1970].

J. MURRAY [1887] and F. CLARKE [1924], (both cited by VERNADSKY, 1954), and V. I. VERNADSKY [1954] paid attention to the fact that concentration of Mn, Fe and other transition metals in the World Ocean does not show any increase, despite their uninterrupted supply from the endogenous and exogenous sources. Considering these facts, V. M. GOLDSCHMIDT [1937] assumed that sorption is the main process responsible for the removal of these metals from seawater. Later, at the beginning of extensive geochemical studies of the Ocean, GOLDSCHMIDT's ideas were advanced by GOLDBERG [1954] and KRAUSKOPF [1956, 1957]. Emphasizing a high sorption activity of hydrous ferric oxides, GOLDBERG and ARRHENIUS [1958] suggested that the sorption of heavy metals from seawater by this sorbent is an autocatalytic process. However, no evidence for the nature of this process has been suggested by the authors.

The processes of the extraction of microamounts of transition metals from seawater by hydrous ferric and manganese oxides is characterized by extremely low rates of reactions [LALOU *et al.,* 1973, 1976; KU, 1977]. Investigations into the individual components of the nodule formation in the Oceans (nodules seawater; associated sediments; specificity of the metal sources, etc.) permit only a rough assessment of the processes and indirect judgement on its mechanism to be made.

Investigations under way during the last two decades by researchers in the various branches of chemistry and geochemistry into the sorption of transition metals from the solutions of complex electrolytes by the hydrous oxides of Fe, Mn and other metals have significantly advanced the ideas of the intrinsic aspects of these processes. The principal results of these investigations are summarized as follows.

1. *Sorbed metal concentration and composition in solution*

Investigations into the processes of heavy metal sorption by hydrous ferric oxides in the ocean basins demonstrate that they occur in a wide range of concentrations the lower boundary being defined by the solubility products of the final products.

It is not uncommon, however, that determination of the lower concentration limit does not give reliable results because of the complex-formation phenomena.

Of particular importance to these investigations is the problem of sorption specificity in the region of relatively low (10^{-1} to 10^{-2} μg/l) and relatively high (over 10^3 μg/l) concentrations. It is shown in a number of works [CHUYKO *et al.,* 1974; KURBATOV *et al.,* 1951; TEWARI *et al.,* 1972; VARENTSOV and PRONINA, 1973] that in the region of relatively low concentrations, the ion-exchange nature of the sorption of heavy metals by hydrous ferric and manganese oxides is not so important as at higher concentrations.

At relatively low concentrations (under 10^{-4} μM), the sorption of Co and Zn is not described by the LANGMUIR equation, whereas K and Na follow this equation over a wide concentration range.

2. *Composition and concentration of the background electrolyte components*

Natural environments where the sorption of heavy metals by hydrous manganese and ferric oxides takes place represent complex solutions of electrolytes with a considerable content of alkaline, alkaline-earth cations and also chloride, sulphate and hydrocarbonate anions. Seawater is a vivid example of such a natural electrolyte. BEEVERS [1966], IDZIKOWSKI [1971, 1972 *a, b,* 1973], NOVIKOV [1972] NOVIKOV and GONCHAROVA [1972, 1977 *a, b*] have indicated that the sorption of some heavy metals (Zn(II), Pb(II), Co(II), Cd(II), Cu(II), Ag(II) and others) by hydrous ferric oxides shows a significant increase with the content of the background electrolyte components. In the case of Na, K, Mg sulphate solutions sorption proceeds at a rate several times (by a factor of about 3) as great as compared with nitrate and chloride solutions of equivalent ionic strength. This effect is interpreted by NOVIKOV [1972] as being due to the ionic hydration of "neutral" salts, being present in solution in significant concentrations, and to the associated increase in the effective concentration of the sorbed component, increase in its polymerization (a salting-out effect), which results in higher sorption at the same pH's. In acidic medium the increase in the background salt concentration leads to lower sorption.

In the case of the transition metal sorption by manganese oxid-hydroxide no significant effect of the background salt components in the pH interval 6—8 has been observed [TEWARI *et al.*, 1972]. The competitive influence of Na^+, Mg^{2+}, Ca^{2+}, manifesting itself in a substantially lower sorption as exemplified by Co, has been observed for the concentrations of these elements corresponding to their amounts in seawater at a Co content of $1 \cdot 10^{-7}$ M in a wide range of pH's: 2—10 [MURRAY, 1975 *b*].

3. *Special features of phase composition, structural and surface characteristics of hydrous ferric and manganese oxides*

Investigations by SIPALO-ŽULJEVIĆ and WOLF [1973] have revealed that La(III) and Co(II) are equally sorbed both by a newly-formed oxide hydroxide in the solution of these components and by a substantially crystallized variety. The only differences are sorption rates. The authors not only point to a surface nature of the process but also stress an important role of the sorbed cation penetration into the sorbent structure.

Results obtained by ANDERSON *et al.* [1973] suggest that sharp differences in the crystallinity of the two MnO_2 modifications (birnessite, δ-MnO_2, and pyrolusite, β-MnO_2) used as sorbents affect only the time of reaching silver equilibrium concentration and not the sorption capacity.

4. *Special features of heavy metal sorption by hydrous ferric and manganese oxides in various pH, Eh intervals and dissolved O_2 concentrations*

Considering the role of such parameters as pH, Eh and dissolved O_2 concentration, in studying the processes of heavy metal sorption by hydrous manganese and ferric oxides, it is significant that conditions in the interface zone differ most significantly from those taking place in a solution mass.

GABANO *et al.* [1965] suggested a model of heavy metal sorption on MnO_2. The authors believe that the surface charge of MnO_2 is governed by the pH of the solution. In the pH interval characteristic of natural waters (pH 5—11) the hydrated manganese dioxide is negatively charged. These ideas are shared by POSSELT *et al.*

[1968]. However, POSSELT *et al.* admit the possibility of the contact oxidation Mn(II)→Mn(III) to account for a high sorptive capacity of Mn(II) as compared with some other ions: Ag(I), Ba(II), Ca(II), Mg(II), Nd(III), Sr(II).

It has been found by some invetigators [BALZANOVA *et al.*, 1977; CHUYKO *et al.*, 1974; DUSHINA, ALESKOVSKY, 1976; SIPALO-ŽULJEVIĆ, WOLF, 1973; DUVAL, KURBATOV, 1952; TEWARI *et al.*, 1972; ANDERSON *et al.*, 1973] that the sorption of heavy metals, particularly those subjected to hydrolysis, increases markedly with increasing pH up to a certain value. At relatively low pH's the phenomena of sorption are regarded as ion exchange between H^+ from the sorbent OH-group and sorbed ion. At alkaline pH's the authors consider hydrolysis to be the main sorption factor. However, as a result of studying Ag sorption by various MnO_2 modifications, ANDERSON *et al.* [1973] emphasize particularly that these phenomena cannot be explained in terms of "surface sorption". The sorption of Ag involves exchange with H^+, foreign ions of the sorbent structure and structural Mn(II) proper.

5. *Relationships between molecular sorption and ion exchange; interaction with the structural ions of oxide hydroxides; chemical reactions within the interface zone in the process of heavy metal sorption by hydrous oxides.*

It was noted in the preceeding Section that the observed behaviour of heavy metal sorption by hydrous oxides can only partially be described by ion-exchange or molecular sorption models.

MURRAY and BREWER [1977] evaluated the relationship between specific (chemical) adsorption, electrochemical adsorption (Coulombic type) and solvation adsorption. Experimental determination of the separate influence of each of these adsorption types presents great problems. Evaluation of the relative contribution of each sorption type is largely performed by calculations using a number of theoretical models. The simpliest case is that of ion adsorption in which the number of the ions adsorbed cannot exceed a value equivalent to a surface charge. It is shown experimentally [MURRAY, 1975 *a, b*] that alkaline metal ions (Na^+, K^+) interact with a hydrous surface oxide only electrostatically. Transition metal ions are sorbed by manganese dioxide more intensively as compared with alkaline and alkaline-earth ions

$$(Na = K < Mg < Ca < Sr < Ba < Ni < Zn < Mn < Co).$$

The ions whose sorption intensity increases markedly with pH are only partly and with differently desorbed with decreasing pH. Such a prominent sorption selectivity on hydrous metal oxides is attributed to their specific (chemical) sorption.

STUMM *et al.* [1976] reviewed the existing models describing the interaction of metals with the surface of oxide-hydroxides. Considering the dependence of the sorption of monomeric metal forms by oxide-hydroxides on pH, these authors did not think it necessary to resort to hydrolysis phenomena. They believed that such a dependence may be interpreted in terms of variation in the basicity of the surface MeO^--groups and chemical affinity of these groups for the sorbed metal ion.

It is shown by NOVIKOV [1972] and NOVIKOV, GONCHAROVA [1972; 1977*a, b*] that the existing numerous ideas of the chemical nature of sorption and coprecipitation of transition and other metal microamounts by hydrous oxide-hydroxides can not provide adequate explanation of the experimentally observed results. These authors propose a model of "coordination coprecipitation and sorption", relying on the formation of various bonds in the system "hydrous oxide-sorbed component".

JAMES *et al.* [1975] considered the various models of metal ion sorption at the hydrous oxide/solution interface and concluded that none of the models reported

is completely satisfactory. The authors note that the observed increase in metal sorption from 0 to 100% in the narrow pH interval can be explained by the formation of hydroxo-complexes. But it is not uncommon that the sorption of metals takes place from solutions with such pH's that only a small proportion of the total amount of metal aquo-compounds is available in the form of soluble hydroxo-complexes. Clarification of the true mechanism of the process is most difficult because of experimental problems and assumptions in the writing down of the reaction schemes. The authors place particular emphasis on the fact that their model of the formation of aquo-hydroxo-complexes [JAMES and HEALY, 1972 *a, b, c;* JAMES *et al.,* 1975] does not make it possible to reveal unequivocally the significance of the participating mechanisms (ion exchange, surface hydrolysis, hydrolysis and specific adsorption of hydrolysis products).

EGOROV [1975] introduced the idea of peptizing, oxy-acidic, hydroxo-complex sorption mechanisms. Ion exchange does not exclude chemisorption interaction which forms the basis of the author's model. JU. V. EGOROV stressed that "primary sorption" implies the effect of completing the solid phase by the sorbed ion and its structural incorporation into the sorbent.

MCKENZIE [1970, 1972] has significantly broadened the ideas of heavy metal sorption by hydrous manganese oxides. This author shows that in the sorption of Co, Cu, Ni by hydrous manganese oxides from chloride solutions at pH 5 the process runs in two stages: 1) rapid sorption of metal ions ($Cu > Co > Ni$) accompanied by the displacement of the exchange ions H^+, K^+, Mn^{2+} from the surface; 2) Co(II), upon sorption, interacts with structural Mn(III). In this case redox reactions take place: $Co(II) \rightarrow Co(III)$; $Mn(III) \rightarrow Mn(II)$, accompanied by the release of Mn into solution. The possibility of these reactions is attributed to the differences in the magnitudes of the Crystal Field Stabilization Energy for these elements.

LOGANATHAN and BURAU [1973] have further advanced the ideas of MCKENZIE. Their works have been refined by MURRAY [1975 *a, b*] showing that no more than 10% of the sorbed Co can be associated with Mn released into the solution from a manganese dioxide as the sorbent. MCKENZIE's ideas [1970, 1972] have been advocated by RENARD and MICHARD [1973] for Pacific manganese nodules.

GIOVANOLI *et al.* [1969, 1976 *a, b*] [GIOVANOLI and STÄHLI, 1970; GIOVANOLI, 1976] have studied a number of transition metal sorption problems by using hydrous oxides to study natural processes. It has been established that the ions of divalent transition metals can enter into the structure of the 10 Å-modification of MnO_2, i.e. buserite (todorokite), promoting the enhancement of crystalline lattice stability of this compound.

A number of geochemical works [GOLDBERG, 1961; HEM, 1963, 1977; MORGAN and STUMM, 1965; STUMM and MORGAN, 1970; MURRAY *et al.,* 1968; MICHARD, 1969; MCKENZIE, 1975; BURNS, 1965, 1976; BURNS and BURNS *et al.,* 1975] have shown that the sorption of Mn, Co and other transition metals by hydrous oxides occurs over a wide concentration range typical of seawater and involves the interface oxidation of the sorbed metals. No experimentally supported model describing the interaction mechanism has been presented by these workers.

It can be concluded from the brief survey of the above studies that most authors note inadequacy of existing models for the explanation of the observed phenomena of sorption interaction between microamounts of metals and hydrous oxides. The reason for such an inadequacy lies in a fragmentation of the studies conducted, inconsistency of the assumptions adopted, problems encounted in the identification of

the system component, starting with a form of the sorbed component, through hydrated metal monomers and polymers of low and high molecular weight compounds up to the colloidal-crystalline hydrous oxides and oxides.

Our studies [PRONINA and VARENTSOV, 1973; PRONINA, VARENTSOV *et al.*, 1973; VARENTSOV, DIKOV *et al.*, 1978; VARENTSOV and PRONINA, 1973, 1976] on the sorption of Mn, Fe, Ni, Co and synthesis of the hydroxide phases of these metals on hydrous ferric and manganese oxides have permitted some of the special features of the process mechanism to be evaluated. High selectivity of the sorption of thes metals from seawater has been established. The initial stages of the process are of an ion exchange nature, largely for Ni, and to a lesser extent for Co, Mn, Fe. At the later stages one can observe the development of nonexchangeable forms of these metals represented by hydroxide phases. The study of the compounds formed on the hydrous ferric oxides (γ-FeOOH) using X-ray diffraction analysis and X-ray photoelectron spectroscopy has made it possible to identify the composition of the newly-formed compounds and to evaluate the accumulated metal valencies. It has been found that in this complex multistage interaction the major role is played by a chemisorption, involving autocatalytic oxidation, of these transition metals. The composition of the resulting phases is to a large extent controlled by the quantitative relationships of the accumulated components in solution and kinetic parameters.

It is the purpose of the present paper, based on experimental studies, to show the principal parameters of the sorption of Mn, Fe, Ni and Co from seawater solution by hydrous manganese oxides, to identify the composition of the newlyformed compounds, to assess the relative role of the factors controlling these processes and possibilities of the extrapolation of the results obtained to develop a model of ore formation in recent basins.

MATERIALS AND METHODS

We used in our experiments as the oxide phase a synthetically obtained hausmannite — Mn_3O_4 as the oxide phase. This sorbent was synthesized in laboratory conditions using the method of MCKENZIE [1971]. The sorbent obtained was identified by X-ray powder diffraction and electron diffraction methods supported the existence of a homogeneous hausmannite phase (see *Fig. 7*). The role of hausmannite in

Dynamics of the sorption synthesis of Fe, Mn, Ni, Co compounds under

No. of runs	Initial concentrations in solution (μg/l)				Final concentrations in solution (μg/l)				Amount of element sorbed from solution (μg/l)			
	Ni	Co	Fe	Mn	Ni	Co	Fe	Mn	Ni	Co	Fe	Mn
1	1640	1580	1320	700	910	938	864	552	730	642	546	148
2	1500	1540	1000	600	995	927	492	396	505	613	508	104
3	1420	1600	1360	400	980	857	805	342	440	743	555	58
4	1280	1360	960	500	811	894	665	624	469	466	295	−124
5	1060	1320	1540	620	885	935	7	703	175	385	1533	−83
6	1140	1260	1000	630	847	934	575	790	293	326	425	−160
7	1000	1000	940	565	600	850	0	1015	400	150	940	−450

* Volume of the solution = 5 l, time of interaction = 72 hours, weighed amount of the sorbent = $\%\ Me_{s.\,ph.} = \frac{Me}{0.3 + Ni + Co + Fe} 100\%$. Me = amount of the sorbed metal (Ni, Co, Fe, in g).

the geochemistry of the processes within recent basins is shown in previous works [GIOVANOLI, 1976; GIOVANOLI *et al.*, 1976; STUMM, GIOVANOLI, 1976 *b*]. Similar experiments were performed with synthetic birnessite. Their results were very similar to those reported below. This paper presents information on the runs in which hausmannite was used as the sorbent.

A synthetic seawater was prepared as described by BRUEVICH [1946]. A deionized water was used for this purpose. The seawater had the following characteristics: $Cl^- = 19‰$, $S = 35‰$, pH 8.10—8.15.

The metals under study, in order to avoid hydrolytic effects, were introduced with the addition of a complex-forming agent, i.e. citric acid, in a 10-fold excess with respect to the molar amounts of the metals. Iron was introduced in the form of ferric ammonium alum, analytical pure grade; manganese — as $MnSO_4$, analytical pure grade; cobalt — as $CoCl_2 \cdot 6\,H_2O$, analytical pure of "nickel-free" grade; nickel — as $NiSO_4 . 7\,H_2O$, analytical pure "cobalt-free" grade. The initial concentrations of the metals are presented in Table 1.

The sorption experiment was conducted in 5-litre polyethylene bottles containing 0.3 g of sorbent. The botles were agitated for 72 hours, and the sorbent was separated centrifugally from the solution. To account for the sorption by the bottle walls and the possible hydrolytic precipitation, blank experiments were carried out. In the final solution the content of Ni and Co was determined by a polarogphic method according to the hydrogen catalytic wave in the presence of dimethylglyoxime [VINOGRADOVA *et al.*, 1968], (the sensitivity of the method in parallel determinations of the content of Ni and Co being not lower than 0.3 μg/l, determination reproducibility ±2.35% — (coefficient of variation), — at the content of the elements equal to 2.9 μg/l); the content of Fe — by photometric reaction with 1.10-phenanthroline [MARCHENKO, 1971], (the molar extinction coefficient equal to $11.8 \cdot 10^3$, the sensitivity of the method being 20 μg/l); the content of Mn — photometrically by a permanganate method [MARCHENKO, 1971], (the molar extinction coefficient being equal to $2.4 \cdot 10^3$). The centrifugally separated sorbent was added to a new portion of the starting solution. Accumulation of the sufficient amounts of metals in the experiment required seven successive interaction cycles to be made, which made it possible to accumulate reasonable amounts of Ni, Co, Mn, Fe (Table 1). The precipitate obtained was washed from the residual impurities of seawater components using deionized water.

TABLE 1

*static conditions from seawater solution on a manganese hydroxide substrate**

Total amount of element sorbed from 5 l solution				Element sorption rate (μg/h)			Total element sorption rate (μg/h)	% of sorption			
Ni	Co	Fe	Mn	Ni	Co	Fe		Ni	Co	Fe	Mn
3,650	3,210	2,280	740	50.69	44.58	31.67	126.94	44.21	40.06	34.54	21.14
6,175	6,275	4,820	1260	35.07	42.57	35.28	112.92	33.33	39.63	50.80	17.33
8,375	9,990	7,595	1550	37.50	51.59	48.54	127.63	30.98	43.12	40.84	14.50
10,720	12,320	9,070	930	32.57	32.36	20.49	85.42	36.61	34.18	30.07	−24.80
11,595	14,245	16,735	515	12.15	26.74	106.46	145.35	16.50	28.22	99.00	−11.16
13,060	15,875	18,860	−285	20.35	22.64	29.51	62.50	25.73	25.91	42.50	−25.39
15,060	16,625	23,560	−2535	27.78	10.41	65.28	103.47	40.00	15.50	100.00	−79.65

0.300 g. Content of the sorbed metals in the solid phase (%): Ni = 17.67, Co = 19.50, Fe = 27.64.

The composition of the starting sorbent and final product was studied by X-ray analysis (Guinier camera, Fe — anticathode), and in a powder camera (57.3 mm, Cr — anticathode, V — filter, G. V. SOKOLOVA, Geological Institute, USSR Acad. Sci.).

The structure of the starting and final products was studied by using a scanning electron microscope (Hitachi, Akashi, Model MS, M-2, Japan) and a high-resolution electron microscope (JEOL, Japan; N. D. SEREBRENNIKOVA, Geological Institute, USSR Acad. Sci.).

The composition and valency state of the metals accumulated were studied by X-ray photoelectron spectroscopy (spectrometer model VIEE—15). Photoelectrons were excited with the aid of Mg Kα-radiation whose photon energy was equal to 1253.6 eV. The binding energy for the narrow lines was determined to an accuracy of ±0.1 eV, the resolution being as high as 1.2 eV. The spectrometer was evacuated to 3.10^{-7} Torr. Spectra calibration was made by the carbon 1_{-s} line for which the value of the electron binding energy (E_{bind}) was taken to be 285.0 eV. Intact samples were applied to a finely corrugated aluminium cylinder in such a way that its surface was covered completely.

The valency state of Fe in the product was determined by MÖSSBAUER spectroscopy. The spectra were taken by using an electrodynamic MÖSSBAUER spectrometer. Used as the γ-quanta source was Co^{57} in a Pd-lattice. Recording was performed by using a NaJ(Tl)-crystal scintillation counter. The procedure took place at room and liquid-nitrogen temperatures.

EXPERIMENTAL RESULTS

Data analysis for the sorption dynamics of the components under study (Table 1) reveals the following features:

(a) The amount of the sorbed Co decreases progressively to the final experimental stages, from 40.06 to 15.50%.

(b) For Ni this trend toward the decrease of the sorbed amount is less pronounced.

(c) For Fe, a gradual and substantial increase in the sorbed amount is observed at the final stages (after stage 5) and reaches 100%.

(d) For Mn, there is a gradual decrease of the sorbed amount (from 21.14 to 14.50%) up to stage 3. Later on (stages 4—7) the de sorption of Mn takes place. The amount of Mn released into the solution at the final stages markedly exceeds its amount in the starting solution.

As result of the 7-time changes of the starting solutions the following relative amounts of metals (%) on the sorbent were accumulated: Ni=17.67, Co=19.50, Fe=27.64. From the data on sorption dynamics (Table 1) there is observed, as a whole, no accumulation of manganese under the experimental conditions. The amounts of manganese released into the solution at the final stages exceed the content of this metal in the starting solution by 2535 μg. These data suggest that the amount of Mn equivalent to 16.14% of the sorbed Co or 17.96% of the sorbed Ni was removed from the substrate structure (Mn_3O_4) in the interaction with the Ni and Co in solution.

Study of the sorbent starting phase, made with the use of a scanning electron microscope *(Fig. 1)* demonstrates that synthetic hausmannite is represented by microglobular aggregates on whose surface there are well developed extremely small needle-like crystallites. It can be seen in the micrographs taken under a transmission

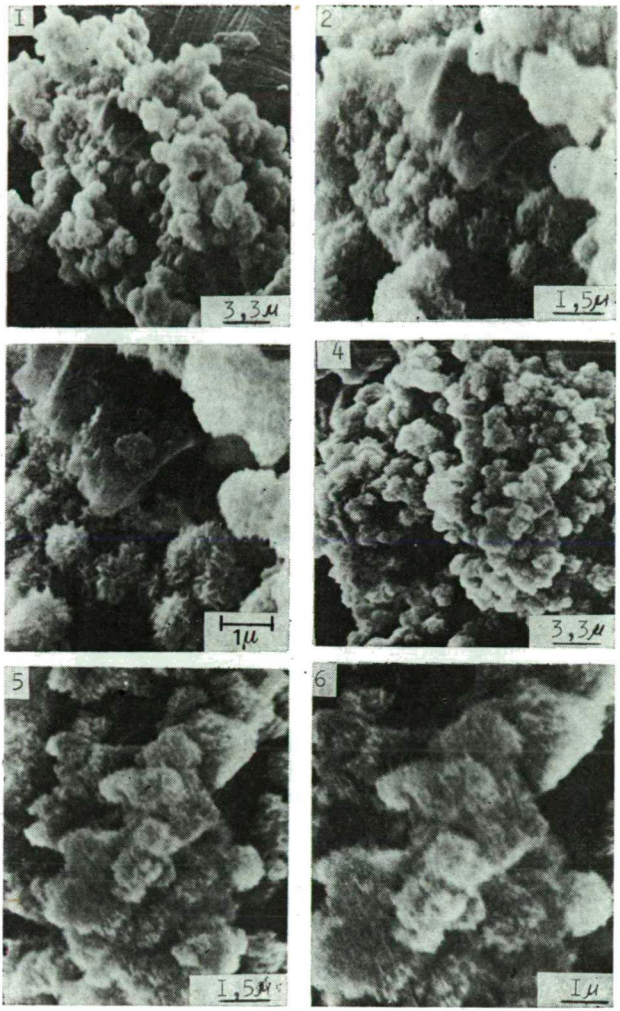

Fig. 1. Micrographs of the initial manganese oxide (Mn_3O_4), taken under a scanning electron microscope. *Photos 1—3* and *4—6* are a successive series taken at increasing magnification. The photos show clearly a microglobular structure of the aggregates with the development of fine needle-like crystallites on the surface

electron microscope with a higher resolution ($4 \cdot 10^3$ x magnification) that the surfaces of the globular aggregates contain the developed, extremely small bipyramidal-octahedral crystals typical of hausmannite *(Fig. 3,* photo 1*)*.

In the micrographs of the newly-formed product *(Fig. 2)*, a significant enlargement of the aggregates, disappearance of the pronounced globularity and development of microlaminated stepped forms of epitaxial outgrowths of the newly-formed phases *(Fig. 3,* photos 2, 3*)* can clearly be seen.

X-ray photoelectron spectroscopy enables one to study the parameters of the atom valency state and their crystallochemical behaviour. The potentialities of this method have been widely discussed recently [MINACHEV *et al.*, 1975; NEMOSHKALENKO,

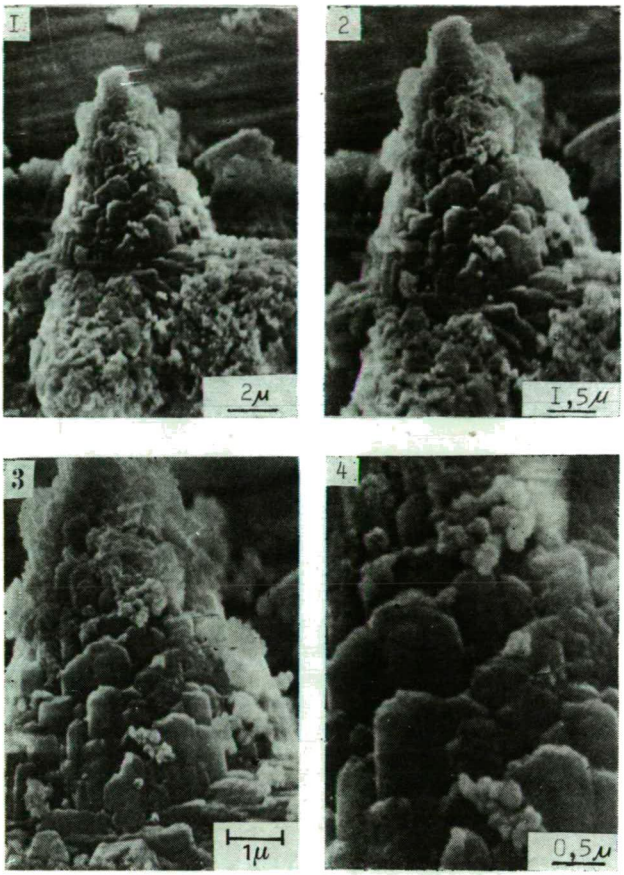

Fig. 2. Micrographs of the product obtained as a result of the sorption of the dissolved forms of Ni, Co, Fe, Mn from seawater by Mn_3O_4 taken under a scanning electron microscope. *Photos 1—4* are a successive series taken at increasing magnification. The photos show clearly a substantial enlargement of the aggregates, disappearance of a prominent globularity, development of microlaminated stepped epitaxial outgrowths of the newly-formed phases

et al., 1976; FROST *et al.*, 1972; MATIENZO *et al.*, 1973; TEWARI and LEE, 1975, 1977; BRIGGS and BOSWORTH, 1977]. A characteristic of this technique is that reliable information on the valency of the ions of interest can be obtained only for the sample surface: the penetration ability of photoelectrons averages 50—70 Å. Therefore, study of the deeper zones of the sample required etching of the sample with argon ions at an energy of 0.7 keV and a current of 6 mA (argon pressure in the sample conditioning chamber being 0.14 Torr). The samples under study were subjected to double and triple etching by steps of 3400—6000 Å. Determination of the structural-chemical behaviour of the sorbed layer was made by the (2p3/2) spectra of Ni, Mn and Co, shown in *Figs. 4a, 5a, 6a.*

Manganese. The Mn (2p3/2) spectrum in the external part of the sorbed layer is characterized by a structure with a clear-cut separation of the low-energy group of peaks (binding energy region 640—644 eV). This low-energy spectrum is dis-

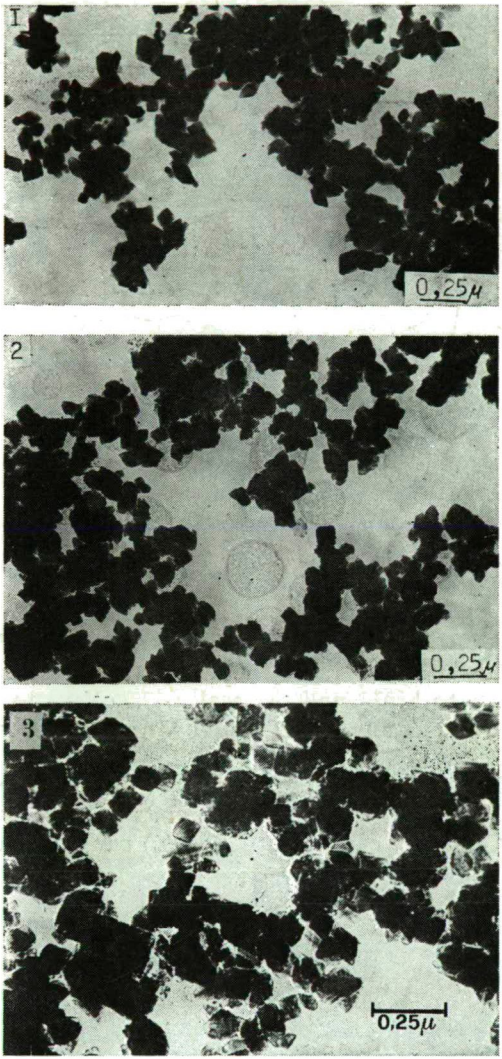

Fig. 3. Micrographs of the sorbent (Mn_3O_4) and products obtained as a result of the sorption of the dissolved forms of Ni, Co, Fe, Mn from seawater by (Mn_3O_4), taken under an electron microscope. *Photo 1.* The initial phase is (Mn_3O_4). Shown clearly are bipyramidal, octahedral crystalline forms of individual grains (40.10^3 x magnification). *Photos 2—3.* The sorbent (Mn_3O_4) after interaction with seawater containing Ni, Co, Fe, Mn (products of parallel experiments). Shown clearly is aggregation of the grains, their less distinct crystalline faces, with indications of the corrosion of the primary grains and development upon them of newly-formed sorption outgrowths: relatively brighter rims and areas around comparatively dark primary grains (40.10^3 · magnification)

tinguished by a considerable breadth and an asymmetry suggesting a superposition of several charge states of Mn. This is supported by a non-uniform, stepped configuration of the spectrum top portion in the given binding energy region. From correlation of the spectrum obtained with those known for various manganese oxides

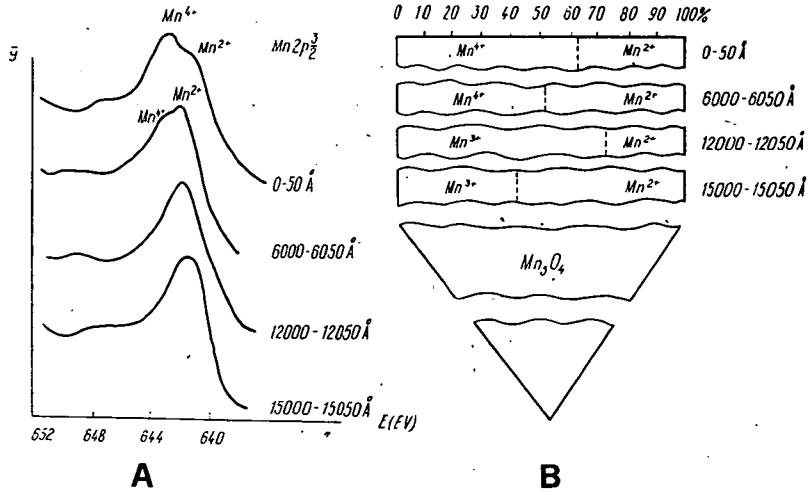

Fig. 4. A) Mn X-ray photoelectron (2p3/2) spectra for the external and internal parts of the newly-formed layer
B) Relationships (%) between the Mn valency states in the external and internal parts of the newly-formed layer

[MINACHEV *et al.*, 1975; ROSENCWAIG *et al.*, 1971; FROST *et al.*, 1972; NEMOSHKALENKO and ALESHIN, 1976] it can be concluded that the peak corresponding to the binding energy 641.6 eV relates to Mn^{2+} and the peak 642.7 eV — to Mn^{4+}. These peaks suggest that the relative amounts of Mn^{4+} and Mn^{2+} are 60 and 40%, respectively (see *Figs. 4a, b)*.

At a depth of 6000 Å, a variation in the relationships between the peaks responsible for Mn^{4+} and Mn^{2+} and the relative amounts of these valency forms of Mn being approximately equal to each other (50:50%) can be observed in the sorbed layer.

For the deeper levels of the sorbed layer (12,000 and 15,000 Å) disappearance of the peak characteristic of Mn^{4+} and appearance of a clear-cut peak (641.4 eV) corresponding to Mn^{3+} are observed. For the depth interval 12,000—12,050 Å the relative amounts of Mn^{3+} and Mn^{2+} are 70 and 30%, respectively. For the levels deeper than 15,000—15,050 Å this ratio decreases substantially: $Mn^{3+}=40$, $Mn^{2+}=60\%$.

Nickel. The Ni (2p3/2) spectra in the external part of the sorbed layer are also distinguished by a considerable breadth, i.e. 3 eV *(Fig. 5a)*. In addition, in the high-energy spectrum portion at a distance of 6—7 eV, there are observed satellite lines. These lines can be readily subdivided into two narrow components with a binding energy of 862.5 and 863.0 eV, respectively. Transition to the intermediate part of the sorbed layer (a depth of 6000 Å) leads to a prominent narrowing of the main line of the Ni (2p3/2) spectrum and its shift to the low-energy side down to 855.5 eV as compared with the binding energy of the Ni main peak in the external part of the layer (856.3 eV). The value 855.5 eV is characteristic of divalent nickel [MINACHEV] *et al.*, 1975; NEMOSHKALENKO, ALESHIN, 1976; ROSENCWAIG *et al.*, 1971; FROST *et al.* 1972], the Ni satellite line has a binding energy of 861.5 eV. The spectrum of Ni in the external part of the layer, as evidenced by its appreciable breadth and the double structure of the satellite line therefore suggests that it represents a superposition of

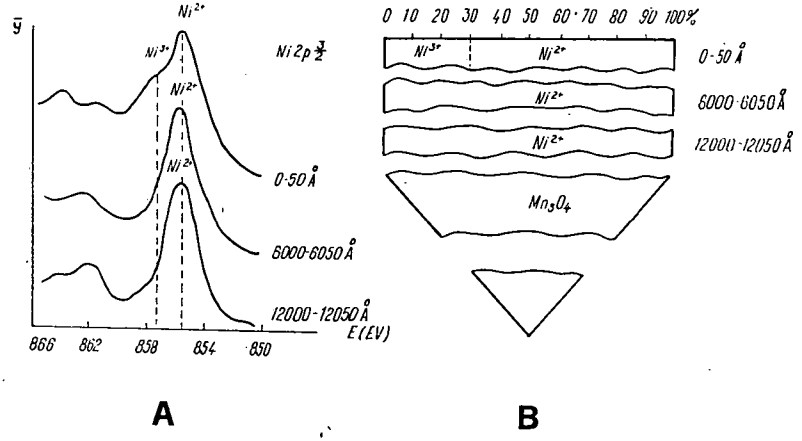

Fig. 5. A) Ni X-ray photoelectron (2p3/2) spectra for the external and internal parts of the newly-formed layer
B) Relationships (%) between the Ni valency states in the external and internal parts of the newly-formed layer

two valency states of Ni, i.e. Ni^{2+} and Ni^{3+} with their relative amounts 70 and 30%, respectively (see *Fig. 5b)*.

In two deeper levels of the sorbed layer, Ni is found largely in a divalent state. In this case the corresponding redistribution of intensity on the satellite lines as well is also observed. The Ni (2p3/2) spectrum in the lower part of the layer (12,000 Å) does not differ from that of the intermediate part of the layer.

Cobalt. The structure of the Co (2p3/2) spectrum is very much the same as that of Ni *(Fig. 6a, cf. Fig. 5a)*. The Co spectrum for the external part of the layer is

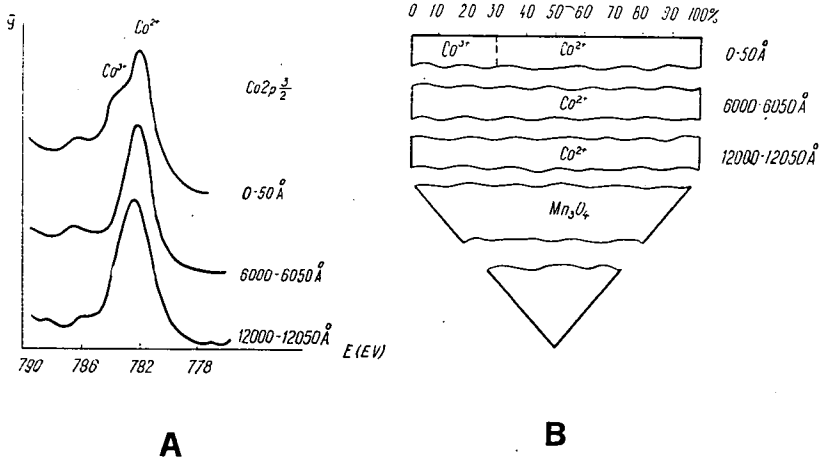

Fig. 6. A) Co X-ray photoelectron (2p3/2) spectra for the external and internal parts of the newly-formed layer. *B)* Relationships (%) between the Co valency states in the external and internal parts of the newly-formed layer

TABLE 2

MÖSSBAUER *spectra parameters of hydrous ferric oxides synthesized on the substrate represented by hydrohausmannite*

Sample	T_{meas} (°K)	Isomeric shift δ E (mm/s) ±0.02 mm/s	Quadrupole splitting E (mm/s) ±0.03 mm/s	Half-width of lines (mm/s) ±0.02 mm/s	Effective magnetic field intensity (kOe)	±0.05	
a	300	0.18	0.68	0.61	—	1.00	0.55
	80	0.17	0.66	0.48; 0.42	—	1.80	
b	300	0.18	0.71	0.61	—	0.53	
	80	0.17	0.69	0.45; 0.60	—	1.50	0.34
c	300	0.18	0.66	0.65	—	0.20	
	80	0.17	0.69	0.54; 0.39	—	1.16	0.15
$Fe(OH)_3$, synthesized	300	0.18	0.66	0.62	—	2.50	
	80	0.17	—	0.54; 0.60	—	3.80	0.66
Goethite from the Red	300	0.15	0.57	0.46	—	7.70	—
Sea (X-ray amorphous)	80	0.15	0.69	0.45	454	—	—
Goethite (α-FeOOH) fine-grained	300	0.20	0.55	0.44	—	—	—
200 Å	80	0.08	0.58	—			

characterized by a significant breadth and shifts to the high-energy side as compared with the internal part of the sorbed layer. As in the case of Ni, this spectrum corresponds to the superposition of Co^{2+} and Co^{3+} in the ratio (%): $Co^{3+}:Co^{2+}=30:70$ *(Figs. 6a, b)*.

It should be noted that the Co spectrum has a satellite structure in the external part of the newly-formed layer. There are serious reasons to believe that the given satellite in the binding energy region 785.2 eV is due to the discrete losses which are associated with the secondary 3d−4s electrons transition on the Co^{3+} ion. The Co spectrum at depths of 6000 and 12,000 Å are identical and characterized by fairly symmetrical lines. The peak of the Co main line for these levels has binding energy in the range 780.5—781.5 eV, which corresponds to the presence of Co^{2+} [MINACHEV *et al.*, 1975; NEMOSHKALENKO, ALESHIN, 1976; ROSENCWAIG *et al.*, 1971; FROST *et al.*, 1972]; the presence of a satellite in the Co spectrum for the external part of the sorbed layer is due to the special features of the nearest surrounding of Co^{2+} and not Co^{3+}, since it follows from studies by ROSENCWAIG *et al.*, [1971] that Co^{3+} has no satellite structure; moreover, this is also suggested by a relatively small distance satellite — $Co^{3+}(2p3/2)$, i.e. 3.3 eV instead of normally observed 4.5 eV.

It is known from experimental studies by MINACHEV *et al.* [1975]; NEMOSHKALENKO, ALESHIN [1976]; FROST *et al.* [1972] that satellites are largely typical of the octahedral configuration Co-ligand, and their absence implies the transition of Co into the tetrahedral surrounding. In the internal part of the sorbed layer, Co^{2+} is therefore distributed largely in tetrahedral voids.

MÖSSBAUER spectroscopy was used to study the crystallochemical features of Fe compunds in the newly-formed layer sorbed on the hausmannite substrate. The study was made on a set of samples *(a, b, c)* obtained in parallel experiments (see Table 2, *Fig. 7*).

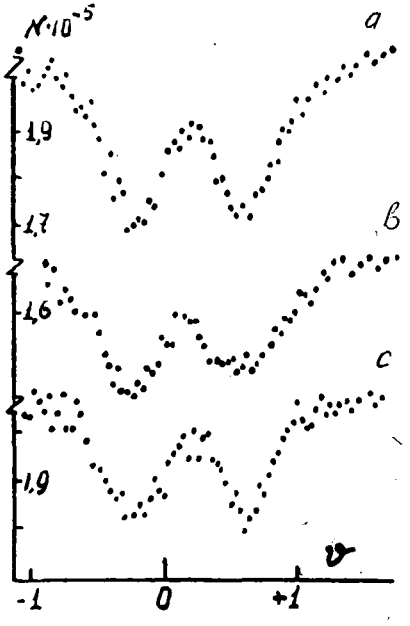

Fig. 7. Mössbauer spectra of the product obtained as a result of the sorption of the dissolved forms of Ni, Co, Fe, Mn from the solution of seawater by Mn_3O_4. The spectra were taken at a temperature of liquid nitrogen. The samples a, b, c are the products of parallel experiments. The parameters of these spectra correspond to $FeOOH.H_2O$. The samples of the a—b—c series show a decrease of crystallinity of $FeOOH.H_2O$

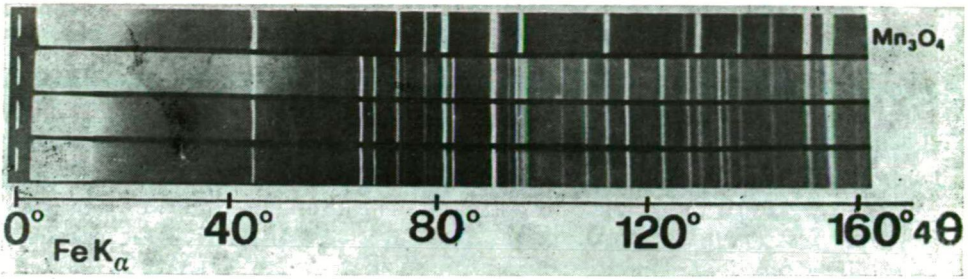

Fig. 8. X-ray powder pattern of varieties of final products (Guinier camera, FeK_{α}-radiation). Note the distinctive new lines of the newly-formed phases. *Sample 1* is the sorbent represented by Mn_3O_4. *Samples 2—4* are the products obtained as a result of the sorption of the dissolved forms of Ni, Co, Fe, Mn from seawater by hausmannite (parallel experiments)

1. *Sample a.* The spectrum represents a quadrupole doublet with an isomeric shift of 0.17 mm/s and a quadrupole splitting $\Delta E = 0.66$ mm/s, these parameters being characteristic of ferri-compounds. The line width is 0.48 mm/s, which is 1.5 times more than the instrumental line width. The magnitude of the effect is of the order of 1.8%.

2. *Sample b.* The spectrum also represents a quadrupole doublet with the same magnitude of isomeric shift and a somewhat larger magnitude of quadrupole splitting, $\Delta E = 0.69$ mm/s. The lines are slightly asymmetrical, their widths being equal to 0.45 mm/s and 0.60 mm/s for the left and the right component respectively (the line widths exceed the instrumental line width by a factor of 1.40 and 1.87, respectively The magnitude of the effect is 1.5%.

3. *Sample c.* The spectrum has a quadrupole doublet similar to the previous case with reverse asymmetry and the magnitude of the effect equal to 1.16.

The constancy of isomeric shift, of the order of 1.17 mm/s, as well as the magnitude of quadrupole splitting, in the range 0.66 to 0.69 mm/s, suggest that in all three cases trivalent iron occurs. As a whole, these parameters are characteristic of ferric oxides, which corresponds most closely to the compound $Fe(OH)_3$. At the same time, the differences observed in the spectra, relate to the magnitude of the effect, that varies, on passing from sample *a* to sample *c,* from 1.80 to 1.16, and also to the line width. It is obvious that this corresponds to variation in a degree of amorphism. In the successive series *a—c* one can observe a decrease in crystallinity, which is represented by the line broadening and variation in the above parameters.

The parameters listed above were obtained for the spectra taken at a temperature of liquid nitrogen. There is practically no parametric variations when passing from room temperature to a temperature of liquid nitrogen, except for a prominent increase of the effect, which characterizes a degree of amorphism. At the same time, for a fine-dispersed goethite and synthesized ferrihydrite at a temperature of liquid nitrogen, one can observe the effect of splitting. The data presented have suggest the availability of the compound type $Fe(OH)_3$ within the newly-formed layer.

The sorbent as starting material and newly-formed phases were identified by using various methods of X-ray analysis (Table 3, *Fig. 8*). It can be concluded from a comparison study of the X-ray patterns by their direct (side-by-side) application that the sorbed layer on the hausmannite substrate is characterized by a number of new reflections (3.39—3.26—2.69—1.97—1.88—1.74 and others) typical of this

layer only. Attempts to refer these reflections to the published tabulated data (ASTM and others) suggest the occurrence within the sorbed layer of the following phases: γ-MnOOH (manganite), CoOOH (heterogenite), Co_2O_3, Ni_2O_3, $NiSO_4 \cdot 2\,H_2O$. These phases are not inconsistent with the X-ray photoelectron spectroscopy data.

TABLE 3

X-ray powder patterns of the starting material and final product, experiments on the chemisorption autocatalytic oxidation interaction of hydrous manganese oxides with the dissolved forms of Fe, Mn, Ni, Co (Guinier camera, FeK_α)

Starting hydroxide		Newly-formed phase		Hausmannite Mn_3O_4 ASTM 16—154		Starting hydroxide		Newly-formed phase		Hausmannite, Mn_3O_4 ASTM 16—154	
d(Å)	I	d(Å)	I	d(Å)	I	d(Å)	I	d(Å)	I	d(Å)	I
4.91	20	—	—	4.94	30	—	—	2.35	0.5	—	—
—	—	4.37	0.5	—	—	—	—	2.33	1.0	—	—
—	—	3.93	0.5	—	—	—	—	2.32	1.0	—	—
3.56	0.5	3.56	0.5	—	—	—	—	2.18	1.0	—	—
—	—	3.43	0.5	—	—	—	—	2.11	0.5	—	—
—	—	3.39	10.0	—	—	2.04	5.0	2.10	2.0	2.04	40
—	—	3.33	0.5	—	—	—		1.97	6.0	—	—
—	—	3.30	0.5	—	—	—	—	1.88	5.0	—	—
—	—	3.26	8.0	—	—	—	—	1.81	4.0	1.82	20
3.06	0.6	3.02	0.5	3.09	50	1.782	5.0	—	—	1.795	50
2.87	1.0	2.82	0.5	2.89	30	—	—	1.75	0.5	—	—
2.76	10.0	2.72	0.5	2.77	90	—	—	1.74	4.0	—	—
—	—	2.69	7.0	—	—	1.696	5.0	1.72	2.0	1.706	30
2.48	9.0	2.45	0.5	2.49	100	1.634	2.0	1.64	0.5	1.642	20
—	—	2.40	1.0	—	—	1.579	7.0	—	—	1.575	80
2.31	2.0	2.37	3.0	2.36	40	1.541	10.0	1.55	0.5	—	—
						1.44	6.0	1.49	0.5	1.468	10

A precision analysis of the studied sample using a Guinier camera with a subsequent side-by-side comparison together with the reference samples and a direct correlation of the X-ray patterns obtained in the same conditions revealed that MnOOH and CoOOH can be discarded. A purely numerical coincidence of the values of the reflections was not supported by the availability of a complete set of the corresponding lines needed for the identification of these compounds. The possibility of the presence of Co_2O_3 and Ni_2O_3 is improbable since the conditions for the synthesis of these compounds, as indicated for the ASTM reference samples and the experimentally obtained phases, are different. Experimental results reported by R. AMMANN and H. GÜDEL at the Bern University also indicate a small probability for the formation of Co_2O_3 and Ni_2O_3 under the conditions of the experiment conducted. The availability of $NiSO_4 \cdot 2\,H_2O$ is somewhat doubtful as in the given conditions this compound is more likely to be present in the form of tetrahydrate. Despite the conclusive evidence for the presence of newly-formed phases within the sorbed layer therefore the problem of their exact identification is still to be solved.

RESULTS AND DISCUSSION

Experiments on the accumulation of Ni, Co, Mn, Fe from seawater by hausmannite required a thorough maintenance of identical conditions throughout the entire 7 cycles (stages). However, the behaviour of each of the four sorbed components is

characterized by markedly specific features. Data on the sorption dynamics (Table1) suggest the following conclusions:

1. The amount of the sorbed Co decreases progressively toward the final experimental stages, from 40.06% down to 15.50%.

2. For Ni, this trend is less marked than for Co.

3. For Fe, there is a less pronounced but gradual increase in the sorbed amount of this metal, which is especially evident during the final (after the fifth) stage, up to 100%.

4. For Mn the initial stages (before the third one) are characterized by a gradual decrease in the sorbed amount of this metal (from 21.14% down to 14.50%). At the later stages (between the fourth and the seventh ones) one can observe a prominent desorption of Mn. The amount of Mn released into the solution at the final stages exceeds noticeably the content of this metal in the starting solution.

It would be possible to conclude from the data on the sorption dynamics that Mn does not accumulate under experimental conditions as the amounts of this metal released into the solution during the final stages exceed its initial amount by 2535 μg. These data therefore suggest that the amount of Mn equivalent to 16.14% of the sorbed Co or 17.96% of the sorbed Ni was removed from the substrate structure (Mn_3O_4) in the interaction with the solution-contained Ni and Co.

Studying the micrographs of the starting sorbent (Mn_3O_4) and the newly-formed products, taken under a scanning microscope, permits the following features to be noted:

(a) The starting sorbent *(Fig. 1)* is characterized by small-globular forms in whose surface there developed very fine needle-like crystallites representing tetragonal bipyramids of Mn_3O_4.

(b) The final product *(Fig. 2)* is represented by large globular aggregates with the distinct patterns of the newly-formed sorbed layer featuring stepped-laminated epitaxial outgrowths.

The process of accumulation of the sorbed components involves aggregation, growth of the sorbent grains and perhaps even formation of epitaxial outgrowths on their surface where previously needle-like crystallites were present. This reduces the active surface of the sorbent substantially during the runs, which, in turn, affects the sorbed amounts of Co and Ni. Similar relations were observed in studies of the dynamics of the sorption synthesis of Ni, Co, Fe, Mn oxide phases on hydrous ferric oxides [VARENTSOV *et al.*, 1978].

X-ray photoelectron spectra of Co, Ni, Mn and MÖSSBAUER spectra of Fe reveal that, for the newly-formed layer there is a distinct trend toward accumulation of these components on the state of relatively high valencies. However, the intensity of oxidation processes at the solution/sorbent (Mn_3O_4) interface is relatively lower than for hydrous ferric oxides (FeOOH), [VARENTSOV *et al.*, 1978]. The most prominent feature in this case is the absence of higher states of Mn oxidation (Mn^{7+} and Mn^{5+}). For the present case, the above pattern of Mn distribution shows up in a relative enrichment of the newly-formed layer with divalent Mn *(Fig. 4)*. At the same time, the Ni and Co spectra of the newly-formed layer retain similarity with the spectra of the compounds synthesized on lepidocrocite. However, in this case the distribution of the Ni and Co valency forms is close to that which was observed not in the surface part of the layer formed on the lepidocrocite substrate but rather at a certain depth, i.e. of the order of 3400 to 3450 Å.

Attention is drawn to a relative general weakening of the processes of Co, Ni, Mn accumulation on hausmannite as compared with lepidocrocite (Table 4). It can be concluded from the data of Table 4 that the process of the component accumulation proceeds in a nonuniform way, i.e. accumulation is highest at the initial stages and, as the newly-formed layer develops, the relative amount of the sorbed components decreases. This conclusion agrees with the data on the sorption dynamics (Table 1). As stated above, the decrease in the sorption rates is associated with a substantial reduction of the sorbent surface.

TABLE 4

Relationships between the intensities of the (2p 3/2) lines of Co, Ni, Mn for the phases newly-formed on the substrates represented by hydrous manganese oxides (hydrohausmannite) and hydrous ferric oxides (lepidocrocite) — [VARENTSOV *et al.*, 1978]

Depth from the surface of the newly-formed layer (Å)	Co	Ni	Mn
		I(2p3/2) hausmannite / I(2p3/2) lepidocrocite	
0—50	0.74	0.68	0.44
6000—6050 (6800—6850)	1.27	1.58	0.93

It is interesting to note that for this case the decrease of the relative share of Ni^{3+} and Co^{3+} with depth occurs more noticeably than in experiments with lepidocrocite, which fact is likely to be due to a specific effect of the substrate and higher rates of the accumulation of these metals.

By and large, the oserved relationships between the valency forms of Ni, Co and Mn confirm an earlier conclusion [VARENTSOV *et al.*, 1978] to the effect that the development of the highly oxidized metal forms in the external part of the newly-formed layer is attributable to the lower accumulation rates of the metals sorbed. It is obvious that the composition of the definite zones of the newly-formed layer is governed by the relationship between the rates of the two processes, i.e. that of the initial sorption of an ion-exchange and hydrolytic nature and a later process of autocatalytic contact oxidation.

A special place is occupied by the solid-phase redox reactions in the diffusion of the sorbed ions into the sorbent structure. It is these reactions to which it is possible to relate an apparent inconsistency of the data on the Mn sorption dynamics (Table 1) and distribution of the valency states of this metal within the newly-formed layer. The results of the experiments conducted and particularly X-ray photoelectron spectra permit a more definite interpretation of the phenomenon consisting in the displacement of Mn^{2+} and Mn^{3+} out of the structure of hydrous manganese oxides in the sorption of Ni and Co [MCKENZIE, 1970, 1972; LOGANATHAN and BURAU, 1973; MURRAY, 1975*a, b*]. The data obtained suggest that along with the sorption of Mn and formation of the phases of this metal within the newly-formed layer (see *Fig. 4*), there is an exchange displacement of Mn^{2+} under the action of Ni and Co ions, and of Mn^{3+} under the action of Co ions from the hausmannite lattice, primarily from the zones of the defect structure. This process is not stoichiometric in that amount of Mn equivalent to 16.14% of the sorbed Co or 17.96% of the sorbed Ni releases into the solution over 82% of Co and Ni therefore accumulate in the sorbed layer.

It is important to note that Fe as the most intensively sorbed component (see Table 1) is present in the newly-formed layer, as evidenced by MÖSSBAUER spectroscopy, nearly in full, in a higher degree of oxidation, i.e. as Fe^{3+} (compound type $FeOOH.H_2O$).

GEOCHEMICAL INTERPRETATION

The criterion of the validity of a genetic model developed by analyzing the observations of a natural process and experimental simulation of some of its elements is conditioned by an adequacy to which this model describes the known facts and new information relating to this process.

Considering recent basins (first of all those of the World Ocean) as ore formation systems, it is possible to distinguish among them the following three categories: (a) sources; (b) transportation medium; (c) ore formation process proper [GREENSLATE *et al.*, 1973; VARENTSOV, 1976]. The above experiments were directed at studying the process of the formation of Mn, Ni, Fe, Co hydrous oxide compounds in the interaction of a component-bearing solution (seawater) with hydrous manganese oxides. The work conducted was based on earlier studies [MICHARD, 1969; MORGAN and STUMM, 1965; STUMM and MORGAN, 1970; PRONINA, *et al.*, 1973; PRONINA and VARENTSOV, 1973; VARENTSOV and PRONINA, 1973, 1976, and others]. These experiments suggest that the hydroxide phases of Mn, Fe, Ni, Co form as a result of a in multistage, involving autocatalytic oxidation, interaction of active surfaces with component-bearing solutions. The initial stages of this process involve sorption and ion-exchange reactions proper with a prominent selective sorption of transition metals. The main reasons for such a high selectivity are the chemical (crystallochemical) affinity of the sorbent and sorbed metal ions, as well as hydrolytic reactions in the interface zone. The later stages involve the reactions of the interface catalytic oxidation of the metals sorbed and their interaction with the sorbed structural ions (hydrous oxides of Fe, Mn and sometimes other transition metals). At the subsequent stages the phases appeared undergo various postsedimentation transformations. Such individual cycles are likely to be multiplied repeatedly in the course of geological time. Experimental laboratory conditions favour the simulation of only separate parts of a natural process taking place at extremely low rates measured by geochronological intervals. The experiments conducted here demonstrate that the composition of the hydroxide compounds of transition metals, appearing as a result of such an autocatalytic process, are governed by a number of critical parameters. The process is most vigorous in the range of weak alkaline pH's (8) and the prominent oxidative values of Eh in the presence of a free soluble O_2. The composition of the newly-formed phases is governed by both the concentrations of the transition metals and their relationship in the component-bearing solution. Such a solution is represented by bottom seawater to which the dissolved metals can be supplied by the currents and in some instances by diffusion from the underlying sediments and other ways.

It has been revealed experimentally that the mineral composition of the compounds results from optimal relationships between the rates of the two basic stages of the process: (a) sorption and (b) catalytic oxidation. It should be noted that the latter stage controls the entire process. The relatively high rates of the first stage leads to the blocking of the second stage, namely interface oxidation. To evaluate how consistently this genetic model explains the known natural phenomena, it is

appropriate to consider, by way of example, the formation of the World Ocean's nodules containing the greatest amounts of transition metals, viz. the equatorial North Pacific [GREENSLATE *et al.*, 1973; ARRHENIUS, 1963; FRAZER, 1977; MENARD and FRAZER, 1978; PIPER, 1977; HORN *et al.*, 1974]. This zone belongs to a subequatorial region of a high biological productivity, relatively low sedimentation rates (under 1 mm/10^3 years), a pronounced erosion activity of underwater currents. The consolidated sediments represented largely by Late Tertiary radiolarian oozes contain, in a scattered form, the considerable amounts of the fragments of altered basic volcanites — palagonites acting as cores for most nodules [HORN *et al.*, 1974]. It is important to note that this nodule zone is adjacent to the western flank of the East Pacific Rise characterized by large-scale hydrothermal activity.

Analysis of the foregoing factors permits the following interpretation to be made. Metals accumulated in the nodules (Mn, Ni, Cu, Co) are present in seawater in solution as the products of biological planktonic transformation occurring in the zone of photosynthesis. The nodule growth is favoured by the presence of the fragments of the altered basic volcanites acting as cores. The presence of hydrous ferric and manganese oxides within the altered basic volcanites makes it possible to regard them as more active sorbents as compared with siliceous radiolarian oozes. The low accumulation rates of the associated sediments favour the process of nodule formation since sedimentary particles produce little or no blocking effect on the active surfaces where transition metals are sorbed. A similar function is performed by bottom currents which, along with the removal of sedimentary material, supply fresh portions of metal-bearing solutions to the zone of natural chromatography. It is obvious that the favourable action of the bottom currents on the nodule formation in this part of the Ocean has been taking place for a long period, presumably since Late Miocene. It is likely that the content of the components in natural water and Eh conditions had a controlling effect on the accumulation rates and composition of Fe—Mn hydroxide phases; for example, the sequence of minerals reflects the growth of oxidative conditions: todorokite — birnessite—δ-MnO_2 (2.4-Å phase), — [CHUKHROV *et al.*, 1976, 1978]. It is interesting to note that characteristic feature of the successive catalytic accumulation of the transition metal hydroxide phases shows up distinctly in the presence of microlaminated epitaxial outgrowths observed under an optical and a scanning microscope. Comparison of the synthetic hydroxide compounds *(Figs. 1, 2)* with the naturally occurring nodules [FEWKES, 1973; MARGOLIS and GLASBY, 1973; SOREM and FOSTER, 1972; WOO 1973; VARENTSOV *et al.*, 1978] points to their having most similar texture features.

A definite role of microorganisms has been assigned to the processes of oxide ferromanganese ore formation in recent basins [DUBININA, 1976; ERHLICH, 1972, 1975; SCHWEISFURTH *et al.*, 1978, and others]. EHRLICH and coworkers [EHRLICH, 1972, 1975] show that the process of microbacterial oxidation is based on the phenomenon of enzymatic (biological) catalysis. Two stages are distinguished in this process [EHRLICH, 1972, p. 66]: (a) sorption; (b) catalytic oxidation proper. In the first stage, the sorption accumulation of transition metals takes place on the active surface. In the second stage, there is catalytic oxidation of the sorbed metals, involving specific enzymes. The intensity or the rate of such an oxidation depends on enzyme concentration. SCHWEISFURTH *et al.* [1978] have found that for a number of microorganisms *(Pseudomonas manganooxidans)* the oxidation of Mn(II) is likely to occur in that case only when the concentration of this metal in solution is under 3.10^{-5} M. Moreover, it is important to note that biocatalytic oxidation of Mn is favoured by the introduction of complexing agents into solution, decreasing the

ionic activity of this metal [SCHWEISFURTH *et al.*, 1978, p. 926]. It has been shown by EHRLICH [1972, p. 67] that the enzymatic oxidation of Mn(II) can take place in a range of relatively not high (for the Ocean) pressures, i.e. up to 567 atm. Thus, the reactions of microbacterial oxidation of transition metals, however, involved they may be, occur in complete agreement with the principal laws of chemical transformations [JENCKS, 1969; BRUCE, BENKOVICH, 1970; THOMAS, THOMAS, 1967]. For the phenomena of microbacterial oxidation of Mn, the mechanism of chemical transformations is likely to be based on the above reactions of catalytic oxidation. However, it can be suggested that these reactions suffer relatively lesser limitations in the basins. Moreover, autocatalytic oxidation is the main process in the formation of oxides of metalliferous sediments [VARENTSOV, 1976; MORGAN, STUMM, 1965].

Among the investigators studying the formation of Fe—Mn nodules, there are those who advocate an exclusively alternative biogenic or abiogenic origin of such ores. The existing situation is similar to that in biological chemistry when in the 1870's there was a lively discussion between J. LIEBIG and L. PASTEUR on the nature of enzymes. Later on, based on the achievements of chemistry and chemical kinetics, it was shown that enzymatic processes (biocatalysis) represent a variety of chemical reactions, without any principal differences.

Thus, taking into consideration all the limitations that are typical of the experiments simulating natural processes, the data obtained may be useful for the fairly satisfactory explanation of the phenomenon of ore formation in recent basins, thereby permitting better understanding of the genetic nature of these processes.

CONCLUSIONS

Results of the experiments conducted and diagnostic data for the compounds synthesized on a substrate represented by manganese oxides (Mn_3O_4) permit the following conclusions to be made:

1. As a result of the data analysis for the sorption dynamics of the dissolved forms of Ni, Co, Mn, Fe from seawater by manganese oxide, study of the starting sorbent and final products under a scanning microscope and by using X-ray photoelectron spectroscopy, MÖSSBAUER spectroscopy, and X-ray identification, it has been established that these components accumulate as a newly-formed sorbed layer.

2. The process is of a complex, multistage nature. The initial stages are characterized by the development of ion-exchange and hydrolytic reactions. In the later stages, the interface autocatalytic oxidation of the components accumulated is observed.

3. The composition of the newly-formed compounds is controlled by the kinetic parameters of the following two main stages of the process: a) the component sorption proper; b) interface catalytic oxidation. Data on the sorption kinetics and X-ray photoelectron spectra of the various levels of the newly-formed layer suggest that the highest oxidized forms of the metals accumulate at the lower sorption rates, when the blocking effect of the first stage does not inhibit the second one. For example, at the final experimental stages at an appreciable decrease of the sorption rates in the external part of the newly-formed layer there are relatively large amounts of the oxidized forms of metals (%): $Mn^{4+}=60$, $Co^{3+}=30$, $Ni^{3+}=30$. Iron, as evidenced by MÖSSBAUER spectroscopy, is present in the sorbed layer in the form: amorphous $FeOOH.H_2O$.

4. The specific feature of the sorption of transition metals by hydrous manganese oxides consists of a partial interaction of Ni and Co with structural Mn^{2+} and

Mn^{3+}. It has been established that, as a result of such an interaction, the amount of Mn equivalent to 16.14% of the sorbed Co or 17.96% of the sorbed Ni is displaced from the substrate into the solution. The main part of Ni and Co accumulates in the sorbed layer.

5. The results presented and survey of the existing situation in the experimental field concerning the problem under consideration enable one to use the above model of the formation of transition metal ore accumulations in recent basins. According to this model, the process is a multistage chemisorption phenomenon in which the principal role is played by interface autocatalytic oxidation of the metals accumulated.

ACKNOWLEDGEMENT

We wish to thank DR. G. P. GLASBY, New Zealand Oceanographic Institute, D.S.I.R., Wellington, New Zealand for critical and constructive comments and reviewing of this paper. The authors are indebted to Academician, Prof. F. V. CHUKHROV, Institute of Geology of Ore Deposits, Petrography, Mineralogy and Geochemistry, USSR Academy of Sciences, Moscow, USSR for helpful suggestions.

REFERENCES

ANDERSON, B. J., JENNE, E. A., CHATO, T. T. [1973]: The sorption of silver by poorly crystallized manganese oxides. Geochim. Cosmochim. Acta v. **37,** No.3, 611—622.

ANDRUSCHENKO, P. F., SKORNYAKOVA, N. S. [1967]: Composition, structure and particular features of the formation of ferromanganese nodules of the Pacific Ocean. In: Manganese deposits of the USSR. M., Nauka Publishers, 94—116.

ARRHENIUS, G. [1963]: Pelagic sediments. In: HILL, M. N. (Editor), The Sea, v. **3,** Interscience, New York, N.Y., 655—727.

BALZANOVA, T. A., TERESHKOVA, M. O., CHUYKO, V. T. [1977]: Thermodynamic interpretation of coprecipitation of some metals by ferric hydroxide. J. Analit. Khimiyi t. **32,** No. 1, 50—55.

BEEVERS, J. R. [1966]: A chemical investigation into the role of sorption processes in ore genesis. Dept. Nat. Development Bureau of Mineral Resources, Geology and Geophysics, report No. **106,** Canberra, 1—63.

BEZRUKOV, P. L., SKORNYAKOVA, N. S., MURDMAA, I. O. [1976]: The problems of the genesis of ferromanganese nodules. In: Ferromanganese nodules of the Pacific Ocean. Proc. Inst. of Oceanology USSR Acad. Sci., M., Nauka Publishers, t. **109,** 241—249.

BREWER, P. G. and SPENCER, D. W. [1974]: Distribution of some trace elements in Black Sea and their flux between dissolved and particulate matter. Mem. Am. Assoc. Petrol. Geol., v. **20,** 137—143.

BRIGGS, D. and BOSWORTH, Y. M. [1977]: Comment on "Adsorption of Co (II) at the oxide-water interface", J. of Colloid and Interface Science v. **59,** No. 1, March 15, 194.

BRUCE, T., BENKOVICH, S. [1970]: Mechanisms of bioorganic reactions. M., Mir Publishers.

BRUEVICH, S. M. [1946]: Average chemical composition of Oceanic water, and "normal" seawater according to the recent data. Probl. Arktiki No. 4.

BURNS, R. G. [1965]: Formation of cobalt (III) in the amorphous $FeOOH \cdot nH_2O$ phase of manganese nodules. Nature v. **205,** 999.

BURNS, R. G. [1976]: The uptake of cobalt into ferromanganese nodules, soil and synthetic manganese (IV) oxides. Geochim. Cosmochim. Acta v. **40,** 95—102.

BURNS, R. G., BURNS, V. M. [1975]: Manganese nodule authigenesis mechanism for nucleation and growth. Nature v. **255,** 130—131.

BURNS, R. G., BURNS, V. M. [1977]: Mineralogy. In: G. P. GLASBY (Editor), Marine manganese deposits. Elsevier Sci. Publ. Comp., Amsterdam—Oxford—New York, 185—248.

CHUKHROV, F. V., GORSHKOV, A. I., RUDNITSKAYA, E. S., BEREZOVSKAYA, V. V., SIVTSOV, A. V. [1978]: On vernadite. Izv. Akad. Nauk SSSR, ser. Geolog., No 6, 5—19.

CHUKHROV, F. V., ZVYAGIN, B. B., GORSHKOV, A. I., ERMILOVA, L. P., KOROVUSHKIN, V. V., RUDNITSKAYA, E. S., YAKUBOVSKAYA, N. D. [1976]: Ferroxyhite — a new modification of FeOOH. Izv. Akad. Nauk SSSR, ser. Geolog., No. 5.

CHUYKO, V. T., NAZARENKO, V. S., KRAVTSOVA, A. A. [1974]: Coprecipitation of nickel by copper and iron hydroxides from ammonium solutions. J. Analit. Khimiyi t. **29,** No. 12, 2437—2441.

DUBININA, G. A. [1976]: Study of the ecology of fresh water basin ferrobacteria. Izv. Akad. Nauk SSSR, ser. Biolog., No. **4**.

DUSHINA, A. P., ALESKOVSKY, V. B. [1976]: Ion exchange as a first stage of solids transformation in electrolyte solutions. J. Pkikladn. Khimiyi No. **1**, 41—49.

DUVAL, J. E., KURBATOV, M. H. [1952]: The adsorbtion of cobalt and barium by hydrous ferric oxide at equilibrium. J. Phys. Chem., v. **56**, 982—984.

EGOROV, JU. V. [1975]: Statics of microelement sorption by oxyhydrates. M., Atomizdat.

EHRLICH, H. L. [1972]: The role of microbes in manganese nodule genesis and degradation, p. 63—70. In: D. R. HORN (Editor), Ferromanganese deposits on the Ocean floor. Conference, Arden House, Harriman, N.Y., 20—22 January, 1972. Lamont-Doherty Geological Observatory, Columbia University and IDOE-NSF, 293 p.

EHRLICH H. L. [1975]: The formation of ores in the sedimentary environment of the deep sea with microbal participation: the case for ferromanganese concretion. Soil Science v. **119**, No. 1, 36—41.

FEWKES, R. K. [1973]: External and internal features of marine manganese nodules as seen with SEM and their implication in nodule origin. pp. 21—29. In: M. MORGENSTEIN (Editor). The origin and distribution of manganese nodules in the Pacific and prospects for exploration. Symposium, Honolulu, Hawaii, 23—25 July, 1973, Valdivia Manganese Exploration Group, University of Hawaii and IDOE-NSF, 175 p.

FRAZER, J. Z. [1977]: Manganese nodule reserves: an updated estimate. Marine Mining v. **1**, Nos. $^1/_2$ pp. 103—123, Crane, Russanand Co., Inc.

FROST, D. C., ISHITANI, A., MCDOWELL, C. A. [1972]: X-ray photoelectron study of transition metals oxides. Molecul. Physic., v. **24**, No. 1, 861.

GABANO, J. P., ETIENNE, P., LAURENT, J. F. [1965:] Etude des propretes de surface du oxyde de manganèse-γ. Electrochimica Acta v. **10**, No. 11, 947—963.

GIOVANOLI, R.[1976:] Vom Hexaquo-Mangan zum Mangan-Sediment Reaktionssequenzen feinteiliger fester Manganoxid-Hydroxide. Chimia **30**, No. 2 (Februar), 102—103.

GIOVANOLI, R., BÜRKI, P., GIUFFREDI, M. and STUMM, W. [1976*a*]: Layer structured manganese oxide hydroxides. IV: The buserite group; structure stabilization by transition elements. Chimia **29**, 517—520.

GIOVANOLI, A., FEITKNECHT, W., MAURER, R. and HÄNI, H. [1976*b*]: Über die Reaktion von Mn_3O_4 mit Säuren. Chimia **30**, No. 6, 307—309.

GIOVANOLI, R. and STÄHLI, E. [1970]: Oxide und Oxidhydroxide des drei- und vierwertigen Mangans. Chimia **24**, 49—61.

GIOVANOLI, R., STÄHLI, E. und FEITKNECHT, W. [1969]: Über Struktur Reaktivität von Mangan (IV) Oxiden. Chimia **23**, 264—266.

GLASBY, G. P. [1974]: Mechanism of incorporation of manganese and associated trace elements in marine manganese nodules. Oceanogr. Mar. Biol., A Rev. 12, 11—40.

GOLDBERG, E. D. [1954]: Marine geochemistry. I. Chemical scavengers of the sea. J. Geol., **62**, 249—265.

GOLDBERG, E. D. [1961]: Chemistry in the Oceans. In: M. SEARS (Editor), Oceanography, Am. Assoc. Adv. Sci. Public., v. **67**, 583—597.

GOLDBERG, E. D., ARRHENIUS, G. [1958]: Geochemistry of pelagic Pacific sediments. Geochim. Cosmochim. Acta v. **13**, 153—212.

GOLDSCHMIDT, V. M. [1937]: The principles of distribution of chemical elements in minerals and rocks. J. Chem. Soc., 655—672.

GREENSLATE, J. L., FRAZER, J. Z., ARRHENIUS, G. [1973]: Origin and deposition of selected transition elements in the seabed, pp. 43—69. In: MAURY MORGENSTEIN (Editor), "The origin and distribution of manganese nodules in the Pacific and prospects for exploration". Symposium, Honolulu, Hawaii, 23—25 July, 1973, Valdivia Manganese Exploration Group, University of Hawaii and IDOE-NSF, 175 pp.

HEM, J. D. [1963]: Chemical equilibria and rates of manganese oxidation. Chemistry of manganese in natural water. Geol. Survey Water-Supply Paper **1667—A**, U.S. Government Printing Office, Washington.

HEM, J. D. [1977]: Reactions of metal ions at surfaces of hydrous iron oxide. Geochim. Cosmochim. Acta v. **41**, 527—538.

HORN, D. R., HORN, B. M., DELACH, M. N. [1974]: Copper and nickel content of Ocean feromanganese deposits and their relation to properties of the substrate, pp. 77—84. In: MAURY MORGENSTEIN (Editor), "The origin and distribution of manganese nodules in the Pacific and prospects for exploration. Symposium, Honolulu, Hawaii, 23—25 July, 1973, Valdivia Manganese Exploration Group, University of Hawaii and IDOE-NSF, 175 pp.

IDZIKOWSKI, S. [1971]: Adsorption of inorganic ions on α-Fe_2O_3 from mixtures of strong electrolytes. Part I. Adsorption of silver, cupric and aluminium ions as a function of indifferent salt concentration. Roczniki Chemii (Ann. Soc. Chim. Polonorum) **45,** 1139—1149. (In Polish)

IDZIKOWSKI, S. [1972]: Adsorption of inorganic ions on α-Fe_2O_3 from mixtures of strong electrolytes. Part II. Relationship between the increase in adsorption and concentrations of the mixture's components. Roczniki Chemii (Ann. Soc. Chim. Polonorum) **46,** 167—177. (In Polish)

IDZIKOWSKI, S. [1972]: Adsorption of inorganic ions on α-Fe_2O_3 from mixtures of strong electrolytes. Part III. Adsorption of cupric and aluminium chlorides in presence of an indifferent electrolyte. Roczniki Chemii (Ann. Soc. Chim. Polonorum) **46,** 1009—1016. (In Polish)

IDZIKOWSKI, S. [1973]: Adsorption of inorganic ions on α-Fe_2O_3 from mixtures of strong electrolytes. Part IV. Adsorption of silver, cupric and aluminium sulphate in presence of an indifferent electrolyte. Roczniki Chemii (Ann. Soc. Chim. Polonorum) **47,** 231—238. (In Polish)

JAMES, R. O. and HEALY, T. W. [1972]: Adsorption of hydrolyzable metal ions at the oxide-water interface. I. Co (II) adsorption on SiO_2 and TiO_2 as model systems. J. of Colloid and Interface Sci., v. **40,** No. 1, July, 42—52.

JAMES, R. O. and HEALY, T. W. [1972]: Adsorption of hydrolyzable metal ions at the oxide-water interface. II. Charge reversal of SiO_2 and TiO_2 colloids by adsorbed Co (II), La (III) and Th (IV) as model systems. J. of Colloid and Interface Sci., v. **40,** No. 1, July, 53—64.

JAMES, R. O. and HEALY, T. W. [1972]: Adsorption of hydrolyzable metal ions at the oxide-water interface. III. A. Thermodynamic model of adsorption. J. of Colloid and Interface Sci., v. **40,** No. 1, July, 65—81.

JAMES, R. O., STIGLICH, P. J. and HEALY, T. W. [1975]: Analysis of models of adsorption of metal ions at oxide-water interfaces. Faraday Discuss., Chem. Soc., v. **59,** 142—156.

JENCKS, W. P. [1969]: Catalysis in chemistry and Enzymology. McGraw-Hill Book Company, New York, St. Louis, San Fransisco, London, Sydney, Toronto, Mexico, Panama.

KRAUSKOPF, K. B. [1956]: Factors controlling the concentrations of thirteen rare metals in seawater. Geochim. Cosmochim. Acta v. **9,** 1—32B.

KRAUSKOPF, K. B. [1957]: Separation of manganese from iron in sedimentary processes. Geochim. Cosmochim. Acta v. **12,** 61—84.

KU, T. L. [1977]: Rates of accretion. In: G. P. GLASBY (Editor), Marine manganese deposits, Elsevier Sci. Publ. Co., Amsterdam—Oxford—New York, 249—267.

KURBATOV, M. H., WOOD, G. B. and KURBATOV, J. D. [1951]: Isothermal adsorption of cobalt from dilute solutions. J. Phys. Chem., v. **55,** 1170—1182.

LALOU, C., BRICHET, E. and RANQUE, D. [1973]: Certains nodules de manganèse trouvés en surface des sediments, sont-ils des formation contemporaines de la sedimentation? C. R. Acad. Sci., Paris, **276** D 1661—1664.

LALOU, C., BRICHET, E., BONTE, PH. [1976]: Some new data on the genesis of manganese nodules. 25th International Geological Congress, Abstracts v. **3,** Sydney, Australia, 779—780.

LOGANATHAN, P. and BURAU, R. G. [1973]: Sorption of heavy metal ions by a hydrous manganese oxide. Geochim. Cosmochim. Acta v. **37,** 1277—1293.

MARCHENKO, Z. [1971]: Photometric determination of elements. M., Mir Publishers, **167,** 231.

MARGOLIS, S. V., GLASBY, G. P. [1973]: Micro-lamination in marine manganese nodules as revealed by scanning electron microscopy. Bull. Geol. Soc. Am., v. **84,** 3601—3610.

MATIENZO, L. J., YIN, L. L., GRIM, S. O. and SWARTZ, W. E. [1973]: X-ray photoelectron spectroscopy of nickel compounds. Inorgan. Chem. **12,** 2762—2769.

MCKENZIE, R. M. [1970]: The reaction of cobalt with manganese dioxide minerals. Australian J. Soil Res., **8,** 97—106.

MCKENZIE, R. M. [1971]: The synthesis of birnessite, cryptomelane and some other oxides and hydroxides of manganese. Miner. Magaz., **28,** 493—502.

MCKENZIE, R. M. [1972]: The sorption of some metals by the lower oxides of manganese. Geoderma **8,** 29—35.

McKENZIE, R. M. [1975]: An electron microprobe study of the relationships between heavy metals and manganese and iron in soil and ocean floor nodules. Aust. J. Soil. Res., **13,** 177—188.

MENARD, H. W., FRAZER, J. Z. [1978]: Manganese nodules on the sea floor: inverse correlation between grade and abundance. Science (3 March, 1978), v. **199,** 969—971.

MICHARD. G; [1969]: Depôt de manganèse par oxidation. Comptes Rendus Acad. Sci., **269** (12 Novem. 1969), ser. D, 1811—1814.

MINACHEV, KH. M., ANTOSHIN, G. V., SHKIRO, E. S. [1975]: Study of the state of nickel in multicomponent zeolite catalysts by X-ray photoelectron spectroscopy. Metallofizika, No. **60,** 55—59. (Kiev)

MORGAN, J. J., STUMM, W. [1965]: The role of multivalent metal oxides in limnological transformations as exemplified by iron and manganese. In: O. JAAG (Editor), Advances in water pollution researches. Proceedings of the Second International Conference held in Tokyo, August 1964, v.1, A, Pergamon Press Book, New York, 103—131.

MURRAY, D. J., HEALY, T. W. and FUERSTENAU, D. W. [1968]: The adsorption of aqueous metal on colloidal hydrous manganese oxide. Adv. Chem. Ser., **79,** 74—81.

MURRAY, J. W. [1974]: The surface chemistry of hydrous manganese dioxide. J. of Colloid and Interface Sci., v. **46,** No. 3, March, 357—370.

MURRAY, J. W. [1975]: The interaction of metal ions at manganese dioxide-solution interface. Geochim. Cosmochim. Acta v. **39,** 505—519.

MURRAY, J. W. [1975]: The interaction of cobalt with hydrous manganese dioxide. Geochim. Cosmochim, Acta v. **39,** 635—647.

MURRAY, J. W., BREWER, P. G. [1977]: Mechanisms of removal of manganese, iron and other trace metals from seawater. In: G. P. GLASBY (Editor), Marine manganese deposits. Elsevier Sci. Publ. Comp., Amsterdam—Oxford—New York, 291—325.

NEMOSHKALENKO, V. V., ALESHIN, V. G. [1976]: Crystal electron microscopy. Kiev, Naukova Dumka Publishers.

NOVIKOV, A. I. [1972]: On the chemistry of coprecipitation of small amounts of elements by hydrated oxides. In: Coprecipitation by hydrated oxides. Issue I, Published by the Tajik State University, Dushanbe, 5—42.

NOVIKOV, A. I., GONCHAROVA, L. K. [1972]: Coprecipitation of Pb by Fe (III) and Zr hydrous oxides. In: Coprecipitation by hydrated oxides. Issue I, Published by the Tajik State University, Dushanbe, 69—90.

NOVIKOV, A. I., KNYAZEV, N. A. [1977]: On the chemistry of coprecipitation of the small amounts of elements by hydroxides. II. Coprecipitation of Zn by ferric hydroxides under conditions of complex formation. In: Coprecipitation by hydroxides. Issue 2, Published by the Tajik State University, Dushanbe, 5—21.

NOVIKOV, A. I., SHAFFERT, A. A. and YAKUBOVA, N. S. [1977]: Study of the relationship between the hydrolysis of 3d-elements and their sorption by hydroxide precipitates. In: Coprecipitation by hydroxides. Issue 2, Published by the Tajik State University, Dushanbe, 81—86.

PIPER, D. Z., WILLIAMSON, M. E. [1977]: Composition of Pacific Ocean ferromanganese nodules. Marine Geology v. **23,** No. 4, 285—303.

POSSELT, H. S., ANDERSON, F. J., WEBER, W. J., JR. [1968]: Cation sorption on colloidal manganese dioxide. Environmental Science and Technology v. **2,** No. 12 (December), 1087—1093.

PRONINA, N. V., VARENTSOV, I. M. [1973]: On the special features of nickel and cobalt sorption from seawater by natural ferric and manganese hydrous oxides. Dokl. Acad. Nauk SSSR, t. **210,** No. 4, 944—947.

PRONINA, N. V., VARENTSOV, I. M., SPEKTOROVA, L. V., SPEKTOROV, K. S., OVSYANNIKOVA, M. N. [1973]: Study of the sorption of nickel and cobalt (biogenic forms) from seawater by natural ferric and manganese hydrous oxides. Geokhimiya No **6,** 876—886.

Renard, D., Michard, G. [1973]: Desorption des elements fixés sur un nodule de manganèse des fonds oceaniques. Compres Rendus Acad. Sci. Paris, v. **277,** (3 Septembre 1973), serie **D,** 749—752.

RENARD, D., MICHARD, G., HOFFERT, M. [1976]: Comportement geochimique du cuivre, du nickel et du cobalt a l'interface eau-sediment. Application a l'enrichissement en ces elements dans les formations ferro-manganesiferes. Mineral. Deposita (Berl.) v. **11,** 380—393.

ROBERTSON, D. E. [1968]: Adsorption of trace elements in seawater on various container surfaces. Anal. Chim. Acta **42,** 533—537.

ROBERTSON, D. E. [1970]: The distribution of cobalt in oceanic waters. Geochim. Cosmochim. Acta **34,** 553—567.

ROSENCWAIG, A., WERTHEIM, G. K., GUGGENHEIM, H. J. [1971]: Origins of satellites on inner-shell photoelectron spectra. Physical Review Letters v. **27,** No. 8 (23 August, 1971), 479.

SCHUTZ D. F. and TUREKIAN K. K. 1965: The investigation of the geographical and vertical distribution of several trace elements in seawater using neutron activation analysis. Geochim. Cosmochim. Acta **29**, 259—313.

SCHWEISFURTH, R., ELEFTHERIADIS, D., GUNDLACH, H., JACOBS, M., JUNG, W. [1978]: Microbiology of the precipitation of manganese. In: KRUMBEIN, W. (Editor), Environmental Biogeochemistry and Geomicrobiology v. **3**, pp. 923—928, Ann Arbor Science Publication. Inc. Ann Arbor, Michigan, USA.

SIPALO-ŽULJEVIĆ, J., WOLF, R. H. H. [1973]: Sorption of lanthanum (III), cobalt (II) and iodide ions at trace concentrations of ferric hydroxide. Microchimica Acta (Wien) 315—320.

SKORNYAKOVA, N. S., ANDRUSCHENKO, P. F. [1970]: Ferromanganese nodules in the Pacific Ocean. In: Sedimentation in the Pacific Ocean. Book 2, M. Nauka Publishers, 202—268.

SLOWEY, J. F., HOOD, D. W. [1971]: Copper, manganese and zinc concentrations in Gulf of Mexico waters. Geochim. Cosmochim. Acta v. **35**, No 2,. 121—138.

SOREM, R. K. FOSTER, A. R. [1972]: Internal structures of manganese nodules and implication in benification. In: D. R. HORN (Editor), Ferromanganese deposits on the ocean floor. Paper from a Conference. Lamont-Doherty Geological Observatory, Columbia University, Palisades New York, January 20, 21, 22 (1972), pp. 167—181, N.S.F., Washington, USA.

SPENCER, D. W., BREWER, P. G. [1969]: The distribution of copper, zinc and nickel in seawater of Gulf of Main and the Sargasso Sea. Geochim. Cosmochim. Acta v. **33**, 325—339.

SPENCER, D. W., ROBERTSON, D. E., TUREKIAN, K. K., FOLSOM, T. R. [1970]: Trace element calibration and profiles at the Geosecs test station in the north-east Pacific Ocean. J. Geophysic. Res., v. **75**, 36, 7688—7696.

STRAKHOV, N. M.: Conditions of the formation of nodular ferromanganese ores in recent basins. Litologiya i Poleznyie Iskopayemyie No. **1**, 3—19.

STUMM, W., Giovanoli, R. [1976]: On the nature of particulate manganese in simulated lake water. Chimia v. **30**, No. 9 (September), 423—425.

STUMM, W., HOHL, H. and DALANG, F. [1976]: Interaction of metal ions with hydrous oxide surfaces. Croatica Chemica Acta (CCACAA) v. **48**, No. 4, 491—504.

STUMM, W. and MORGAN, J. J. [1970]: Aquatic chemistry. Wiley-Interscience, New York, N.Y., 583.

TEWARI, P. H., CAMPBELL, A. B. and LEE, W. [1972]: Adsorption of Co^{2+} by oxides from aqueous solution. Can. J. Chem., v. **50**, 1642—1648.

TEWARI, P. H. and LEE, W. [1975]: Adsorption of Co (II) at the oxide-water interface. J. Colloid and Interface Sci., v. **52**, 77—88.

TEWARI, P. H. LEE, W. [1977]: Comments on "Adsorption of Co (II)". J. of Colloid and Interface Sci., v. **59**, No. 1, March 15, 195—196.

THOMAS, J. M., THOMAS, W. J. [1967]: Introduction to the principles of heterogeneous catalysis. Academic Press, London—New York.

VAN DER WEIJDEN, C. H. [1976]: Experiments on the uptake of zinc and cadmium by manganese oxides. Marine Chemistry v. **4**, 377—387.

VAN DER WEIJDEN, C. H. [19]76: Some geochemical controls on Ni and Co concentration in marine ferromanganese deposits. Chemical Geology v. **18**, 65—80.

VARENTSOV, I. M. [1972]: On the main aspects of the formation of ferromanganese ores in recent basins. In: Doklady sovetskikh geologov, probl. No. 4, Mineral. Mestorozhdeniya, International Geological Congress, 24th Session, Nauka Publishers, M., 158—173.

VARENTSOV, I. M. [1976]: Geochemistry of transition metals in the process of the formation of ferromanganese ores in recent basins. In: Doklady sovetskikh geologov, Mineral. Mestorozhdeniya, International Geological Congress, 25th Session, Nauka Publishers, M., 79—96.

VARENTSOV, I. M., DIKOV, YU. P., BAKOVA, N. V. [1978]: On the model of the formation of Fe—Mn ores in recent basins (experiments on the synthesis of Mn, Fe, Ni, Co oxide phases on hydrous ferric oxides). Geokhimiya 1198—1210.

VARENTSOV, I. M., PRONINA, N. V. [1973]: On the study of mechanisms of iron-manganese formation in recent basins: the experimental data on nickel and cobalt. Mineral. Deposita v. **8**, No. 2, 161—178.

VARENTSOV, I. M. and PRONINA, N. V. [1976]: Experimental study of ferromanganese ores formation in recent basins: data on iron, manganese, nickel and cobalt. 25th International Geological Congress, Abstracts (Sydney), v. **3**, 799.

VERNADSKY, V. I. [1954]: Essays on geochemistry. Essay 3. Geospheres. History of manganese. Ebergy of geospheres. In: Selected Works, t. 1, Published by the USSR Acad. Sci., M., 61—97.

VINOGRADOVA, E. N., PROKHOROVA, G. V., SEVASTYANOVA, T. N. [1968]: Polarographic determination of Ni and Co in soils and natural waters. Vestn. Moskovsk. Universiteta, No. **5**, 74—75.

Woo, C. C. [1973]: Scanning electron micrographs of marine manganese micronodules, marine pebble-sized nodules and fresh water manganese nodules. pp. 165—171. In: M. MORGENSTEIN (Editor), The origin and distribution of manganese nodules in the Pacific and prospects for exploration. Symposium, Honolulu, Hawaii, 23—25 July, 1973, Valdivia Manganese Exploration Group, University of Hawaii and IDOE-NSF, 175 pp.

Manuscript received, July 5, 1979

I. M. VARENTSOV
Senior research worker,
Geological Institute,
USSR Academy of Sciences,
Moscow, USSR

N. V. BAKOVA
Junior research worker,
Geological Institute,
USSR Academy of Sciences,
Moscow, USSR

YU. P. DIKOV
Senior research worker,
Institute of Geology
of Ore Deposits, Petrography,
Mineralogy and Geochemistry,
USSR Academy of Sciences,
Moscow, USSR

T. S. GENDLER
Senior research worker,
Institute of the Physics
of the Earth,
USSR Academy of Sciences
Moscow, USSR

PROF. DR. R. GIONAVOLI
Bern University,
Institute of Inorganic,
Analytic and
Physical Chemistry,
Bern, Switzerland

Acta Mineralogica-Petrographica, Szeged, XXIV/1, 91—97, 1979

ORE MICROSCOPIC, X-RAY AND TRACE ELEMENTAL DATA ON MANGANESE ORES FROM SANDUR, KARNATAKA, INDIA

J. S. R. KRISHNA RAO, B. VENKATA NAIDU and K. VISWESWARA RAO

INTRODUCTION

One of the best manganese deposits occurs in Sandur belt belong to the Dharwar super group. Originally these ores were considered by FERMOR [1909] as 'lateritic' later NAGANNA [1971] made a detailed study of these deposits and suggested them, as 'syngenetic sedimentary'; however, recently DIXIT [1976] suggested these are probably due to 'alterite' affiliations. According to him alterite is defined as a rock by intensive tropical chemical weathering of varied rock types as metalavas, greywackes, tuffaceous and metasedimentary schists, amphibolites, intrusive sheets and dykes of basic rocks and at times even the acidic rocks like quartz and felsite porphyrites, granites and gneisses. In view these interesting observations, the present authors examined some typical manganese ores from this belt. The ores were subjected to X-ray examination and a minor elemental study was carried out. The results are presented herewith suggesting no genetic relation with alterite, but the typical textures and minerals are sedimentary metamorphic and have undergone supergene enrichment.

MINERALOGY

The following minerals were identified in polished sections — cryptomelane, ramsdellite, pyrolusite and bixbyite. The iron minerals like magnetite, goethite, associated with manganese minerals were also observed. Manganosite, jacobsite, woodruffite, hydrohausmannite, braunite, lithiophorite, coronadite were identified by X-rays in addition to those observed in polished sections.

Cryptomelane

This is the most abundant mineral in the ores. Cryptomelane is microcrystalline to amorphous, presenting gel structures and it is isotropic. Another important feature is the round oolitic structure with regular layering. The matrix is clay.

The cell dimensions calculated ($a=9.85$ Å; $c=2.87$ Å) were tallying with the A.S.T.M. Card data.

The mineral shows close similarity in structure and granularity with that of Nicopol-Chiatura type.

Pyrolusite

It is the next abundant mineral to cryptomelane. It is tabular, crystalline with characteristic pleochroism and strongly anisotropic. The cell dimensions calculated ($a=4.41$ Å; $c=2.86$ Å) were tallying with the A.S.T.M. Card data. The pyrolusite

is developing from cryptomelane and shows a radiating structure or coarse grain size. The hand specimens are massive and show layering (a few mm thick).

Ramsdellite

Ramsdellite is fibrous closely associated with pyrolusite. It is greyish white, pleochroic and anisotropic. The cell dimensions calculated (a=4.54 Å; b=9.28 Å; c=2.86 Å) and compared with the A.S.T.M.Card data.

Bixbyite

Bixbyite shows wide variation and it is usually found in polished sections, but often detected in X-ray patterns. It has a unit cell a=9.3847 Å and this is compared with that of A.S.T.M.Card data. Bixbyite is crystalline, idioblastic found in a matrix of pyrolusite. The color is yellowish with moderate reflectivity. It is isotropic.

Magnetite—Goethite—Jacobsite

These are observed in X-ray patterns but magnetite is observed rarely in polished sections.

Manganosite

It is also a common mineral but only observed in X-ray patterns.

Some of the specimens metabasalt or andesite from the area were polished and studied for manganese minerals. Oxidation of magnetite into goethite were observed and no manganese mineral was detected.

X-RAY STUDIES

The following minerals were detected in X-rays to confirm the minerals already discussed above. The *d*-spacings and peak intensities are given in Table 1.

TABLE 1

Mineral	*d* (Å)	*I*
Pyrolusite	1.6178	8
	1.3571	5
	1.5502	7
Cryptomelane	3.1060	10
	2.1440	5
	1.5275	6
Woodruffite	2.52	7
	1.48	8
	1.97	5
Manganosite	1.3371	8
Goethite	2.238	4
	2.433	7
Hydrohausmannite	2.47	8
	1.53	5
Ramsdellite	2.53	8
	1.88	5
	1.6413	6

Coronadite	2.4042	4
	2.2061	4
	1.5417	8
Jacobsite	1.6431	8
	1.5071	10
Braunite	2.3613	5
	1.6634	10
	1.4207	8
Bixbyite	1.8371	2
	1.6563	10

The above *d*-spacings and *I* values of the minerals were compared and tallying with A.S.T.M. Card data.

TEXTURES AND STRUCTURES

Colloform, gel layers, oolitic texture and concretions were observed in pyrolusite and cryptomelane minerals. Scaly forms due to replacing other materials, cavities of different sizes, radiating structures of pyrolusite have been observed in polished sections. Based on the above textures and structures the ores of Sandur under examination can be grouped into primary and secondary ores given below.

Primary ores

Colloform *(Fig. 1)*, gel layers *(Fig. 2)* and oolitic *(Fig. 3)* are present. The minerals chiefly cryptomelane, ramsdellite, manganosite, braunite and hydrohausmannite.

Secondary ores

Scaly forms due to replacing other materials *(Fig. 4)*, presence of cavities in different sizes, radiating structures *(Fig. 5)* developing from the cryptomelane are present. The minerals are chiefly pyrolusite, bixbyite etc.

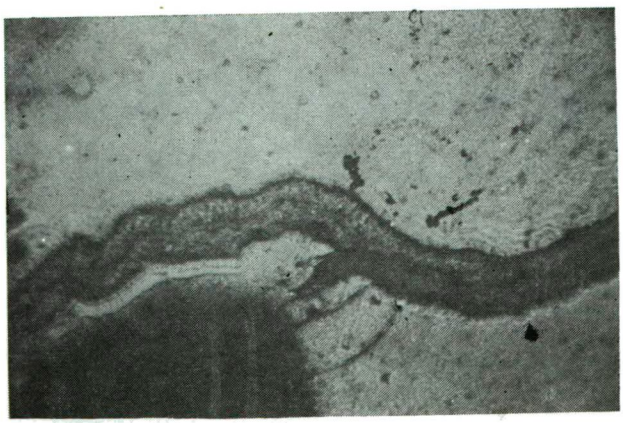

Fig. 1. Colloform banding in cryptomelane. Black color showing the cavity. Sandur, Karnataka. Polished section, ×70

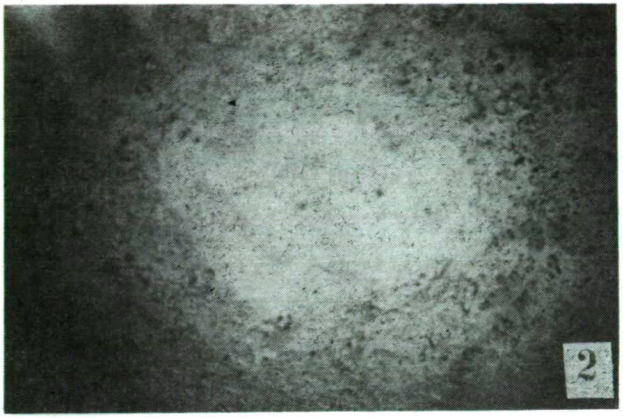

Fig. 2. Gel structure in cryptomelane, Sandur, Karnataka, polished section, ×70

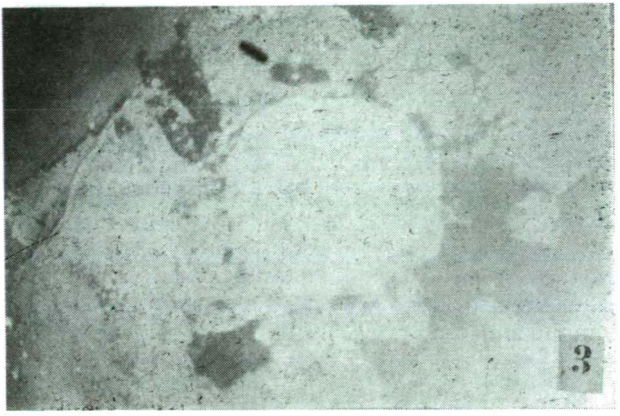

Fig. 3. Oolitic texture in cryptomelane. The gangue is clay material. Sandur, Karnataka. Polished section, ×70

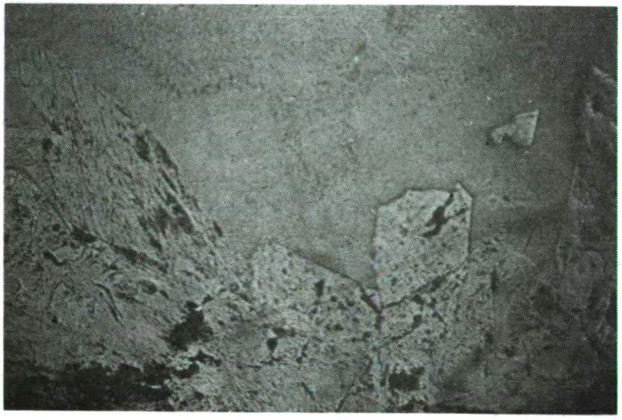

Fig. 4. Scaly forms of pyrolusite replacing cryptomelane. Sandur, Karnataka. Polished section, ×70

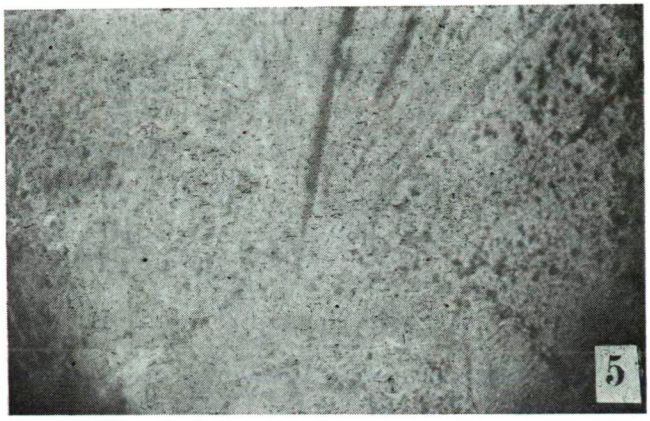

Fig. 5. Radiating structure of pyrolusite developing from the cryptomelane banding. Sandur, Karnataka. Polished section, ×70

TRACE ELEMENTS AND THEIR DISTRIBUTION

Four samples have been analysed for trace elements and the concentrations of the elements is given in ppm in the Table 2.

TABLE 2

Sample No.	847	829	997	954
Co	9	106	ND*	ND*
Ni	8	43	ND*	ND*
V	36	140	ND*	2
Cr	82	190	>1000	>1000
Y	4	8	17	3
Cu	800	>1000	23	300
Ga	31	3	ND*	6
Pb	32	147	ND*	ND*
Sn	26	64	78	63

ND* = Not detected.

Co and Ni

According to Dana [1959] the two elements Co and Ni are present together in most of the primary deposits, yet supergene processes result in their separation. The total absence of these two elements in the secondary deposits (sample Nos. 997 and 954) is the result of intensive supergene processes. Ni and Co were generally absent in the minerals of cryptomelane [SUPRIYA ROY, 1966].

Cu, Pb and V

Considerable amounts of these elements have been detected in coronadite [DANA, 1959]. This is true with the sample Nos. 847 and 829 in which coronadite is found by X-rays. However, the presence of a little Cr may be due to the replacement of Mn by Cr in coronadite.

Cu and Cr

SREENIVAS and ROY [1961] made observations on the cation exchange in some manganese minerals by electrodialysis and as a result they found replacement of K^+ by Cu^+ and replacement of a part of the Mn^{4+} by Cr^{3+} giving internal compensation for the loss of K^+. Applying these experimental results to the natural formation of minerals it is possible of higher concentration of Cr and Cu in the sample Nos. 997 and 954. Moreover there is a close resemblance in the ionic sizes of Mn^{4+} and Cr^{3+} ($Mn^{4+}=0.60$; $Cr^{3+}=0.63$).

Yttrium

Yttrium is present in small amounts (mostly $<0.01\%$) in jacobsite, manganosite, in collodial pyrolusite and cryptomelane.

PARAGENESIS

Manganese was originally deposited as MnOOH and then transformed to various oxides as it is metamorphosed. The scheme of transformation is given below.

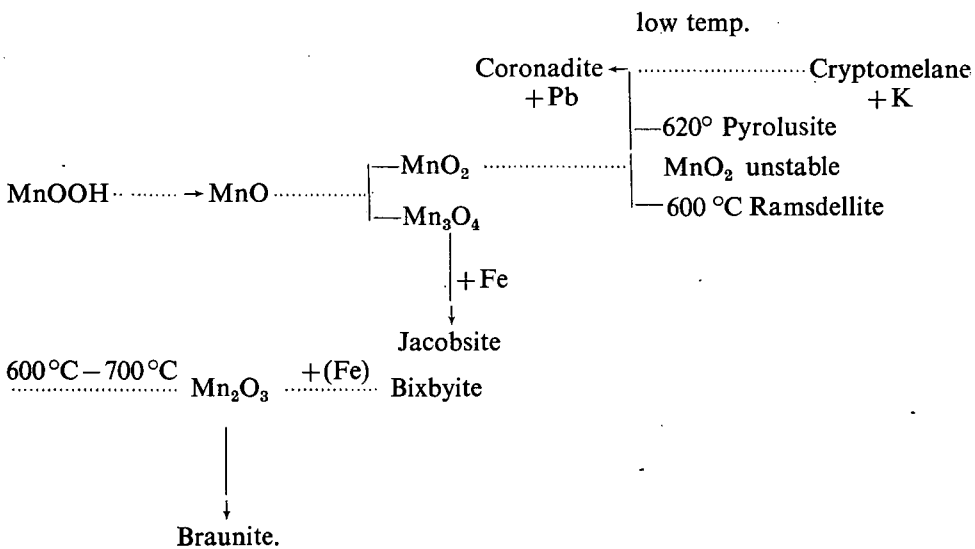

As shown in the above the MnOOH after dehydroxylization gives manganosite, this mineral oxidized with active oxygen and forms $MnO_2+Mn_3O_4$.

The MnO_2 forms different minerals at different temperatures leaving behind, the unstable MnO_2. However, either alteration of the minerals like pyrolusite cryptomelane and ramsdellite etc., or de-oxidation of unstable MnO_2 forms Mn_2O_3 braunite, bixbyite with Fe and other minerals.

The various manganese minerals were worked by supergene processes and the most important mineral in the deposit is the cryptomelane. It may be stated the manganese mineralization is sedimentary metamorphic and have undergone supergene enrichment.

ACKNOWLEDGEMENTS

We are thankful to the Geological Survey of India for sparing some typical samples from Sandur. The Director, National Geophysical Research Institute, Hyderabad (India) is thanked for facilitating us, to do the trace elemental determination.

We acknowledge PROF. G. H. MOH, Mineralogisch-Petrographicsches Institut, Heidelberg, West Germany, for carrying out the X-ray analyses.

The financial assistance of U.G.C. is also greatly acknowledged.

REFERENCES

DANA, E. S. [1959]: A Text Book of Mineralogy. 4th ed. Asia Publishing House, Bombay—Calcutta—New Delhi.

DIXIT, R. L. N. [1976]: Proceedings of the First Symposium on the Geology, Exploration, Mining, Mineral Processing and Metallurgy of Ferrous and Ferro-Alloy Minerals. (Abstr.) Bangalore, Karnataka (India)

FERMOR, L. L. [1909]: Manganese Ore Deposits of India. Mem. Geol. Surv. India **37**.

MASON, BRIAN [1966]: Principles of Geochemistry. 3rd ed. John Wiley and Sons Inc. New York—London Sydney.

NAGANNA, C. [1976]: Proceedings of the First Symposium on the Geology, Exploration, Mining, Processing and Metallurgy of Ferrous and Ferro-Alloy Minerals. Bangalore, Karnataka (India).

RAMDOHR, P. [1969]: The Ore Minerals and their Intergrowths. 3rd ed. Pergamon Press, Oxford—London.

ROY, SUPRIYA [1966]: Syngenetic Manganese Formations of India. Jadavpur University, Calcutta.

SREENIVAS, B. L. and R. ROY [1961]: Observations on cation Exchange in some Manganese Minerals by Electrodialysis. Econ. Geol., **56**, 198—203.

Manuscript received, March 20, 1979

J. S. R. KRISHNA RAO,
B. VENKATA NAIDU
and
K. WISWESWARA RAO
Dept. of Geology, Andhra University
Waltair-530 003, India

Acta Mineralogica-Petrographica, Szeged, XXIV/1, 99—111, 1979

THERMAL DEGRADATION OF THE OIL SHALE KEROGEN OF PULA (HUNGARY) AT 473 AND 573 K

M. HETÉNYI

INTRODUCTION

The burial of the organic matter of sediments, the change of environmental parameters and mostly the increase of pressure and temperature produce the continuous transformation of the organic matter. The experiences on the processes taking place in nature, the theoretical considerations as well as the simulation experiments carried out in laboratories allowed the conclusion that the decisive parameter of the evolution of organic matter of sediments is the temperature. As to our knowledge the role of pressure is less significant.

Though the transformation is continuous, it can be divided into three phases without sharp boundaries on the basis of the nature of processes and of the type of the predominating products. The first phase, i.e. the main process of diagenesis, is an insoluble three-dimensional organic compound of complex great molecule; the formation of kerogen takes place partly by microbiological partly by chemical processes, first of all by polycondensation. The degradation of the complex molecule starts already at the end of this phase; the second phase will be the thermal degradation, i.e. the main process of katagenesis as a result of which oil and gas will be produced. During the metagenesis taking place in great depth first of all methane develops. The end-product of this evolution is anthracite or graphite.

The process is governed by the regularity that a given system tries to be in equilibrium with its environment. The system reacts to the changes of the environment with the suitable transformations. The equilibrium between the organic matter of the sediment and the enviroment is interrupted due to the burial and to the increase of pressure and temperature. The kerogen having got the new conditions is able to create an equilibrium with the new physico-chemical parameters if it will be ever more ordered, if it approximates ever more the graphite structure. Thus it is necessary that the H/C ratio should be decreased, the system should be evolved to a more coalified, more aromatic one. One of the factors of approaching the end-state (the graphite structure) is that due to the steric hindrance the cyclic components of the macromolecule, the nuclei of the units constituting the kerogen itself try to an arrangement lying parallel with the surface [TISSOT et WELTE, 1978]. Consequently, the units hindering this arrangement (aliphatic chains, hetero-atomic bonds) will be gradually eliminated. The authors above outlined the process of degradation as follows: the most sensible sites of degradation are the bonds containing hetero-atoms, especially oxygen. The carbonyl and carboxyl groups are extremely instable. Thus, during diagenesis the thermal degradation is started by the break of these

bonds. As a result of this H_2O and CO_2 are released, further smaller structural units are broken off the macromolecule which become the main components of bitumens. The greater fragments formed by this process contain mostly hetero-atoms, i.e. oxygen (resins, asphaltenes, BAM-bitumen). During katagenesis the increase of temperature results in the break of different types of bonds partly in the kerogen, partly in the bitumens produced by the preceding process. The fragments produced in this way are for the most part hydrocarbons. This phase is called by VASSOEVICH [1969] the main phase of oil formation. In the remaining kerogen the C-content and the relative quantity of the aromatic compounds is gradually increasing as it is evidenced by the elementary and IR-analyses. In the phase of metagenesis, after the release of less stable groups such a poly-condensed nucleus remains which is unable to hydrocarbon generation.

The experimental simulation of natural thermal degradation may provide assistance to discover the process of genesis, the reaction mechanism taking place in nature. Since it is impossible to simulate the long geological periods, the reaction rate is increased by the increase of temperature. The artificial "maturation" of a relatively immature kerogen under known laboratory conditions seems to be the most expedient way and then to compare it with the deeper-lying samples of a given basin. This problem has been studied by numerous researchers and many of them dealt with the thermal degradation of the oil shale kerogen. When taking into consideration the fact that the main though not only mode of industrial utilization of the oil shale is to convert the organic matter to oil during thermal treatment, this interest seems to be obvious. The usual temperature of conversion lies between 743 and 823 K, thus a group of authors studying the industrial utilization investigated the evolution process in the temperature range of 773 ± 100 K. By means of the lower temperature degradation (473–623 K) the type of organic matter, its gas and oil potential, the mechanism of the degradation process as well as its kinetics can be investigated. From the point of view of the industrial utilization the possibility of the in situ processes called the attention to the lower temperature degradation. This procedure may provide a more economic production than the usual retorting technique.

The major part of author believes the degradation mechanism of the oil shale kerogen to consist of two processes at least. As a first step the kerogen is transformed into bitumen and after further heating shale oil will be produced. The process is accompanied by gas generation and a part of kerogen remains in solid state. FRANKS *et al.* [1922] having registered the formation of sulfur-smelling gas and water as well of bitumen from the oil shale heated between 573 and 623 K and having observed the darkening of the oil shale, came to the conclusion that the kerogen of the oil shale consists of two types of matter. One of them is the so-called oil-producing matter from which the bitumen and with the subsequent transformation of it the oil are generated. The other type is the coal-producing matter from which the coal is developed.

CARLSON *et al.* [1937] investigated the gases produced from the Green River oil shale during the thermal treatment between 523 and 623 K and stated that the gas formation takes place in two stages, i.e. in the initial phase due to the decomposition of kerogen, in the second phase due to the cracking of bitumen.

The main components of the gas-state products are CO_2 and CH_4 at lower temperature (i.e. around 473 K), and C_4-C_{12} hydrocarbons at higher temperatures (i.e. around 573 K). After the statement of HOERING and ABELSON [1963] the C-isotope ratio of the gas-state products developed from kerogen is similar to that of the

natural gases related to the crude oil. These observations allow to transmit the results of laboratory experiments to the natural processes.

The more particular investigation of the degradation mechanism resulted in the further refinement of the two-stage degradation. VITOROVIČ and JOVANOVIČ [1968] believe that during heating (573–673 K) the oil shale is transformed into insoluble bitumen and this process is accompanied by CO_2 and H_2O loss. Further heating produces soluble bitumen and this is accompanied by H_2S and CO_2 loss. Then the soluble bitumen is cracked to oil.

According to CANE [1951] the degradation mechanism of kerogens of algal origin is as follows:

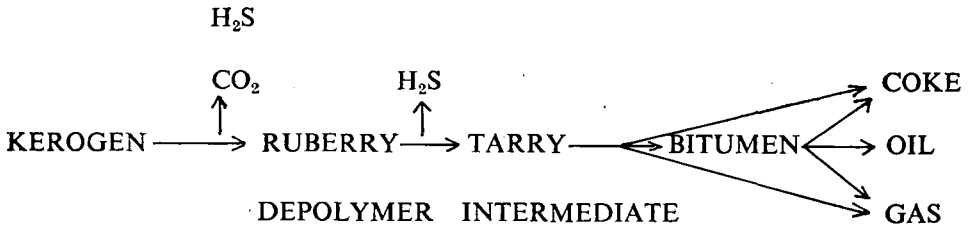

This mechanism was experimentally evidenced by the thermal degradation of the Australian torbanite.

Most of the authors believe the process to be kinetically a first-order reaction (DIRICCO, 1956; GIRAUD *et al.*, 1970; WEITKAMP *et al.*, 1970] or a pseudo-first-order reaction [CANE, 1948, 1976] emphasizing that this is an extremely complex process the mechanism of which are insufficiently explained so far.

In this work the thermal degradation of the kerogen of the oil shale of Pula (Hungary) was investigated at 473 and 573 K in neutral gas atmosphere, heating the samples in different durations. The produced bitumen was extracted, its quantity was determined, and the detailed investigation will be neglected here. The characterization of the non-converted kerogen will be comprehended below, and the results of reaction kinetic computations will be described, respectively.

EXPERIMENTAL

Preparation of the sample

The samples to be investigated are oil shales from Hungary, formed in the Pliocene, its precursor is the *Botryococcus braunii* KÜTZ. It was formed in saline water in a crater lake of 283—285 K [JÁMBOR and SOLTI, 1976]. The air-dry sample was ground to the grain size of 0.05—0.15 mm. The moisture, ash, CO_2 and organic carbon contents were determined (see Table 1). The soluble organic matter was extracted in Soxhlet extractor by means of chloroform (BIT-A), then by the mixture of benzene—acetone—methanol of 75:15:15 ratio (BAM-bitumen). Kerogen was separated from the inorganic components by differences in specific gravity, i.e. by physical accumulation. Table 1 shows the degree of purity (ash content, CO_2) of the kerogen as well as the data characteristic of the organic matter content (C_{org}). Though the ash content of kerogen is rather high, i.e. 9 percent, it has been believed that it would be more expedient to investigate a less pure concentrate which has undergone no chemical effect during the isolation procedure since this will provide the possibility to make comparison with the more diagenized samples of the basin.

TABLE 1

Some organic and inorganic data of the oil shale and kerogen

	Oil shale	Kerogen
Ash %	49,9	9,0
CO_2 %	9,5	2,2
C_{inorg} %	2,6	0,6
Bit-A %	3,3	—
BAM %	1,3	—
C_{org} %	27,4	70,2

Thermal degradation method

5—10 g of the kerogen prepared in the afore-mentioned way was weighted into glass-boat and was put into ignition glass tube. The heating of the ignition tube was carried out in a furnace equipped with programmed heating. The system was thoroughly washed with nitrogen at room temperature, then it was heated at 473±5 resp. 573±5 K during one, seven and fourteen days under continuous nitrogen flow. The gas-state products were not retained. Fluids (water, and occasionally oil) were condensed in air-cooled trap. The sample was cooled to room temperature also under nitrogen flow. The solid rest was extracted in the mixture of benzene:acetone:methanol in Soxhlet equipment in order to determine the H/C ratio and quantity of the bitumen formed during degradation. The solid matter remained after extraction (unconverted kerogen) was dried at 333 K.

The effect of thermal treatment on the unconverted kerogen has been characterized by the H/C ratio, by the volatile material ratio and by the C_R/C_T ratio.

The determination of the hydrogen and carbon contents was carried out in CHN-1 analysator.

The volatile material ratio equals to the material loss at 773 K heated during 30 minutes in inert atmosphere referring to unit carbon, according to the ASTM Standard (Standard Methods of Laboratory Sampling and Analysis of Coal and Coke D271—48 in 1952, Book of ASTM Standard, 1952).

The C_R/C_T ratio was adapted by GRANSCH and EISMA [1966] from coal chemistry to characterize the organic matter of the sediments. The value of the quotient is determined by the type and diagenesis degree of the organic matter. If one of these factors is the same in all samples to be compared, the deviation of the quotient is caused only by the other parameter. Adapting the procedure applied in coal chemistry, the samples were pyrolized at 1173 K during 90 minutes under nitrogen atmosphere and the carbon content of the original material (C_T) and of the thermally treated sample (C_R) was measured. The kerogen investigated by us is immature and is far of the coalified state, consequently, the treatment at lower temperature seemed to be suitable to its characterization. The oil shale samples were heated at 573, 773, 873 and 1173 K and the C_R/C_T ratio was determined at each temperature. It has been found that thermal treatment ought to be carried out at 773 K (or maximum at 873 K) in order to compare the samples of the same degree of diagenesis from the point of view of comparison of the organic matter contents [HETÉNYI *et al.*, 1977]. In the present measurements we started from a given kerogen concentrate which has been artificially "matured" during the experiments. Thus, the type of the organic matter is the same and from the quotient conclusions can be drawn to the degree of diagenesis. To choose the temperature 773 K is verified also by the

fact that in the low temperature thermal degradation (423—623 K) of the Green River oil shale kerogen taken as basis for comparison CUMMINS *et al.*, [1974] used to characterize the unconverted kerogen the "carbon residue ratio". This represents the amount of carbon residue formed at 773 K per unit of organic carbon.

Results

The conversion of the organic matter of oil shale into oil takes place at about 743—823 K under industrial conditions. The process of degradation, however, starts at much lower temperature. Nevertheless, depending on the temperature applied and on the duration of degradation the composition of products will change and the structure of the unconverted kerogen will more or less change as compared to the original untreated kerogen. In our laboratory experiments considerable quantity of gas has developed from the organic matter degraded at 473 and 573 K during one, seven and fourteen days, since the first moments of the thermal treatment. Small quantity of water, resp., at 573 K small quantity of oil also developed which were condensed already to the effect of air-cooling in the flask fitted to the outlet of the ignition tube. The colour of kerogen deepened from the original ochre-yellow: first it became lighter than darker brown. The gases were not analyzed, in order to obtain information these were transported through a tube filled with soda-asbest. From fading it has been registered that relatively great amounts of CO_2 were developed. The gas formation can be followed since the start of the process, the gas quantity has perceptibly decreased in the course of the process.

The quantity of water and oil is very small. The pH-value of water proved to acid in general (i.e. 3 to 5). At 473 K no oil formation was observed. At 573 K slight oil film developed during one day, during seven, resp., fourteen days a drop of dark-brown oil of high H/C ratio (1.91) was formed. On the basis of the IR-spectra of the oil, it contains long-chain oxygen-bearing compounds.

After the thermal treatment the solid phase was extracted again. Since during preparation the originally present soluble organic matter was removed, the repeated

TABLE 2

Quantity and composition of BAM-bitumen

Heating time (days)	BAM-bitumen			
	Quantity %	C %	H %	Atomic H/C ratio
0 (Original oil shale)	1,3	70,2	10,3	1,76
		473 °K		
1	2,5	74,6	10,9	1,75
7	0,8	62,8	8,7	1,69
14	0,7	67,9	9,6	1,69
		573 °K		
1	1,9	—	—	—
7	0,8	69,7	9,7	1,67
14	0,8	76,5	10,6	1,66

extraction produced the thermally developed bitumen. The quantity of the so-called BAM-bitumen formed during the thermal degradation of kerogen at 473 and 573 K and being soluble in the mixture of benzene:acetone:methanol of 75:15:15 ratio can be seen in Table 2 in percentage of the starting kerogen. The quantity of bitumen formed during degradation is remarkable: after one-day treatment 2.5 percent at 473 K resp. 1.9 percent at 573 K. Our paper does not aim the particular investigation of the formed soluble organic matter, the quantities of the BAM-bitumen was determined only in order to characterize the quantitative relations of the converted and unconverted organic matter, resp., to study the reaction mechanism itself. In first approximation this fraction was characterized by the atomic H/C ratio. According to the data of Table 2 considerable change follows in the quantitative relationships of the bitumen fractions after one and seven days. After the thermal treatment of seven and fourteen days only 30—40 percent of the bitumen produced during one day remains, the other part is degraded. It is worthy of mention that after the seven-day treatment and under the applied experimental conditions the quantity of the extractable BAM-bitumen remains constant independently of the time and temperature, i.e. about 0.8%. At the same time, the atomic H/C ratio proves to be relatively the same both at 473 and 573 K and both during seven and fourteen days, i.e. 1.69 resp. 1.66—1.67.

The atomic H/C ratio of the extracted bitumen is 1.75 after the treatment at 473 K and during one day, i.e. it shows the same value as the original oil shale (1.76). Though the decrease of the H/C value is rather slight, when taking this into account together with the quantitative relations this may lead to the conclusion that at the given temperature the part of the primary bitumen formed from kerogen was further degraded as a secondary process. Also during the degradation of the bitumen the components rich in hydrogen were first removed, thus the remaining soluble organic matter becomes somewhat more "coalified".

It seems so that under the applied experimental conditions the equilibrium follows in this phase of degradation during seven days; the bitumen production is presumably continued and at the same time the formed bitumen is degraded again.

TABLE 3

Properties relating differences in the kerogen of the heated residues

Heating time (days)	C %	H %	Atomic H/C ratio	Volatile material ratio	C_R/C_T
0	70,2	10,3	1,76	128	0,07
			473 °C		
1	71,3	10,0	1,68	115	0,11
7	73,1	9,6	1,58	106	0,14
14	69,4	9,0	1,55	107	0,21
			573 °K		
1	70,7	9,7	1,65	106	0,20
7	71,1	9,1	1,53	100	0,23
14	72,6	8,8	1,45	87	0,28

The decrease of the perceptible gas products in this phase as well as the facts above relate to the formation of other types of compounds during the secondary degradation of the formed bitumen, and to the restricted measure of bitumen formation and degradation as compared to the first phase of the process, respectively.

The unconverted kerogen remained after the removal of the soluble thermal fraction has been characterized by its H/C ratio, volatile content and C_R/C_T ratio. These data are in close relationship with the structure of the kerogen. The H/C ratio expresses the number of H-atoms per C-atoms, i.e. it is the measure of the saturation of the system. The volatile material ratio, i.e. the quantity of the components mobilized at 773 K (gas, water, oil) referring to the unity organic carbon, may reflect the state of condensation of the system. If kerogen is built up by strongly condensed cyclic structures, small quantity of volatile material will be released. In our case the C_R/C_T ratio, or the degradation factor [GIRAUD, 1974] shows the degree of diagenesis. The carbon and hydrogen contents, the H/C ratios, the volatile material ratio as well as the degradation factor of the original kerogen and of the unconverted kerogen degraded at 473 and 573 K during one, seven and fourteen days are comprehended in Table 3.

The degradation factor of the studied original kerogen is very low (0.07). The organic matter is immature and is of high H/C ratio (1.76). According to other gradual degradation experiments proceeded by $KMnO_4$ it was produced mostly by straight-chain fatty acids and is a highly polymerized organic macromolecule, the proportion of the aromatic constituents can be neglected.

In the course of the simulation experiments by means of which only the effect of time and temperature tried to be investigated disregarding the other factors, the degradation factor is definitely growing. At both temperatures the value shows slight rise between one and seven days, between seven and fourteen days the rise is steeper *(Fig. 1)*. The two curves are nearly parallel with each other, i.e. at 473 K

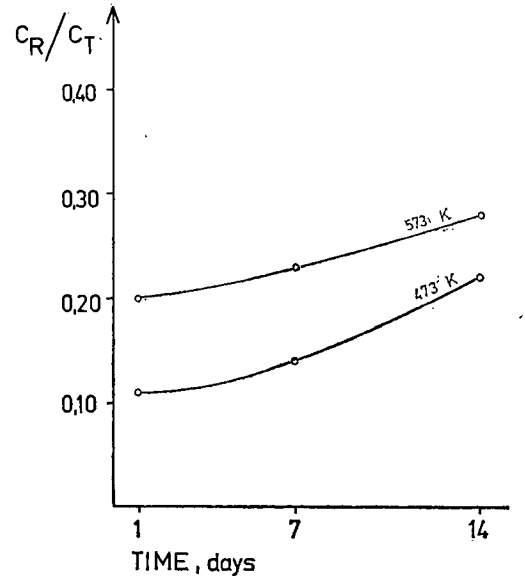

Fig. 1. Change of the C_R/C_T ratio during the heating period

the time dependence of the C_R/C_T value is similar. As a function of the duration of thermal treatment the H/C ratio shows slight decrease *(Fig. 2)*. The change is somewhat more expressed at 573 than at 473 K.

Regarding the absolute values of the two quotients, of the degradation factor as well as of the atomic H/C ratio, a relatively immature kerogen remains after the simulation experiments. On the basis of these quotients the thermally treated organic matter can be qualified also as alginite kerogen. The H/C and at 1173 K the C_R/C_T values are 1.4—1.8 resp. 0.09—0.27 in case of the alginite kerogen [GRANSCH and EISMA, 1966]. The same values of the unconverted kerogen comprehended in Table 3

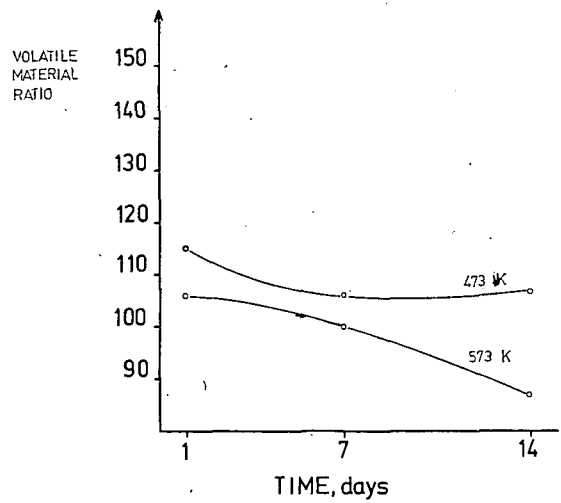

Fig. 2. Change of the volatile material ratio during the heating period

are within the given limits, especially when taking into consideration the lower temperature at which the degree of degradation was measured (773 K). During this relatively short low-temperature degradation process the oil shale kerogen of Pula did not reach the state of the humic coals where the C_R/C_T (measured at 1173 K), resp., the H/C ratio would be 0.60—1.00 resp. 1.4—0.4. To reach these values higher temperature is needed. At 573 K the increase of duration would produce, further degradation. During the thermal degradation carried out with the Green River oil shale the change of the H/C ratio is similar: at 473 K after 90-days thermal treatment 1.31, after 360 days 1.21. At 573 K this value decreased from 1.38 to 1.25 during 0.5 and 4.0 days [CUMMINS *et al.*, 1974].

The proportion of the volatile material decreases between one and seven days at 473 K *(Fig. 3)* and remains unchanged between seven and fourteen days. At the same time, at 573 K the whole process shows a decreasing tendency, moreover between seven and fourteen days this tendency becomes more expressed. Apparently, at 473 K the measure of condensation of the sample hardly changes as a function of time. The less stable groups are released already at the beginning of thermal treatment in form of gas and occasionally of small quantity of water. Equilibrium follows in the bitumen formation. The decrase of the quantity of the unconverted material is continuous. The further degrading part of the forming bitumen is released also in form of gas. The measure of degradation is slight, thus the measure of conden-

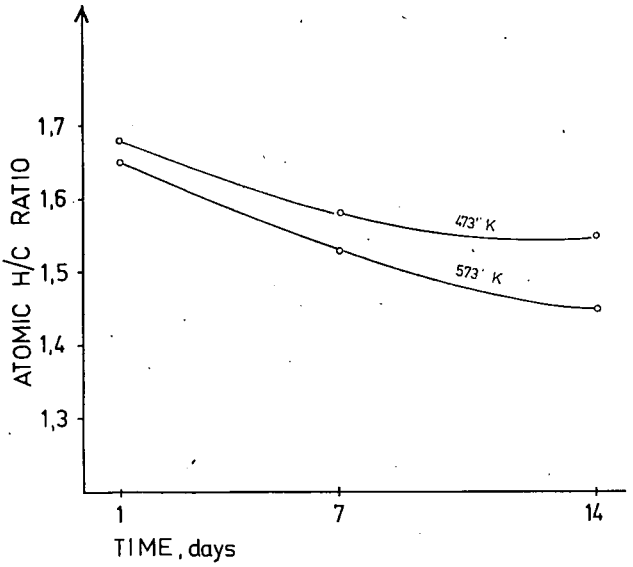

Fig. 3. Change of the atomic H/C ratio during the heating period

sation of the unconverted kerogen hardly differs from that of the original kerogen. At 573 K the degradation becomes more expressed, after seven days small quantity of oil has also developed. Both the formation and the further transformation of the bitumen increased. The oil consists of long-chain compounds which derive from the kerogen itself through the bitumen. By means of the break of longer-chain peripheric units the kerogen becomes relatively more condensed, thus the proportion of the volatile material decreased. These experiences are in harmony with the measurements of CUMMINS *et al.* [1974] mentioned above, i.e. the proportion of volatile material of the Green River oil shale degraded at 473 K is relatively constant as a function of the duration of degradation and at 573 K definite decrease can be observed. In case of the oil shale kerogen of Pula the volatile material is less in its proportion at 473 K but definite decrease has been measured. This deviation can also be attributed to the less mature state of the oil shale of Pula.

The thermal degradation of oil shale kerogens proceeding at lower temperatures is a reaction consisting of numerous complex part-processes. Regarding kinetically the whole of the process the reaction is first-order [DIRICCO, 1956; HUBBARD and ROBINSON, 1950; CUMMINS and ROBINSON, 1972], or pseudo-first-order, at least [CANE, 1976].

Consequently, the temporal change of kerogen concentration is as follows:

$$-\frac{dc}{dt} = kt$$

When taking the starting quantity of organic matter as unit, and when the quantity of degraded kerogen is x at any t time, the quantity of the unconverted kerogen will

be: $1-x$. Integrating the equation above and substituting these values, the equation of a straight line will be obtained:

$$-k = \frac{2.303 \log (1-x)}{t}$$

When plotting $\log (1-x)$ as a function of time, a straight line ought to be obtained if the reaction is a first-order one. The specific reaction rate, "k", can be computed from the rise of the straight line.

In Table 4 the quantity of the converted kerogen degraded at 473 and 573 K during one, seven and fourteen days, that of the unconverted kerogen $(1-x)$ as well as the logarithm of the latter are demonstrated. When plotting these values *(Fig. 4)* a straight line has been obtained at both temperatures. The rise of these lines were determined and the k-values were computed. At 473 K $k=5.31 \cdot 10^{-2}$/day; at 573 K $k=8.86 \cdot 10^{-1}$/day. As a result of a temperature increase of 100 K the specific reaction rate has increased by about 17-times.

TABLE 4

Quantity of the converted and unconverted organic matter and the specific reaction rate

SAMPLE	Temperature (K)	Time (days)	x	$1-x$	$\log (1-x)$	k (per days)
OIL SHALE	473	1	0.076	0.924	−0.0343	$3.18 \cdot 10^{-1}$
		14	0.114	0.886	−0.0526	
KEROGEN	473	1	0.027	0.973	−0.0119	
		7	0.030	0.970	−0.0132	$5.31 \cdot 10^{-2}$
		14	0.033	0.967	−0.0146	
	573	1	0.122	0.878	−0.0565	
		7	0.170	0.830	−0.0799	$8.86 \cdot 10^{-1}$
		14	0.217	0.783	−0.1059	

When comparing the values determined in this way with those computed by CUMMINS and ROBINSON [1972], i.e. at 473 K $k=2.4 \cdot 10^{-4}$/day and at 573 K $k=2.9 \cdot 10^{-2}$/day, it can be seen that the specific reaction rate of the kerogen investigated by us is greater at both temperatures. Especially great difference is found at lower temperature. This can be explained by the fact that the oil shale kerogen of Pula is rather immature as evidenced also by the measurements, thus a lot of groups of weaker bonds is connected to the matrix which break off rapidly at relatively low temperature. The process was accompanied by intense gas formation, very small quantity of water was observed, resp., considerable quantity of bitumen was formed. When increasing the temperature the stronger bonds could also be affected by the thermal degradation, consequently taking the k-values at 573 K of the kerogens of Pula and of Green River the differences are smaller.

At this temperature the kerogen is degraded into bitumen but during the sequent degradation not only water and gas develop, but small quantity of oil co-subuld also be observed.

By means of the thermal degradation experiments the conversion the insoluble organic matter itself, i.e. of the kerogen had to be investigated, thus it was separated from the inorganic components. The measurements of CUMMINS and ROBINSON

[1972] were carried out on oil shale and not on kerogen. The presence of the inorganic components has presumably effect on degradation, i. e. it may change the rate of it. Consequently, the comparison of the values concerning the Green River oil shale and the kerogen analyzed by us is not exact. To support our assumption the oil shale of Pula has also been thermally degraded at 473 K, i.e. at the temperature where

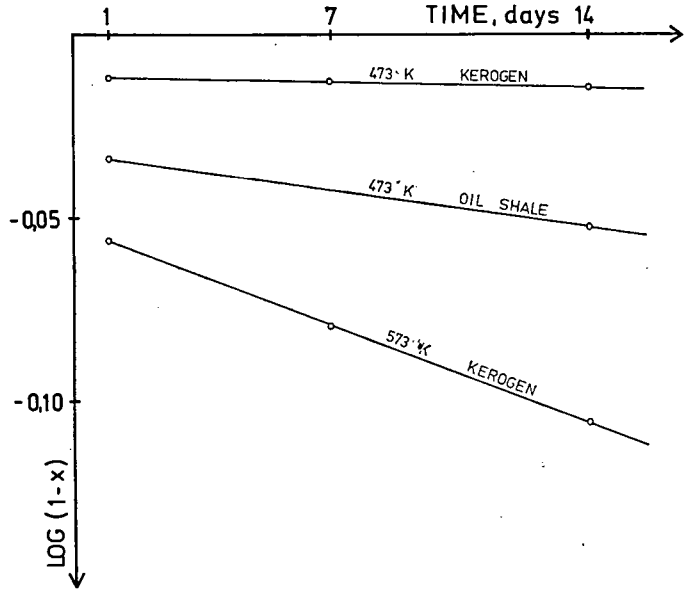

Fig. 4. First-order plot for 473 and 573 K data

the greater difference has been observed in the k-values. The $\log(1-x)$ — time relation is plotted in *Fig. 4,* then having determined the rise of the curve the k-value was computed: $k=3.18 \cdot 10^{-1}$/day. As a result of the effect of inorganic components the specific reaction rate increased by more than one order of magnitude.

SUMMARY

The thermal degradation of the oil shale kerogen of Pula (Hungary) was investigated at 473 and 573 K during one, seven and fourteen days in neutral gas atmosphere. The degradation mechanism, the structural changes of the unconverted kerogen were investigated as well as kinetic computations were carried out.

The organic matter of the original oil shale is a complex macromolecule formed from algal fatty acids, the proportion of its aromatic components is low.

In the course of thermal degradation considerable quantity of bitumen developed, the further decomposition of which produced gas-state compounds at 473 K and small quantity of oil at 573 K. The quantity of the extractable bitumen is independent of time and temperature after seven days, of course under the given experimental conditions. Equilibrium follows in the formation and decomposition. The atomic H/C ratio, i.e. the type of bitumen shows considerable differences after one day, after the thermal treatment of seven, resp., fourteen days it is practically the same.

As a result of thermal treatment first the least stable groups, the short-chain units are broken off, this is manifested in the intense gas formation since the start of the reaction. This is followed by the degradation of the longer-chain peripheric compounds: the main phase of formation of the bitumen fraction. After one day the role of secondary processes increases as a function of time until the formation and degradation of bitumen get the equilibrium. In the course of the secondary degradation also the hydrogen-rich components are first eliminated, the atomic H/C ratio decreases, but this "coalification" is of very small measure.

The formation of gas, water and oil takes place directly from the kerogen or through the bitumen state. Simultaneously, structural changes are taking place in the kerogen molecule which result in the increase of its condensed state and coalification.

On the basis of the atomic H/C ratio and of the degradation factor the original kerogen is immature, and after maturation followed during the thermal treatment and measured by the parameters above it does not reach the state of humic coals and lignites, either. The character and measure of change are similar to those measured in the simulation experiments of the Green River oil shale. The difference showing in the values of quotients can be attributed to the less mature state of the oil shale kerogen of Pula. For the same reason, the proportion of the volatile material at 473 K does not depend on the duration of thermal treatment of the Green River oil shale, while in case of the kerogen of Pula the increase of duration of thermal treatment is accompanied by slight but definite decrease of this proportion. It is assumed that the less stable groups of the immature kerogen are able to gradual elimination already at this relatively low temperature while in case of more mature oil shale the degradation follows only at higher temperature (573 K). The thermal energy of 573 K is suitable to activate the structural units in respect of which no considerable difference exists between the two materials. Thus, at this temperature the volatile material ratio decreases in both samples as a function time, i.e. the sample became more condensed.

From the kinetic point of view the thermal degradation is a first-order reaction. The specific reaction rate is $5.31 \cdot 10^{-2}$/day at 473 K. As a result of the temperature increase of 100 K this value increases by about 17-times, i.e. at 573 K it is $8.81 \cdot 10^{-1}$/day. Both values are higher than the corresponding values of the Green River oil shale. As it has been demonstrated by the data concerning the structural characteristics of the unconverted kerogen (H/C, C_R/C_T, proportion of volatile material) the thermal behaviour of the two samples differs first of all at low temperature (473 K) just due to the structural features. This difference is shown also in the results of the kinetic computations, especially when the kerogen of the oil shale Pula is not isolated but the oil shale itself is degraded. In this case, presumably due to the catalytic effect of the inorganic components the reaction rate increases, the specific reaction rate will be $3.18 \cdot 10^{-1}$/day at 473 K.

ACKNOWLEDGEMENT

The author expresses her gratitude to Dr. Á. Jámbor making available for her the samples investigated.

REFERENCES

Cane, R. F. [1948]: The chemistry of the pyrolysis of torbanite. Journal et Proceedings, p. 62—68.
Cane, R. F. [1951]: The mechanism of the pyrolysis of torbanite. — In: Oil shale and cannel coal, 2, Institute of Petroleum, London.

CANE, R. F. [1976]: The origin and formation of oil shales. — In: Oil shale, edited by T. F. YEN and G. V. CHILINGARIAN. Elsevier Scientific Publishing Company, p. 27—61.
CARLSON, A. J. [1937]: Inorganic environment in kerogen transformation. — In: W. E. ROBINSON of Mines Research, 7968, p. 40.
CUMMINS, J. J., F. G. DOOLITTLE and W. E. ROBINSON [1974]: Thermal degradation of Green River kerogen at 150° to 350 °C. Composition of products. BuMines RI 7924, p. 18.
CUMMINS, J. J. and W. E. ROBINSON [1972]: Thermal degradation of Green River kerogen at 150° to 350 °C. Rate of product formation. BuMines RI 7620, p. 15.
DIRICCO, L. and P. L. BARRICK [1956]: Pyrolysis of oil shale. Industrial and Engineering Chemistry, Vol. **48**, No. 8, p. 1316—1319.
FRANKS, A. J. and B. D. GOODIER [1922]: Preliminary study of the organic matter of Colorado oil shales — In: W. E. ROBINSON and K. E. STANFIELD: Constitution of oilshale kerogen: Bibliography and Notes on Bureau of Mines Research, 7968, p. 39—40.
GIRAUD, A. [1970]: Application of pyrolysis and gas chromatography to geochemical characterization of kerogen in sedimentary rock. AAPG Bulletin **54**, No. 3, p. 439—455.
GRANSCH, S. A. and E. EISMA [1966]: Characterization of the insoluble organic matter of sediments by pyrolysis — In: Advances in Organic Geochemistry, edited by G. D. HOBSON and G. C. SPEERS, p. 407—427, Pergamon Press.
HETÉNYI, M., K. MAITZ and É. TÓTH [1977]: Contributions to the knowledge of the Hungarian oil shale kerogen I. Preliminary report on the results of the pyrolysis and selective oxidation. Acta Miner. Petr., **XXIII/1**, p. 165—175.
HOERING, T. C. and P. H. ABELSON [1963]: Annual report of the director of the Geophysical' Laboratory, 1962—1963, Carnegie Inst. Wash. Year Book, **62**, p. 229—234.
HUBBARD, A. B. and W. E. ROBINSON [1950]: A thermal decomposition study of Colorado oil shale. BuMines Rept. of Inv. 4744, p. 24.
JÁMBOR, Á. and G. SOLTI [1976]: Geological conditions of the Upper Pannonian oil shale deposit recovered in the Balaton Highland and at Kemeneshát (Transdanubia, Hungary) — Annual Report of the Hungarian Geological Institute of 1974. p. 193—220.
TISSOT, B. P. and D. H. WELTE [1978]: From kerogen to petroleum — In: B. P. TISSOT and D. H. WELTE: Petroleum formations and occurrence, Springer-Verlag, p. 148—184.
VITOROVIČ, D. K. and L. J. JOVANOVIČ [1968]: Solubility of Aleksinac oil shale kerogen III. Solubility of preheated kerogen. Glasnik Hemijskog Drustva, Vol. **33**, No. 8—9—10, p. 581—588.
WEITKAMP, A. W. and L. C. GUTHERLET [1970]: Application of a microretort to problems in shale pyrolysis. Ind. and Eng. Chem., Process Design. Development, v. **9**, No. 3, p. 386—395.

Manuscript received July 31, 1979

MISS DR. M. HETÉNYI
Institute of Mineralogy, Geochemistry
and Petrography
Attila József University
H-6701 Szeged, Pf. 428
Hungary

Acta Mineralogica-Petrographica, Szeged, XXIV/1, 113—124, 1979

SEVERAL FEATURES OF THE OIL SHALE AND OIL-SHALE-KEROGEN BITUMENS OF PULA (HUNGARY)

L. PÁPAY

ABSTRACT

In favour of determining the soluble organic matter of the oil shale of Pula according to the main chemical groups, bitumens were destructed to fractions by means of column chromatography, and each fraction was analyzed by infrared spectroscopy and C-H analysis, respectively. Similarly, the analysis of the soluble organic matter formed from the kerogen concentrate accumulated physically from the oil shale under thermal treatment, was also carried out. It is characteristic of all samples that these consist of oxygen-containing compounds, e.g. carbon-acid esthers, ketons and alcohols. Further, the long straight-chain hydrocarbons occur first of all in the hexane fractions in different quantities while the salts of carbon acid are contained mainly by the methanol fractions.

The original bitumen of the oil shale and the bitumen formed from kerogen concentrate after thermal treatment show the most striking difference that in the latter one aromatic compounds of small quantities are found while in the oil shale bitumens these are absent. To decide whether these aryl compounds were formed from the alkyl and cycloalkyl compounds due to the catalytic effect of clay minerals or were released from the kerogen matrix, or both effects play predominant role in the formation, further investigations are in progress.

INTRODUCTION

In Hungary economically negligible but abundant organic matter containing surficial outcrop was found in Transdanubia, in the environs of Pula, in 1973, as a filling matter of a basalt crater-lake [JÁMBOR, SOLTI, 1975]. The section most abundant in organic matter is found between 13.5 and 19.0 m. In the samples great quantities of the plankton alga *Botryococcus braunii* KÜTZING are found in addition to the rich spore-pollen content [NAGY, 1976]. According to the palynological and diatom analyses sedimentation took place in standing water of shallow depth. The temperature of water might be 283—285 K at the time of diatom flourishing, i.e. warmer than the recent climate. These diatomaceous formations were generated in the Upper Pannonian brackish phase [HAJÓS, 1976]. The chemical analyses indicated that the sedimentary rock of Pula can be qualified as a limy-clayey oil shale the organic matter of which is a highly polymerized kerogen of algal origin [ARATÓ and BELLA, 1976].

The abundant organic matter content of the oil shales of Pula provides favourable possibilities to extract relatively pure kerogen of greater quantity, consequently to carry out investigations aiming the determination of the peculiarities of the kerogen. Such analyses are e.g. to investigate the decomposition products of kerogen produced by temperature increase and by oxidation, and the results are suitable to draw conclusions to the original organic matter components of the oil shales. The kerogen of Pula being considered to be stable at the beginning of its thermal history was treated similarly as TISSOT *et al.* [1971, 1974] have treated the kerogen of the Toarcian shale of the Parisian Basin.

Nowadays it is generally accepted the most of the oil shales have been generated by algal accumulation. It has been evidenced that in different occurrences, i.e. in the Siberian balkhashite as well as in the Australian coorongite and torbanite the presence of the *Botryococcus braunii* is common [BLACKBURN and TEMPERLEY, 1936]. The polymerisation and film-producing oxidation of lipids are the chemical proves of the preservation of algae since the non-polymerized material is decomposed during the biological decomposition.

According to THORNE *et al.* [1964]: "Oil shale was formed by the deposition and lithification of finely divided mineral matter and organic debris in the bottom of shallow lakes and seas. The organic debris resulted from the mechanical and chemical degradation of small aquatic algal organisms."

The investigation results of the kerogen of oil shale of Pula of Upper Pannonian age and deriving from shallow depth provide the possibility to reconstruct the thermal history of kerogen deriving from boreholes of the Southern Great Plain, being of similar age but deriving from much greater depths. Further, taking into account the same age the role of burial depth can also be elucidated.

In literature other kinds of correlation methods are also known. The chemical analysis of the very young coorongite assumed to be the intermediary of the Australian torbanite promotes the cognition of composition of the kerogen [CANE, 1969]. The general model determined by means of mass spectrometry, pyrochromatography and of other methods is as follows: the structural backbone is a carboxylic acid terminating in long alkyl chains the chain consisting of ester and ionic functions, between the chains probably peroxide and hydroxyl groups are found. It is postulated that some of the cross links of macromolecules are oxygen bonds of ether-type. The hydrocarbon fractions of coorongite have been investigated in detail [DOUGLAS *et al.*, 1969]. Based on these investigations it is probable that the hydrocarbons of isoprene skeleton were produced by the chlorophyl of the *Botryococcus braunii* as a result of bacterial activity or autolysis. The same authors refer also to the fact that in the hydrocarbon fraction of the older Scotch torbanite and of the Scotch Westwood Shale also isoprene-skeletal alkanes were found and the latter one contains also the remains of Botryococcus braunii. The particular investigation of the hydrocarbon fractions is believed to be very important since this may throw light upon the formation conditions of the organic matter.

By all means, the results render probable the imagination that both the kerogen and the oil were produced by mixed lipid matter. In both of them the precursor is a material in which the difference of small measure in the structure produces very different behaviour during diagenesis and during the geological times produces different end-products. After the suitable burial period the intermediaries deriving from lipids of less ability to reactions are decomposed to oil-like molecules while from the more reactive members of the same groups produce inert kerogen through polymerisation and condensation reactions [CANE, 1976].

The analytical results of the soluble organic matter also contribute to know the inert and stable kerogen. In the non-reservoir old sediments the quantity of soluble matter amounts only to hundredth or tenth percent, in different oil shales this value is greater by an order of magnitude. In Table 1 the data of several foreign oil shale bitumen are demonstrated after YEN [1976] in addition to those of the oil shale of Pula.

Since the quantity and character of the soluble organic matter depends partly on the environmental effects and partly on the source matter, i.e. on kerogen, it

TABLE 1

Bitumen contents of some foreign oil shales and of the oil shale of Pula (Hungary)

Name and location	Age	Bitumen content (%)
Torbanite, Scotland	Permian	1.6
Green River, Colo. USA	Eocene	2.0
Alginite, Australia	Permian	1.2
Coorongite, Australia	Recent	46.0
Pula, Hungary	Pliocene	4.6

proved to be expedient to analyze the soluble fractions of the organic matter of the oil shale of Pula. The interpretation of the results is simplified by the fact that the starting organic matter is autochthonous.

EXPERIMENTAL

Analyses were carried out on the average sample (alginite) of the oil shale from the Pula-region. The air-dry sample was powedered down to less than 0.15 mm, in agate mill. The soluble organic matter was extracted in the Soxhlet-equipment first by chloroform (Bit-A), then by a mixture of benzene:acetone:methanol (70:15:15), (BAM-bitumen). The ratio of solvent/solid matter was 4:1. During the thorough extraction the solvent was changed several times. The extraction time was long: to remove the Bit-A of 3.3% on the average needed 80—90 hours, while the extraction of BAM-bitumen of 1.3% on the average needed 140—160 hours when starting from 50 g dry matter.

Though the Soxhlet-equipment is widely used in several countries to extract bitumens, it seems so that in case of a sediment of such abundant organic matter content the method of extraction should be changed. Some preliminary measurements were carried out, i.e. in three-necked boiling flask the solvent and the matter to be extracted (ratio 30:1) were simultaneously mixed and refluxed. By means of this method extraction time could be decreased to the tenth.

The crude extracts were fractioned on neutral alumina of III—IV activity by means of a rapid and simple method, i.e. of the suction column chromatography. (The principle of this procedure: chromatography is carried out by means of a suction flask under vacuum. The ratio of matter/adsorbent changed between 1:70 and 1:100, respectively. The material to be fractionated was carried on the column solved in hexan, resp., benzene. The solution of each fraction was followed in UV-light. The eluation of each fraction required several litres of solvent. The solution was condensed to 40—50 ml by means of distillation under decreased pressure. The remaining part was removed on steam-bath and in drying furnace at 343—353 K, respectively.)

The column chromatographic data of Bit-A and BAM-bitumens of the oil shale of Pula are demonstrated in Tables 2 and 3 below; the starting material quantities are 1.1390 and 1.1110 g, respectively. The data of the Tables indicate numerically the differences between the bitumens, the difference showing already in crude state. After the evaporation of the solvent Bit-A is solid, easily powderable and is light-brown colour, while BAM-bitumen is of brownish-black colour and slightly sticky. On the basis of the features of the extracting solvent it can be expected that the BAM-bitumen contains more polar material mixture than Bit-A. In fact, however,

TABLE 2

Column chromatographic results of Bit-A of the oil shale of Pula

Sign of the fraction	Denomination	Quantity (ml) of the solvent	Quantity (g) of the fraction	Proportion (%) of the fraction
a	hexane	5300	0.0730	6.41
b	hexane:benzene 1:1	5200	0.1120	9.83
c	benzene	6400	0.1790	15.71
d	chloroform	3700	0.2690	23.61
e	acetone	3400	0.1660	14.57
f	methanol	2750	0.0815	7.15
			0.8805	77.28

TABLE 3

Column chromatographic results of the BAM-bitumen of the oil shale of Pula

Sign of the fraction	Denomination	Quantity (ml) of the solvent	Quantity (g) of the fraction	Proportion (%) of the fraction
a	hexane	6200	0.0830	7.47
b	hexane:benzene 1:1	3000	0.0334	3.00
c	benzene	5000	0.0517	4.65
d	chloroform	3000	0.0850	7.65
e	acetone	4150	0.1489	13.40
f	methanol	3000	0.0850	7.65
			0.4870	43.82

the BAM-bitumen can be solved in chloroform under slight heating and this indicates that the solvent mixture dissolves the material bound more strongly at the grain's surface, but applying the suitable protic solvent mixture the soluble matter can be removed in one step. (In the literature several authors use only solvent mixtures.) It is characteristic of the chromatographed bitumen fractions that their colour is gradually deepened from the high yellow to different shades of brown. Most of the fractions are of ointment consistency at room temperature, the solid ones also melt below 373 K except the methanol-part. The composition of each fraction has been controlled by means of thin-layer chromatography. The silicagel plates of 10×20 cm (Kieselgel G nach STAHL) were activated during 2 hours at 393 K. The matter was dropped onto the starting point solved in chloroform. Development was made with benzene.

It is characteristic of the first three fractions of both the Bit-A and of the BAM-bitumen that these are mixtures of mostly apolar matter, the other fractions consist of polar compounds. The quality of the different matter was identified by means of IR-records. (The matter to be analyzed was washed down from the silicagel by means of suitable solvent, i.e. by KBr of spectroscopic purity. After evaporation of the solvent the KBr containing the matter can be pastilled and then the IR-record can be carried out.)

To determine the functional groups the spectra of the fractions of column chromatography as well as those of some spots of differing R_f value were recorded. Records were made by means of the IR-spectroscope UNICAM SP 200. In case

of solid matter the method of KBr pastilling (200 mg KBr+2 mg matter to be analyzed), in case of greasy fractions the film-technique were used. In the course of interpretation the designation of each vibration type was carried out after the HOLLY—SOHÁR—VARSÁNYI [HOLLY—SOHÁR, 1975] system, i.e.

ν_s: symmetric stretching vibration
ν_{as}: asymmetric stretching vibration
β_s: scissoring (in-plane symmetric deformation) vibration
β_{as}: rocking (in-plane asymmetric deformation) vibration
γ_s: wagging (symmetric perpendicular deformation) vibration
γ_{as}: twisting (asymmetric perpendicular deformation) vibration
δ_s: symmetric deformation vibration
δ_{as}: asymmetric deformation vibration

In *Figs. 1* and *2* the Bit-A column chromatographed fraction of the oil shale of Pula, resp., the IR-spectra of the spots of different R_f value are found.

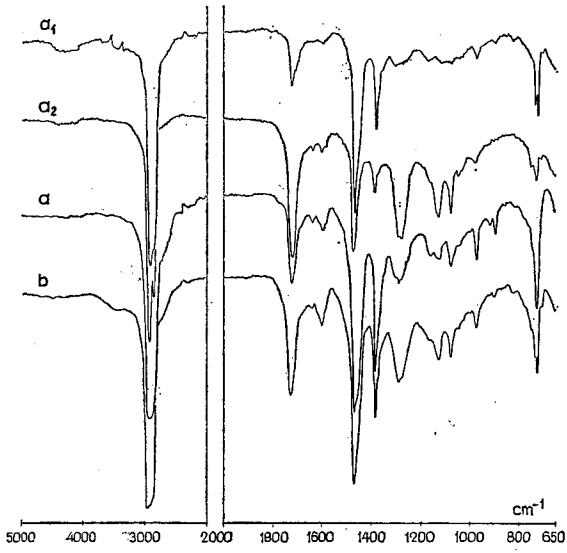

Fig. 1. The IR spectra of the spots of different R_f value and several Bit-A column chromatographed fractions

In the spectrum of the spot of $R_f=0.9$ separated on thin layer from the Bit-A fractions (a_1) the following bands are characteristic of the long chain paraffin hydrocarbons: 2900, 2850 (ν C—H), 1470 (δ_{as} CH_3,β_s CH_2), 1380 (δ_s CH_3) and 720 (β_{as} CH_2) cm^{-1}. Slight contamination is shown at 1720 cm^{-1} (νC=0), and undersaturation at 1610 cm^{-1} (ν C=C). In the spectrum of the spot occurring in the range of $R_f=0.6$—0.7 and separated on thin layer from the Bit-A fractions (a_2) the intensity of ν CO (1720 cm^{-1}) increased, the accompanying vibrations are found in the "finger print" range. In addition to the isolated C=C (1640 cm^{-1}) the conjugated undersaturation (1600 cm^{-1}) can also be observed, the quantity of both of them is small. In this R_f range straight-chain ketons are found.

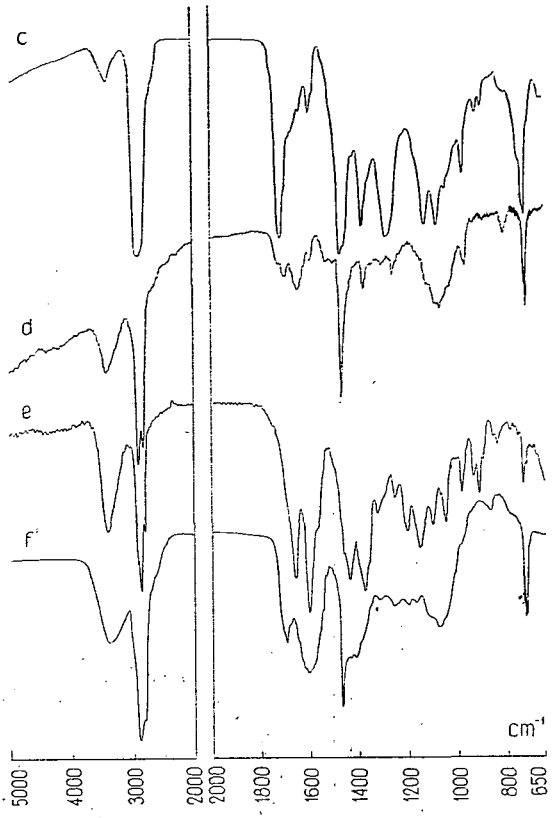

Fig. 2. The IR spectra of the further Bit-A column chromatographed fractions

It is to be noted that when evaluating the spectrum of coorongite the band-pair of 1140 and 1085 cm^{-1} was believed to be of ether-type bond which formed the cross-bonds of macromolecules [CANE, 1969]. It is probable that among the chains of the compounds constituting some, especially the *b* and *c* fractions of the oil shale of Pula C—O—C bonds are also found.

The original *a* (hexan) and *b* (hexan:benzene=1:1) fractions consist of the mixture of "pure" compounds mentioned above. The fraction *a* contains mostly aliphatic hydrocarbons while in fraction *b* the straight chain ketons are predominant. In both cases the spectra show slight undersaturation at 1640—1600 resp. 980—900 cm^{-1} (ν C=C; resp. γ C—H vinyl).

It is characteristic in general of the other fractions of Bit-A that deformation vibrations occur at 3450 cm^{-1} referring to the presence of νOH, these occur with different intensities.

In the *c* (benzene) part the ν OH vibration appears first but considering the whole spectrum it agrees with the fraction *b* the only difference being the somewhat saturation here.

In the *d* (chloroform) fraction the caraboxyl group skeletal vibration is relatively very small. The supplementary γ OH vibration of the ν OH band can be observed at 1070 cm^{-1}. The long straight chain alcohols predominate.

The spectrum of the fraction *e* (acetone) shows differences as compared to the records above mostly in the shorter wavelength range. The *v* CO band is displaced by about 40 cm^{-1} and occurs at lower wave number, i.e. at 1680 cm^{-1}. The band at 1610 cm^{-1} referring to undersaturation is more intense than in the foregoing case. At the joint band of the β_s CH_2 and δ_{as} CH_3 in this case the vibration of δ_s CH_3 is more intense. At 1160 cm^{-1} the transmittance of the ν_{as} C—O—C band approaches that of the carbonyl group. These features together are characteristic of the branched undersaturated conjugated esters. At the same time, the fraction contains alcohol-type compounds, too, because the *v* OH band is very strong. The corresponding deformation vibrations cannot be identified in the finger print range due to superpositions.

It is conspicuous in the spectrum of the fraction *f* (methanol) that it is relatively poor in bands and some bands being narrow in general became widened. In addition to the long chain alcohols mentioned above the spectrum shows the presence of carboxyl acid salt. The wide band at 1570 cm^{-1} (ν_{as} CO_2^-) and the widening al 1400 cm^{-1} (ν_s CO_2^-) can be attributed to the carboxylate ion. It proved to be successfut to separate the salt of carboxylic acid which contains mainly Ca-ions. The spectrum also indicates carbonyl contamination.

The IR-records of the BAM-bitumen fractions *(Fig. 3)* indicate the presence of similar functional groups as mentioned above, but the composition of certain parts is different from those of the Bit-A fractions. Based on the spectra the following compounds can be found in the BAM-bitumen.

Part *a* (hexan) consists mostly of long aliphatic paraffin hydrocarbons but the presence of cycloparaffins can also be assumed. Slight undersaturation and carbonyl contamination also occur.

Fraction *b* (hexan:benzene=1:1) contains aliphatic saturated ketons and carboxyl acid ester.

In the fraction *c* (benzene) somewhat more undersaturation and hydroxil contamination are found though this is very similar to the fraction *b*.

In the fraction *d* (chloroform) oxo-compound also occur in addition to the long-chain alcohols; the band of carbonyl group is widened indicating the presence of carbonyl group conjugated by C=C double bond.

The fraction *e* (acetone) contains highly undersaturated branched matter having conjugated oxo and hydroxil which are esters and alcohols.

In the fraction *f* (methanol) compounds containing long-chain undersaturated alcoholic hydroxil group as well as salt of carboxylic acid, resp. their mixture are found. The spectrum indicates carbonyl contamination, too.

ANALYSIS OF THE SOLUBLE ORGANIC MATTER OF THE THERMALLY TREATED OIL SHALE KEROGEN

Major part of the organic matter of oil shales consists of kerogen being insoluble in traditional solvents and from which shale oil is produced by means of destructive distillation. Our experiments carried out at lower temperatures than pyrolisis (max. 573 K) aimed the more thorough knowledge of the decomposition processes of kerogen.

In the course of the analyses physically isolated thus unchanged kerogen concentrate was used which has been of ash content of about 9 percent. The inorganic components are first of all clay minerals, quartz, feldspar and small quantity of

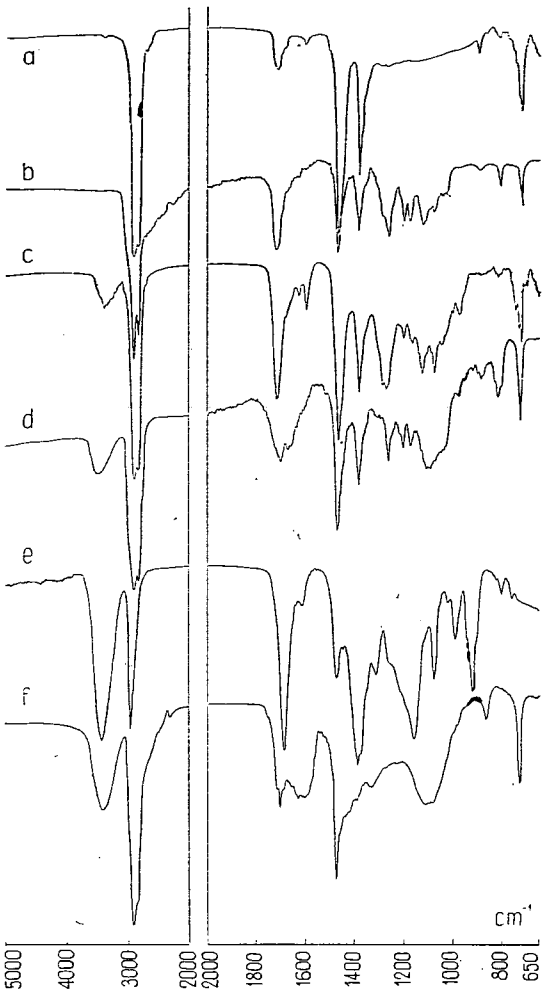

Fig. 3. The IR spectra of the BAM-bitumen column chromatographed fractions

carbonate. Experiments proved that at low temperatures (423, 473 and 573 K) soluble organic matter was formed from kerogen. The total soluble organic matter was removed from the sample treated thermally during one day at 573 K in nitrogen flow (i.e. under the expected greatest influence) by means of mixture of BAM-solvent and the analyses described in the characterization of oil shale bitumens were carried out. The material quantity to be separated (0.0740 g) was chromatographed on alumina of III—IV activity. Data of column chromatography are comprehended in Table 4.

The comparison between the data of Table 4 and the fractions corresponding to the original bitumens of the oil shale shows that the compounds formed from kerogen are mostly apolar while the quantity of the polar matter relatively decreased. More information can be obtained from the IR-spectra *(Fig. 4)*.

TABLE 4

Column chromatographic results of the soluble organic matter of the oil shale kerogen after thermal treatment (Pula)

Sign of the fraction	Denomination	Quantity (ml) of the solvent	Quantity (g) of the fraction	Proportion (%)
a	hexane	1400	0.0190	25.68
b	hexane: benzene 1:1	1900	0.0050	6.76
c	benzene	2900	0.0270	36.49
d	chloroform	1850	0.0020	2.70
e	acetone	1350	0.0070	9.46
f	methanol	1600	0.0110	14.86
			0.0710	95.95

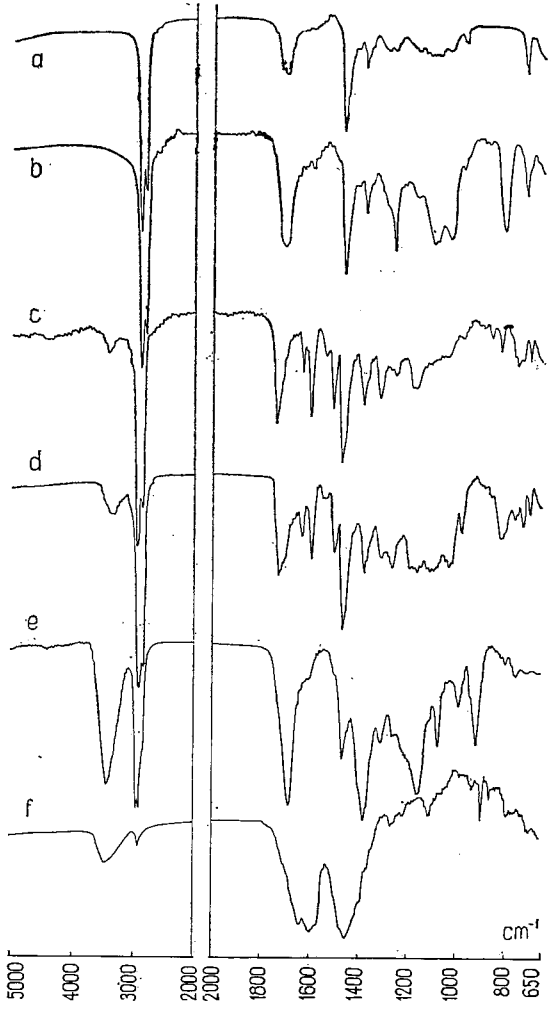

Fig. 4. The IR spectra of the thermally treated oil shale kerogen column chromatographed fractions

Having evaluated the spectra of bitumens produced by the thermally treated oil shale kerogen vibrations of qualitative new type were found in certain fractions which do not occur in the spectrum of the bitumens of the original oil shale. Depending on the quantity, in the range between 1600 and 1500 cm^{-1} small shoulders or peaks of medium intensity indicate the aromatic skeletal vibrations. The corresponding deformation vibrations are found at 750 cm^{-1} (γ =CH) and at 710 cm^{-1} (γ CC).

Similarly to the recent analyses in some fractions of Bit-A of the original oil shale treated first thermally and subsequently extracted, the presence of aromatic compounds was indicated by the IR-spectra. Though the total quantity of the aryl-compounds in not predominant the exact interpretation of their formation needs further experiments.

One of the formation possibilities is as follows: aromatization takes place from the different alkyl or cycloalkyl components due to the catalytic effect of clay minerals; further it is also possible that in the easily removable parts e.g. alkyl-aril compounds are released from the kerogen matrix due to the thermal effect and by means of the breaking of bonds, and which contain also aromatic skeleton, as well.

According to the IR-records of the thermally treated kerogen concentrate the composition of each fraction is as follows:

The fraction *a* (hexan) consists mostly of hydrocarbons of long alkyl chains with slight carbonyl contamination. The wide shoulder at 1600 cm^{-1} derives rather from undersaturation than from aromatic skeletal vibrations since the complementary deformation bands cannot be observed.

In the fraction *b* (hexan:benzene=1:1) mostly the keton-type compounds predominate. The chain is long and not branched. The spectrum shows minimal aromatic contamination.

In the fraction *c* (benzene) partly alkyl-aril skeletal oxo-compounds are found with slight OH-contamination.

In the fraction *d* (chloroform) the spectrum indicates somewhat more alcoholic OH-groups, the skeleton is, however, aliphatic and of aromatic structure.

The fraction *e* (acetone) consists of esters and alcohols being conjugated, undersaturated and of branched chain.

The spectrum of the fraction *f* (methanol) indicates great amounts of inorganic matter. In addition to the salt of carboxylic acid compounds of undersaturated alcoholic functional groups are found.

In favour of obtaining further information the C—H analysis of the column chromatographed fractions was also carried out, in addition to the IR-records.

Analysis was done by means of the KÖRBL-method, in which the oxidation of carbon compounds is carried out in oxygen flow at 823 K and the active catalizing effect of thermal decomposition products of silver permanganate is used. The quantities of carbon dioxide and water were determined gravimetrically. In Table 5 the C—H analytical results of the oil shale bitumens and of the chromatographed fractions of the bitumen formed as a result of thermal treatment from the kerogen concentrate and isolated physically from the original oil shlae, are comprehended. As comparison, the quantities of elements constituting the "original" not chromatographed bitumen of the oil shale are shown below (in percent):

Bit-A:	C: 72.9	H: 11.8	S: 0.14
BAM-bitumen:	C: 72.6	H: 11.2	S: 0.17

TABLE 5

C-H analyses of the shale kerogen bitumen fractions after thermal treatment and of the oil shale bitumens of Pula

Eluation agent of the fractions separated in the column	Bit-A		BAM-bitumen		Oil shale kerogen after thermal treatment	
	C %	H %	C %	H %	C %	H %
hexane	83.95	13.02	80.95	12.55	81.93	12.75
hexane:benzene 1:1	82.22	12.85	79.82	12.45	80.07	11.90
benzene	79,52	12.75	78.38	12.35	78.88	11.64
chloroform	78.50	12.51	77.72	12.40	77.36	10.86
acetone	66.75+	11.07	61.19+	10.58	64.61+	9.82
methanol	63.60+	9.62	62.02+	9.50	67.90+	10.44

+ Having completed the analyses incombustible matter of 1—3 percent remained.

Data of Table 5 also show that the individual fractions are mixtures and not pure materials. It is fairly evidenced by numerical data, i.e. when comparing the data of the hexan-fractions with those of the spot (R_f: 0.9) separated from the hexan fraction of Bit-A which represent C_{20} hydrocarbons: C: 84.77%, H: 13.56%.

Data of the analysis also indicate that the quantity of oxygen increases during progressive chromatography since the lacking percent is attributed to this element.

In the final fraction (*f*) the presence of inorganic matter was indicated also by the IR-spectra while the record of the fraction *e* did not show this. It is probable that also in this part small quantity of salt of carboxylic acid is found, but it can be also assumed that sulfur culminates in this fraction and is represented by thioester, in the spectrum, however, its weak bands, e.g. C—S, S=O are overshadowed by the more characteristic bands.

DISCUSSION

The data of soluble organic matter concerning the oil shale of Pula show that the major part of bituments consists of oxygen-bearing compounds, i.e. carboxylic esters, alcohols, etc. which derive from the lipid-like material of algae. The long-chain aliphatic structure is mostly characteristic of the compounds and branched hydrocarbons occur only in smaller quantities, mainly in the acetone fraction.

The relatively high oxygen content relates to the fact that the organic matter is free of stronger effects, it is in the initial phase of its evolution. This verified also by the fact that in the oil shale, resp., oil shale kerogen samples treated atrelatively low temperatures the presence of the aromatic skeleton can be determined. In case of the samples of the Southern Great Plain deriving from greater depths (1990—2100 m) and being more diagenized but of the same Upper Pannonian age the quantity of oxygen decreased according to the previous investigations and the proportion of the condensed compounds increased.

The investigation of the soluble organic matter is closely related to the investigation of the oil shale kerogen. Because of the low maturity grade the oil shale kerogen of Pula is highly suitable to follow the thermal-historic processes under laboratory conditions. The analysis of the soluble products will provide further data

concerning the changes in the kerogen structure due to thermal treatment. In the future the analysis of bitumens will be supplemented by the analysis of the oil produced under thermal treatment in favour to obtain further information on the oil shale kerogen and to make clear the genetic problems.

ACKNOWLEDGEMENTS

Acknowledgements are said to DR. ÁRON JÁMBOR (Hungarian State Geological Institute) for the disposal of samples, further tot the workers of the Department for Organic Chemistry of the József Attila University, first of all to DR. IRÉN VINCZE for the useful directives indispensable to the chemical analyses and to DR. GIZELLA BARTÓK-BOZÓKI and ÉVA GÁCS-GERGELY for the precise analytical works.

REFERENCES

ARATÓ, K. and M. BELLA [1976]: Results of technological and chemical analyses of the oil shale of Pula and Gérce (Transdanubia, Hungary). — Annual Report of the Hungarian Geological Institute of 1974 p. 287—300.

BLACKBURN, K. B. and B. N. TEMPERLEY [1936]: Botryococcus and the algal coals. — Trans. Roy. Soc. Edinburgh **58,** p. 841—868.

CANE, R. F. [1969]: Coorongite and the genesis of oil shale. — Geochim. et Cosmochim. Acta **33,** p. 257—265.

CANE, R. F. [1976]: The origin and formation of oil shale. — In: Oil shale. Edited by T. F. YEN and G. V. CHILINGARIAN. Elsevier Scientific Publishing Company p. 27—61.

DOUGLAS, A. G., G. EGLITON and J. R. MAXWELL [1969]: The organic geochemistry of certain samples from the Scottish Carboniferous Formation. — Geochim. et Cosmochim. Acta **33,** p. 579—590.

HAJÓS, M. [1976]: Diatom flora in Upper Pannonian sediments of borehole Put-3 at Pula village (Transdanubia, Hungary). — Annual Report of the Hungarian Geological Institute of 1974 p. 263—285.

HOLLY, S. and P. SOHÁR [1975]: Absoption spectra in the infrared region. Akadémia Kiadó, Budapest.

HUNT, J. M., G. W. JAMIESON [1956]: Oil and organic matter in source rocks of petroleum. — AAPG Bull., **40,** p. 477—488.

JÁMBOR, Á., G. SOLTI [1975]: Geological conditions of the Upper Pannonian oil shale deposite recovered in the Balaton Highland and Kemeneshát (Transdanubia, Hungary). — Acta Miner. Petr., Szeged, **XXII/1,** p. 9—28.

NAGY, E. [1976]: Palynological investigation of Transdanubian oil-shale exploratory boreholes. — Annual Report of the Hungarian Geological Institute of 1974 p. 247—262.

POUCHERT, C. J. [1975]: The Aldrich Library of Infrared Spectra. Second Edition. Milwaukee Wisc., Aldrich Chemical Company.

THORNE, H. M., K. E. STANDFIELD, G. U. DINNEEN and W. I. MURPHY [1964]: Oil shale technology: A review. Information Circular 8216 U.S. Bureau of Mines. Washington.

TISSOT, B., Y. CALIFET-DEBYSER, G. DEROO and J. L. OUDIN [1971]: Origin and evolution of hydrocarbons in early Toarcian shales, Paris basin, France. — AAPG Bull., **55,** p. 2177—2193.

TISSOT, B., B. DURAND, J. ESPITALIE and A. COMBAZ [1974]: Influence of nature and diagenesis of organic matter in formation of petroleum. — AAPG Bull., **58,** p. 499—506.

VERNING, G. [1973]: Vékonyréteg-kromatográfia a szerves kémiában (La chromatographie en couche mince techniques et applications en chimie organique.) Műszaki Könyvkiadó, Budapest.

Manuscript received, May 25, 1979

DR. LÁSZLÓ PÁPAY
Institute of Mineralogy, Geochemistry
and Petrography
Attila József University
H-6701 Szeged, Pf. 428.
Hungary

Acta Mineralogica—Petrographica, Szeged, XXIV/1, 125—136, 1979

EXAMINATION OF FACTORS EFFECTING THE RESULTS OF HIGH TEMPERATURE PYROLYSIS STUDIES USED TO CHARACTERIZE NON-SOLUBLE DISPERSE ORGANIC MATERIAL IN SEDIMENTARY ROCKS. CRITICAL EVALUATION OF GRANSCH AND EISMA'S METHOD

István Koncz

SUMMARY

Pyrolysis examinations used to study disperse organic matter are review and evaluated here. The information content and use of CR/CT rations obtained by Gransch and Eisma's method in connection with hydrocarbon prospecting problems are analysed here. Due to difficulties during the geochemical interpretation of CR/CT values obtained according to Gransch and Eisma the method had to be reevaluated critically. The effects of pyrolysis temperature upon the CR/CT rations are analysed on natural and artificial rock samples. The reasons underlying the decrease of CR/CT ratios at pyrolysis temperatures above 700 °C are examined.

INTRODUCTION

By now it is generally recognized that known fossil hydrocarbon reserves originate from the organic (bio-organic) material content of the sedimentary rocks [1, 2]. The greatest part of known hydrocarbon reserves comes from the thermal decomposition of organic material in sedimentary rocks while burried [3].

The best part of organic material in sedimentary rocks is in dispersed form. Concentrated (non-dispers) organic material in sedimentary rocks i.e. coal is mostly of humic type and forms the least fraction of the total organic material present, in the continental sector of the stratisphere. Rocks with lower organic carbon contents contain dispersed material. Sapropelic organic material is their major component. Methane and other higher homologes are formed in significant amounts from sapropelic organic material. Methane is the major component formed from humic type organic material.

Based on the qualitative and quantitative distribution of the organic material in sedimentary rocks the greatest part of hydrocarbons can be concluded to originate from dispers organic material.

Analysis of recent sediments demonstrate that their dispersed organic material content is generally insoluble in organic solvents. During the burial process of sedimentary rocks the non-soluble part of the dispersed organic material undergoes thermal decomposition yielding components more and more soluble in organic solvents or present in gaseous form. During this stage both the composition and the properties of the non-soluble fractions are altered.

In order to predict the outcome of hydrocarbon prospecting it is insufficient to explore the geological structures which potentially allow for hydrocarbon formation. Scientifically founded hydrocarbon prospecting is impossible without information relating to the amount of hydrocarbons formed in promising, potentially hydrocarbon-bearing formations.

Theoretically there are two possibilities to determine hydrocarbon prospecting perspectives and the amount of hydrocarbons formed: direct determination of the hydrocarbons formed, and indirect prediction, i.e. estimation of hydrocarbon quantities from the quality of the non-soluble organic material. Since hydrocarbons are mobile in the crust of Earth direct determination of their quantities frequently yield erroneous results. Depending on their mobility and volatility the error can be negative or, if hydrocarbons of allochton origin are encountered, positive. Quality estimates based on the quality (identity) of the non-soluble organic material are free from mobility-linked uncertainties.

Since analytical techniques make feasible only the description of the current status none of the methods can do without the reconstruction of the initial conditions and the intermediary transformations which is based on so-called geochemical analogies.

To our best knowledge the amount of hydrocarbons formed depends on the amount, type and maturity, i.e. the extent of thermal decomposition of the organic material present.

Due to analytical constraints the organic (non-carbonate) carbon content, C_{org} of the sedimentary rocks is used to characterize the amount of organic material present. In order to express the effects of the type and degree of transformation of the organic material it is advisable to express the amount of decomposition products relative to a carbon unit. Accordingly, at the beginning of decomposition formation (i.e. at initial conditions) the amount of organic carbon content is unity.

The amount of hydrocarbon formed, relative to carbon unit, depends on the type and the degree of transformation of the dispersed organic material. The type of organic material (i.e. humic, sapropelic or intermediary), as an initial condition, is determined by the conditions prevalent at the time of deposition formation. The degree of transformation, i.e. the extent of thermal decomposition depends on both time and temperature.

PYROLYSIS TESTS. AN OVERVIEW

Hydrocarbon formation processes can be modelled in the laboratory by so-called pyrolysis tests by heating the rock sample in an inert atmosphere. In order to achieve the extent of transformation completed under true geological conditions temperatures much higher than naturally found during hydrocarbon formation have to be applied.

The type and amount of decomposition products formed during further transformations of the organic material present in the rock sample can be directly obtained by pyrolysis tests. Also, decomposition products of slightly transformed organic materials can indicate the type of the organic material originally present. No information regarding the amount of decomposition products already formed in the rock sample can be obtained from the pyrolysis tests. However, by combining the results of pyrolysis tests and the reconstructed mechanism of geochemical transformations the amount of decomposition products can be estimated.

Pyrolysis tests are widely used for the characterization of the dispersed organic material in oil shales, coals and sedimentary rocks. Pyrolysis tests, quite abundant as testified by the References list, differ both in the sample, parameters and components tested as well as in the test conditions. So many variants of the pyrolysis test are known that their exhaustive evaluation, or even a detailed listing is beyond the scope of this paper.

As regards the material tested there are pyrolysis tests using organic material islaoted from [4], and not-isolated-from the inorganic matrix [5, 6]. Isolation from the inorganic matrix is a time consuming and never-complete process, frequently accompanied by alterations in the chemical structure of the organic material. On the other hand during pyrolysis of the organic material not separated from the inorganic matrix decomposition products originating but from the organic material are formed. Also, products due to interactions of the organic and inorganic material appear frequently. According to a few methods only the carbonates are removed from the inorganic matrix such as, e.g. in the methods based on the determination of the total organic carbon content. The total organic material [7] or its part not soluble in organic solvents [5] (i.e. the sample after extraction) is used for the pyrolysis tests.

As regards test conditions pyrolysis tests differ both in the duration, temperature and pressure (atmospheric or vacuum) of pyrolysis. Furthermore, tests were described with stepwise [8] or continous [9] temperature increases.

As regards the parameters and components tested pyrolysis tests differ whether the decomposition products [10, 11, 12, 13], the residual material [5] or both are tested.

Time and apparatus requirements of various pyrolysis tests differ significantly, consequently the information content of the results obtained is also widely different. A fast, and simple (as regards hardware) version of a laboratory pyrolysis unit was developed by GRANSCH and EISMA [5, 14]. Also, it can be easily automated.

THE METHOD OF GRANSCH AND EISMA

The rock sample used in the method described by GRANSCH and EISMA is carbonate free and contains no soluble organic material. Dispersed organic material is not separated completely from the inorganic matrix. However, carbonates should be removed because their presence contributes a positive error to the method based on the determination of the organic carbon content. After the removal of carbonates with hydrochloric acid, part of the original pyrite content, non-hydrochloric soluble metal oxides, silicates (mostly clay minerals) and silicium dioxide is left over as inorganic matrix. In order to eliminate the uncertainties caused by the mobilization of the decomposition products the method of GRANSCH and EISMA was used for the determination of non-soluble dispersed organic material.

Tests were carried out as follows: the carbon content (CT) of a carbonate-free and extracted, finely ground rock sample was determined by the so-called PREGL—DUMAS method. Another portion of the sample was pyrolyzed in purified nitrogen stream at 900 °C for 1.5 hr. The carbon content of the sample after pyrolysis (CR) was once again determined by the PREGL—DUMAS method.

GRANSCH and EISMA used the relative amount of non-volatile carbon (CR/CT) to characterize the non-soluble organic content of the sample. Volatile (pyrolysable) carbon content was calculated as

$$1 - \frac{CT}{CR}$$

Some authors call the CR/CT ratio the *diagenetic coefficient* or the *degree of diagenesis* [15,16].

Neither the diagenetic coefficient, nor the katagenetic coefficient terms are fortunate because the result obtained needs not to be assigned to any specific stage of organic material transformation. In fact, any such assignment is highly misleading.

The pyrolysis temperature, 900 °C used by GRANSCH and EISMA is the standardized pyrolysis temperature used for the characterization of the *"fixed organic carbon content"* of coals. In this test the weight loss of a finely ground coal sample in inert gas atmosphere at 900 °C is measured (naturally, corrections are made for the moisture and ash contents of the sample). With coal samples weight losses due to heat decomposition of the inorganic matrix are negligable or can be accounted for by correction. Since the best part of any sedimentary rock sample is inorganic, weight losses characterize not only the organic material but also the inorganic matrix. Therefore, GRANSCH and EISMA modified the fixed carbon test method by measuring the pyrolysis-induced-weight-loss of the organic carbon content.

They note [5] that "Determination of the CR/CT ratio is an empirical approach. The values might be influenced by the inorganic material present." Effects of the inorganic matrix were investigated in clay-enriched mixtures of relatively high organic carbon content, 1—9% w/w. Slight increase could be attributed to the inorganic matrix. Based on the identical or similar CR/CT values of the valuable and covering layers slight changes were attributed to the presence of inorganic matrix. Thus, they concluded that "CR/CT ratios reflect characteristics strictly connected with the non-soluble organic material." CR/CT ratio characterizes the over-all non-soluble organic material present. Therefore, its value depends on both the type of the non-soluble organic material and the degree of its transformation. It is in contrast with such parameters as color and shape of pollen, reflection of vitrinites which depend only on the degree of transformation.

Consequently, CR/CT ratios can be used for the determination of the degree of transformation only when the non-soluble organic material is of the same type. On the other band, if the degree of transformation of the non-soluble organic material determined by other methods is the same, differences in the CR/CT ratios can be used to determine the type of organic material. Results of pyrolysis tests carried out with humic coal samples indicate that irrespective of the degree of transformation CR/CT ratios below 0.6 indicate the presence of organic material suitable for hydrocarbon formation (more sapropelic). When the CR/CT ratio is higher than 0.6 other methods have to be used to determine the degree of transformation in order to distinguish between organic materials suitable and not suitable for hydrocarbon generation.

GRANSCH and EISMA compared their pyrolysis test results with the results of other methods and found good agreement, identical tendencies and conclusions. With concentrated dispersed organic material, i.e. peat, lignite and humic coals the CR/CT ratios correlated well with the fixed carbon content values. They conluded that similarily to the fixed organic carbon content the CR/CT ratio is also unsuitable for the determination of the degree of transformation with volatile rich, slightly transformed bituminous and other coals. Also, humic coals display CR/CT ratios above 0.6 even at low degrees of transformation (in early stages of diagenesis). CR/CT ratios of West Venezuelan sediments display good correlation with the maximum depth of burial, ratios increase with depth. This correlation proves that with similar organic material CR/CT ratios increasing proportionally to depth indicate that the deeper the sediment (i.e. the higher the temperature) the higher the degree of transformation. The relationship of CR/CT ratios and the relative amount of extractable organic material (i.e. ratio of extracted and total carbon content) was also tested in samples obtained at approximately identical depths, i.e. which were of approximately identical as regards the degree of transformation. It was found that at high extracted/total carbon ratios the CR/CT ratios were high and *vice versa.*

This relationship indicates that with identical degrees of transformation lower CR/CT ratios indicate the presence of organic material more suitable for hydrocarbon generation. Similar conclusions were reached by comparing the H/C atom ratios and CR/CT ratios of various organic materials with low degrees of transformation. The higher the H/C ratio (i.e. hydrogen rich, more sapropelic organic material, more suitable for hydrocarbon generation) the lower the CR/CT ratios and *vice versa* (i.e. humic materials).

CRITICAL EVALUATION OF THE GRANSCH—EISMA-METHOD

Some 500 samples from the Hungarian part of the Pannonian Basin were tested by the method of GRANSCH and EISMA. Measured CR/CT values were compared with the results of other methods (i.e. vitrinite reflection, selective oxidation) for a limited number of samples [16]. Except for a few samples the results correlated excellently. CR/CT ratios obtained on samples of Bulgarian sedimentary rocks could also be interpreted [18]. Kaolinite-coal composite samples of 6—8% organic carbon content prepared from coals of known degree of transformation obtained from the Perniski and Donec basins were tested by Bulgarian scientists and measured CR/CT values were compared with the volatile contents and vitrinite reflexion [19]. Results agreed vell. CR/CT ratios measured by the method of GRANSCH and EISMA could be used to follow the transformation of the disperse organic material and formed the basis of the reaction kinetic description of hydrocarbon formation [16, 17, 20, 21].

However, problems encountered occasionally during the interpretation of CR/CT ratios measured with sediment samples from the Pannonian Basin necessitated the reevaluation and critical analysis of the method of GRANSCH and EISMA. In most rock samples obtained from depths of 2.5 km and temperatures of 130—140 °C CR/CT values were above 0.6. However, significantly lower values were obtained occasionally and on the basis of extracted/total carbon ratios these samples could not be considered more sapropelic. To explore more these contradictions the effects of pyrolysis temperature upon the CR/CT values were tested with a natural clay-marl rock sample of average carbon content (CT=0.556%) and a coal-quartz mixture of 0.355% organic carbon content in a temperature range of 760—980°. Results are shown in Table 1 and *Fig. 1.* In order to eliminate the effects of various CR/CT ratios percent changes of the CR/CT ratio at identical pyrolysis temperatures

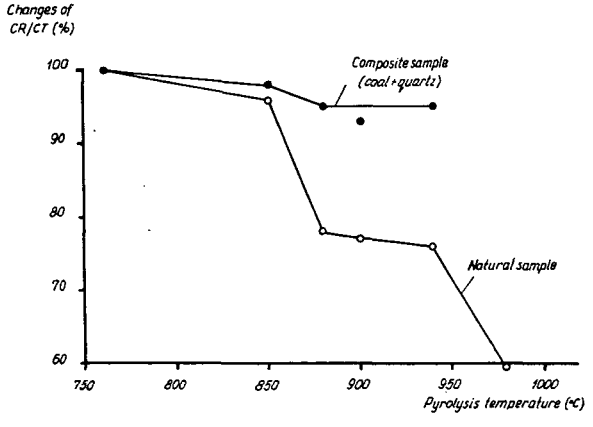

Fig. 1. Changes of the CR/CT ratio with the pyrolysis temperature

are shown. The CR/CT ratio measured at 760° is taken 100% and CR/CT ratios measured at higher temperatures are expressed with respect to this value. (Naturally, the question whether higher CR/CT ratios obtained at lower pyrolysis temperatures were due to temperature effects or merely to inadequately short pyrolysis times, had to be answered. Therefore, CR/CT values were obtained in the 400—900° temperature range with pyrolysis times above 90 min. CR/CT values obtained in 90; 120; 150 and 1440 min pyrolysis tests were identical within experimental error. Thus, higher CR/CT values at lower pyrolysis temperatures were caused by lower temperature).

It can be seen that in the case of the composite sample decrease of the CR/CT ratio with increasing temperature is not significant (7% up to 900°) but is considerable with the natural sample (23% up to 900°).

Effects of the pyrolysis temperature upon the CR/CT ratios in natural samples were studied in higher temperature ranges (350—950°). The results, percentage changes of the CR/CT ratio are shown in *Fig. 2* and Table 2. The CR/CT ratio measured at 350 °C was taken 100% and other values expressed in percent relative to this figure. It can be seen that the amount of carbon lost with the pyrolysis products (1−CR/CT) is negligible, i.e. CR/CT is close to unity. The greatest part o carbon is lost in the 400—500 °C range. Carbon is lost in this range mostly as hydrocarbon [6, 10]. There is almost no carbon loss in the 500—700 °C range. However, further carbon is lost from 800—900 °C upwards. The relative amount of pyrolysable carbon at 700 °C (1−CR/CT or volatile carbon) can be considered the hydrocarbon generating potential of the sedimentary rock.

Effects of pyrolysis temperature in a narrower temperature range (500—900 °C) were also studied with a large number of samples. Results are shown in Table 3 as percent changes of the CR/CT ratio taking the CR/CT ratio at 500 °C hundred percent. 500 °C was selected as initial pyrolysis temperature because previous experiments proved (Table 2) that the majority of volatile hydrocarbons is lost up to 500 °C. Up to 700 °C the decrease of the CR/CT ratio remained within the experimental error (4%), then at 800 °C it became slightly higher while at 900 °C it became significant (10—27%) and varied greatly from sample to sample. The extent of the decrease could not be correlated with the depth where the samples tested were taken from. The CR/CT ratio at 700 °C is also shown in Table 3, along with the CR/CT at 900 °C, as it is a parameter related to the amount of carbon lost by pyrolysis. The difference between CR/CT values at 700° and 900 °C (ΔCR/CT) are also shown in

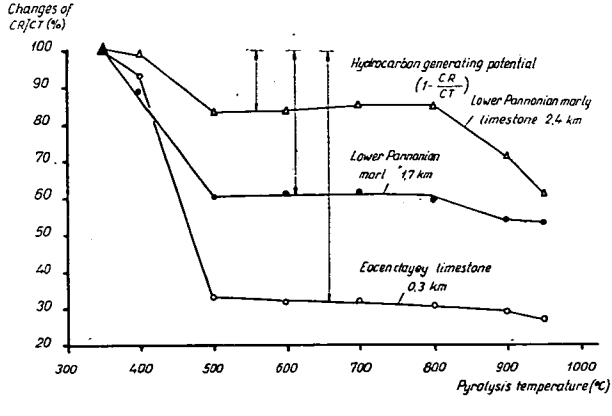

Fig. 2. Changes of the CR/CT ratio with the pyrolysis temperature

TABLE 1

Relative changes (%) of the CR/CT values with the pyrolysis temperature (CR/CT=100% at 760 °C) with natural (clay-marl) and composite (coal+quartz) samples

Sample	CT %	Pyrolysis temperature, °C						CR/CT	
		760	850	880	900	940	980	760 °C	900 °C
Clay-marl	0.556	100%	96%	78%	77%	76%	59%	0.914	0.707
Coal+quartz	0.355	100%	98%	95%	93%	95%	—	0.820	0.763

TABLE 2

Relative changes (%) of the CR/CT values of sedimentary rocks with the pyrolysis temperature (CR/CT=100% at 350 °C)

Sample characteristics				Pyrolysis temperature, °C								CR/CT	
Age	Rock	Depth (km)	CT %	350	400	500	600	700	800	900	950	350 °C	500—800 °C
Eocen	clayey limestine	0.3	31.01	100	93	33	32	32	30	29	27	0.975	0.294—0.320
Lower Pannonian	marl	1.7	2.66	100	89	60	61	61	59	54	53	1.000	0.589—0.614
Lower Pannonian	marly limestone	2.4	1.32	100	99	83	83	85	85	71	61	0.946	0.784—0.808

TABLE 3

Relative changes (%) of the CR/CT values of sedimentary rocks with the pyrolysis temperature (CR/CT=100% at 500 °C)

Sample characteristics				Pyrolysis temperature, °C				CR/CT		ΔCR/CT*
Age	Rock	Depth (km)	CT %	500	700	800	900	700 °C	900 °C	
Eocen	clayey limestone	0.3	31.01	100	98	92	88	0.313	0.282	0.031
Lower Pannonian	marl	1.7	2.66	100	100	97	90	0.611	0.544	0.067
Sarmatian	marl	2.3	3.38	100	97	90	73	0.605	0.458	0.138
Lower Pannonian	marly limestone	2.4	1.32	100	100	100	85	0.808	0.670	0.138
Lower Pannonian	clayey marl	2.7	0.60	100	99	91	82	0.868	0.714	0.154
Lower Pannonian	clayey marl	2.7	0.63	100	100	94	81	0.881	0.708	0.176
Lower Pannonian	aleurolite	3.0	0.56	100	100	90	75	0.818	0.613	0.205
Helvetian	clayey marl	3.7	1.25	100	98	90	84	0.924	0.799	0.125
Range of decrease (%)					0—3	0—10	10—27			

* ΔCR/CT=(CR/CT) 700 °C—(CR/CT) 900 °C

the Table. This difference as a function of depth changes as expected. Both CR/CT ratios at 700 and 900 °C increase with depth, the relative amount of pyrolysable carbon decreases, the degree of transformation increases, the hydrocarbon generating potential of the organic material is increasingly depleted.

Further test were carried out to learn the cause of the second thermal decomposition from 800 °C onwards, following the first thermal decomposition yielding mostly hydrocarbons, and which is practically completed by 500 °C. The second thermal decomposition step increases the relative amount of pyrolysable carbon and significantly decreases the CR/CT ratio.

Samples pre-pyrolysed at 700 °C were subjected to further pyrolysis at 800° and 900 °C and the amount of carbon monoxide swept out by the purified, oxygen-free nitrogen carrier was analysed similarily to the oxygen determinations [22]. The only difference was that in the latter case the glowing carbon filling was substituted by the sample investigated. The amount of carbon monoxide relased at 800° and 900 °C was expressed as pure carbon and compared with the "carbon-loss" relative to the pyrolysis at 700 °C. It was found that the amount of carbon lost as carbon monoxide increased with the temperature and its value agreed well with the "carbon-loss" due to pyrolysis at 800 and 900 °C temperatures. No volatile carbon lost as carbon monoxide could be detected above the experimental error with composite (coal+quartz) samples, in agreement with the results of pyrolysis tests.

We could conclude that "carbon-loss" at higher pyrolysis temperatures (800 and 900 °C), i.e. thermal decomposition accompanied by the decrease of the CR/CT ratio was caused by the interaction of inorganic and organic material in the sample and the oxygen content of the organic material. It is known that if the pyrolysis products of an organic material are transmitted through a carbon bed heated to 1100 °C temperature those containing oxygen form quantitatively carbon monoxide. (This process is made use of when the oxygen content of organic materials is determined.) In the presence of platinum catalyst conversion to carbon monoxide takes place at lower (900 °C) temperatures. Naturally, the reaction takes place without catalyst even at lower temperature if there is oxygen present in the organic material or if there are oxygen releasing components (such as oxides of metals of changing valency) in the inorganic material of the sample. Sedimentary rock samples prepared for pyrolysis tests may contain such oxides non-soluble in hydrochloric acid (e.g. Cr_2O_3, etc.). Tests carried out with coals and organic material isolated from sedimentary rocks proved that the oxygen content of the organic material is significant at low degrees of transformation and it decreases rapidly with increasing degree of transformation due to thermal decomposition resulting in water-and-carbon-dioxide-formation. Thus, the oxygen content of the organic material might enhance the decrease of the CR/CT ratio only with organic materials of low degree of transformation. However, carbon left over by pyrolysis at 700 °C might partially react with the metal oxides present in the catalytical environment provided by the clay minerals resulting in the formation of carbon monoxide and dioxide. Carbon dioxide is further reduced to carbon monoxide by any carbon present according to the BOUDOUARD reaction.

This assumption was to be proved by adding oxidizing metal oxides (Fe_2O_3; V_2O_5, $PbCrO_4$) to the samples. Magnesium oxide was used as control since its presence could not increase the degree of oxidation. Composite samples were prepared from quartz and carbon black ignited in nitrogen flow. Results are summarized in Table 4 along with the CR/CT values of the samples containing no additives. Changes of the CR/CT ratio caused by admixed metal oxides are expressed with respect to

TABLE 4

Relative changes (%) of the CR/CT ratios of composite and natural samples with metal oxide admixing (CR/CT = 100% at 700° and 900 °C, without additives)

Type of sample	CT (%)	Pyrolysis temp. °C	CR/CT without additive	Added metal oxide			
				Fe_2O_3	V_2O_5	$PbCrO_4$	MgO
Composite (carbon black + quartz)	1.380	900	1.000	86	84	66	100
Natural (sedimentary rock)	2.068	900	0.605	77	85	58	95
		700	0.697	100	100	86	100
Natural (sedimentary rock)	0.972	900	0.602	87	80	67	100
		700	0.869	95	95	93	94

the CR/CT ratio of the sample containing no admixed metal oxide. It can be seen that non-oxidizing quartz had no effect upon the CR/CT ratio with oxygen-free carbon black. (CR/CT obtained at 900 °C temperature was 1.000.) Oxidizing metal oxides added to the samples decreased the CR/CT ratio. As expected theoretically, non-oxidizing MgO had no effect on the CR/CT ratio. With natural rock samples there was only one case when the presence of oxidizing metal oxide decreased the CR/CT ratio at 700 °C beyond the experimental error. At 900 °C, however, significantly decreased CR/CT ratios were obtained in all cases. (Practically the same results were obtained when the amount of oxidizing metal oxides present was halved.)

These tests proved that inorganic materials, the major components of rock samples play a significant role in determining the decreased CR/CT ratios of samples pyrolysed at 900 °C.

CONCLUSIONS

Pyrolysis test can be used to model hydrocarbon formation taking place in sedimentary rocks. Results of the pyrolysis tests can be used to determine the degree of transformation of a given type of disperse organic material.

Pyrolysis tests were carried out according to GRANSCH and EISMA resulting in the relative amount of non-soluble organic carbon not pyrolysed at 900 °C (CR/CT ratio).

In order to explore the origin of certain problems encountered during the geochemical interpretation of the CR/CT ratios measured at 900 °C their method of determination was evaluated critically. The effects of pyrolysis temperature on the CR/CT ratios were studied. Results of the pyrolysis tests carried out with natural and composite samples can be summarized as follows:

1. The relative amount of non-pyrolysable organic carbon (CR/CT ratio) decreases rather rapidly up to 500 °C, depending on the type of organic material and the degree of transformation. The ratio is almost constant in the 500—700 °C range but decreases further, or remains constant, above 700 °C.

2. Decreased CR/CT ratios above 700 °C are due to the interaction of the organic and inorganic part of the sample and/or the oxygen content of the organic material present.

3. The value of the CR/CT ratio measured at 700 °C depends on the type of the organic material and the degree of its transformation.

4. The value of the CR/CT ratio measured at 900 °C depends, apart from the type of the organic material and the degree of its transformation, on the interactions of the organic and inorganic parts of the sample and/or the effects of the oxygen content of the inorganic parts — secondary effects which have no influence under the conditions of natural hydrocarbon formation.

5. Interaction of the organic and inorganic material might be due to oxides of metals of changing valency non-or only partly soluble in hydrochloric acids. At pyrolysis temperatures above 700 °C these metal oxides promote carbon monoxide formation from part of the organic carbon present. If the organic material contains oxygen it can lead alone to carbon monoxide formation above 700 °C.

6. Secondary effects can be characterised by the difference of CR/CT ratios measured at 700 and 900 °C (ΔCR/CT).

ACKNOWLEDGEMENTS

Tests used throughout this study were carried out at the Institute of Organic Chemistry of the L. Eötvös University of Sciences, Budapest under the contract "Complex Organo-Geochemical Investigations" signed with the Geological Department of the Industrial Laboratory for Oil and Gas Research (OGIL). The author is indebted to J. KOMJÁTI, Head of the Department, for permission to publish these results, DR. (MRS.) K. MEDZIHRADSZKY and coworkers, Inst. Org. Chem. L. Eötvös Univ. Sci. for the careful experimental work and DR. A. BALÁZS, Head of the Department, Dept. of Chemistry, OGIL for valuable discussion.

REFERENCES

[1] VASSZOJEVICS, N. B. [1967]: Teorija oszadocsno-nigracionnogo proiszhozsdenyija nyefti, Izv. Akad. Nauk SzSzSzR., Szer. Geol., N°. 11, p. 135—156.

[2] VASSZOJEVICS, N. B. [1973]: Osznovnüe zakonomernoszti, harakterizujuscsie organicseszkogo vescsesztva szovremennüh i iszkopaemüh oszadkov — Priroda organicseszkogo vescsesztva szovremennüh i iszkopaemüh oszadkov, Moszkva, "Nauka", p. 11—51.

[3] PHILIPPI, G. T. [1965]: On the depth, time and mechanism of petroleum generation, Geochim et Cosmochim. Acta **29,** p. 1021—1049.

[4] HARWOOD, R. J. [1977]: Oil and gas generation by laboratory pyrolysis of kerogen, Am. Ass. Petr. Geol. Bull., vol. **61,** No. 12, p. 2082—2102.

[5] GRANSCH, J. A., EISMA, E. [1966]: Characterisation of the insoluble organic matter of sediments by pyrolysis, Adv. in Organic Geochemistry, Proc. of the 3rd International Congress, p. 407—426. London.

[6] ESPITALIÉ, J. *et al.* [1977]: Méthode rapide de caracterisation des roches méres de leur potentiel petrolier et de leur degré d'évolution. Revue de l'IFP, vol. **XXXII,** 1, p. 23—42.

[7] CLAYPOOL, G, B., REED, F. R. [1976]: Thermal analysis for source-rock evaluation: quantitative estimate of organic richness and effects of lithologic variation. AAPG Bull., vol. **60,** 4, p. 608—626.

[8] LEVENTHAL, J. S. [1976]: Stepwise pyrolysis gas chromatography of kerogen is sedimentary rocks. Chemical Geology **18,** p. 5—20.

[9] COLIN BARKER [1976]: Pyrolysis techniques for source-rock evaluation. AAPG Bull., **58,** 11, p. 2349—2361.

[10] SOURON, C., BOULET, R., ESPITALIÉ, J. [1974]: Étude par spektrométrie de masse de la décomposition thermique sous vide de kerogénes appartenant a deux lignées évolutives distinctes. Revue de l'IFP, **XXIX,** p. 661—678.

[11] GIRAUD, A. [1970]: Application of pyrolysis and gas chromatography to geochemical characterization of kerogen in sedimentary rock. AAPG Bull., **54,** 3, p. 439—455.

[12] JONATHAN, D., L'HOTE, G.M DU ROUCHET, J. [1975]: Analyse geochimique des hydrocarbures légers par thermovaporisation. Revue de l'IFP, **XXX,** p. 65—88.

[13] DU ROUCHET, J. [1978]: Indices chimiques pour l'evaluation de l'état diagenetique des huiles et des roches sapropéliques. Revue de l'IFP, **XXXIII,** p. 33—45.

[14] KHANH, T., VAN DER WEITE, B. M. [1969]: Determination automatique du degré de carbonisation de la matiére organique de roches. Bull. Centre Red. Pau-SPNA, p. 449—457.
[15] BAJOR, M.: Einige Kenngrössen der organischen Geochemie bei der Suche nach Erdöl. Erdöl u. Kohle **22,** 9, p. 515—519 (1969).
[16] BALÁZS, Á., KONCZ, I. [1973]: Der Diagenesegrad der unlöslichen dispersen organischen Substanz von Gesteinen. Vorträge zu geochemischen und chemisch-physikalischen Problemen der Erdöl-Erdgas-Erkundung und -Förderung, Band I, Geochemie, p. 501—513. Budapest.
[17] KONCZ, I. [1977]: Kerogen thermal decomposition reactions: simulation of kinetics by measurements of katagenetic factor. 8th International Congress on Organic Geochemistry, Abstracts of Reports **1,** p. 114. Moscow.
[18] VELEV, V., VÜCSEV, V., KONCZ, I., PETROVA, R., TÓTH, P. [1978]: Problemü i rezultatü izucsenija organicseszkogo vescsesztva oszadocsnüh porod Vengrii i Bolgarii. Geologica Balcanica **8,** 1, p. 55—80.
[19] VELEV, V., MARKOVA, K., SISKOV, G.: Koeficientite na proporcionirane na ugleroda v organicsnoto vescsesztvo-pokazateli na uglefikacijata i kriterij pri kategorizacijata na neftemaj csinite szkali. (in press)
[20] BALÁZS, Á., KONCZ, I. [1975]: Geochemische Untersuchungen übertiefer Bohrungen. Compendium 74/75, Vorträge der 24. Haupttagung der DGMK, Band I, p. 84—97, Hamburg.
[21] KONCZ, I. [1977]: A szénhidrogén-genezis reakciókinetikai megközelítése. Kőolaj-Földgáz **10 11,** 8, 225—228.
[22] UNTERZAUCHER, J. [1940]: Ber. dtsch. Chem. Ges., **73,** 391.

Manuscript received, April 10, 1979

DR. I. KONCZ
Dept. of Chemistry,
Industrial Laboratory for Oil and
Gas Research (OGIL),
Nagykanizsa, H-8800, Hungary

Acta Mineralogica-Petrographica, Szeged, XXIV/1, 137—147, 1979

GEOTHERMAL INHOMOGENEITY IN THE HUNGARIAN GREAT PLAIN (PANNONIAN BASIN)

L. VÖLGYI

ABSTRACT

Investigations tried to analyze the geothermal conditions of the Pannonian Basin by processing the thermal data obtained from deep boreholes and to explore in detail the measures of inhomogeneities and tendencies of changes.

In a global sense the Pannonian Basin as a crustal structural unit can be characterized by a gradient corresponding to the terrestrial geothermal mean value. On the basis of regional comparison, however, considerable inhomogeneity occurs characterized by higher minima and high maxima approaching the world average. Based on statistic evaluations, the extreme values of spatial changes show changes of geothermal gradient of 4 to 8 °C/100 m as a function of the geographical situation and of the depth. The reliable isotherm calculations have shown similar inhomogeneity. The measure of vertical inhomogeneity is 4.2—6.8 °C/100 m being valid of the depth interval of 650 to 2860 m, in case of the isotherms calculated to 60—140 °C.

Studying the change of geothermal gradient as a function of depth four basic types can be distinguished:

1) the gradient increasing with depth, this can be approached by a straight line,
2) the gradient increasing at the beginning and decreasing later with depth, this can be approached by a sine wave,
3) the mixed gradient type of uncertain evaluation,
4) special gradients of obvious local anomalies.

Having studied the areas explored by deep-bores "hot-sites" lying in minimal depth as well as "cold-sites" lying in maximal depth could be determined. The result of processing of geothermal data, which can be generalized is that the value of the average geothermal gradient unambiguously decreases in sedimentary sequence parallel with increasing depth and concerning the depth interval between 100 and 5500 m this value is 7.0—4.0 °C/100 m.

INTRODUCTION

The endogene heat plays decisive role in the "internal life" of the earth since its origin to the recent. The views on the origin of this endogene heat can be divided into two groups. According to one of the research groups the earth preserved a part of the cosmic heat of the high-temperature origin but during its evolution it gradually cools and shrinks. The members of the other group (mostly the followers of the theory of condensation from cosmic dust) pronounce for the continuous heat generation. Estimations concerning the heat resources of the earth show recently rather diverse values. It seems to be probable that the heat quantity which can be derived from radioactive decay (43.34×10^{16} cal/hours) amounts to amount 24-fold of the emitted heat quantity (1.8×10^{16} cal/hours). This latter value supports the followers of heating, i.e. of the earth's expansion. Be, however, the recent balance of thermal budget of the earth either positive or negative, it can be stated that none of the theories could avoid the problem of terrestrial heat. This in itself is also the evidence of the significance of geothermics in several fields of geology.

Taking in general the geothermal situation of the earth, it follows from the second principle of thermodynamics that between the sites of different temperatures thermal transport is started from the warmer towards the cooler parts.

As to the investigations the global thermal field of the earth can be regarded to be stationary when taking the recent of the earth's history. The value of the earth's heat flux is estimated to be 1.5×10^{-6} cal/cm^2, in general.

Disregarding the insolation and eradiation phenomena the internal thermal field of the earth endures distortion partly due to the "heat source", partly due to the inhomogeneities of thermal conduction.

Regional (megatectonic) and local reasons may be responsible for the distortion of the terrestrial thermal field. The former will be discussed later in relation with the Pannonian Basin. In general, it can be said that the distribution of the isotherms of the terrestrial thermal field and of the main streamlines is considerably influenced by the spatial configuration of the rocks of different thermal conduction in the investigated area, resp., depth interval. In local sense, the "heat sources" (heat-producers) of physical sense play extraordinarily significant role. In addition to the well-known heat-producing geological processes, e.g. radioactivity or ore oxidation, the role of abyssal water is of more general validity especially in Hungarian conditions. As a result of the great specific heat and of the relatively low thermal conductivity of rocks the water flowing in subsurface regions keeps its basic temperature, thus, in the nature the temperature of water often differs from that of its environment (hot waters, karst water).

In connection with the so-called "depth thermal disturbance" generating under deep-geological conditions it is worthy to mention some physical facts. To the realization of thermal equilibrium, i.e. to the formation of stationary field theoretically infinite time is needed, after the thermodynamic calculations. When investigating the date of the stage approaching this state to 90 percent, a significant time value (about 10 million years) is obtained also in geological sense if e.g. deriving the site of thermal disturbance from the depth of the Moho-surface [STEGENA, L., SALÁT, P., 1972].

GEOTHERMAL SITUATION OF THE PANNONIAN BASIN

The geothermal conditions of a geological unit, area or region can be characterized most clearly by the average geothermal gradient or by its invert. As it has been stated in my previous work [VÖLGYI, L., 1978] on the basis of several hundred corrected temperature data deriving from the boreholes of the Great Plain constituting the major part of Hungary's area, the extreme values and averages of the geothermal gradient (resp. invert) are as follows:

extreme values:	4—8 °C/100 m = 25 − 12.5 m/°C
average values:	5.5 °C/100 m = 18 m/°C

Numerous authors tried to find relationship between the geological structure and the geothermal gradient. On the basis of the most frequent data of the rather different evaluations the following average values could be determined.

Average of continents (tabular and folded areas):
2.03 °C/100 m = 33 m/°C

Areas of ancient shields:

0.8 °C/100 m = 125 m/°C

Volcanic areas, young geosynclines:

9.7 °C/100 m = 10.3 m/°C

Shelves (mostly Scotland):

2.2 °C/100 m = 45.4 m/°C

Super-deep boreholes (USA, Soviet Union):

1.8 – 3.1 °C/100 m = 56.5 – 32.2 m/°C

On the basis of some data of Hungarian deep boreholes the decrease of the geothermal gradient is also probable:

3.8 – 4.0 °C/100 m = 26.3 – 25.0 m/°C

Thus, considering the average extreme values of the crustal-structural types of the earth, i.e. the minimal 0.8 and the maximal 9.7 °C/100 m geothermal gradient, it can be stated that the Pannonian Basin represents nearly exactly the mean value.

The Pannonian Basin is a young geosyncline which is surrounded by crust parts of continental folded structure. Thus, in regional environmental sense it is a combined type, because the average of 5.5 °C/100 m exceeds the continental average (3.03 °C/100 m) but does not reach the world maxima of volcanic areas and young geosynclines.

The considerable deviation of the extreme values relates to large-scale local changes and provides a fair basis to real interpretation. The minimal extreme value is higher than the continental average which obviously proves the relative "hot" crustal position. The fact, however, that the maximal extreme value nearly reaches the maxima of 9.7 °C/100 m of the volcanic areas, is in clear relationship with the real geological conditions.

CRUSTAL-STRUCTURAL BACKGROUND OF THE DISTORTION OF THE TERRESTRIAL THERMAL FIELD IN HUNGARY

Based on areal comparative studies it can be accepted as an evidence that the Pannonian Basin possesses a higher heat flow value as compared to its environment [STEGENA, 1973]. According to him the geoisotherms of 1 km indicate 50—70 °C in Hungary's area while in the surroundings these amount only to 30—40 °C. Thus, the area of Hungary is a "relative geothermal maximum" with high heat flux values.

When evaluating the regional geological situation the search for geothermal reasons is to be carried out only down to the lower boundary of the crust, i.e. to the surface of the Moho-discontinuity. On the basis of the Carpatho-Dinaride crust-surveying seismic profile the crustal thickness below the Pannonian Basin amounts only to 26 km [MITUCH, E., POSGAY, K., 1972]. Along this profile the change of the thickness ratios of the upper crust (granite velocity zone) and of the lower crust (basalt velocity zone) is remarkable. In Hungary's area the basalt-zone is extraordinarily thinned (5 to 8 km thickness). This indicates the approach of the Moho-surface to the earth's surface which is produced by isostatic compensation of the average subsidence of 3000 m of the Pannonian. This phenomenon is considered by STEGENA *et al.*, [1975], to be a mantle diapir which has been generated by the subduction connected to the surrounding mountains. The subduction zones are dealt with by SZÁDECZKY-KARDOSS, E., [1973]. The subduction zones reported by him coincide with the megatectonic lines known so far. It is without doubt that the zonal arrangement of the hydrocarbon and carbon-dioxide deposits joins the

directions of the megatectonic lines. The thermal disturbance, however, prevails in the Pannonian Basin on a regional scale. The tectonic lines may prove only local anomalies at least.

Investigating the velocity of heat flow in harmony with the geological events it seems to be probable that the recent upper crustal relative geothermal anomaly is produced by the thermal disturbance followed at the Pannonian-Miocene boundary. In accordance with STEGENA, L., when studying the origin of heat surplus the decisive significance of heat transport (convective transport) should be regarded a regional factor produced by upward directed material transport.

The statement of SVETZOV, P. P., [1974] is remarkable, i.e. concerning the anomalously high temperatures occurring in the Piedmont and Intramontane Basins of the Alpine folded zone. Accordingly, this thermal anomaly can not be always sufficiently explained only by the endogene heat of the earth. In these basins the thick sequences of clayey and fine-detrital rocks being in state of compaction are believed to by supplementary heat flow sources. "This type of strate forms a heat-shade promoting the accumulation of heat in the "nest" below the shade".

The vertical heat transporting role of the volcanic activity proceeded in the Miocene and Pannonian is without doubt. Further, it is obvious that only a part of heat deriving from volcanic activity was emitted to the earth's atmosphere. Recently, by means of vitrinite reflectance measurements it can be evidenced that in the surroundings of the Miocene volcanites the paleo-temperature of the Early Pannonian was considerably higher than in our days. Since that time these formations lie in a gradually subsiding basin, but relatively these are "cooled". This is possible only if the heat surplus of volcanic origin was transferred into the sedimentary sequence and when spreading it an average compensation temperature was produced in the Pannonian sediments.

As to the author's opinion the convective heat transporting activity of the upward flowing hot waters deriving from great depths through fractures and fissures should also be considered a similar supplementary heat flow source. The role and significance of the water flows in basins were always emphasized by Hungarian experts.

EVIDENCES OF GEOTHERMAL INHOMOGENEITY

In this paper the data deriving from the area east of the Danube and from (hydrocarbon prospecting and exploring) deep-bores were used. In the previous work [VÖLGYI, L., 1978] the measures and tendencies of abyssal thermal changes were studied and more considerable inhomogeneity was obtained than expected before.

When plotting the data of geothermal gradient as a function of depth isotherm curves can be constructed which provide the theoretical depth-distribution function of a temperature value. This, however, bears practical significance if correctly determined gradients and depth data are used.

Corrected isotherm calculations

The calculations of isotherms was corrected so that less but more reliable basic data were taken into account. In favour of this only the measurement data were used which approached the temperature value of the isotherm to be computed to ± 10 °C. In this way the number of reliable data decreased from 450 to 165 but this made possible to carry out linear interpoiation within a depth interval of ± 200 m.

The procedure has been as follows:

t = measured temperature, °C, within the interval of ± 10 °C,

t_i = isotherm value (°C),

i = 60, 80, 100, 120, 140,

M = depth of temperature measurement (m),

M_i = calculated depth of the isotherm *i* in the geological formation of definite age of the given area.

Consequently:

$$M_i = \frac{M \cdot t_i}{t}.$$

The distribution in depth of the calculated isotherms are shown in *Fig. 1*. The comprehensive evaluation of this gives the following result.

According to the data, above 140 °C the uncertainties are great. This is caused by the fact that the average depth of the boreholes varies around 2600 m, thus data of sufficient quantity are available only to this depth (due to the accuracy criteria).

It can be demonstrated that the depth variance of the isotherms between 60 and 120 °C is of an order of magnitude of several hundred metres as it can be seen in Table 1:

TABLE 1

Isotherm (C)	Depth limits (m)	Average depth (m)	M_z (m)
60	650—1280	965	630
80	980—1680	1330	700
100	1320—2080	1700	760
120	1660—2500	2080	840
140	2000—2860	2430	860

M_z = depth interval.

Average and extreme values of geothermal gradients

To control the previous statistic work the calculations of geothermal gradients following from the isotherm calculations was also carried out.

The result is shown in Table 2:

TABLE 2

Isotherm (°C)	Isothermal gradient* (°C/100 m)		Invert (m/°C)
	Interval	Average values	
60	7.54—3.83	5.07	19.69
80	7.04—4.11	5.18	19.27
100	6.74—4.28	5.23	19.10
120	6.56—4.36	5.24	19.08
140	6.45—4.51	5.30	18.84
Average to 60—140:	4.22—6.86	5.20	19.19

* taking 11 °C near-surface temperature.

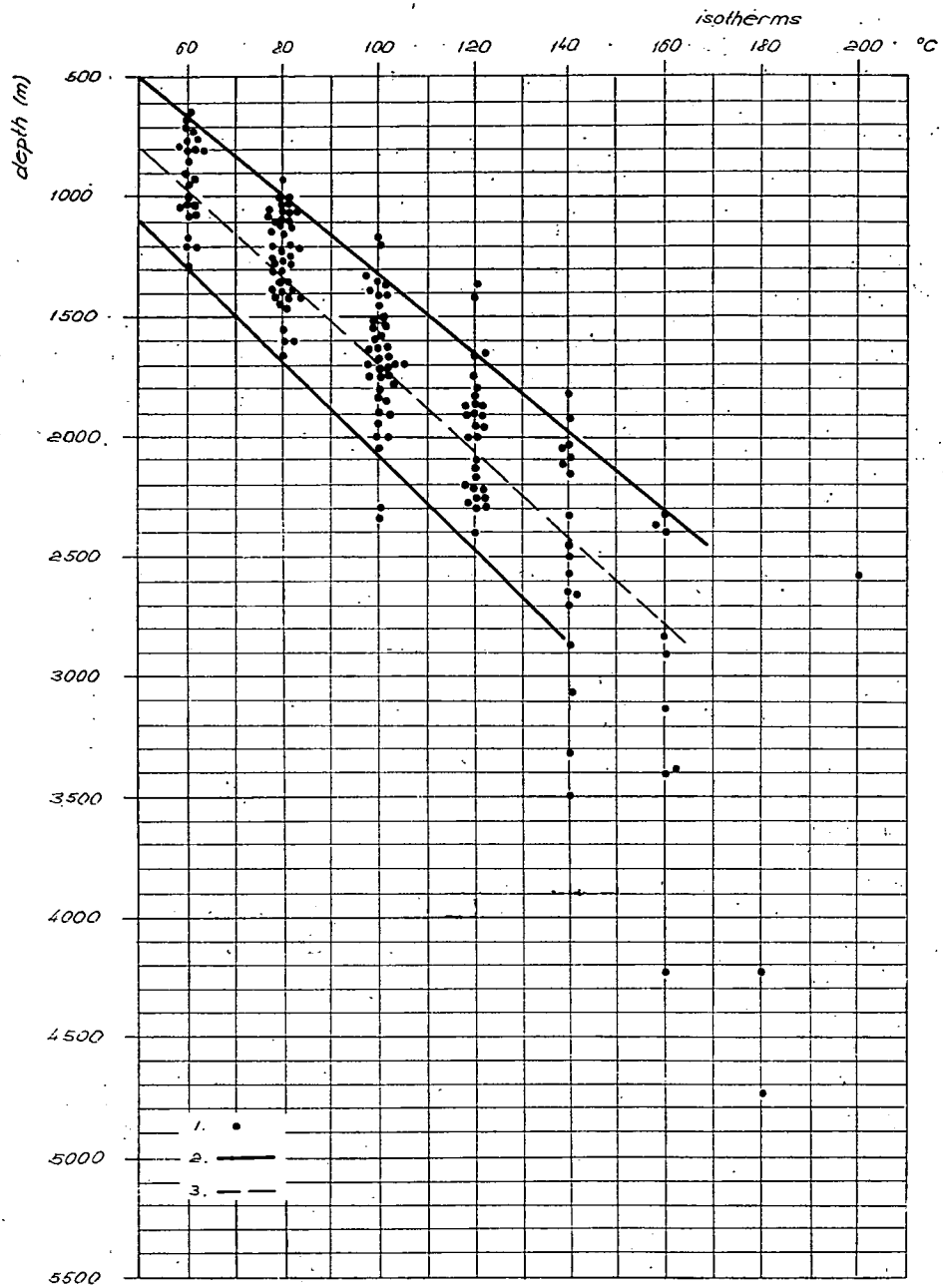

Fig. 1. Distribution in depth of the calculated isotherms. 1) calculated depth of isotherms; — 2) extreme values of gradients; — 3) average gradient.

Comparison of the average and extreme values between the statistic and corrected (i.e. computed from isotherms) methods is given in Table 3:

TABLE 3

Method	Geothermal gradient (°C/100 m)		Invert (m/°C)
	Extreme	Average	
statistic	4.0—8.0	5.5	18.2
corrected	4.2—6.8	5.2	19.2

The measure of vertical inhomogeneity of the Great Plain is 4.2—6.8 °C/100 m according to the corrected geothermal gradient calculations. It is valid of the intervals of 60 to 140 °C and 650 to 2860 m.

GEOTHERMAL REGION TYPES IN THE GREAT PLAIN

In this part the investigation results carried out in connection with local change of the geothermal gradients will be discussed. On the basis of the collected data two fundamentally differing types will be introduced by means of several concrete instances.

E.g. "hot-sites" lying in minimal depth:

Mezőhegyes	in 457 m	58 °C
	in 1095 m	90 °C
Tótkomlós	in 762 m	68 °C
	in 1008 m	86 °C
	in 1486 m	121 °C
	in 2190 m	150 °C
Hunya	in 3925 m	203 °C

E.g. "cold-sites" lying in maximal depths:

Nagyecsed	in 1174 m	55 °C
Cegléd	in 1389 m	92 °C
Mindszent	in 2472 m	107 °C
Furta	in 2341 m	100 °C
Algyő	in 1106 m	58 °C
	in 1506 m	75 °C
	in 2054 m	107 °C
	in 2423 m	126 °C
	in 2545 m	132 °C
	in 3196 m	163 °C
Makó	in 3500 m	147 °C
	in 4095 m	173 °C
Hódmezővásárhely	in 4790 m	181 °C
	in 5418 m	203 °C

These few examples also indicate that how relative are the "cold" and "hot" notions since the location bears significance only as a function of depth. In evaluation the space coordinates should be taken into account.

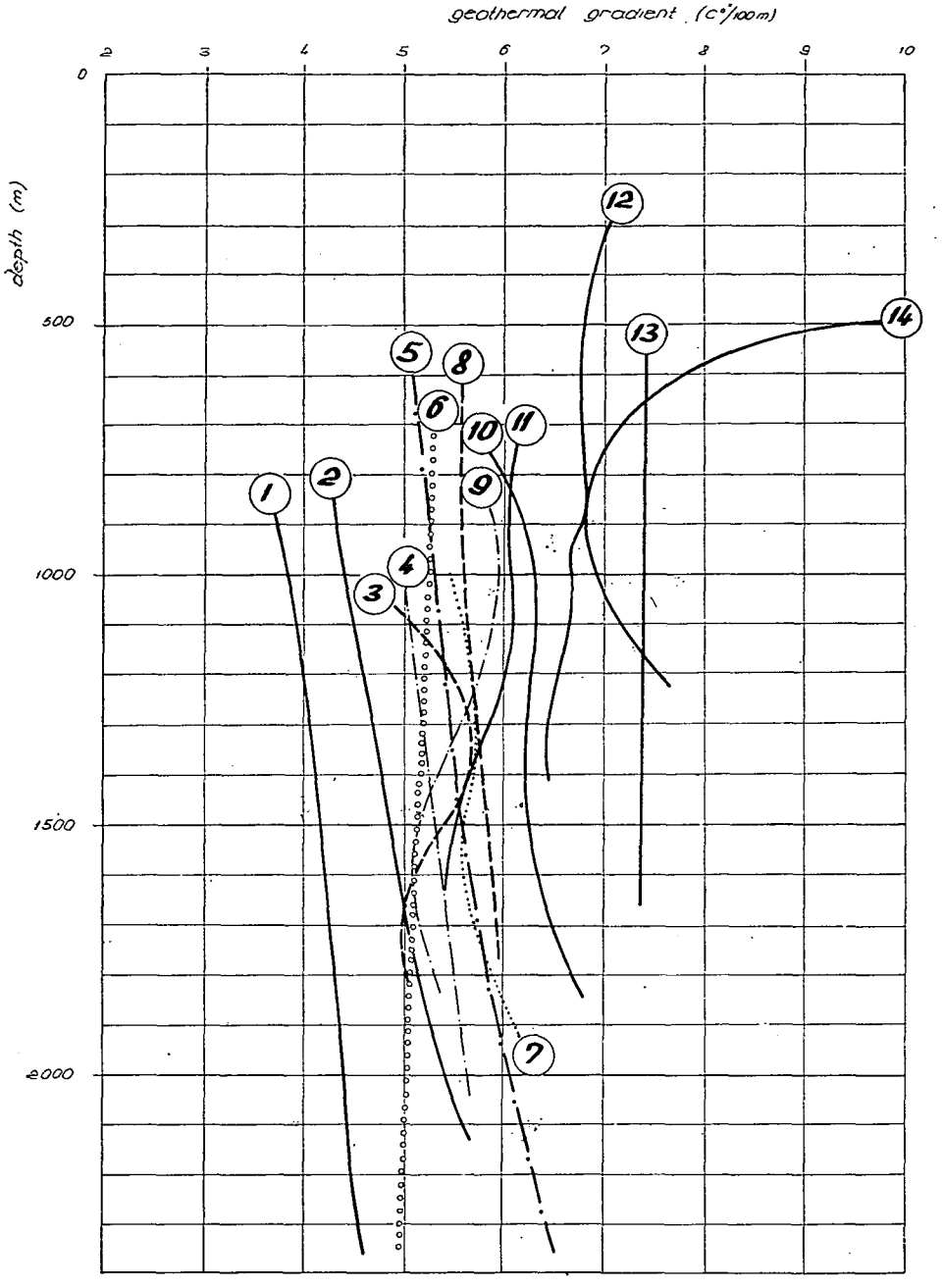

Fig. 2. Local changes of the geothermal gradient (Great Plain). — Names of exploratory wells № 1—14 see in the text

In everyday sense, the area characterized by hot waters from small depths is called "hot-site" but in absolute value the temperature of 203 °C is qualified also as "cold-site" when it is below the depth of 5400 m.

Types of geothermal gradients

The change of the geothermal gradient as a function of site and depth is shown in the figure of complex change of geothermal gradient *(Fig. 2)*. This shows the areal average run of the temperature gradients of 14 regions of the Great Plain. The result is certainly astonishing. It is clear that a given gradient value is rather meaningless if one tries to know the real situation.

In the 14 areas constant gradient is found only in one case. The gradient of all the other areas are changing as a function of depth, in all possible varieties.

Gradients increasing and decreasing as a function of depth are found, as well as tendencies of repetition or completely turn also occur. These concrete changes of geothermal gradients averaged to each regions call the attention to the search for the local geological reasons. The gradient types are as follows:

(a) *Gradient increasing with depth* (this can be approached by a straight line). The representative areas (number of lines in the figure in brackets):
Algyő (1)
Kiskunhalas (2)
Szank (4)
Üllés (5)
Kaszaper (8)
Pusztaföldvár (10; not typical)

(b) *Gradient first increasing then decreasing with depth* (this can be approached by a sine-wave):
Kisújszállás (3)
Hajdúszoboszló (11)
Kunmadaras (7)
Szandaszőlős (9)

(c) *Mixed gradient type of uncertain evaluation:*
Endrőd (6) — decreasing tendency
Ebes (12) — curve of decreasing tendency

(d) *Special gradients of obvious local anomalies:*
Tótkomlós (13) — independent of depth, high constant gradient,
Mezőhegyes (14) — gradient suddenly decreasing along a hemicircle then increasing with depth.

TENDENCIES OF VERTICAL INHOMOGENEITY IN GREATER DEPTHS

The results of particular investigations introduced in the previous chapters fairly represent the conditions of geothermal gradients in the sedimentary sequence of the Pannonian Basin down to about 2500—3000 metres depth but do not provide information for greater depths. Thus, though the number of data is insufficient, it is expedient to investigate the change of geothermal gradient as a function of depth using all the data available *(Fig. 3)*.

When determining the minimal — average — maximal tendency of changes of the geothermal gradient as a function of depths by means of graphic plotting, according to *Fig. 3* the approximate values shown in Table 4 will be obtained:

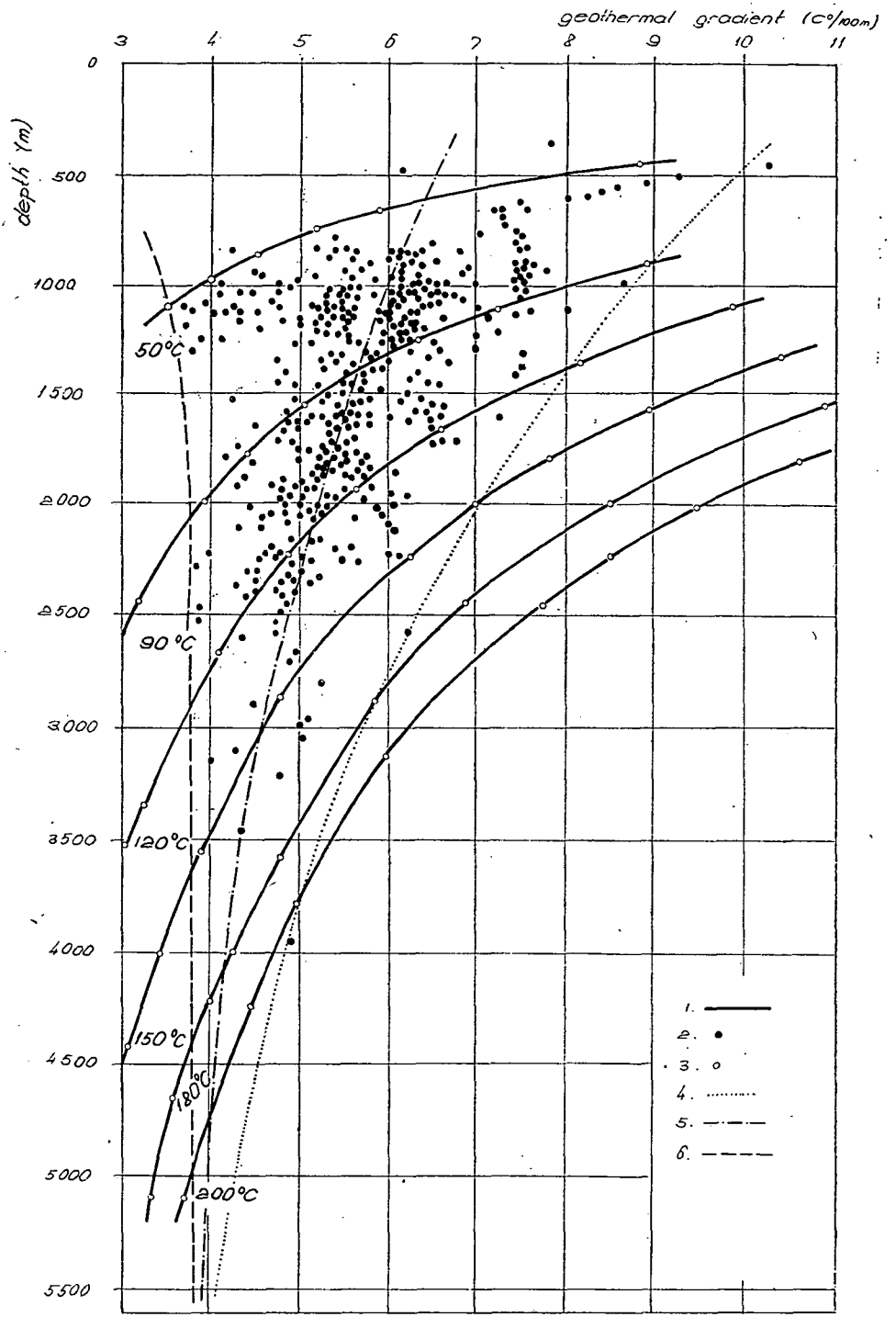
geothermal gradient (C°/100m)
3
4
5
6
7
8
9
10
11
depth (m)
0
500
1000
1500
2000
2500
3000
3500
4000
4500
5000
5500
50°C
90°C
120°C
150°C
180°C
200°C
1.
2.
3.
4.
5.
6.

TABLE 4

Isotherm	Depth — Temperature gradient					
	Minimal		Average		Maximal	
°C	M	°C/100 m	M	°C/100 m	M	°C/100 m
50	1100	3.5	600	6.4	400	10.0
90	2100	3.7	1400	5.7	900	8.9
120	2900	3.75	2150	5.1	1400	8.0
150	3600	3.8	3000	4.7	2000	7.0
180	4400	3.8	4000	4.25	2900	6.0
200	>5000	3.8	4700	4.15	3700	5.0

It can be stated that with increasing depth
— the minimal value hardly changes (3.5—3.8);
— the maximal value considerably decreases (10.0—5.0);
— the average value unambiguously decreases.

The decrease of the average geothermal gradient with increasing depth is believed a tendency, the fact of which is without doubt.

The measure of decrease of the average geothermal gradient determined by author is 7.0—4.0 °C/100 m concerning the depth interval of 100 to 5500 m.

The reasons of this phenomenon should be searched by means of further particular investigations. To elucidate this problem it would be advantageous to investigate the role of convection flows and the thermal conduction coefficient of the terrestrial heat flows.

REFERENCES

MITUCH, E., POSGAY, K. [1972]: Hungary. In: "The crustal structure of Central and Southeastern Europe based on the results of explosion Seismology (ed.: SZÉNÁS, GY.). Geophys. Trans. Spec. Edit., Budapest, 118—130.

STEGENA, L., SALÁT, P. [1972]: A mélyfúrásokkal kapcsolatos geotermikus kutatások alapösszefüggései (Basic relationships of geothermal researches connected to deep-bores). — Publication of the MTESZ — Magyar Geofizikusok Egyesülete.

STEGENA, L. [1973]: A Pannon-medence kainozóos evolúciója (Cenozoic evolution of the Pannonian Basin). — Geonómia és Bányászat, **6**, 1—4.

STEGENA, L. *et al.* [1975]: A Pannon-medence későkainozóos fejlődése (Late Cenozoic evolution of the Pannonian Basin). — Földtani Közl., **105**, 2.

SVETZOV, P. P. [1974]: Geothermal conditions of Mesozoic and Cainozoic hydrocarbon-bearing basins (in Russian), Nauka, USSR.

SZÁDECZKY-KARDOSS, E. [1973]: A Kárpát-pannón terület szubdukciós övezetei (Subduction zones of the Carpatho-Pannonian area). — Földtani Közl., **103**, 3—4.

VÖLGYI, L. [1978]: The role of geothermal conditions of Hungary in hydrocarbon prospection. — Acta Geol. Acad. Sci. Hung., Tom. **21**, 1—2.

Manuscript received, November 20, 1978

DR. LÁSZLÓ VÖLGYI
Petroleum Exploring Enterprise,
H-5000 Szolnok, Munkásőr u. 43.
Hungary

Fig. 3. Change of the geothermal gradient as a function of depth (data of the Great Plain). — 1) isotherms, being fundamental from the point of view of hydrocarbons, — 2) measured data, — 3) points of curve construction, — 4) maximal gradient, — 5) average gradient, — 6) minimal gradient

Acta Mineralogica-Petrographica, Szeged, XXIV/1, 149—165, 1979

EROSION SURFACES AND FACIES CHANGES IN THE DANUBE TECTONIC TRENCH

B. MOLNÁR

INTRODUCTION

Having explored the Pliocene and Quaternary formations of the Great Plain along the profile of nearly N—S direction lying in the line of the river Tisza, the Hungarian State Geological Institute initiated to drill new boreholes in a profile of W—E direction. For the time being the profile includes the boreholes of Kunadacs, of the Kecskemét environs and of Nyárlőrinc. Under the guidance of the Department for Flatlands of the Hungarian State Geological Institute the core samples of the boreholes were investigated by many-sided sedimentological and paleontological methods. Within this complex processing this paper tries to give a report on the micromineralogical and grain-size analysis of sand strata from the borehole of Nyárlőrinc.

Nyárlőrinc is situated 19 km east of Kecskemét, at the side of the Danube—Tisza Interfluve inclining towards the river Tisza, about 13 km west of the river. The borehole Nyárlőrinc Ny-1 was drilled in 1975 in the axis of the "Danube tectonic trench" demonstrated by SÜMEGHY, J. [1953].

In the borehole profile of 800 metres of Nyárlőrinc from down topwards Upper Pannonian strata to 688 m, Uppermost Pliocene, Levantine strata between 273 and 688 m [after FRANYO, F.] or as suggested recently by BARTHA, F. [1971, 1975] and by JÁMBOR, Á., KORPÁS—HÓDI, M. [1971] Uppermost Upper Pannonian strata are found. The latter author regard the Uppermost Pliocene sequence to be a part of the Upper Pannonian. Finally, between 0 and 273 m the Pleistocene sequence is found. Holocene is absent.

In the "Danube tectonic trench" the Pliocene and Quaternary strata become thicker towards Szentes, Mindszent and Szeged and their lower boundary gets deeper than determined in the profile of Nyárlőrinc indicating a more intense subsidence as compared to its environment. E.g. at Mindszent the Upper Pannonian — Levantine resp. the Levantine — Pleistocene boundaries occurred in a depth of 1210 resp. 690 m, i.e. much deeper than at Nyárlőrinc.

The micromineralogical analysis of 103 samples deriving from the interval between 0 and 800 m of the Nyárlőrinc profile was carried out. In favour of micromineralogical analysis the samples were first divided into fractions, then the minerals of the fraction of 0.1 to 0.2 mm were separated to light and heavy minerals by means of bromoform, the boundary between them lying at a specific weight of 2.8.

Based on the previous investigations it was expected that at Nyárlőrinc in addition to the fluviatile facies the aeolian ones will also occur within the Pleistocene sediments, thus the shape of the quartz grains of these samples were also determined

by means of the grain-shape method of CAILLEUX [CAILLEUX, A., 1952; MOLNÁR, B., 1961]. Grain-shape investigations were carried out in the grains of more than 0.2 mm diameter if possible, in case of finer-grained material the grains of 0.1 to 0.2 mm diameter were used.

In case of the clastic sediments of the Great Plain the change in grain-size composition strongly affects the heavy-mineral composition, thus in favour of right conclusions the compositional analyses of grains were also carried out [MOLNÁR, B., 1969].

The investigation results are comprehended in Tables and the data were demonstrated in profiles, respectively (Tables 1—2, *Figs. 1—2*). When grouping the results according to ages the following statements can be concluded.

INVESTIGATION RESULTS OF THE UPPER PANNONIAN FORMATIONS

The Upper Pannonian formation were explored between 688 and 800 metres, i.e. in a length of 112.0 m. On the basis of the profile of FRANYÓ, F. [1976] showing the sedimentary evolution the Upper Pannonian sequence of Nyárlőrinc is characterized by the predominance of the pelitic clastic sediments. Consequently, this strata sequence is less suitable to micromineralogical investigations, thus the analyses of only eight samples were carried out. The grain composition of the investigated samples did not exceed the fine-grained sand either investigating the coarsest strata of the sequence. It can be read off from Table 1, resp., from the column III of *Fig. 1* that the prevailing grain size varied between 0.04 and 0.12 mm.

It is characteristic of the heavy-mineral composition of the sedimentary sequence that it is poor in heavy minerals (Table 1). In all samples chlorite predominates, the quantity of which varies between 68.8 and 84.2 percent. Nevertheless, when summing up the 10.2 percent biotite and 13.2 percent chlorite content of the sample of least; i.e. 68.8 percent chlorite content, it is obvious that phyllosilicates predominate also in this sample.

Garnet and weathered minerals (0.6 to 6.3 and 1.8 to 5.9 percent, respectively) occurred in much smaller quantities, but in all samples. In order of better review these minerals were framed in Table 1. Other minerals, e.g. hypersthene, other orthorhombic pyroxenes, augite and diopside which are demonstrated together in *Fig. 1*, did not occur in a quantity which proved to have been suitable to demonstration. The stereomicroscopic photos of Plate I reflect also this rather monotonous mineral composition consisting mostly of chlorite.

The mineral composition of the Upper Pannonian sequence of Nyárlőrinc shows good agreement with that the Upper Pannonian sequences of Szentes, Mindszent, Szeged and of that of the South Great Plain, in general [MOLNÁR, B., 1963, 1965*a*, 1965*b*, 1966*a*, 1966*b*, 1966*c*; GEDEON—RAJETZKY, M., 1975].

As to our recent knowledge, this part of the Upper Pannonian sedimentary sequence is a lacustrine sediment both in the Great Plain and thus also at Nyárlőrinc. The homogeneous lacustrine sedimentation conditions and the selective weathering may be the reasons of this poorish mineral composition.

The CAILLEUX's grain-shape method showed predominantly sharp splintery quartz grains in the Upper Pannonian section of the borehole, profile. Lightsurfaced, slightly rounded quartz grains occurred only in 6.0 to 17.0 percent (*Fig. 1*, column II). The stereomicroscopic photo of Plate V (4) fairly shows that quartz grains are really sharp a splintery. According to CAILLEUX, A. this composition relates to fluviatile transport and deposition in water.

TABLE 1

Heavy mineral composition of bore-profile of Nyárlőrinc

Number	Depth m	Dominantly magmatic minerals										Dominantly metamorphic minerals										Other minerals							Total quantity minerals in the examined fraction	Dominant grain diameter mm	AGE	FACIES
		Hypersthene	Other rhombic pyroxenes	Augite	Diopside	Basaltic—Hornblende	Magnetite—Ilmenite	Apatite	Zircon	Biotite	Chloritized Biotite	Chlorite	Tourmaline	Epidote	Clinosoisite	Zoisite	Rutile	Hornblende	Actinolite—Tremolite	Anthophyllite	Garnet	Staurolite	Kyanite	Calcite-dolomite	Limonite	Pyrite	Other micas	Weathered minerals				
52	398.0 I.	5.2	7.3	3.8	3.5	0.6	11.1	1.4	—	—	—	2.1	1.0	1.0	0.7	—	—	6.2	0.3	1.0	32.4	—	0.3	0.3	—	0.7	—	21.1	5.5	1.00		
53	398.0 II.	3.8	3.8	2.7	2.7	0.3	8.9	1.0	0.3	—	—	4.1	1.0	2.4	2.4	0.7	—	9.2	1.0	0.3	26.0	0.3	1.4	1.0	—	1.4	—	25.3	50.4	1.20		
54	399.4 —400.0	—	2.6	0.9	—	0.9	1.3	0.9	—	0.4	—	52.2	0.9	1.3	0.9	—	—	4.8	0.9	0.9	2.2	—	0.9	4.4	—	—	9.6	14.0	0.8	0.15		
55	433.20—433.8	0.3	3.5	1.0	3.5	0.3	4.5	0.3	—	—	—	42.4	0.7	1.4	1.7	—	—	4.9	0.3	0.3	8.4	—	0.7	4.9	—	—	3.8	17.1	3.0	0.14		
56	439.19—440.01	0.6	2.9	0.9	4.1	0.6	2.9	1.6	—	0.3	—	14.8	—	0.9	1.9	0.6	—	6.4	0.9	0.3	26.0	0.6	0.3	7.3	—	5.4	3.8	16.9	7.3	0.24		
57	447.2 —448.3	—	1.6	—	0.5	—	0.5	2.1	—	—	—	65.8	—	1.1	0.5	—	—	1.6	1.1	—	2.7	—	0.5	2.7	—	1.1	6.4	11.8	1.8	0.11		
58	456.70—457.32	0.3	4.4	2.3	3.7	0.3	4.7	2.3	—	—	—	20.9	1.0	0.3	2.0	—	—	4.7	1.3	0.3	10.1	—	0.7	4.4	—	—	3.0	33.3	2.3	0.14		
59	460.16—461.4	2.0	2.6	3.2	1.2	—	8.1	0.9	0.3	—	—	23.5	0.6	0.6	1.5	—	—	7.0	—	—	28.7	0.3	0.6	0.6	0.3	1.7	0.6	15.7	1.6	0.09		
60	472.00—473.05	0.3	1.5	1.2	2.8	0.3	3.1	0.3	—	—	—	19.5	0.6	0.6	0.9	—	—	4.6	0.9	—	15.8	—	0.6	26.0	—	0.9	5.6	14.5	8.5	0.22		
61	475.40—479.00	—	3.6	2.3	3.9	—	3.2	1.3	0.3	—	—	24.1	—	1.3	1.0	—	—	9.10	0.6	—	25.6	—	0.3	5.2	—	1.0	3.2	14.0	4.5	0.19		
62	489.12—489.83	0.3	2.3	1.7	1.7	0.3	6.7	2.3	0.3	—	—	24.8	0.7	1.0	1.3	—	—	4.4	1.3	0.3	22.8	—	—	6.0	—	0.7	3.3	17.8	2.7	0.16		
63	492.00—495.14	—	2.0	1.6	3.2	—	2.4	0.8	—	0.8	—	47.4	0.4	0.4	1.2	—	—	4.9	0.4	0.8	6.9	—	0.4	3.6	—	—	4.9	17.9	2.3	0.20		
64	496.69—500.00	—	3.3	0.3	1.2	—	5.5	1.5	—	0.6	—	34.4	0.3	0.9	2.7	—	—	3.9	1.5	0.3	15.2	—	1.2	4.0	—	0.3	4.0	18.9	3.3	0.20		
65	501.15—503.20	—	5.1	2.0	1.3	—	7.8	1.7	—	—	—	15.2	—	0.3	3.0	—	0.3	2.0	0.3	—	35.7	—	1.0	4.4	—	1.3	—	18.6	3.2	0.7		
66	508.00—510.80	—	4.9	0.4	2.4	—	1.2	0.4	—	0.8	—	47.8	0.4	1.6	0.8	0.4	—	4.5	1.6	—	8.5	—	0.4	2.4	—	—	6.9	14.6	3.7	0.14		
67	510.80—516.0	0.4	2.9	0.8	2.9	—	6.1	0.4	—	—	—	47.8	0.4	0.4	2.0	0.4	0.4	4.1	1.2	—	11.1	—	—	5.7	—	—	2.0	11.0	1.00	0.19		
68	522.00—527.80	0.6	3.1	1.5	4.0	—	7.4	0.6	—	0.3	—	11.8	—	0.9	2.8	—	—	2.2	1.2	—	35.9	—	1.5	3.4	—	0.9	1.5	20.4	4.7	0.24		
69	539.30—545.60	—	3.2	0.5	3.2	—	2.3	0.5	—	—	—	52.1	0.5	0.9	1.4	0.5	—	3.2	—	0.9	11.5	—	0.5	4.6	—	0.9	1.8	11.5	2.7	0.20		
70	545.60—550.10	0.4	3.0	1.1	1.9	—	4.2	0.8	—	—	—	35.7	0.4	0.4	0.8	—	0.4	2.3	0.8	—	12.9	—	1.5	4.2	—	0.4	1.5	27.3	3.9	0.21		
71	550.48—550.98	—	6.1	1.8	2.5	—	8.7	2.2	—	—	—	16.2	—	1.1	2.2	—	—	4.3	0.7	0.4	20.6	—	0.7	2.2	—	—	0.4	29.9	3.8	0.18		
72	561.80—565.92	0.3	3.4	1.9	3.4	—	6.2	0.9	—	—	—	16.8	0.9	1.2	1.2	—	0.3	1.5	1.2	—	23.9	—	0.9	6.2	0.3	—	2.2	27.3	4.1	0.21		
73	570.80—577.10/b	—	1.0	1.0	1.7	—	6.8	1.4	—	0.3	—	35.5	—	1.0	1.0	—	—	0.3	0.7	0.3	14.3	—	1.0	3.1	—	—	2.7	27.9	4.2	0.22		
74	577.10—579.95	—	2.1	3.1	2.1	—	8.6	—	—	0.3	—	28.7	0.7	0.3	1.0	—	—	0.3	1.0	0.3	16.5	—	0.3	5.5	—	—	1.0	28.2	3.3	0.23		
75	580.50—585.10/b	0.5	0.5	0.9	0.9	—	5.1	0.9	—	3.2	—	43.6	—	1.4	1.8	—	—	0.5	0.9	0.5	9.7	—	0.9	0.5	0.9	1.4	4.6	21.3	0.3	0.16		
76	585.10—591.40/b	—	3.3	1.7	3.0	—	4.7	2.0	—	0.6	—	34.0	0.6	0.6	2.6	0.3	—	0.3	0.3	0.3	11.7	0.3	0.3	2.7	—	1.0	2.7	27.0	2.7	0.14		
77	591.40—595.25	0.6	7.4	1.3	1.6	—	2.6	0.6	—	2.2	—	38.7	0.3	1.0	1.9	0.6	—	—	0.3	0.3	13.1	—	1.0	5.1	—	0.3	2.2	18.9	4.1	0.15		
78	595.31—596.30	—	0.8	0.4	1.2	—	5.2	—	—	—	—	33.5	—	0.8	1.6	—	—	1.6	—	—	5.9	—	0.4	4.8	—	3.2	1.6	39.0	7.4	0.31		
79	598.02—600.98	0.7	2.8	1.1	2.8	—	3.6	0.3	—	1.1	—	35.3	—	1.4	1.4	0.3	—	1.1	—	0.3	6.1	—	0.7	0.3	—	0.3	1.4	39.0	5.0	0.24		
80	604.40—605.55	0.4	2.9	1.8	2.6	—	5.1	1.8	—	0.7	—	11.8	0.7	1.8	2.0	—	0.4	—	0.7	0.4	25.0	—	0.7	0.4	—	0.7	1.1	39.0	3.8	0.30		
81	609.13—609.47	—	2.6	1.3	3.3	—	4.6	1.0	0.3	4.0	—	32.6	0.3	1.3	0.3	0.3	—	—	0.3	—	12.2	—	0.3	3.0	—	—	6.9	25.4	2.5	0.14		
82	610.22—611.50	—	4.8	1.5	5.2	—	7.4	0.7	—	—	—	7.1	0.7	3.0	1.9	0.4	—	0.4	0.8	—	37.1	—	1.1	2.2	—	1.5	0.4	23.8	6.1	0.22		
83	613.5 —615.00	1.4	2.0	0.7	2.0	—	3.8	1.7	—	2.0	—	31.8	0.3	1.0	1.0	—	—	0.3	0.7	—	10.0	—	1.0	2.7	—	1.4	2.0	34.2	2.0	0.12		
84	623.60—624.23	—	5.2	0.7	4.5	—	4.2	1.4	—	0.3	—	7.6	0.7	3.8	5.5	2.1	—	0.3	0.7	—	32.9	—	1.4	—	—	0.7	1.7	26.3	5.7	0.19		
85	627.40—630.00	—	3.8	3.0	3.0	—	10.9	2.3	—	1.1	—	11.7	—	2.6	2.6	0.4	—	—	0.4	—	28.3	0.4	1.5	2.3	—	0.8	0.4	24.5	2.3	0.16		
86	635.00—635.75	—	2.8	0.7	1.0	—	7.3	1.7	0.3	0.3	—	12.8	—	1.7	1.7	—	—	—	0.7	0.7	18.3	—	1.0	9.7	—	1.7	4.8	32.8	3.4	0.42		
87	637.05—640.00	—	1.3	—	—	—	—	1.3	—	2.7	—	76.2	—	1.3	—	—	—	—	—	—	4.7	—	0.6	6.0	—	0.6	1.3	4.0	0.8	0.10		
88	650.41—651.09	0.7	2.3	1.0	2.0	—	7.3	1.0	—	0.3	—	12.9	0.7	2.3	2.0	0.3	—	—	0.7	—	36.5	0.3	2.6	0.3	—	—	0.7	26.1	8.2	0.26		
89	657.00—657.53	0.3	2.8	0.6	2.8	—	10.0	2.2	—	1.2	—	20.9	1.2	1.5	1.2	—	—	0.6	—	—	25.1	0.3	0.6	1.6	—	6.2	0.3	20.6	2.1	0.90		
90	659.59—661.70	0.3	4.5	0.6	2.1	—	8.2	2.1	—	0.6	—	16.4	1.2	4.5	1.5	—	—	—	—	0.3	26.3	—	0.9	2.4	—	4.5	0.3	23.3	4.2	0.70		
91	663.25—664.20	—	1.2	0.8	0.8	—	2.4	1.2	—	0.8	—	13.0	0.8	1.2	0.8	0.4	—	—	0.4	1.2	4.0	—	0.8	35.8	—	3.2	1.2	30.0	1.3	0.21		
92	667.80—668.61	—	3.0	0.7	3.0	—	7.7	1.0	—	0.7	—	37.3	—	1.7	1.0	—	—	—	—	0.3	16.5	—	1.3	1.3	—	1.3	1.0	22.2	3.6	0.38		
93	675.53—676.42	—	1.5	—	1.9	0.4	5.4	1.5	—	—	—	17.2	0.8	1.5	2.7	—	—	—	—	0.4	35.1	—	0.8	7.7	—	1.2	1.5	20.4	2.3	0.20		
94	678.70—681.41/a	—	2.1	0.5	3.7	—	9.0	1.8	—	0.3	—	12.7	0.5	2.9	3.2	—	—	—	0.3	—	28.2	—	1.6	9.2	—	0.5	0.8	22.7	5.8	0.14		
95	682.91—684.20	—	3.2	1.0	2.5	—	6.1	2.2	0.3	0.3	—	17.3	1.0	1.0	3.0	—	—	—	0.3	—	34.9	—	1.3	1.3	—	0.3	1.0	23.0	5.3	0.27		
96	690.48—690.59	—	—	0.7	—	—	—	—	—	6.2	—	84,2	—	0.7	—	—	—	—	—	—	1.4	—	0.7	—	—	—	0.7	5.4	3.80	0.04	UPPER PANNONIAN	LACUSTRINE
97	692.67—694.60	—	—	—	1.3	—	0.6	1.9	—	—	—	73.5	—	5.1	0.6	0.6	—	—	—	—	6.3	—	1.3	1.9	—	0.6	2.5	3.8	2.3	0.10		
98	695.01—695.32	—	—	—	0.7	—	—	2.0	—	1.3	—	80.6	0.7	2.0	—	—	—	—	—	—	2.7	—	0.7	1.3	—	2.0	—	6.0	4.7	0.05		
99	700.90—701.24	—	—	—	—	—	—	0.8	—	3.1	—	89.0	—	—	—	—	—	—	0.8	—	1.5	—	—	—	—	0.8	—	4.0	3.7	0.06		
100	705.18—705.47	—	0.7	—	—	—	—	—	—	—	—	87.5	—	1.5	—	—	—	—	—	—	0.7	—	—	—	—	—	3.7	5.9	0.5	0.06		
101	763.57—769.02/a	—	—	0.6	—	—	—	—	—	10.2	13.2	68.8	—	1.2	—	—	—	0.6	—	—	0.6	—	—	—	—	—	3.0	1.8	2.9	0.12		
102	763.57—769.02/b	0.7	—	—	0.7	—	0.7	1.4	—	—	—	77.3	—	—	2.1	—	—	—	1.4	—	2.1	—	0.7	3.6	—	0.7	3.6	5.0	3.3	0.12		
103	769.30—775.08/a	—	—	0.7	2.0	—	0.7	0.7	—	1.4	—	80.1	0.7	0.7	1.4	0.7	—	0.7	—	—	2.0	—	0.7	0.7	—	—	2.0	4.8	2.6	0.12		

TABLE 2

Heavy mineral composition of bore-profile of Nyárlőrinc

Number	Depth m	Dominantly magmatic minerals										Dominantly metamorphic minerals												Other minerals					Total quantity minerals in the examined fraction	Dominant grain diameter mm	AGE	FACIES
		Hypersthene	Other rhombic pyroxenes	Augite	Diopside	Basaltic—Hornblende	Magnetite—Ilmenite	Apatite	Zircon	Biotite	Chloritized Biotite	Chlorite	Tourmaline	Epidote	Clinosoisite	Zoisite	Rutile	Hornblende	Actinolite—Tremolite	Anthophyllite	Garnet	Staurolite	Kyanite	Calcite-dolomite	Limonite	Pyrite	Other micas	Weathered minerals				
1	2.0 — 3.0 m	3.2	1.9	1.3	3.5	—	5.7	0.9	—	0.3	—	3.8	1.3	1.3	2.5	—	—	8.8	0.6	0.9	30.0	0.3	0.6	3.8	—	1.6	—	27.7	4.2	0.21	TOCENE	EOLIAN
2	6.63— 7.20 m	2.4	4.0	3.4	2.7	0.7	7.4	0.3	0.3	0.3	—	2.7	1.3	1.3	2.4	—	—	8.5	0.7	1.3	36.9	0.3	0.7	—	—	0.7	—	21.7	4.2	0.16		
3	8.5 m	1.9	0.5	1.9	1.9	—	5.6	—	—	—	—	4.2	2.3	2.3	2.8	—	—	2.3	0.5	0.5	44.8	0.5	0.5	2.3	—	—	—	25.2	1.04	0.14		
4	15.69—15.93 m	1.9	3.1	3.5	3.1	—	7.4	1.2	—	0.4	—	1.9	0.4	1.2	2.3	—	—	5.4	0.4	0.8	29.2	—	0.4	0.4	—	1.2	—	35.8	3.2	0.14		
5	19 m	1.3	—	0.4	1.8	—	6.7	1.8	—	0.4	—	5.4	0.4	3.6	3.6	—	—	9.4	0.4	—	38.0	—	—	10.2	—	—	—	16.6	0.5	0.12		
6	21.5 m	4.5	0.8	1.6	1.6	—	7.3	—	0.4	—	—	—	0.4	2.4	2.4	—	—	7.7	—	—	32.9	—	1.2	—	0.8	—	—	36.0	6.0	0.20		
7	31.0 m	4.1	2.5	4.1	0.8	—	7.5	0.4	—	—	—	7.9	—	1.6	3.3	—	—	5.4	—	0.8	26.6	0.8	0.4	0.4	—	—	—	33.4	2.1	0.11		
8	36.0 m	2.5	2.0	1.5	0.5	—	5.0	1.0	0.5	—	—	6.8	2.5	3.0	3.9	—	—	2.0	—	—	31.8	0.5	0.5	2.5	1.0	—	—	32.5	4.5	0.13		
9	38.20—38.66 m	2.1	3.5	4.8	3.5	0.3	4.8	0.3	—	0.3	—	2.4	1.4	0.7	1.7	—	—	16.6	1.7	0.7	24.3	0.3	0.3	0.3	—	1.7	1.4	26.9	2.3	0.20		
10	51.5 m	3.5	2.3	2.3	3.5	—	4.6	0.8	—	—	—	5.8	1.5	0.4	3.1	—	—	7.7	—	0.8	27.8	0.4	1.5	—	0.4	—	—	33.6	2.1	0.13		
11	58.0 m	0.7	1.5	0.7	1.8	—	5.2	0.4	—	—	—	10.4	1.1	1.1	2.6	0.7	—	13.3	—	0.4	33.0	—	1.5	0.4	—	—	—	25.2	3.6	0.19		
12	62.5 m	1.1	1.1	2.6	1.1	0.8	11.3	1.1	—	0.4	—	11.3	1.1	3.4	2.2	0.4	—	10.5	0.8	1.1	24.5	0.4	1.1	—	—	—	0.4	23.3	1.9	0.17		
13	64.5 m	2.2	1.5	1.5	2.6	—	7.7	1.8	—	—	—	4.8	0.4	0.7	2.9	—	—	11.4	—	0.4	23.5	0.4	1.5	7.7	—	—	1.1	27.9	7.6	0.16		
14	70.0 m	1.6	5.7	3.3	2.0	—	8.6	—	—	—	—	2.5	—	0.8	1.6	—	—	8.6	1.6	0.4	43.7	—	0.4	—	—	0.8	0.8	17.6	2.8	0.12		
15	74.3 m	0.9	0.4	1.7	—	—	3.4	0.4	—	8.1	—	14.0	0.4	1.3	0.4	—	—	1.3	—	0.4	19.6	—	—	21.3	0.4	—	—	26.0	5.1	0.06		
16	77.5 m	1.8	1.3	0.4	0.9	—	3.9	1.3	—	0.4	—	11.8	—	0.9	1.8	—	—	17.1	0.9	1.3	17.1	1.8	0.4	5.7	0.4	—	—	30.8	3.7	0.11		
17	81.0 m	1.5	0.8	2.3	1.9	—	3.9	0.8	—	1.2	—	9.6	0.4	2.3	1.2	0.4	—	12.0	0.8	0.8	10.0	0.8	0.8	25.0	1.5	—	1.2	20.8	5.1	0.11		
18	89.60—90.81 m	2.1	5.9	4.2	3.4	1.4	8.3	—	—	—	—	2.7	0.7	1.4	2.4	0.3	—	10.3	0.7	0.7	16.2	—	2.0	—	—	—	1.0	36.3	3.4	0.14		
19	97.3 m	2.0	2.4	2.4	4.5	0.4	6.6	0.8	—	0.4	—	5.8	0.4	4.1	5.8	—	—	9.5	0.4	1.6	16.0	0.4	0.4	6.2	—	—	1.2	28.7	3.2	0.15		
20	99.3 m	0.7	4.0	1.4	4.3	—	3.6	0.4	0.4	—	—	6.9	1.8	4.7	0.7	—	—	6.5	0.4	1.4	22.4	0.4	0.7	4.0	—	—	0.4	34.9	3.4	0.14		
21	101.0 m	2.0	2.8	2.4	3.2	—	5.6	0.4	—	—	—	15.1	0.4	1.6	2.8	—	—	8.0	1.6	1.2	23.9	—	1.2	1.6	—	—	—	26.2	3.2	0.22		
22	112.0 m	1.0	2.3	0.6	3.3	—	5.5	0.6	—	0.6	—	4.6	1.6	0.6	1.0	0.3	—	5.2	0.3	0.3	10.8	—	1.0	17.6	2.0	—	0.3	40.5	4.7	0.12		
23	113.20 m	2.4	3.7	2.0	1.0	—	7.1	1.3	—	1.7	—	6.8	1.3	1.0	2.7	—	—	9.8	1.0	0.7	13.9	0.3	0.7	11.2	—	—	0.3	31.1	1.0	0.08		
24	123.0 m	0.9	—	—	—	—	—	—	—	7.3	—	35.2	—	—	—	—	—	1.4	—	0.4	—	—	—	7.8	—	—	44.3	2.7	5.3	0.07	PLEISTOCENE	FLUVIATILE
25	124.0 m	—	0.7	1.1	0.4	—	1.1	—	—	4.5	—	22.1	0.4	0.7	0.4	—	—	1.5	0.7	—	5.6	0.4	0.4	29.6	—	—	19.5	10.9	6.5	0.09		
26	134.0 m	1.8	1.4	3.2	3.9	1.4	5.3	1.0	—	0.4	0.4	12.0	0.4	1.4	1.4	0.4	—	15.8	1.4	—	19.4	—	1.0	—	—	0.7	4.9	22.4	2.8	0.31		
27	139.74—140.87 m	0.4	—	0.8	2.1	—	2.6	0.4	—	2.3	—	24.3	0.4	0.8	—	—	—	19.1	2.1	0.4	2.6	—	—	3.0	—	5.1	5.9	27.7	3.4	0.13		
28	154.7 m	0.5	1.3	1.3	1.8	1.3	0.9	2.2	—	1.3	—	21.3	0.5	0.5	0.5	0.5	—	21.7	4.0	0.5	4.8	—	0.5	0.9	—	6.2	6.2	21.3	3.3	0.11		
29	158.0 m	0.4	0.4	1.3	—	0.4	1.7	—	—	1.7	—	16.0	0.9	0.9	1.3	0.4	—	6.9	1.7	0.4	2.2	—	0.4	43.1	—	—	6.1	13.8	3.5	0.12		
30	161.5 m	1.5	1.5	4.4	2.2	—	2.6	0.4	—	1.1	—	7.3	0.4	0.7	1.8	—	—	7.0	0.4	0.4	14.7	—	0.7	14.7	—	—	1.8	36.4	16.3	0.25		
31	164.0 m	1.5	2.2	3.3	2.9	0.4	8.4	0.4	—	1.1	—	7.3	0.7	1.8	2.2	—	—	9.5	0.7	1.1	17.0	0.4	1.5	4.4	—	—	4.0	29.2	16.0	0.28		
32	167.4 m	0.9	0.9	1.8	0.9	—	—	—	—	0.9	—	30.7	—	—	0.4	0.4	—	5.9	1.3	—	0.4	0.4	0.4	29.4	—	—	10.8	14.5	9.2	0.12		
33	169.3 m	1.0	1.4	1.0	1.7	—	2.8	0.7	—	4.2	—	39.9	0.3	0.7	0.7	—	—	10.2	1.4	—	0.3	—	—	8.1	—	0.7	12.3	12.6	3.5	0.09		
34	188.7 m	0.3	1.4	1.4	0.7	0.3	2.8	—	—	—	—	13.7	0.3	0.7	—	0.3	—	7.0	0.3	0.3	1.0	0.3	0.3	23.6	0.7	—	7.0	37.6	4.5	0.20		
35	202.5 m	1.7	1.7	3.5	1.4	0.7	6.3	1.0	—	1.0	—	21.9	0.3	1.4	1.7	0.3	—	13.2	0.3	0.7	7.3	—	1.0	3.1	—	—	3.1	28.4	3.5	0.19		
36	205.8 m	0.6	3.2	0.6	2.8	0.6	8.2	0.9	—	0.3	—	13.5	1.3	0.9	0.6	0.6	0.3	10.1	0.6	—	6.3	0.3	0.6	13.0	—	0.3	3.8	30.6	4.2	0.22		
37	209.0 m	—	1.3	0.3	0.6	0.3	3.3	2.9	—	—	—	20.2	0.6	1.6	1.0	0.3	—	6.6	0.6	—	3.0	—	1.0	16.4	—	—	12.5	27.5	6.7	0.25		
38	212.7 m	0.3	3.5	2.9	0.6	—	8.0	1.6	—	—	—	5.7	1.3	2.5	1.6	0.6	0.3	10.2	0.3	0.3	8.6	0.6	1.0	19.5	—	—	1.0	29.6	8.0	0.18		
39	215.5 m	0.7	2.4	1.7	0.7	0.3	3.1	0.7	—	2.0	—	36.2	—	1.7	0.3	—	0.3	3.7	0.3	0.3	4.4	0.3	0.3	4.7	—	—	22.0	13.9	9.0	0.34		
40	217.5 m	0.8	1.6	2.7	2.4	1.6	10.6	0.4	—	—	—	6.3	—	1.6	0.4	1.2	—	9.8	0.4	0.4	16.1	0.4	1.6	2.7	—	—	1.2	37.8	6.2	0.36		
41	238.87—241.80 m	—	6.1	3.5	6.1	0.9	3.0	0.9	—	—	—	20.0	1.8	1.3	0.9	—	—	9.6	3.0	—	9.1	—	0.4	0.9	—	2.6	0.9	29.0	4.1	0.21		
42	257.6 m	—	3.8	2.6	4.0	1.5	3.3	0.7	—	—	—	29.9	1.8	1.5	0.7	0.4	—	7.4	1.1	—	9.6	—	0.7	0.4	—	—	5.5	25.1	3.5	0.18		
43	272.6 m	—	1.6	3.1	5.2	1.0	3.1	0.5	—	—	—	21.9	0.5	2.1	0.5	—	—	6.8	1.0	0.5	6.2	—	1.6	2.1	—	—	4.2	38.1	2.7	0.14		
44	289.9 m	—	2.1	—	0.7	—	1.4	0.7	—	—	—	73.2	—	—	—	—	—	2.1	1.4	—	0.7	—	—	5.7	—	—	7.8	4.2	4.4	0.08	LEVANTINE	LACUSTRINE —FLUVIATILE
45	301.5 m	1.2	4.7	2.4	3.9	2.0	11.5	1.2	—	—	—	15.8	0.4	0.8	1.6	—	—	5.9	0.4	—	24.9	—	1.2	0.8	—	0.8	2.8	17.7	1.2	0.28		
46	307.7 m	—	3.2	1.1	2.8	—	3.9	—	—	—	—	36.9	1.4	0.7	0.7	—	—	8.5	0.3	—	3.5	0.3	—	2.1	—	0.3	6.8	27.5	3.3	0.11		
47	315.0 m	1.6	4.0	—	1.2	5.7	11.3	0.4	0.8	—	—	10.1	0.8	1.6	0.8	—	—	6.5	0.4	—	20.7	0.4	0.4	3.6	—	0.4	2.4	26.9	5.5	0.36		
48	335.0 m	0.7	5.0	2.0	2.8	3.2	3.6	1.1	—	—	—	18.3	0.7	1.1	0.3	—	—	13.6	1.1	0.7	12.5	—	0.3	1.1	—	1.8	2.1	28.0	7.3	0.26		
49	365.5 m	—	3.4	0.4	3.0	0.4	5.3	0.4	0.4	—	—	30.2	1.1	3.0	1.9	—	0.4	6.4	1.9	—	6.4	—	1.1	3.0	—	—	10.6	20.7	4.9	0.18		
50	382.6—384.0 m	—	1.4	1.4	2.8	0.5	1.4	0.5	—	0.5	—	57.9	0.9	0.9	—	—	—	8.0	1.4	—	4.2	—	0.9	0.9	—	2.3	1.9	12.2	2.1	0.13		
51	396.0 m	2.6	4.5	2.6	4.1	—	6.0	0.8	—	0.4	—	6.0	0.8	2.3	1.1	—	—	8.3	2.3	—	37.8	—	0.4	0.4	—	0.4	1.1	18.1	35.8	0.17		

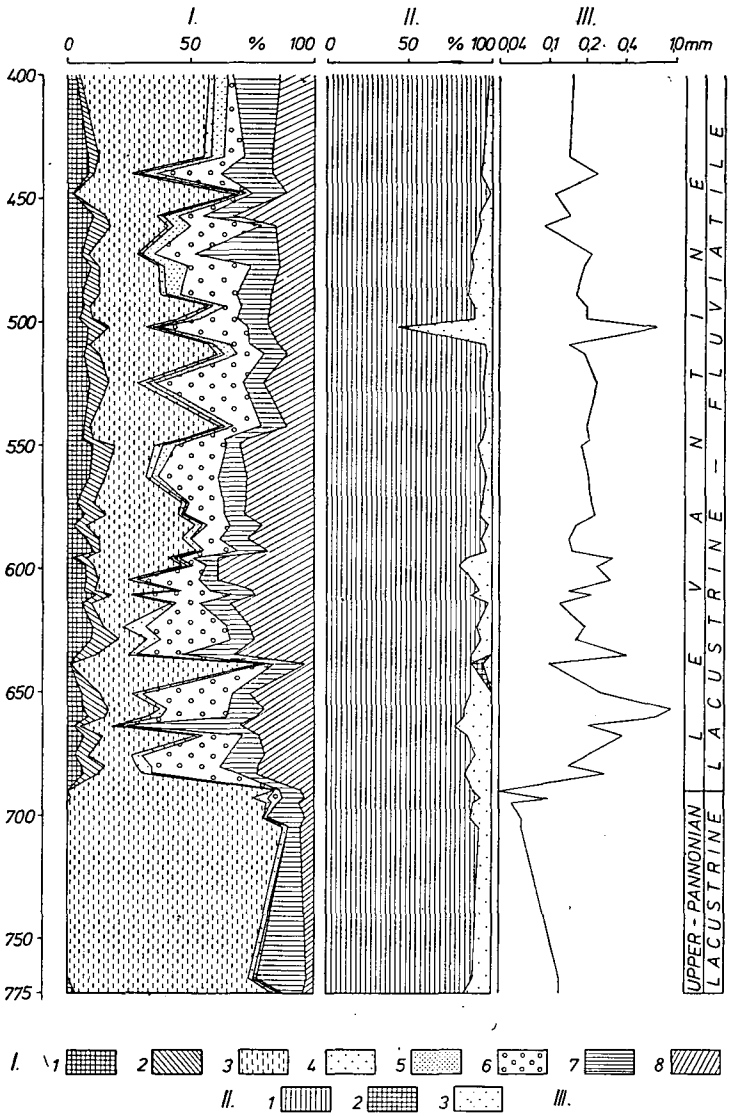

Fig. 1. Results of heavy mineral, grain-shape and grain-size analyses of the section between 400 and 775.8 m of the borehole at Nyárlőrinc

I. 1. hypersthene, other orthorhombic pyroxenes, augite and diopside, 2. magnetite-ilmenite, 3. chlorite, 4. epidote, 5. hornblende and actinolite-tremolite, 6. garnet, 7. other minerals together, 8. weathered mineral.

II. 1. sharp, splintery, 2. rounded, mat, 3. rounded bright-surfaced grains

III. Median grain diameter of the analyzed samples (Md-value)

INVESTIGATION RESULTS OF THE UPPER PLIOCENE (LEVANTINE) SEDIMENTS

The borehole of Nyárlőrinc explored the Levantine formations between 273 and 688 m, i.e. in a tickness of 415 m. After the profile of FRÁNYÓ, F. [1976] as well as according to our grain composition analysis the Levantine formations contain much more sand strata than the Upper Pannonian ones. 52 samples were investigated from the sequence and this is more than in case of the Upper Pannonian since the explored sequence is thicker and within the sequence there are more sand strata.

Previously, the sedimentological investigations demonstrated that the Levantine formations are of cyclic development, the sand strata within each cycles are arranged according to definite regularities [MOLNÁR, B., 1973]. In harmony with the former statements, the profile of Nyárlőrinc is of cyclic structure [MOLNÁR, B., 1973]. Regarding the grain composition of the section between 420 and 688 m this is a sequence which becomes finer from down. Between 113 and 420 m, reaching down to the Pliocene another sedimentary cycle can be distinguished with upward refining sediments.

The grain-size of sand strata of the sequence various between rather wide limits, i.e. between 0.08 and 1.2 mm. The sand strata are coarser in the lower and finer in the upper third of the sedimentary cycles (Tables 1—2, *Figs. 1—2*).

The heavy-mineral composition of the Levantine strata is more abundant than that of the Upper Pannonian. All samples contain several mineral species. In addition to the hypersthene and amphibole shown at the beginning of Table 1—2, in the sample the other orthorhombic pyroxenes, i.e. augite, diopside, magnetite-ilmenite and augite occur. This is fairly shown by the column of 1—2, of *Figs. 1—2*. The two combined columns pass through the whole Levantine without breaking as against the Upper Pannonian.

In the sequence chlorite plays a predominant role though as against the 80 percent of the Upper Pannonian strata its average quantity amounts here only to about 30 percent. Deviation is, however, rather significant, because its quantity varies between 2.1 and 73.2 percent and the wide limits of grain-size distribution is responsible for this, since this considerably affects the change of mineral composition. The decrease of chlorite as compared to the Upper Pannonian is unambiguous.

Epidote and clinozoisite occurred also in smaller quantites is most of the samples, as well as the hornblende when moving upwards. The quantity of garnet is also changing but is represented by about 15 to 20 percent being more abundant than in the Upper Pannonian. Garnet plays important role in composition, as well. The weathered mineral content of the Levantine is more than that of the Upper Pannonian but proved to be less than that of the Pleistocene. In two sites, i.e. in a depth of 472 resp. 663 metres the high quantities of carbonate minerals represented by 26.0 resp. 35.8 percent can be observed, and is indicated in Table 1 within the Levantine sequence. Nevertheless, this phenomenon is characteristic rather of the Pleistocene. In these samples the rock detritus of carbonate material is also important in addition to calcite and dolomite. The greater quantities of carbonate minerals of predominantly epigenic origin can be traced back to the more varying lacustrine-fluviatile sedimentation and to the climatic changes, respectively.

The photos of Plate II fairly show the more diversified mineral composition as compared to that of the Upper Pannonian. In the photos of the Upper Pannonian chlorite predominated, in these pictures, however, numerous other minerals can also be seen.

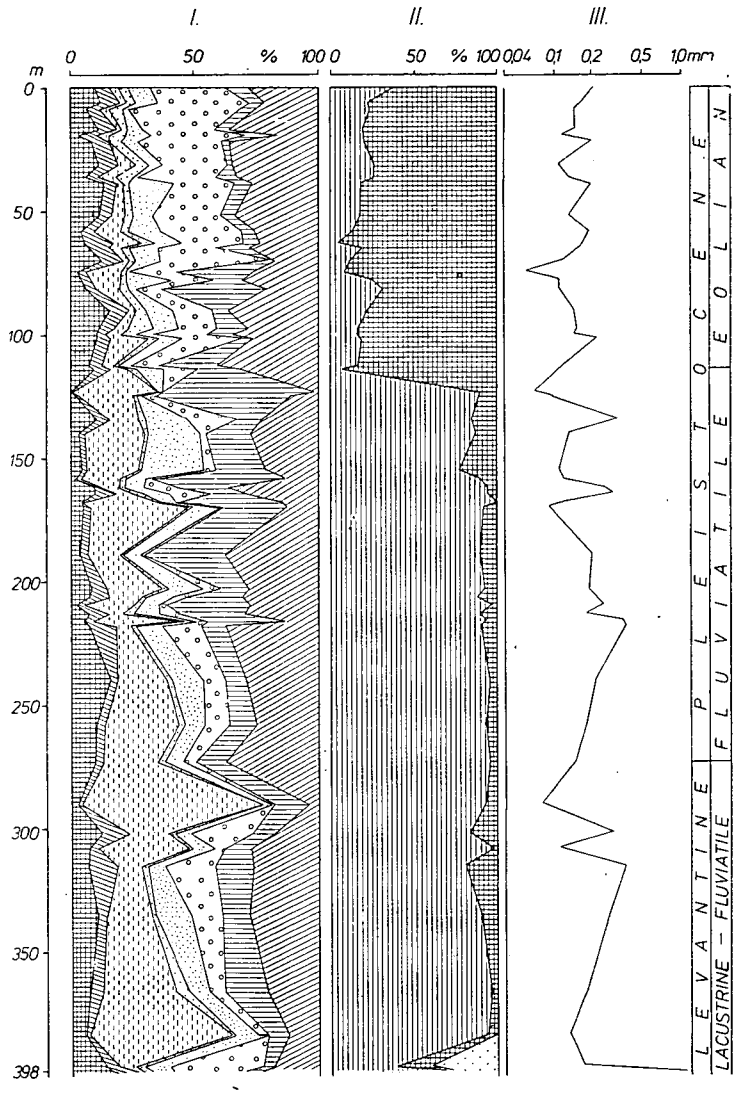

Fig. 2. Results of heavy mineral, grain-shape and grain-size analysis of the section between 0 and 400 m of the borehole at Nyárlőrinc

In the Levantine strata the CAILLEUX's grain-shape analysis have shown also mostly sharp splintery grains (*Figs. 1—2;* Table V, photo No. 3). The bright-surfaced slightly rounded grains reach greater amounts at two sites, i.e. between 396 and 398 m (24 to 40%) and in 501 m (57%). Out of the investigated strata these proved to be the coarsest ones, thus this is responsible for the extreme values. On the other hand, in the former lake-shore strip the wearing effect of the rolling sea might prevail to greater extent.

In the upper part of the Levantine when moving upward between 289 and 439 metres the rounded, unglazed aeolian quartz grains also occur in an average

quantity of not more than 10 percent, but changing between 1.0 and 29.0%. At the same time, in the upper part of the Levantine, between 289 and 384 m the more rounded quartz grains eroded more considerably by water disappear. The appearance of the aeolian grains as well as the disappearance of the bright-surfaced rounded grains may be the "forecast" of the Pleistocene aeolian facies. Thus, in the Levantine though being more variegated than the Pannonian, the sharp splintery grains prevail which is fairly shown by the photo No. 3 of Plate V.

When summing up it can be stated that at Nyárlőrinc considerable change followed with respect to the source area after the sedimentation of the Upper Pannonian sequence. The Levantine, with its varying mineral composition is now similar to the mineral composition of the Danube alluvium [MOLNÁR, B., 1964]. The only difference is its greater chlorite content. Consequently, at Nyárlőrinc the "Danube Tectonic Trench" is filled up by the Danube since the Levantine. This might proceed in form of alluvium transported into the former lake.

INVESTIGATION RESULTS OF THE PLEISTOCENE SEQUENCE

The borehole explored the Pleistocene sequence between 0 and 273 metres. In this sequence the sand strata are frequent, thus 43 samples were analyzed. On the basis of the results the Pleistocene sequence can be divided into two parts: between 113.2 and 273.0 metres and between 0 and 113.2 metres, respectively. Their introduction follows this order.

Pleistocene fluviatile sequence

The section of the borehole between 113.2 and 273.0 metres, i.e. an interval of nearly 160 metres is the continuation of the sedimentary cycle started in the Levantine. From this section of 160 metres 20 samples were analyzed. According to the terminating phase of the sedimentary cycle the grain-size composition of the sands is somewhat finer than that of the underlying one. The grain-size varied between 0.07 and 0.36 mm, i.e. within relatively narrow interval. The grain-size composition of the coarsest samples did exceed the medium-grained sand, neither.

The heavy mineral composition of the Pleistocene sequence is the unbroken continuation of the underlying Levantine with the only difference that out of the igneous minerals the hypersthene and basaltic amphibole occurring previously only in the upper part of the Levantine become here more frequent (Table 2). The other minerals of igneous origin are of similar quantity as in the Levantine.

The extreme values of chlorite are only 6.3 and 39.9%. The average quantity is also somewhat lower than in the Levantine. This is shown also by column No. 3. I of *Fig. 2*. The metamorphic tourmaline, epidote, clinozoisite and kyanite occur nearly in all samples but all these minerals show a quantity of max 2%. Hornblende becomes ever significant from down upwards. In several samples it exceeds 10 percent, moreover in one samples its amount is 21.7%. In the Levantine its quantity reached or exceed 10 percent only once, i.e. 13%. Garnet is somewhat less than in the Levantine, its quantity varies randomly between 0 and 17 percent.

Calcite—dolomite resp. the carbonatic rock detritus showed extreme values in the Levantine only twice. Within the interval of 113.2—273.0 m of the Pleistocene their quantity exceeded 10 percent already in eight samples, moreover, in three samples its amount proved to be 30.0%, in one sample 43.1%.

The greater quantities of carbonate minerals can probably be explained by the climatic changes of the Pleistocene. It is well-known that the Levantine and Pleisto-

cene strata of the Great Plain often contain lime concretions. A part of the carbonatic rock detritus of Nyárlőrinc is also fine lime concretion or the crumbled part of it.

It is worthy of mention in Table 2 the high percentages of the mineral assemblage denominated "other micas" consisting in this case predominantly of muscovite and sericite. It can be observed in several boreholes of the Great Plain that in the terminating phase of the sedimentary cycle, i.e. when low-energy fluviatile transportation took place, the mica of large specific surface accumulates, if it is present. The accumulation here can be explained also by this fact. The change in grain-size considerably influences the quantity of micas. In case of the finer-grained sand, for instance, the analyzed fraction of 0.1—0.2 mm means the coarsest part of the sample, which contains large quantities of mica. In case of coarser samples this proves to be inverted [MOLNÁR, B., 1969]. In this section of the Nyárlőrinc borehole the samples of same or nearly same grain-size composition contain rather different quantities of mica, i.e. muscovite or sericite. E.g. the samples No. 40 or 41 of Table 2, where 22.0 resp. 1.2% mica was found though both of the samples are nearly of the same grain-size, i.e. of 0.34 and 0.36 mm, respectively.

The weathered minerals slightly accumulate as compared to the Levantine. In the colder phases of the Pleistocene the chemical weathering affected the minerals but similarly to the Upper Pannonian or Levantine complete weathering can be observed only in less minerals, thus these minerals remain in the strata as weathered minerals.

The microphotos of the section between 113.2 and 273.0 m are shown by the pictures 1—2 of Plate II. As it can be seen, hornblende occur in greater amounts. Minerals occurring first or occurred only once can also be found, e.g. actinolite-tremolite. Consequently, the photos also indicate the ever varied mineral composition when moving upwards, i.e. to the Pleistocene strata.

According to the CAILLEUX's grain-shape analysis in this section of the Pleistocene sequence the quartz grains are also predominantly sharp and splintery (Plate V, Photos No. 1—2). The quantity of the sharp splintery grains varied between 85.4 and 100.0 percent. The slightly rounded, bright-surfaced partly water-worn grains are practically absent similarly to the upper part of the Levantine. On the contrary, the aeolian rounded, mat quartz grains are present in a quantity changing between 0 and 19%. Their appearance may be the forecast of the subsequent Pleistocene aeolian facies, as a continuation of the upper part of the Levantine.

It is seen from the fact above that similarly to the Levantine, the lower part of the Pleistocene sequence is the continuation of it as fluviatile deposition of Danube. Regarding its mineral composition the heavy mineral composition characteristic of the recent alluvium of Danube is much more emphasized as compared to that of the Levantine. This is reflected first of all by the smaller amounts of chlorite and by the greater amounts of hornblende. Thus, at Nyárlőrinc the filling role of Danube continued also in the Pleistocene.

Pleistocene aeolian sequence

In the Nyárlőrinc borehole 23 samples consisting of rather homogeneous mainly fine-grained sand were analyzed from the section between 0 and 113.2 m. The predominating grain-size of the samples varied between 0.06 and 0.22 mm. Only the grain-size composition of four samples differed from that of the fine-grained sands. Out of them two proved to be fine-grained, the grain-size composition of the others was shifted towards the medium-grained sands, the latter one reaching only max.

0.02 mm. This means that in this sedimentary sequence the sand strata were transported and deposited by a rather equilibrated average energy.

It is characteristic of the heavy mineral composition of the section between 0 and 113.2 m that the quantities of the minerals shown in column 1. I of Table 2, i.e. hypersthene and other orthorhombic pyroxenes, as well as those of augite and diopside together, increased as compared to the older sedimentary sequences. This is valid also of magnetite and ilmenite. It is a more significant change, however, that the chlorite quantity considerably decreased, its value varies between 0 and 15.5%, its average quantity varies only between 5 and 10%. Tourmaline, epidote and clinozoisite show similar quantities as the underlying Pleistocene fluviatile strata, i.e. their average quantity is about 2%, though in certain cases this amounts to 4%. Zoisite is insignificant. The quantities of amphibole are similar, those of actinolite-tremolite are somewhat lower. Important change is the considerable increase of the garnet quantity. Its quantity is above 10% in all samples, its extreme values vary between 10.0 and 44.8%. Its quantity increases upwards, in general.

The quantities of calcite—dolomite and of the carbonatic rock detritus, resp. shows random change, similarly to the Pleistocene fluviatile section. The extreme values vary between 0 and 25%, i.e. are somewhat lower than in the Pleistocene fluviatile sequence. Their appearance and the reason of it resp., are the same as in case of the Pleistocene fluviatile sequence.

Muscovite and sericite comprehended under the term "other micas" in the Tables were identified in ten out of the 23 samples. Their maximal quantity, however, proved to be 1.2% indicating the practical disappearance of these minerals from this sequence. The weathered mineral content varied between 16.0 and 40.5%, thus this value is greatest in the whole profile of the borehole. The reason if this can be traced back to the less intense chemical weathering of the cold Pleistocene climate, similarly to the Pleistocene fluviatile strata.

The total heavy mineral content of the fraction of 0.1—0.2 mm of the investigated samples which means practically the relation of heavy and light minerals in weight percent, seems to be rather uniform, i.e. between 0.5 and 7.6 percent. In the older part of the sequence the fluctuation proved to be more considerable. This is caused by the greater differences in the grain-size composition, further by the fact that the fluviatile transport could produce smaller "outcrops" which resulted in mineral accumulation within the sequence. This can be observed to greater extent in the older section of the profile.

The CAILLEUX's grain-shape analysis showed considerable changes in this part as compared to the former ones *(Fig. 2, III)*. While downwards the sharp splintery grains predominated, in the section between 0 and 113.2 m this was changed. Here the worn and mat grains become predominating, thus in harmony with the CAILLEUX-method the aeolian grains play preponderant role [CAILLEUX, A., 1952]. Upward from 113.2 m the maximal quantity of the sharp splintery grains amounts only to 35%. The quantity of the aeolian grains, however, varies between 64.1 and 94.9%. The slightly rounded bright-surfaced grains are lacking. The photos introduced in Plate VI fairly show this phenomenon. As against the previous stereomicroscopic photos here the strongly rounded grain prevail. The same phenomenon can be observed in case of the heavy minerals. The heavy minerals in Plates I and II are sharp and splintery, those in Plate III and IV are rounded.

The differences in heavy mineral composition indicate also the aeolian transport, e.g. the considerable percentual accumulation of magnetite, ilmenite and of the hard

garnet, the considerable decrease of chlorite and micas. It is well-known that blown sands contain no or rather small quantity of mica.

Previous investigations indicated that in the Danube—Tisza Interfluve, thus also at Nyárlőrinc a thicker aeolian sequence is deposited consisting of aeolian sand and loess or of its varieties [MOLNÁR, B., 1961]. The faunal analyses of E. KROLOPP carried out in the material of Nyárlőrinc verified this fact. As to personal communication, in a depth of 124 m and below the material of Nyárlőrinc contains fluviatile molluscs. Above 124 m, however, no fluviatile species are found. The sand strata in 124 m of the Nyárlőrinc borehole are fluviatile also according to the grain-shape and heavy mineral analysis. Unfortunately, between 113.2 and 124 m finer sediment is found, thus this could not be analyzed. This silt layer, however, is the terminating phase of the fluviatile cycle following before the complete deceleration of filling and consisting of fine-grained material, thus it is closely assigned to the fluviatile facies.

The coincidence of data is not accidental and this proves the correctness of the previous investigations, i.e. that in the Danube—Tisza Interfluve at thicker aeolian sedimentary sequence is found.

The heavy mineral composition of the blown sand differs from the Pleistocene fluviatile strata only in the percentual quantities of the minerals compared to each other, otherwise the same minerals occur. Thus, in the meantime the source area did not change. The material of the blown sand derives also from the Danube alluvium. This sand, however, was developed so that it was transported by aeolian way through several ten kilometres. Consequently, the former fluviatile sand transformed into aeolian sand. The roundness value of sand grains are often higher even than those of the blown sand in the Danube—Tisza Interfluve. Thus, the sand got its recent position through being transported in a greater distance.

SUMMARY

On the basis of grain-size composition, micromineralogical and grain-shape investigations carried out in the Nyárlőrinc borehole the following conclusions can be drawn:

1. The material of the Nyárlőrinc borehole derives from source areas differing from each other.

(a) The Upper Pannonian section of the sequence is poor in heavy mineral species, it contains mostly metamorphic minerals, predominantly chlorite.

(b) The Levantine and Pleistocene part of the profile is rich in minerals. Its material of varied composition consisting mostly metamorphic minerals being nearly similar to the recent sand of the Danube derives from the river.Thus, Danube appeared in this area in the Early Pliocene (Levantine).

2. Regarding the material transport, in the Pleistocene sequence of the Nyárlőrinc borehole two phases can be distinguished. Between 113.2 and 273 m the fluviatile formation, while between 0 and 113.2 m the aeolian formation are characteristic. The material of both phases derive from the Danube. Sand was blown up from the Danube valley, and after aeolian transport through several ten kilometres it was deposited in its recent location.

REFERENCES

BARTHA, F. [1971]: A magyarországi pannon biosztratigráfiai vizsgálata. — In: Magyarország pannon-kori képződmények kutatásai. — Akadémiai Kiadó, Budapest, p. 9—172.

BARTHA, F. [1975]: A magyarországi pannon képződmények horizontális és vertikális összefüggései és problematikája. — Földt. Közl., **105**, 4, p. 399—418.

CAILLEUX, A. [1952]: Morphoskopische Analyse der Geschiebe und Sandkörner und ihre Bedeutung für die Paläoklimatologie. — Geol. Rundschau **40**, Stuttgart, p. 11—19.
FRANYÓ, F. [1976]: Jelentés a nyárlőrinci fúrás anyagvizsgálatáról. — MÁFI Adt.,(Manuscript).
GEDEON—RAJETZKY, M. [1975]: A mindszenti és csongrádi kutatófúrások mikromineralógiai vizsgálata különös tekintettel az anyagszállítás egykori irányaira. — MÁFI Évi Jel. 1971. évről, p. 169—184.
JÁMBOR, Á., KORPÁS—HÓDI, M. [1971]: A pannóniai képződmények szintezési lehetőségei a Dunántúli Középhegység D-i előterében. — MÁFI Évi Jel. 1969. évről, p. 155—192.
MOLNÁR, B. [1961]: A Duna—Tisza közi eolikus rétegek felszíni és felszínalatti kiterjedése. — Földt. Közl., **91**, 3, p. 300—315.
MOLNÁR B. [1963]: A délalföldi pliocén és pleisztocén üledékek tagolódása nehézásvány-összetétel alapján. — Földt. Közl., **93**, 1, p. 97—107.
MOLNÁR, B. [1964]: Magyarországi folyók homoküledékeinek nehézásvány-összetétel vizsgálata. — Hidrol. Közl., **44**, 8, p. 347—355.
MOLNÁR B. [1965*a*]: Adatok a Duna—Tisza köze fiatal harmadidőszaki és negyedkori rétegeinek tagolásához és származásához nehézásvány-összetétel alapján. — Földt. Közl., **95**, 2, p. 216—225.
MOLNÁR, B. [1965*b*]: Ősvízrajzi vizsgálatok a Dél-Tiszántúlon. — Hidrol. Közl., **45**, 9, p. 397—404.
MOLNÁR, B. [1966*a*]: Pliocén és pleisztocén lehordási területváltozások az Alföldön. — Földt. Közl., **96**, 4, p. 403—413.
MOLNÁR, B. [1966*b*]: Lehordási területek és irányok változásai a Dél-Tiszántúlon a pliocénben és a pleisztocénben. — Hidrol. Közl., **44**, 3, p. 121—127.
MOLNÁR, B. [1966*c*]: Lithogical and Geological Study of the Pliocene Formation in the Danube—Tisza Interstream Regin. Part I. — Acta Miner. Petr., Acta Univ. Szegediensis **17**, 2, p. 131—142.
MOLNÁR, B. [1969]: A szemnagyság és a nehézásvány-összetétel összefüggései. — Földt. Kutatás **12**, 2, p. 8—17.
MOLNÁR, B. [1973]: Az Alföld harmadidőszak végi és negyedkori feltöltődési ciklusai. — Földt. Közl., **103**, 3—4, p. 294—310.
SÜMEGHY, J. [1953]: A Duna—Tisza közének földtani vázlata. — MÁFI Évi Jel. 1950. évről, p. 233—263.

Manuscript received, March 20, 1979

DR. B. MOLNÁR
Attila József University
Department of Geology and Paleontology
H-6701 Szeged, Pf. 428,
Hungary

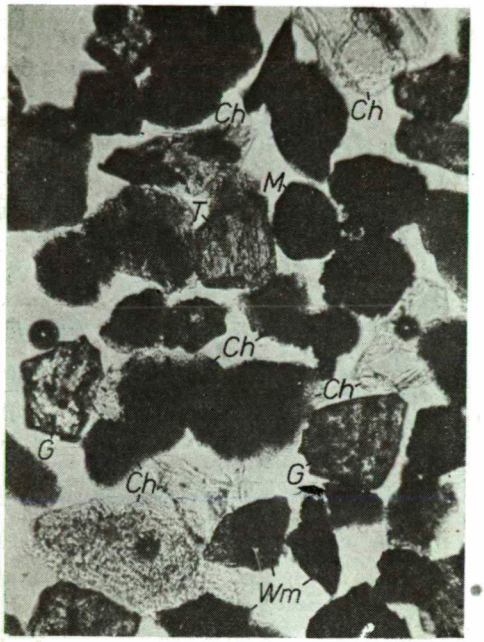
Ch
Ch
M
T
Ch
Ch
G
Ch
G
Wm

1

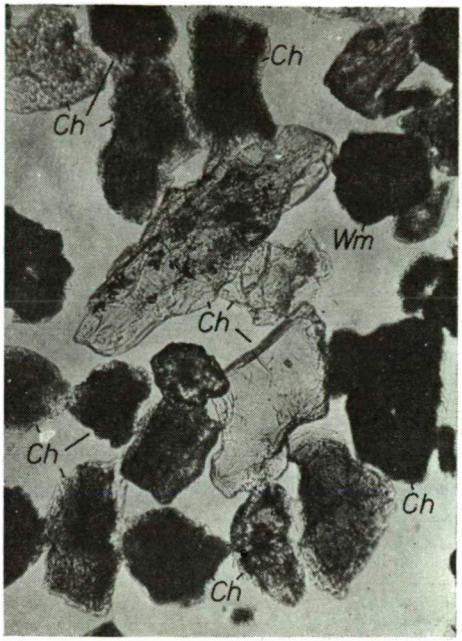
Ch
Ch
Wm
Ch
Ch
Ch
Ch

2

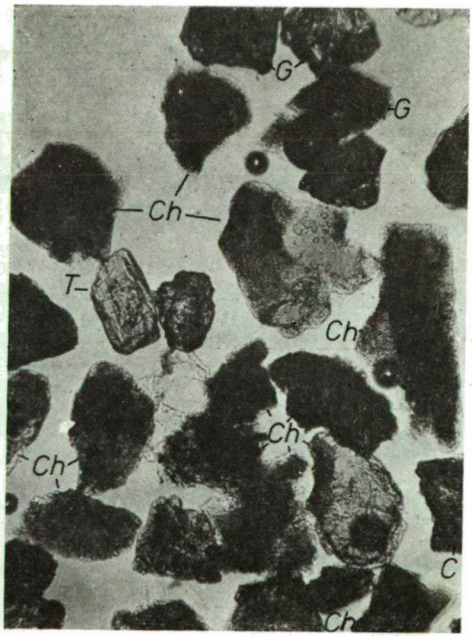
G
G
Ch
T
Ch
Ch
Ch
C
Ch

3

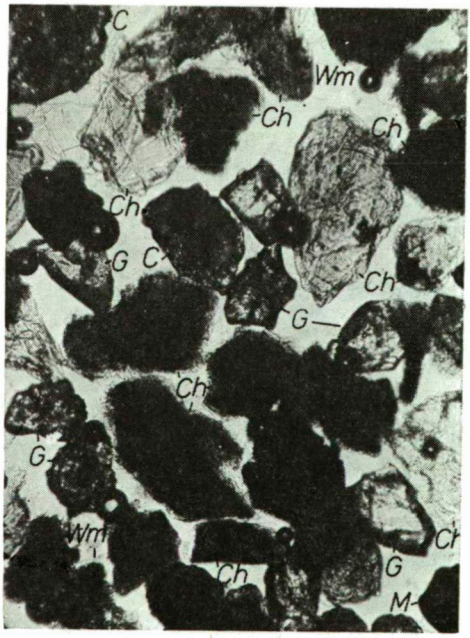
C
Wm
Ch
Ch
Ch
G
C
Ch
G
Ch
G
Wm
Ch
Ch
G
M

4

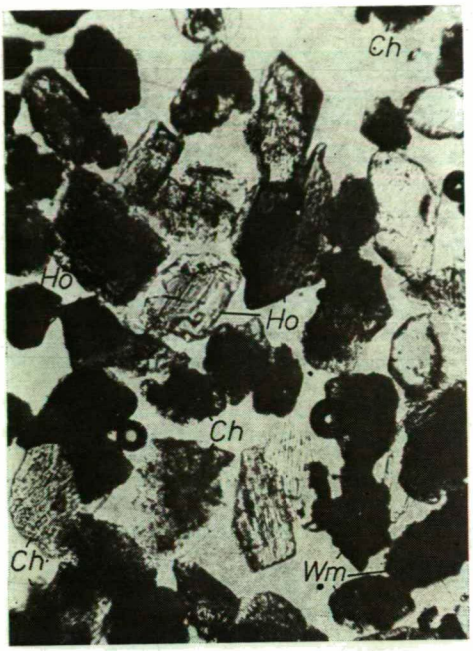
Ch
Ho
Ho
Ch
Ch
Wm

1

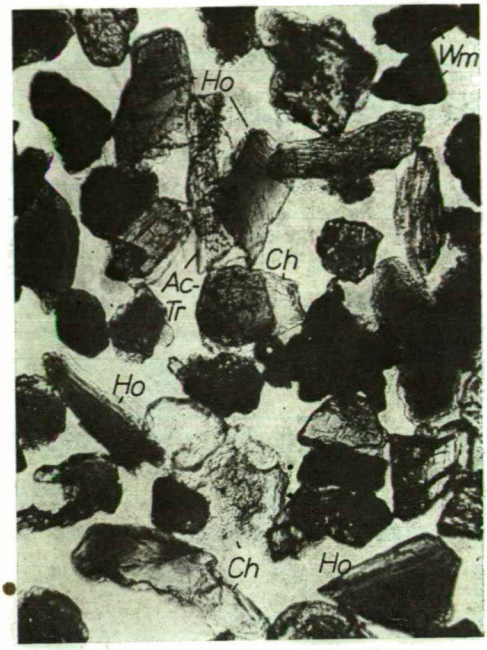
Wm
Ho
Ch
Ac
Tr
Ho
Ch
Ho

2

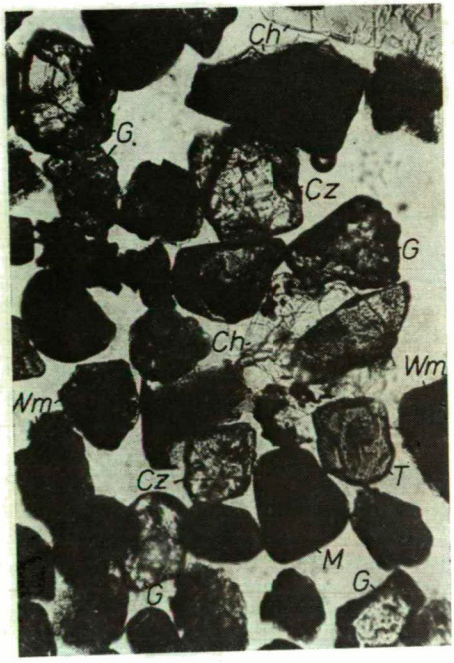
Ch
G
Cz
G
Ch
Wm
Wm
T
Cz
M
G
G

3

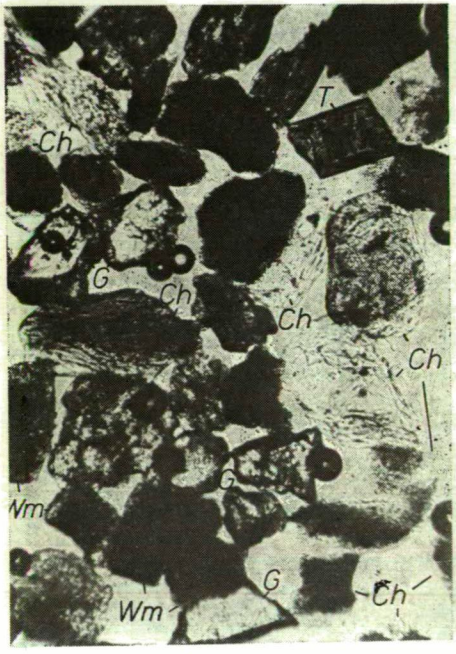
T
Ch
G
Ch
Ch
Ch
G
Wm
G
Ch
Wm

4

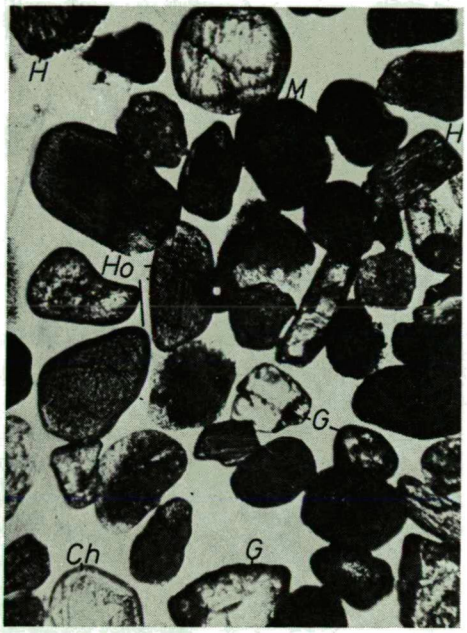

1

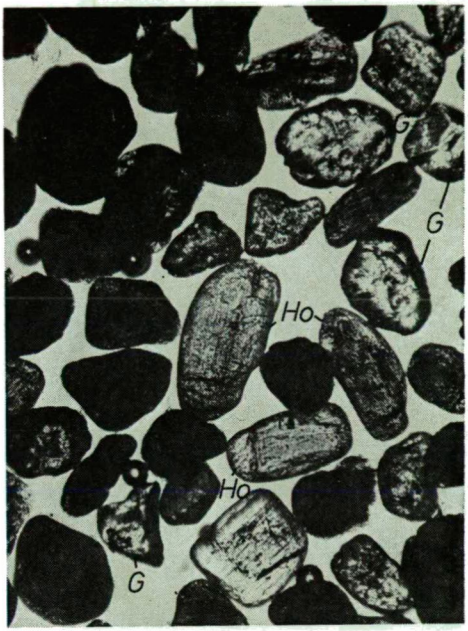

2

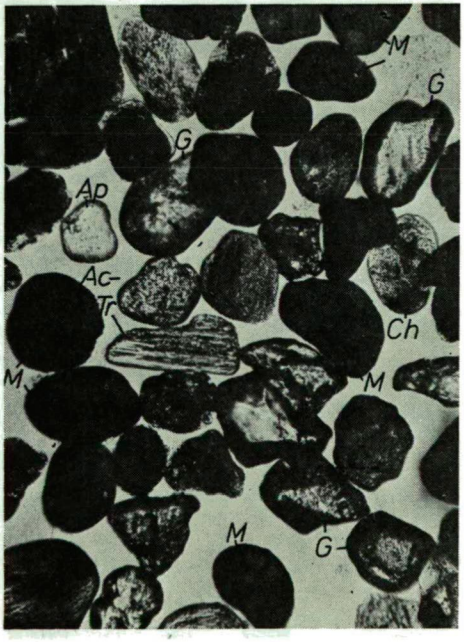

3

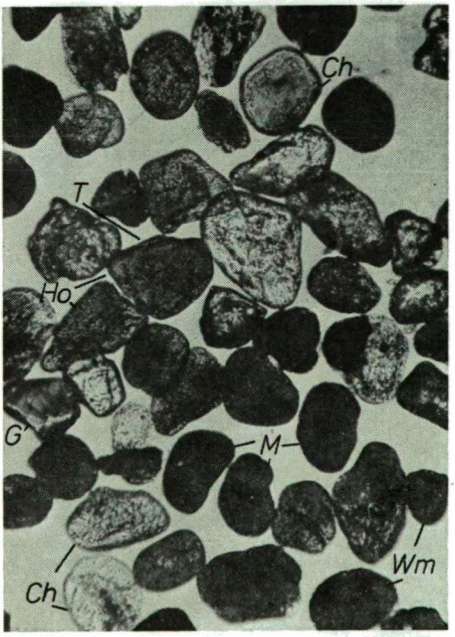

4

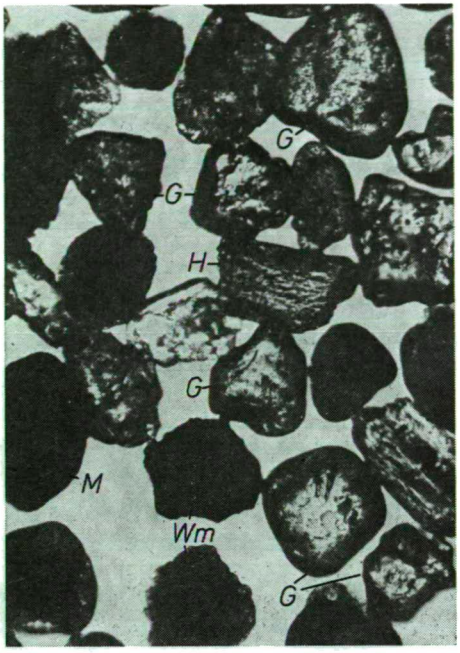

1

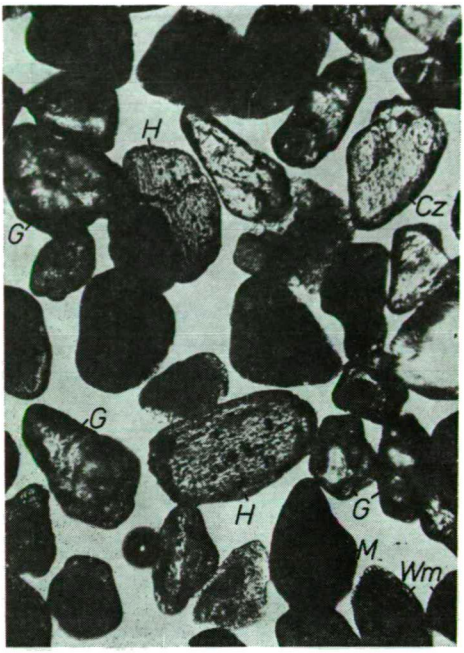

2

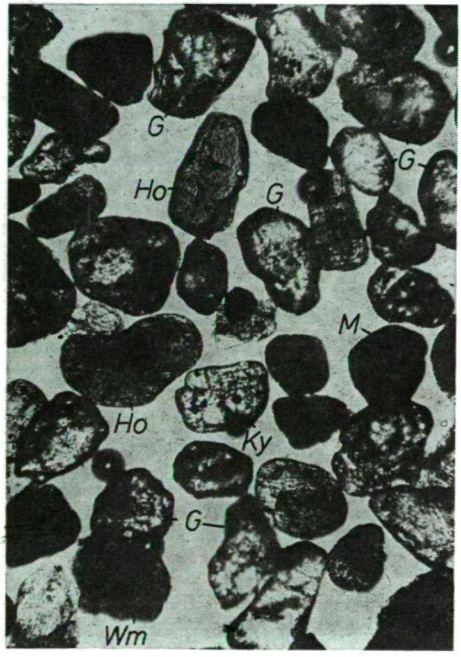

3

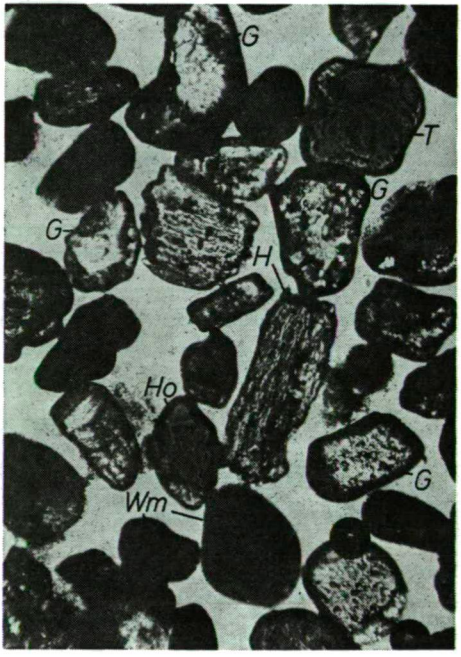

4

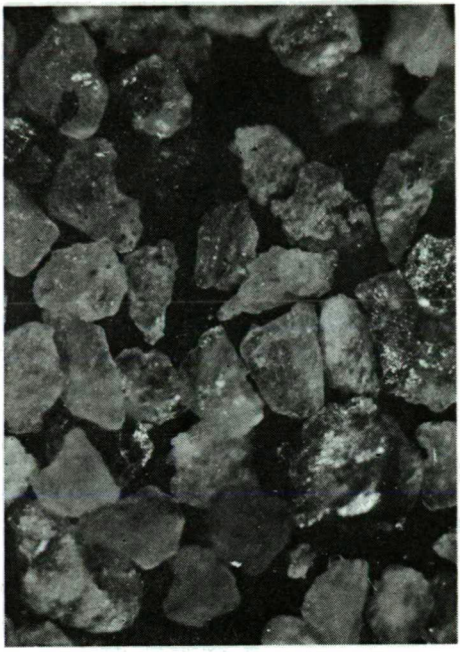

1

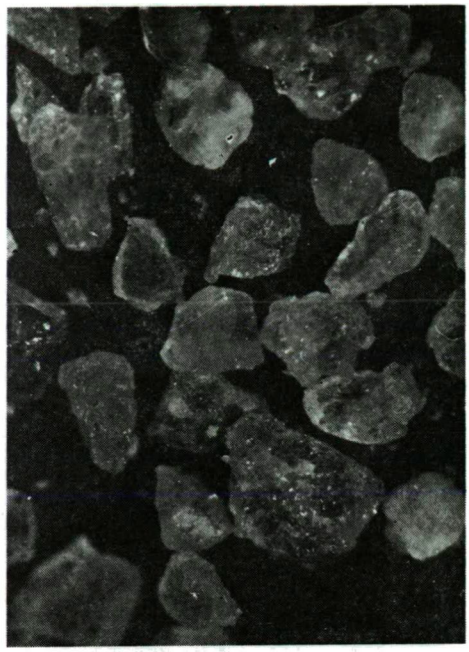

2

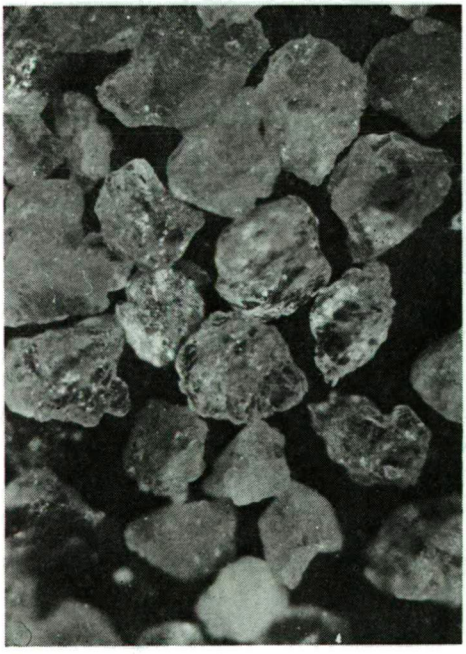

3

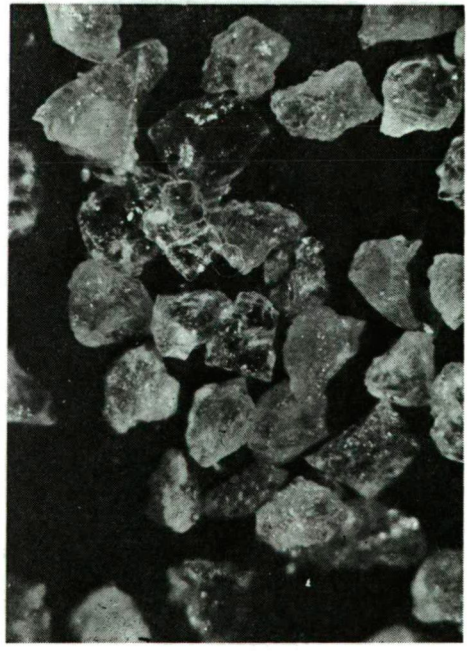

4

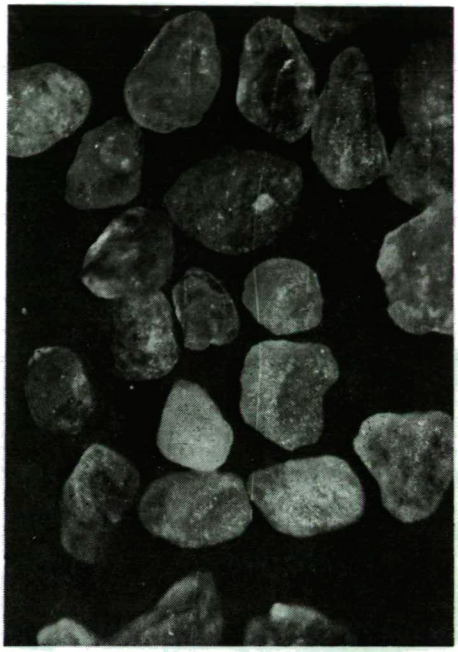

1

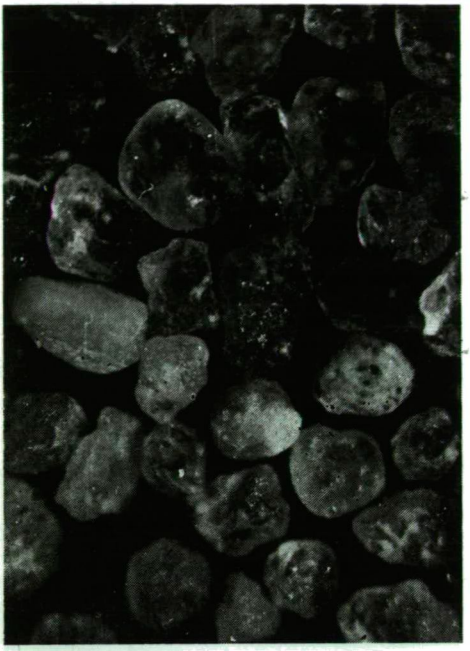

2

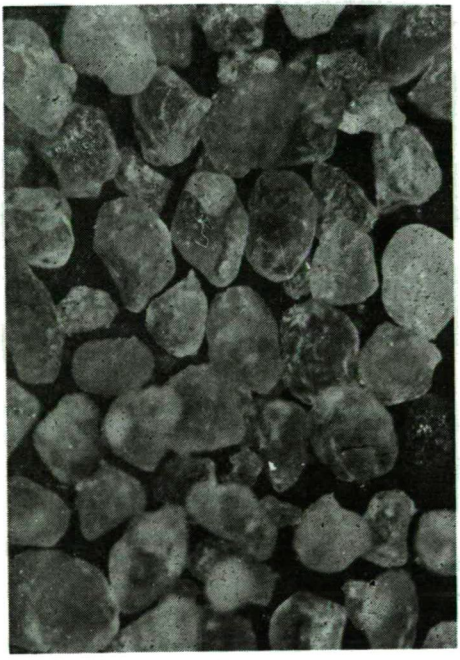

3

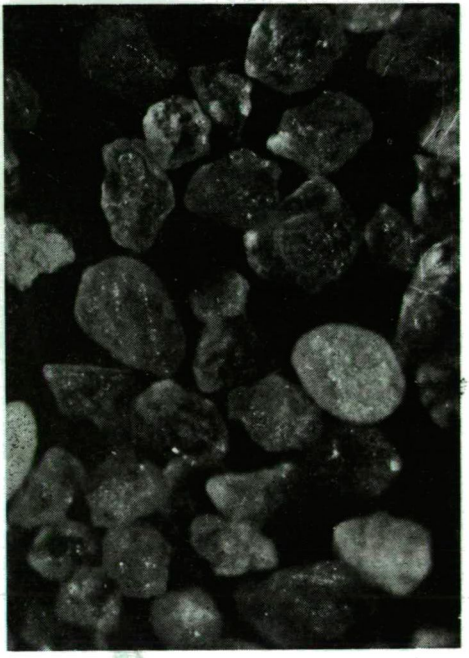

4

EXPLANATION OF PLATES I—VI

PLATE I: Heavy minerals of sand samples of the Upper Pannonian (Pliocene) in the Nyárlőrinc borehole: The photos of plates I—IV were made by mineralogical microscope with paralleled nicols, interbedding the minerals in nitrobenzol of n=1.552. In all photos the heavy minerals of the 0.1—0.2 mm fraction can be seen. *Abbreviations of minerals: H:* hypersthene, *Au:* augite, *Di:* diopside, *BH:* basaltic amphibole, *M:* magnetite, *Ap:* apatite, *B:* biotite, *Ch:* chlorite, *T:* tourmaline, *Cz:* clinozoisite, *Ho:* hornblende, *Ac—Tr:* actinolite—tremolite, *G:* garnet, *Ky:* kyanite, *C:* calcite-dolomite, or carbonatic rock detritus, *Wm:* weathered mineral.

1. 692.67—694.60 m
2. 763.57—769.02 m
3. 769.30—775.08a m
4. 769.30—775.08b m

PLATE II: Heavy minerals of the Pleistocene fluviatile (1—2) and Levantine fluviatile-lacustrine (3—4) sand samples from the Nyárlőrinc borehole.

1. 139.74—140.37 m
2. 154.7 m
3. 439.19—440.0 m
4. 496.69—500.0 m

PLATE III: Heavy minerals of the Pleistocene blown sand samples from the Nyárlőrinc borehole.

1. 77.5 m
2. 89.60—90.81 m
3. 112.0 m
4. 113.2 m

PLATE IV: Heavy minerals of the Pleistocene blown sand samples from the Nyárlőrinc borehole.

1. 2.0—3.0 m
2. 21.5 m
3. 31.0 m
4. 51.5 m

PLATE V: The Pleistocene fluviatile (1—2), Levantine fluviatile-lacustrine (3) and Upper Pannonian lacustrine (4) sharp, splintery quartz grains. Photos of Plate V—VI were made under binocular stereomicroscope. The quartz grains assigned to the fractions 0.1—0.2 resp. 0.2—0.32 mm are shown.

1. 139.74—140.87 m
2. 158.0 m
3. 678.70—681.41 m
4. 769.30—775.08 m

PLATE VI: Worn quartz grains of the Pleistocene blown-sand samples from the Nyárlőrinc borehole.

1. 8.5 m
2. 21.5 m
3. 81.0 m
4. 113.2 m

Acta Mineralogica-Petrographica, Szeged, XXIV/1, 167—186, 1979

PALYNOLOGICAL INVESTIGATIONS ON SEDIMENTS OF THE LOWER DANIAN (FISH CLAY, DENMARK) I

M. KEDVES

ABSTRACT

The first part of the spore-pollen investigations into the Fish Clay layers in Denmark, the *Angiospermatophyta* pollen grains are summarized in the present paper. We have succeeded in demonstrating altogether 57 form-species. Of these 24 are *Normapolles*, 18 *Postnormapolles*, resp. 14 *Longaxones*. There are described the following new taxons: *Semioculopollis croxtonae* n. fsp., *S. daniensis* n. fsp., *Trudopollis bangii* n. fsp., *T. hojrupensis* n. fsp., *Pompeckjoidaepollenites stockmarrii* n. fsp., *P. daniensis* n. fsp. *Jarzenipollenites trinus* [STANLEY, 1965] n. fgen. n. comb., *Vacuopollis pflugii* n. fsp., *Minorpollis hojstrupensis* n. fsp.. *Triatriopollenites grabowskae* n. fsp. The assemblage are of Upper Cretaceous character. There occurred none of the forms particularly characteristic of the Paleocene.

INTRODUCTION

The attention of geologists and palaeontologists has been engaged for a long time past by the problem of transition between the Cretaceous and Tertiary Periods. On palynological basis, too, this problem is extremely complicated. This is the cause of that a considerable part of the investigations is concentrated on the Danian, Monsian and Thanetian layers. The Danian stage is considered as the uppermost part of the Upper Cretaceous or the lower part of the Paleocene, but the designation Danian-Paleocene is frequent in palynological works. The problem is complicated by that the palaeophytogeographical regions are most express in the Upper Cretaceous and Paleocene Periods. The investigation into the Danian stage is regarded as particularly important in more than one paper. Cf. the K-TEC research programme of the Canadian work-team (BÉLAND, P., FELDMAN, P., FOSTER, J., JARZEN, D., NORRIS, G., PIROZYNSKI, K., REID, G., ROY, J.—R., RUSSEL, D., TUCKER, W.). This work-team called the attention to the palaeontological and palaeoecological importance of the supernova theory.

At datings on palynological basis, the knowledge of the spore-pollen composition of the type locality is absolutely indispensable. There are unfortunately, some cases, like that of Danian, when no sporomorphs are contained in the stratotype [KEDVES, 1967]. In this case, Fish Clay is the only comparative matter to be regarded as typical.

The stratigraphy of *Dinoflagellatae* of the sediments of the Danian, Upper Maastrichtian in Denmark was elaborated by HANSEN [1977].

MATERIAL AND METHOD

In answer to my request, an opportunity presented itself for me to investigate the following samples:
Stevns Klint — from CATHERINE A. CROXTON (The Geological Survey of Greenland),
Højrup — from JENS STOCKMARR (Geological Survey of Denmark),
Højstrup, bor. 5 DG 7, K75119, lab. no 127, 25—31 cm below top of core — from INGER BANG (Geological Survey of Denmark),
North Jütland, quarry named Dania.

At the preparation, there were applied different methods but the classical $ZnCl_2$ separation proved to be best.

RESULTS

Fgen.: OCULOPOLLIS PF. 1953b

The form-genus is complicated in respect of its electronmicroscopic structure as well. There was demonstrated endexine at *O. zaklinskaiae* GÓCZÁN 1964 by HEGEDŰS, KEDVES and PÁRDUTZ [1971]. This is an ancient characteristic within the *Normapolles* stemma. On the basis of the foregoing scanning electronmicroscopic results [KEDVES and RADVÁNSZKI 1975, ONORATINI and AZEMA 1973, MEDUS 1977], the form-genus is heterogenous, and on the basis of the ultrasculpture, two main types can be separated. The taxonomical value of these is not cleared up, as yet.

1. *O. minoris* W. KR. 1973 (Plate I, 1, 2)

As to its contour, it is no typical representative of the species described from the Maastrichtian layers of Oebisfelde.

2. Cf. *O. minoris* W. KR. 1973 (Plate I, 3, 4)

The oculi are of different sizes at the two different surfaces.

3. *O.* fsp. (Plate I, 5, 6)

Its measure is little prominent, its characteristic is given by the oculi, growing narrow in the direction of poles.

Fgen.: SEMIOCULOPOLLIS GÓCZÁN, W. KR. and PACLT. 1967

1. *Semioculopollis croxtonae* n. fsp. (Plate I, 7, 8)

Diagnosis

It has the form of an equatorial contour triangle. The surface is granulated, finely verrucate. The extragerminal exine is 1.3 μ thick, consisting light-microscopically only of ectexine its stratification can difficultly be observed, the infratectum is narrow. The exogerminalia are narrow colpi. The annulus is express, 3 μ thick. The vestibulum is narrow, it has an express endannulus which is 1.5 μ thick. The endoapertures are large, the pores have 3 μ diameters, the pollen is heteropolar, on one of the sides there are narrow oculi.
Maximum size: 24 μ (20—30 μ).
Holotype: Plate I, 7, 8, slide Stevns Klint-7, co-ordinates 6.4/110.2.
Locus typicus: Stevns Klint.
Stratum typicum: Fish Clay.
Derivatio nominis: In honour of Dr. C. A. CROXTON.
Differential diagnosis: The size of *S. praedicatus* (WEYL. and KRIEG. 1953) W. KR. 1967 is smaller and its surface is rugulate, the exine structure of *S. lapillus* (PF. 1953b) W. KR. 1967 is intrabaculate.
Occurrence: Stevns Klint, Højrup, Dania.

2. *Semioculopollis daniensis* n. fsp. (Plate I, 9, 10)

Diagnosis

Contour is triangular, with convex sides. The surface is punctate. The extragerminal exine is 1.5—2 μ thick. The tectum, infratectum and foot layer are equally thick. The exogerminalia are narrow colpi. The annulus is 4 μ thick, somewhat centripetal. The vestibulum is narrow. The endannulus is not express, the nexine does not incurve, centripetally. At one of the sides, there are express oculi. The diameter of endopores is 2.5 μ.

Maximum size: 24 μ (20—28 μ).

Holotype: Plate I, 9, 10, slide Dania-33, co-ordinates 7.6/112.2.

Locus typicus: Dania (N. Jütland).

Stratum typicum: Fish Clay.

Derivatio nominis: From the locality of the type.

Differential diagnosis: It is separated well from *S. croxtonae* n. fsp. by the ornamentation of the surface, the missing endannulus, and the narrow endopores.

Occurrence: For the time being it is only known from the locality of the type.

Fgen.: TRUDOPOLLIS PF. 1953b emend. W. KR. 1967

The exine ultrastructure investigation into the *T. mechanicus* PF. 1953b was carried out by HEGEDŰS, KEDVES and PÁRDUTZ [1972]. Its endexine could not be demonstrated, that is a more developed pecularity. The infratectum consists of short elements of varied shapes. This reminds us of the recent *Amentiflorae*.

1. *Trudopollis bangii* n. fsp. (Plate I, 11, 12)

Diagnosis

Contour is triangular with convex sides. The extragerminal exine is 1.8 μ thick. The tectum is somewhat thicker than the infratectum and foot layer, respectively. The exogerminalia is narrow colpi. The annulus is centripetal and 4 μ thick. There is only a very small, narrow vestibulum. It has an express, centripetally incurved 1.3 μ thick endannulus. There is a large, triangular atrium, in the direction of the poles of the pollen.

Maximum size: 25 μ (20—28 μ).

Holotype: Plate I, 11, 12, slide Dania-20, co-ordinates 15.4/117.7.

Locus typicus: Dania (N. Jütland).

Stratum typicum: Fish Clay.

Derivatio nominis: In honour of DR. I. BANG.

Differential diagnosis: It is separated from *T. concretor* PF. 1953b by the shape of the annulus and endannulus.

Occurrence: For the time being, it is only known from the locality of the type.

2. *T.* fsp.$_1$ (Plate I, 13, 14)

Contour is triangular, with convex sides. The surface is smooth or finely scabrate. The extragerminal exine is 1 μ thick, the tectum, infratectum, and foot layer are equally thick. The exogerminalia are narrow colpi. There is an express 2.5 μ thick centripetal annulus. There is a narrow, comparatively long vestibulum. The endannulus is 0.9 μ thick, incurving centripetally inside. The atrium is granular.

Note. — *T. retifectus* WEYL. and KRIEG. 1953 is similar, but has a intrareticulate structure.

Occurrence: Højstrup.

3. *Trudopollis hojrupensis* n. fsp. (Plate I, 15, 16)

Diagnosis

Contour is triangular, with straight or somewhat convex sides. The surface is granulate or finely rugulate. The extragerminal exine is 1 μ thick, the infratectum is narrower than the tectum, resp. the foot layer. The exogerminalia are short, narrow colpi. The annuli are 3.5 μ thick, they incurve somewhat inside. The vestibulum is long, narrow. The endannuli are comparatively narrow (0.9 μ), they incurve only a little centripetally. The endogerminalia are broad pores (3 μ).

Maximum size: 22 μ (18—25 μ).

Holotype: Plate I, 15, 16, slide D_3-95, co-ordinates 19.5/117.4.

Locus typicus: Højrup.

Stratum typicum: Fish Clay.

Derivatio nominis: From the locality of the type.

Differential diagnosis: *T. orthomechanicus* PF. 1953b is similar but its exine is of baculate structure.

Occurrence: For the time being, it is only known from the locality of the type.

4. *T.* fsp.$_2$ (Plate I, 17, 18)

Contour is triangular, with convex sides. The surface is scabrate. The extragerminal exine is 2 μ thick, the tectum, infratectum, foot layer are equally thick. The annulus is 3 μ thick and centripetally incurves. There is an expressed vestibulum. The endannulus is 2 μ thick, wedge-shaped. The atrium is narrow.

Note. — It was found in two damaged specimens from the locality Højrup. There is not known any similar pollen in the literature.

Fgen.: HUNGAROPOLLIS GÓCZÁN 1964

HEGEDŰS, KEDVES and PÁRDUTZ [1971] have performed ultrastructure investigations into the genus and ascertained a particular type, not the same as the other *Normapolles*.

1. Cf. *H.* fsp. (Plate I, 19, 20)

Contour is triangular, with convex sides. The surface is scabrate. In one of the poles, there is a formation, similar to a not express papillus. The extragerminal exine is 4 μ thick, the infratectum is extremely narrow, the tectum and foot layer are equally thick. The endogerminalia are long, narrow colpi. The annulus is 3.5 μ thick, incurving centripetally. The vestibulum is narrow. The endannulus is 3 μ thick, the atrium is small.

Occurrence: Højrup.

Fgen.: POMPECKJOIDAEPOLLENITES PF. 1953b emend. W. KR. 1967

The ultrastructure investigation into the *P. subhercynicus* PF. 1953b emend. W. KR. 1967 exine was performed by KEDVES and PÁRDUTZ [1970]. The channels of the tectum and the granular infratectum refer to the origin from *Amentiflorae*. The perforated tectum and the similarly to *Amentiflorae* referring coni at the surface have been ascertained by the scanning electronmicroscopic results [STANLEY and KEDVES 1975].

1. *Pompeckjoidaepollenites stockmarrii* n. fsp. (Plate I, 21, 22)

Diagnosis

The equatorial contour is triangular, with convex sides. The surface is granulate, the sculpture elements often anastomose, a rugulate sculpture comes about. The extragerminal exine is 1.3 μ thick, the tectum, infratectum, and foot layer are equally

thick. The annuli are 3—4 μ thick, incurving centripetally. The vestibulum is small, wedge-shaped. The endannulus is wedge-shaped, 0.7 μ thick. The atrium is broad, the platea is express, broad.
Maximum size: 38 μ (35—43 μ).
Holotype: Plate I, 21, 22, slide D_3-54, co-ordinates 10.1/103.3.
Locus typicus: Højrup.
Stratum typicum: Fish Clay.
Derivatio nominis: In honour of DR. J. STOCKMARR.
Differential diagnosis: It is well-separated by the broad express platea from *P. absurdus* (WEYL. and KRIEG. 1953) W. KR. 1967.
Occurrence: For the time being, it is only known from the locality of the type.

2. *P. subhercynicus* PF. 1953b emend. W. KR. 1967 (Plate I, 23, 24)

Cf. its electronmicroscopical results at the form-genus. In our material, typical individuals of the form-species also occurred.
Occurrence: Højrup, Højstrup, Dania.

3. *Pompeckjoidaepollenites daniensis* n. fsp. (Plate I, 25, 26)

Syn. — 1969, KEDVES — *Pompeckjoidaepollenites* fsp. B, Pl. 2, 9—12.

Diagnosis

The equatorial contour is triangular, with very convex sides. The surface is scabrate, or finely punctate. The extragerminal exine is 1.2 μ thick, the infratectum is thinner than the tectum, resp. foot layer. The exogerminalia are narrow colpi. The annulus is narrow, incurving only a little, its thickness is 2.2 μ. The vestibulum is narrow, the endannulus is not express. It has a wedge-shaped, 0.8 μ thick, small atrium. The platea is only little express, narrow.
Maximum size: 16 μ (14—20 μ).
Holotype: Plate I, 25, 26, slide Dania-36, co-ordinates 18.9/107.5.
Locus typicus: Dania (N. Jütland).
Stratum typicum: Fish Clay.
Derivatio nominis: From the locality of the holotype.
Differential diagnosis: It is separated by its smaller size and narrow platea from *P. subhercynicus* PF. 1953b emend. W. KR. 1967.
Occurrence: Dania (N. Jütland), U. Sparnatian (Guitrancourt B_1 32, Faciés Argiles des Flandres: Templeuve-en-Pévèle B_1-25), Cuisian: Fosses I—III.

4. *Pompeckjoidaepollenites hojrupensis* n. fsp. (Plate II, 1, 2)

Diagnosis

Contour is triangular, with very convex sides. The surface is smooth. The extragerminal exine is 1 μ thick, the infratectum is narrower than the tectum, resp. the columellar layer. The exoapertures are only somewhat elongated pores, comparatively broad colpi. The annulus is 2.2 μ thick, prominent, somewhat incurving. The atrium is narrow, short. The endannulus is 1 μ thick, centripetally incurving. The platea is narrow, a little express.
Maximum size: 17 μ (15—18 μ).
Holotype: Plate II, 1, 2, slide D_3-75, co-ordinates 21.4/104.3.
Locus typicus: Højrup.
Stratum typicum: Fish Clay.
Derivatio nominis: From the locality of the type.
Differential diagnosis: It is separated by its surface and prominent annulus from *P. daniensis* n. fsp.

Occurrence: For the time being, it is only known from the locality of the holotype.

5. *P.* fsp. (Plate II, 3, 4)

It occurred with a single damaged specimen from the locality Stevns Klint

Fgen.: NUDOPOLLIS Pf. 1953b

Transmission electronmicroscopic data about *N. terminalis* (Th. and Pf. 1953) Pf. 1953b, by Kedves and Párdutz [1970]. The scanning elaboration of the same form-species was performed by Stanley and Kedves [1975]. The electronmicroscopic results refer to *Myricaceae* origin.

1. *N. terminalis* (Th. and Pf. 1953) Pf. 1953b (Plate II. 5, 6)

Occurrence: Højrup, Dania (N. Jütland).

Fgen.: PLICAPOLLIS Pf. 1953b

The SEM and TEM data of *P. pseudoexcelsus* (W. Kr. 1958) W. Kr. 1961 equally refer to *Myricaceae* origin [Kedves and Párdutz 1970, Stanley and Kedves 1975].

1.1. *P. pseudoexcelsus* (W. Kr. 1958) W. Kr. 1961 subfsp. *turgidus* Pf. 1953a (Plate II, 7, 8)

Occurrence: Dania (N. Jütland).

1.2. subfsp. *semiturgidus* Pf. 1953a (Plate II, 9, 10)

Occurrence: Højrup.

1.3. subfsp. *luteticus* Kds. 1969 (Plate II, 11, 12)

Occurrence: Stevns Klint, Højrup.

1.4. subfsp. *minor* Pf. 1953a (Plate II, 13, 14)

Occurrence: Højrup.

Fgen.: JARZENIPOLLENITES n. fgen.

Fgen. type: *J. trinus* (Stanley 1965) n. comb. (Plate II, 15—20)

Syn. — 1965, Stanley — *Alnus trina* n. sp., Pl. 43, 4—6

Diagnosis

The equatorial contour is triangular, with convex sides. There are three germinal apertures, these are pores, and there is a small centripetal annulus. Germinalia are connected with one another by arcuses. The surface is smooth or punctate.

Genus type: in Stanley, Pl. 43, 4—6.

Locus typicus: North Cave Hills, Harding Co., South Dakota.

Stratum typicum: Ludlow member, Fort Union Formation, Paleocene.

Derivatio nominis: In honour of Dr. D. M. Jarzen.

Differential diagnosis: The surface of *Ulmoideipites* Anderson 1960 is expressly sculptured, rugulate.

Species diagnosis: See at Stanley [1965].

Note. — The pollen grain published under the name *Simarubaceae* [Bratzeva 1969, Pl. 61, 7], may probably belong to the described form-genus. The form of Jarzen [1976], Plate I, 4; *Alnus* type is identical with the *J. trinus*.

Occurrence: North Cave Hills, Harding Co., South Dakota, Paleocene, Saskatchewan (Canada), Maastrichtian and Paleocene, Dania (N. Jütland).

2. *J.* fsp. (Plate II, 21, 22)

Occurrence: Stevns Klint.

Fgen.: INTERPOLLIS W. Kr. 1961

A modern TEM and SEM elaboration is known from Stanley and Kedves [1975]. The ultrastructure of the *I. microsupplingensis* W. Kr. 1961 differs from the

other fossil *Angiospermatophyta* pollen grains. By the SEM investigations, coni, characteristic of *Amentiflorae* were established.

1. *I. supplingensis* (PF. 1953a) W. KR. 1961 (Plate II, 23—26)
The observed specimens are smaller than the typical forms.
Occurrence: Højrup, Dania (N. Jütland).

2. *I. velum* W. KR. 1961 (Plate II, 27, 28)
Occurrence: Højrup.

3. *I. microsupplingensis* W. KR. 1961 (Plate II, 29—36)
A very great form-variation could be observed.
Occurrence: Højrup, Højstrup, Stevns Klint, Dania (N. Jütland).

Fgen.: VACUOPOLLIS PF. 1953b

TEM data are from *V. orthopyramis* PF. 1953b (Upper Cretaceous). The exine structure of this, differs from that of the other *Normapolles* [HEGEDŰS, KEDVES and PÁRDUTZ 1972]. At the surface of *V. concavus* (PF. 1953a) W. KR. 1960 from the Eocene there are coni. This is general enough within the *Normapolles* stemma and is an *Amentiflorae* characteristic.

1. *Vacuopollis pflugii* n. fsp. (Plate III, 1, 2)
Diagnosis

Contour is triangular, with concave sides. The surface is punctate-scabrate. The extragerminal exine is 1.6 μ thick, the infratectum is somewhat thicker than the tectum and foot layer.Th e infratectum is of columellar structure. The exogerminalia are 1 μ broad short colpi. The annulus is extremely narrow, hardly observable. The foot layer is only partially missing from the pore region.
Maximum size: 25 μ (23—28 μ).
Holotype: Plate III, 1, 2, slide Stevns Klint-8, co-ordinates 9.6/114.2.
Locus typicus: Stevns Klint.
Stratum typicum: Fish Clay.
Derivatio nominis: In honour of PROF. DR. H. PFLUG.
Occurrence: For the time being, it is only known from the locality of the type.

Fgen.: MINORPOLLIS W. KR. 1959

1. *Minorpollis hojstrupensis* n. fsp. (Plate III, 3, 4)
Diagnosis

Equatorial contour is triangular, with convex sides. The surface is smooth. The extragerminal exine is 0.6 μ thick, the infratectum is very narrow, its structure cannot be identified. It has an extremely small centripetal annulus. The exogerminalia are short colpi.
Maximum size: 9 μ (8—10 μ).
Holotype: Plate III, 3, 4, slide Højstrup-12, co-ordinates 16.7/117.7.
Locus typicus: Højstrup.
Stratum typicum: Fish Clay.
Derivatio nominis: From Højstrup, the locality of the type.
Differential diagnosis: It is separated from *M. gallicus* KDS. 1969 by its thinner wall and smaller size.
Occurrence: For the time being, it is only known from the locality of the type.

2. *M. gallicus* KDS. 1969 (Plate III, 5—8)
Occurrence: Højrup, Dania (N. Jütland).

Fgen.: TRIATRIOPOLLENITES PF. 1953a

1. *Triatriopollenites grabowskae* n. fsp. (Plate III, 9—16)

Diagnosis

The equatorial contour is triangular, with stratight or somewhat convex sides. The surface is punctate. The extragerminal exine is 2 μ thick, the tectum, infratectum and foot layer are equally thick. The exact structure of the infratectum cannot be identified with light microscope, it is probably of granular structure. The exogerminalia are 1 μ broad, short colpi. The infratectum becomes thick in the germinal region, the annulus is 2 μ thick. The atrium is intragranulate.

Maximum size: 16 μ (14—17 μ).

Holotype: Plate III, 9, 10, slide D_2—1—1, co-ordinates 11.6/120.2.

Locus typicus: Højrup.

Stratum typicum: Fish Clay.

Derivatio nominis: In honour of DR. I. GRABOWSKA.

Differential diagnosis: It is separated from *T. rurobituitus* PF. 1953a by its comparatively thick wall and smaller size.

Occurrence: Højrup, Dania (N. Jütland).

Note. — This species was published by GRABOWSKA [1968] from the L.—M. Eocene layers of Szczecin, without any nearer determination, Pl. III, 81.

2. *T. cycloquietus* W. KR. 1961 (Plate III, 17, 18)

Occurrence: Højrup, Dania (N. Jütland).

3. *T.* fsp. A (Plate III, 23, 24)

Equatorial contour is triangular, with convex sides. The surface is scabrate. The extragerminal exine is 1 μ thick, the tectum, infratectum and foot layer are equally thick. The exoapertures are comparatively long colpi. The annulus is 2.5 μ thick. The atrium is finely intrapunctate.

Occurrence: Højstrup.

4. *T. rurensis* PF. and TH. 1953 (Plate III, 25, 26)

Occurrence: Højrup.

5. *T.* fsp. B (Plate III, 27—30)

Occurrence: Højrup.

Fgen.: MYRTACEIDITES COOKSON and PIKE 1954 em. R. POT. 1960

1. *M.* fsp. (Plate III, 31, 32)

Occurrence: Højrup.

Fgen.: SPARGANIACEAEPOLLENITES THIERGART 1937

1. *Sp.* cf. *cuvillieri* (GRUAS-CAV. 1966) W. KR. 1970, *Sparganiaceae* (Plate III, 33, 34)

Occurrence: Højrup.

Fgen.: LABRAPOLLIS W. KR. 1968

1. Cf. *L. rotundoides* W. KR. 1968 (Plate III, 35, 36)

Occurrence: Højrup.

2. *L. labraferoides* (W. KR. 1961) W. KR. 1968 (Plate III, 19—22, 37, 38)

Occurrence: Dania (N. Jütland), Stevns Klint.

3. *L. globosus* (PF. 1953a) W. KR. 1968 (Plate III, 39, 40)

Occurrence: Dania (N. Jütland).

Fgen.: PORTNIAGINAEPOLLENITES KDS. 1974

1. *P.* fsp. (Plate IV, 1, 2)

Contour is approximately circular. The surface is scabrate. The extragerminal exine is 2 μ thick, the tectum is thicker than the foot layer. The infratectum is of express, columnar structure. The diameter of pores is 1.5 μ, the annulus is small. The atrium is also small but express.
Occurrence: Højrup.

Fgen.: TRIPOROPOLLENITES PF. and TH. 1953
1. *T. undulatus* PF. 1953a, *Ulmaceae* (Plate IV, 3—6)
Occurrence: Højrup, Højstrup.
2. *T. robustus* PF. 1953a subfsp. *robustus,* cf. *Betulaceae* (Plate IV, 7, 8)
Occurrence: Højrup.
3. *T. festatus* TAKAHASHI 1961, *Betulaceae* (Plate IV, 9, 10)
Occurrence: Stevns Klint.

Fgen.: SUBTRIPOROPOLLENITES PF. and TH. 1953
The ultrastructure investigation into *S. constans* PF. 1953a subfsp. *constans* was carried out by KEDVES and STANLEY [1976]. The anastomosing infratectum consisting of irregular, short elements refers to *Amentiflorae* origin.
1. *S. constans* PF. 1953a subfsp. *constans* (Plate IV, 11, 12)
Occurrence: Højrup, Dania (N. Jütland).
2.1. *S. anulatus* PF. and TH. 1953 subfsp. *anulatus, Juglandaceae* cf. *Carya* (Plate IV, 13, 14)
Occurrence: Højrup.
2.2. *S. anulatus* PF. and TH. 1953 subfsp. *nanus* PF. and TH. 1953, *Juglandaceae* cf. *Carya* (Plate IV, 15—18)
Occurrence: Dania (N. Jütland).
3. *S.* fsp. (Plate IV, 19, 20)
Contour is circular or ellipsoid. The surface is smooth. The exine is 1 μ thick, the tectum, infratectum and foot layer are equally thick. The exact structure of the infratectum cannot be identified with light microscope. The diameters of pores are 1.5 μ, there are narrow, annulus-like formations around them.
Occurrence: Højstrup.

Fgen.: ARECIPITES WODEH. 1933
1. *A.* fsp., *Palmae* (Plate IV, 21, 22)
Occurrence: Højstrup.

Fgen.: CUPULIFEROIPOLLENITES R. POT. 1960
1. *C. insieyanus* (TRAVERSE 1955) R. POT. 1960, *Fagaceae, Castanea* (Plate IV, 23, 24)
Occurrence: Højstrup.
2. *C. pusillus* (R. POT. 1934) R. POT. 1960, *Fagaceae,* cf. *Castanea* (Plate IV, 25—28, Plate V, 1, 2)
Occurrence: Højstrup, Stevns Klint.
3. *C. oviformis* (R. POT. 1931) R. POT. 1960, *Fagaceae, Castanea* (Plate V, 3, 4)
Occurrence: Dania (N. Jütland).

Fgen.: PSILATRICOLPORITES (VAN DER HAMMEN 1956a) VAN DER HAMMEN and WIJMSTRA 1964
1. *Ps.* fsp. (Plate V, 5, 6)
Contour is ellipsoid, the surface is smooth. The extragerminal exine is 1.6 μ thick, the tectum, infratectum and nexine are by and large of equal thickness. The

exact structure of the infratectum cannot be identified with light microscope. Colpi are narrow, reaching the poles, with an about 1 μ broad cavern. The endogerminalia are narrow, split-like fugae.
Occurrence: Stevns Klint.

2. *Ps.* cf. *microparmularius* KDS. and DIN. 1978 (Plate V, 7, 8)
Occurrence: Højrup.

Fgen.: INTRABACULITRICOLPORITES KDS. 1978

1. *I.* fsp.$_1$ (Plate V, 9, 10)

Contour is elliptical. The surface is smooth, the tectum being finely perforated. The exine is 0.8 μ thick, the infratectum is thicker than the tectum and nexine. The colpi are narrow slit-like, reaching the poles almost always. Colpi are surrounded by a 0.8 μ broad cavern. The endopores are elliptical, orientated in the direction of the longitudinal axis of the pollen, their size being 1.5×2 μ.
Occurrence: Højstrup.

2. *I.* fsp.$_2$ (Plate V, 11, 12)

Contour is elliptical, in the middle somewhat enlarging. The surface is smooth, the tectum, infratectum and nexine are equally thick. The infratectum is of expressly columellar structure. The colpi are united with the cavium, encurving a little outside at the poles. Colpi are surrounded by an about 1 μ broad cavern. The endopores are more or less circular, with 3 μ diameters.
Occurrence: Dania (N. Jütland).

3. *I.* fsp.$_3$ (Plate V, 13, 14)

Contour is elliptical. The surface is smooth or scabrate. Under the ectexine, endexine can be separated light-microscopically, its thickness being identical with one layer of ectexine. The tectum, infratectum and foot layer are equally thick. The infratectum consists of fine columellar elements. Colpi are narrow slit-like, not reaching the poles. The cavern is about 0.6 μ broad. The endopores are narrow slit-like.
Occurrence: Stevns Klint.

4. *I.* fsp.$_4$ (Plate V, 15, 16)

Contour is approximately circular. The surface is smooth. The exine is 1.3 μ thick, under the ectexine a thick endexine can be separated. The tectum, infratectum and foot layer are equally thick. The infratectum is of very fine columellar structure. Colpi are narrow slit-like, with a 0.3 μ broad cavern. Colpi are united with the cavium in the poles. The endopores are elliptical (1×2 μ).
Occurrence: Stevns Klint.

5. *I.* fsp.$_5$ (Plate V, 21, 22)

Contour elliptical. The surface is smooth or scabrate. The exine is 2.5 μ thick, consisting light-microscopically of ectexine and endexine. The infratectum is thicker than the tectum and foot layer. The infratectum is of expressly columellar structure. Colpi are slit-like, with a 1.5 μ broad cavern and reaching the poles generally. The endogerminalia are elliptical (1.5×3—4 μ).
Occurrence: Dania (N. Jütland).

Fgen.: NYSSAPOLLENITES THIERGART 1937

1. *N.* fsp., *Nyssaceae* v. *Mastixiaceae* (Plate V, 17, 18)
Occurrence: Højrup.

2. Cf. *N.* fsp., *Nyssaceae* v. *Mastixiaceae* (Plate V, 19, 20)
Occurrence: Stevns Klint.

Fgen.: RETITRICOLPORITES (VAN DER HAMMEN 1956) VAN DER HAMMEN and WIJMSTRA 1964

1. *R.* fsp. (Plate V, 23, 24)

Occurrence: Højrup.

Fgen.: ILEXPOLLENITES (THIERGART 1937) R. POT. 1960

1. I. fsp., *Aquifoliaceae, Ilex* (Plate V, 25, 26)

Occurrence: Højrup.

DISCUSSION

It is to be mentioned at evaluating the demonstrated spore-pollen assemblages that — although 57 angiospermous pollen form-species could be demonstrated — the investigated material is not rich in sporomorphs and the lack of certain types can only be evaluated under reserve. In PFLUG's material (1953a, b) from Wehmingen there are, according to our present-day knowledge, some species characteristic of the Paleocene, as well; *Stephanoporopollenites hexaradiatus, Extratriporopollenites audax,* etc. I have to mention the richness in species of the *Nudopollis* genus, as well, which is not characteristic of the material from Denmark. KRUTZSCH [1966], classifying the Danian into the Paleocene, distinguishes two main assemblage types. The type from Zahna is comparatively poor in sporomorphs. The richness of *Erdtmanipollis* fspp. is interesting. From this assemblage, the *Stephanoporopollenites* fgen. is missing, as well as the *Pompeckjoidaepollenites,* too; this latter is, however, frequent enough in the material from Denmark. The assemblages (A—C) of Roda type are very rich in the *Angiospermatophyta* pollen grains. The occurs the so-called Paleocene form of *Stephanoporopollenites, Tetrapollis, Extratriporopollenites.* From among the more developed types, *Milfordia, Pentapollenites* and *Compositoipollenites* occur.

Our demonstrated assemblage differs from those dealt with above just in the lack of the forms which are characteristic of the Paleocene. Compared with the results from the Maastrichtian till now, it can mostly be placed over the spore-pollen assemblage of KRUTZSCH and MIBUS [1973] from Walbeck. The connective link with the assemblage from Denmark is represented in this assemblage by the presence of *Interpollis* and *Pompeckjoidaepollenites.* On the other hand, the richness of the *Trudopollis, Oculopollis* fgen., the presence of *Bohemiapollis, Complexiopollis, Extremipollis, Paravacuopollis,* etc. in the assemblage of Walbeck is a good delimiting characteristic.

Summarizing, the spore-pollen assemblage of Fish Clay (Lower Danian) contains, apart from the *Normapolles* originating from the Upper Cretaceous, several *Postnormapolles,* as well, which are characteristic of the Lower Tertiary. The forms which are particularly characteristic of the early Paleocene sediments, are missing. After the Walbeck assemblage of Maastrichtian age, the Fish Clay can be located very well on palynological basis, as the representative of the lower part of the Danian, and the other assemblages (Wehmingen, Zahna, Roda) are to be classified into the Upper Danian. Thus the Danian is, from palynological point of view, of double character. Within the Danian, considerable changes took place in Europe in the development of the vegetation. The measure of the palynological difference between the Walbeck-assemblage and that from Fish Clay is by and large identical with that between the Upper Danian assemblages. In Fish Clay, the younger elements are given by the forms which are characteristic of the Eocene, as well, without the pollen grains which are characteristic of the Early Paleocene. By this is given the characteristic of this assemblage originating from the boundary of the Cretaceous and Tertiary Periods.

ACKNOWLEDGEMENTS

I am deeply indebted to DR. C. A. CROXTON, DR. I. BANG, and DR. J. STOCKMARR for kindly holding to my disposal the samples for my investigations.

PLATE I

1, 2. — *Oculopollis minoris* W. KR. 1973, D_3—2—3; 20.3/110.5.
3, 4. — Cf. *Oculopollis minoris* W. KR. 1973, D_3—75; 2.4/116.0.
5, 6. — *Oculopollis* fsp., D_2—1—8; 20.7/111.1.
7, 8. — *Semioculopollis croxtonae* n. fsp., Stevns Klint—7; 6.4/110.2.
9, 10. — *Semioculopollis daniensis* n. fsp., Dania—33; 7.6/112.2.
11, 12. — *Trudopollis bangii* n. fsp., Dania—20; 15.4/117.7.
13, 14. — *Trudopollis* fsp.$_1$, Højstrup—27; 11.8/117.4.
15, 16. — *Trudopollis hojrupensis* n. fsp., D_3—95; 19.5/117.4.
17, 18. — *Trudopollis* fsp.$_2$, D_3—88; 22.9/116.0.
19, 20. — Cf. *Hungaropollis* fsp., D_3—49; 14.5/111.2.
21, 22. — *Pompeckjoidaepollenites stockmarrii* n. fsp., D_3—54; 10.1/103.3.
23, 24. — *Pompeckjoidaepollenites subhercynicus* PF. 1953b emend. W. KR. 1967, Dania—7; 18.2/102.4.
25, 26. — *Pompeckjoidaepollenites daniensis* n. fsp., Dania—36; 18.9/107.5.
× 1000

PLATE II

1, 2. — *Pompeckjoidaepollenites hojrupensis* n. fsp., D_3—75; 21.4/104.3.
3, 4. — *Pompeckjoidaepollenites* fsp., Stevns Klint—29; 22.8/104.4.
5, 6. — *Nudopollis terminalis* (TH. and PF. 1953) PF. 1953b, D_2—1—5; 4.4/107.1.
7, 8. — *Plicapollis pseudoexcelsus* (W. KR. 1958) W. KR. 1961 subfsp. *turdigus* PF. 1953a, Dania—5; 19.5/112.5.
9, 10. — *Plicapollis pseudoexcelsus* (W. KR. 1958) W. KR. 1961 subfsp. *semiturgidus* PF. 1953a, D—3—35; 8.7/101.6.
11, 12 — *Plicapollis pseudoexcelsus* (W. KR. 1958) W. KR. 1961 subfsp. *luteticus* KDS. 1969, Stevns Klint—40; 22.2/111.5.
13, 14. — *Plicapollis pseudoexcelsus* (W. KR. 1958) W. KR. 1961 subfsp. *minor* PF. 1953a, D_2—1—1; 12.2/118.7.
15, 16. — *Jarzenipollenites trinus* (STANLEY 1965) n. fgen. n. comb., Dania—16; 12.2/112.4.
17, 18. — *Jarzenipollenites trinus* (STANLEY 1965) n. fgen. n. comb., Dania—36; 12.4/114.1.
19, 20. — *Jarzenipollenites trinus* (STANLEY 1965) n. fgen. n. comb., Dania—10; 22.0/110.2.
21, 22. — *Jarzenipollenites* fsp., Stevns Klint—6; 21.8/114.2.
23, 24. — *Interpollis supplingensis* (PF. 1953a) W. KR. 1961, D_2—1—8; 1.2/113.2.
25, 26. — *Interpollis supplingensis* (PF. 1953a) W. KR. 1961, Dania—18; 5.5/118.7.
27, 28. — *Interpollis velum* W. KR. 1961, D_2—1—2; 16.5/120.9.
29, 30. — *Interpollis microsupplingensis* W. KR. 1961, D_3—67; 11.4/112.4.
31, 32. — *Interpollis microsupplingensis* W. KR. 1961, D_3—76; 12.3/119.2.
33, 34. — *Interpollis microsupplingensis* W. KR. 1961, D_2—1—8; 8.1/126.3.
35, 36. — *Interpollis microsupplingensis* W. KR. 1961, Stevns Klint—37; 6.0/114.9.
× 1000

PLATE III

1, 2. — *Vacuopollis pflugii* n. fsp., Stevns Klint—8; 9.6/114.2.
3, 4. — *Minorpollis hojstrupensis* n. fsp., Højstrup—12; 16.7/117.7.
5, 6. — *Minorpollis gallicus* KDS. 1969, D—2—1; 17.3/106.3.
7, 8. — *Minorpollis gallicus* KDS. 1969, Dania—1; 17.3/104.4.
9, 10. — *Triatriopollenites grabowskae* n. fsp., D_2—1—1; 11.6/120.2.
11, 12. — *Triatriopollenites grabowskae* n. fsp., Højstrup—39; 10.7/116.4.
13, 14. — *Triatriopollenites grabowskae* n. fsp., Højstrup—40; 18.4/116.3.
15, 16. — *Triatriopollenites grabowskae* n. fsp., Højstrup—8; 11.6/120.6.
17, 18. — *Triatriopollenites cycloquietus* W. KR. 1961, D—1—x—9; 4.7/123.8.

19, 20. — *Labrapollis labraferoides* (W. Kr. 1961) W. Kr. 1968, Stevns Klint—20; 4.7/111.4.
21, 22. — *Labrapollis labraferoides* (W. Kr. 1961) W. Kr. 1968, D_3—1; 22.1/123.1.
23, 24. — *Triatriopollenites* fsp. A, Højstrup—33; 15.0/117.3.
25, 26. — *Triatriopollenites rurensis* Pf. and Th. 1953, D_3—5; 5.2/108.3.
27, 28. — *Triatriopollenites* fsp. B, D_3—20; 23.0/123.6.
29, 30. — *Triatriopollenites* fsp. B, D_2—1—1; 22.9/105.9.
31, 32. — *Myrtaceidites* fsp., D_2—2—6; 8.9/106.5.
33, 34. — *Sparganiaceaepollenites* cf. *cuvillieri* (Gruas—Cav. 1966) W. Kr. 1970, *Sparganiaceae*, Højstrup—41; 13.1/115.8.
35, 36. — Cf. *Labrapollis rotundoides* W. Kr. 1968, D_2—2—x—1; 16.7/119.1.
37, 38. — *Labrapollis labraferoides* (W. Kr. 1961) W. Kr. 1968, Dania—18; 5.5/112.4.
39, 40. — *Labrapollis globosus* (Pf. 1953a) W. Kr. 1968, Dania—1; 18.1/120.7.
× 1000

Plate IV

1, 2. — *Portniaginaepollenites* fsp., D_3—3; 9.4/109.7.
3, 4. — *Triporopollenites undulatus* Pf. 1953a, *Ulmaceae;* D_3—67; 14.0/110.7.
5, 6. — *Triporopollenites undulatus* Pf. 1953a, *Ulmaceae;* Højstrup—2; 7.4/105.4.
7, 8. — *Triporopollenites robustus* Pf. 1953a subfsp. *robustus*, cf. *Betulaceae*, D_2—1—5; 18.2/104.7.
9, 10. — *Triporopollenites festatus* Takahashi 1961, *Betulaceae*, Stevns Klint—1; 13.6/104.5.
11, 12. — *Subtriporopollenites constans* Pf. 1953a subfsp. *constans*, D_3—37; 18.7/119.2.
13, 14. — *Subtriporopollenites anulatus* Pf. and Th. 1953, subfsp. *anulatus*, *Juglandaceae* cf. *Carya*, D_3—95; 6.5/110.5.
15, 16. — *Subtriporopollenites anulatus* Pf. and Th. 1953 subfsp. *nanus* Pf. and Th. 1953, *Juglandaceae* cf. *Carya*, Dania—19; 4.7/114.8.
17, 18. — *Subtriporopollenites anulatus* Pf. and Th. 1953 subfsp. *nanus* Pf. and Th. 1953, *Juglandaceae* cf. *Carya*, Dania—13; 9.5/102.2.
19, 20. — *Subtriporopollenites* fsp., Højstrup—49; 18.5/110.7.
21, 22. — *Arecipites* fsp., *Palmae*, Højstrup—5; 9.2/120.7.
23, 24. — *Cupuliferoipollenites insleyanus* (Traverse 1955) R. Pot. 1960, *Fagaceae, Castanea*, Højstrup—8; 4.5/118.3.
25, 26. — *Cupuliferoipollenites pusillus* (R. Pot. 1934) R. Pot. 1960, *Fagaceae*, cf. *Castanea*, Stevns Klint—39; 13.5/120.8.
27, 28. — *Cupuliferoipollenites pusillus* (R. Pot. 1934) R. Pot. 1960, *Fagaceae*, cf. *Castanea*, D_3—3; 2.3/115.5.
× 1000

Plate V

1, 2. — *Cupuliferoipollenites pusillus* (R. Pot. 1934) R. Pot. 1960, *Fagaceae*, cf. *Castanea*, D_3—5; 19.3/124.3.
3, 4. — *Cupuliferoipollenites oviformis* (R. Pot. 1931) R. Pot. 1960, *Fagaceae, Castanea*, Dania—10; 8.3/110.1.
5, 6. — *Psilatricolporites* fsp., Stevns Klint—44; 18.6/104.0.
7, 8. — *Psilatricolporites* cf. *microparmularius* Kds. and Din. 1978, D_2—1—7; 19.1/114.5.
9, 10. — *Intrabaculitricolporites* fsp.$_1$, Højstrup—10; 16.8/114.6.
11, 12. — *Intrabaculitricolporites* fsp.$_2$, Dania—31; 8.9/116.1.
13, 14. — *Intrabaculitricolporites* fsp.$_3$, Stevns Klint—5; 9.0/120.2.
15, 16. — *Intrabaculitricolporites* fsp.$_4$, Stevns Klint—3; 12.7/118.3.
17, 18. — *Nyssapollenites* fsp., *Nyssaceae* v. *Mastixiaceae*, D_3—20; 22.1/116.6.
19, 20. — Cf. *Nyssapollenites* fsp., *Nyssaceae* v. *Mastixiaceae*, Stevns Klint—10; 12.8/116.8.
21, 22. — *Intrabaculitricolporites* fsp.$_5$, Dania—16; 3.3/104.5.
23, 24. — *Retitricolporites* fsp., D_2—1—9; 17.2/121.5.
25, 26. — *Ilexpollenites* fsp., *Aquifoliaceae, Ilex*, D_3—34; 14.7/112.7.
× 1000

REFERENCES

ANDERSON, R. Y. [1960]: Cretaceous-Tertiary Palynology, Eastern Side of the San Juan Basin, New Mexico. — State Bur. of Min. and Mineral Res., **6,** 1—59.

BRATZEVA, G. M. [1969]: Palynological studies of Upper Cretaceous and Paleogene of the Far East. — Acad. Sci. of the USSR, **207,** 1—56.

BRATZEVA, G. M. [1976]: Pollen of a new form genus, *Buravicolpites,* from the Eocene of the Far East. — Rew. of Palaeobotan. Palynol., **21,** 317—327.

GÓCZÁN, F. [1964]: Stratigraphic Palynology of the Hungarian Upper Cretaceous. — Acta Geologica **8,** 230—264.

GÓCZÁN, F., J. J. GROOT, W. KRUTZSCH, and B. PACLTOVÁ [1967]: Die Gattungen des "Stemma *Normapolles* PFLUG 1953b" *(Angiospermae)* Neubeschreibung und Revision europäischer Formen (Oberkreide bis Eozän). — Paläont. Abh. B. **2,** 427—633.

GRABOWSKA, I. [1968]: Paleogen z wiercenia Szczecin 1G—1 w swietle analizy sporovo-pylkowej. — Kwartalnik Geologiczny **12,** 155—166.

HANSEN, J. M. [1977]: *Dunoflagellatae* stratigraphy and echinoid distribution in Upper Maastrichtian and Danian deposits from Denmark. — Bull. Geol. Soc. Denmark **26,** 1—26.

HEGEDÜS, M., M. KEDVES and Á. PÁRDUTZ [1971]: Ultrastructural investigations on fossil *Angiosperms* exines of Upper Cretaceous. — Advancing Frontiers of Plant Sciences **28,** 317—325.

HEGEDÜS, M., M. KEDVES and Á. PÁRDUTZ [1972]: Ultrastructural investigation of Upper Cretaceous *Angiosperm* exines II. — Acta Biol. Szeged **18,** 55—69.

JARZEN, D. M. [1977]: *Angiosperm* pollen as indicators of Cretaceous-Tertiary environments. — Syllogeus **12,** 39—49.

KEDVES, M. [1967]: Sur quelques problèmes de stratigraphie palynologique appliquée au Tertiaire inférieur en Europe. — Pollen et Spores **9,** 321—334.

KEDVES, M. [1969]: Études palynologiques des couches du Tertiaire inférieur de la Région Parisienne IV. Pollens des *Normapolles.* — Pollen et Spores **11,** 385—396.

KEDVES, M. [1974]: Paleogene fossil sporomorphs of the Bakony Mountains Part II. — Studia Biol. Hung., **13,** 1—124.

KEDVES, M. [1978]: Paleogene fossil sporomorphs of the Bakony Mountains Part III. — Studia Biol. Hung., **15,** 1—166.

KEDVES, M. and F. DINIZ [1978]: Contribution á la connaissance de pollens des *Angiospermes* du Crétacé supérieur de Portugal. — Manuscrit.

KEDVES, M. and Á. PÁRDUTZ [1970]: Études palynologiques des couches du Tertiaire inférieur de la Région Parisienne. VI Ultrastructure de quelques pollens d'*Angiospermes* de l'Éocène inférieur (Sparnacien). — Pollen et Spores **12,** 553—575.

KEDVES, M. and Á. PÁRDUTZ [1973]: Ultrastructure investigations of *Angiospermatophyta* pollens from the Lower Eocene. — Acta Bot. Acad. Sci. Hung., **18,** 135—154.

KEDVES, M. and M. RADVÁNSZKI [1975]: The application of scanning electronmicroscopical method in some plant microfossils. — Acta Bot. Acad. Sci. Hung., **21,** 51—59.

KEDVES, M. and E. A. STANLEY [1976]: Electronmicroscopical investigations of the *Normapolles* group and some other selected European and North American *Angiosperm* pollen II. — Pollen et Spores **18,** 105—127.

KRUTZSCH, W. [1958]: Sporen und Pollengruppen aus der Oberkreide und dem Tertiär Mitteleuropas und ihre stratigraphische Verbreitung. — Z. angew. Geol., **3,** 519—548.

KRUTZSCH, W. [1959]: Einige neue Formgattungen und -arten von Sporen und Pollen aus der mitteleuropäischer Oberkreide und dem Tertiär. — Palaeontographica B, **105,** 125—157.

KRUTZSCH, W. [1961]: Beitrag zur Sporenpaläontologie der präoberoligozänen kontinentalen und marinen Tertiärablagerungen Brandenburgs. — Ber. Geol. Ges. DDR **5,** 290—343.

KRUTZSCH, W. [1966]: Die sporenstratigraphische Gliederung der Oberkreide im nördlichen Mitteleuropas. Methodische Grundlagen und gegenwärtiger Stand der Untersuchungen. — Abh. zentr. geol. Inst., **8,** 79—111.

KRUTZSCH, W. [1968]: *Brosipollis* und *Labrapollis,* zwei neue Pollengenera aus dem Tertiär Mitteleuropas. — Rev. of Palaeobotan. Palynol., **6,** 61—70.

KRUTZSCH, W. [1970]: Atlas der mittel- und jungtertiären dispersen Sporen- und Pollen- sowie der Mikroplanktonformen des nördlichen Mitteleuropas. — VEB Gustav Fischer Verlag, Jena.

KRUTZSCH, W. [1973]: Über einige neue Sporen und Pollenformen aus dem Maastricht Norddeutschlands. — Abh. zentr. geol. Inst., **18,** 77—98.

KRUTZSCH, W. and J. MIBUS [1973]: Sporenpaläontologischer Nachweis von kontinentalen Maastricht in Walbeck (Bezirk Magdeburg, DDR). — Abh. zentr. geol. Inst., **18,** 99—108.

KRUTZSCH, W., J. PCHALEK and D. SPIEGLER [1960]: Tieferes paläozän (?Montien) in Westbrandenburg. — Proc. XXI Int. Geol. Congr., **6,** 135—143.

MEDUS, J. [1975]: Fine Structure of *Oculopollis parvooculus* GOCZAN and *Oculopollis semimaximus* W. KR. — Grana **15,** 113—116.
MEDUS, J. [1977]: Indications de l'ultrastructure d'une espèce de forme du Crétacé supérieur, *Oculopollis maximus* W. KRUTZSCH. — Rev. Palaeobotan. Palynol., **24,** 209—215.
ONORATINI, G. and C. AZEMA [1973]: Une palynoflore du Santonien inférieur dans le Gard. — Rev. de Micropaléont., **16,** 214—222.
PFLUG, H. D. [1953]: Zur Entstehung und Entwicklung des angiospermiden Pollens in der Erdgeschichte. — Palaeontographica B, **95,** 60—171.
POTONIÉ, R. [1960]: Synopsis der Gattungen der Sporae dispersae. — Beih. Geol. Jb. **39,** 1—189.
STANLEY, E. A. [1965]: Upper Cretaceous and Paleocene plant microfossils and Paleocene *Dinoflagellates* and *Hystrichosphaerids* from Northwestern South Dakota. — Bull. of American Paleontology **49,** 179—384.
STANLEY, E. A. and M. KEDVES [1975]: Electronmicroscopical investigations of the *Normapolles* group and some other selected European and North American *Angiosperm* pollen I. — Pollen et Spores **17,** 233—271.
TAKAHASHI, K. [1961]: Pollen und Sporen des westjapanischen Alttertiärs und Miozäns. Teil II. — Mem. Fac. of Sci., Kyushu Univ. D, **11,** 279—345.
THOMSON, P. W. and H. D. PFLUG [1953]: Pollen und Sporen des mitteleuropäischen Tertiärs. — Palaeontographica B, **94,** 1—138.
WEYLAND, H. and G. KRIEGER [1953]: Die Sporen und Pollen der Aachener Kreide und ihre Bedeutung für die Charakterisierung der Mittleren Senons. — Palaeontographica B, **95,** 6—29.

Manuscript received, January 10, 1979

DR. MIKLÓS KEDVES
Department of Botany,
Attila József University,
H-6701 Szeged, Pf. 428
Hungary

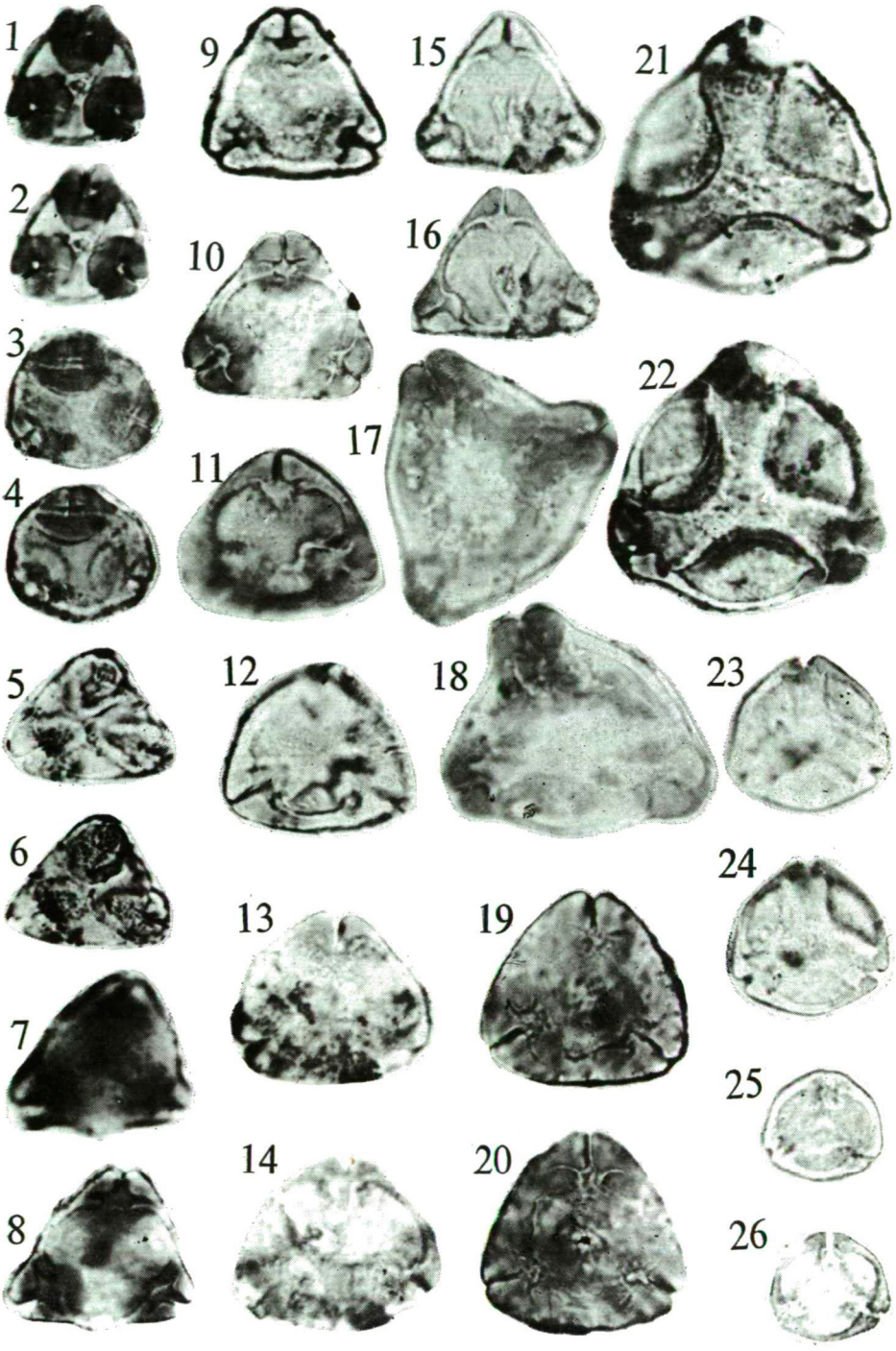
1
2
3
4
5
6
7
8
9
10
11
12
13
14
15
16
17
18
19
20
21
22
23
24
25
26

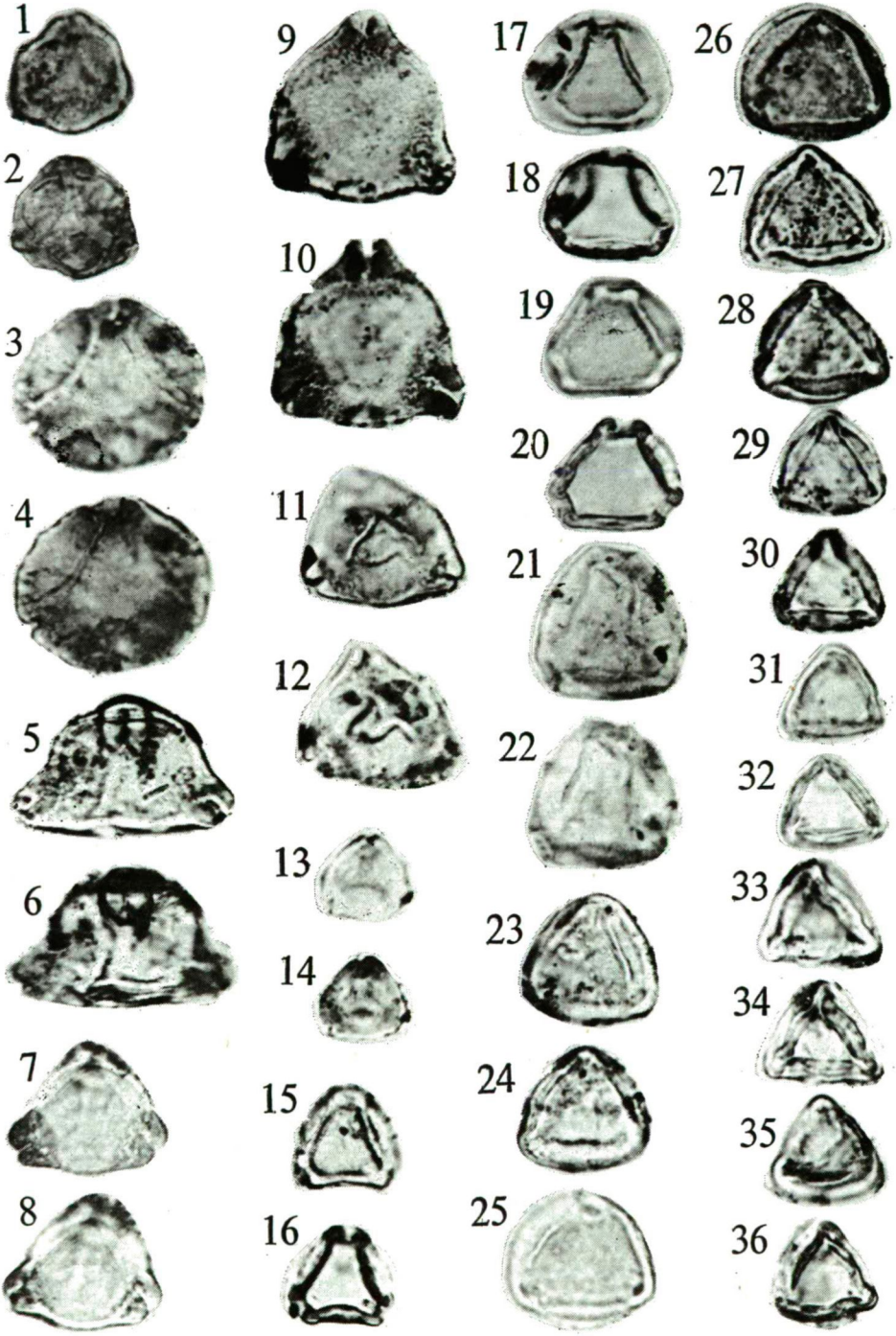
1
2
3
4
5
6
7
8
9
10
11
12
13
14
15
16
17
18
19
20
21
22
23
24
25
26
27
28
29
30
31
32
33
34
35
36

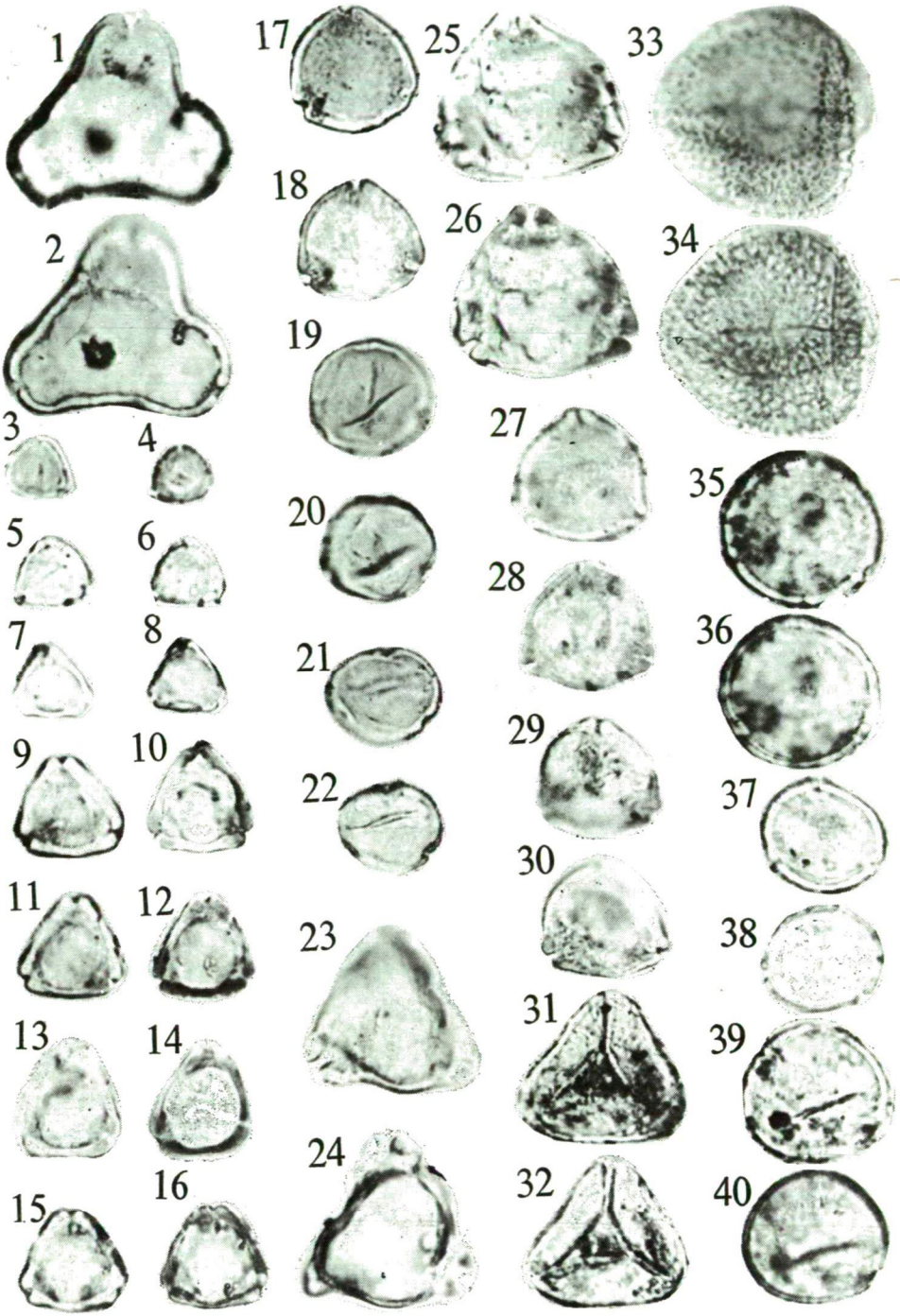
1
2
3
4
5
6
7
8
9
10
11
12
13
14
15
16
17
18
19
20
21
22
23
24
25
26
27
28
29
30
31
32
33
34
35
36
37
38
39
40

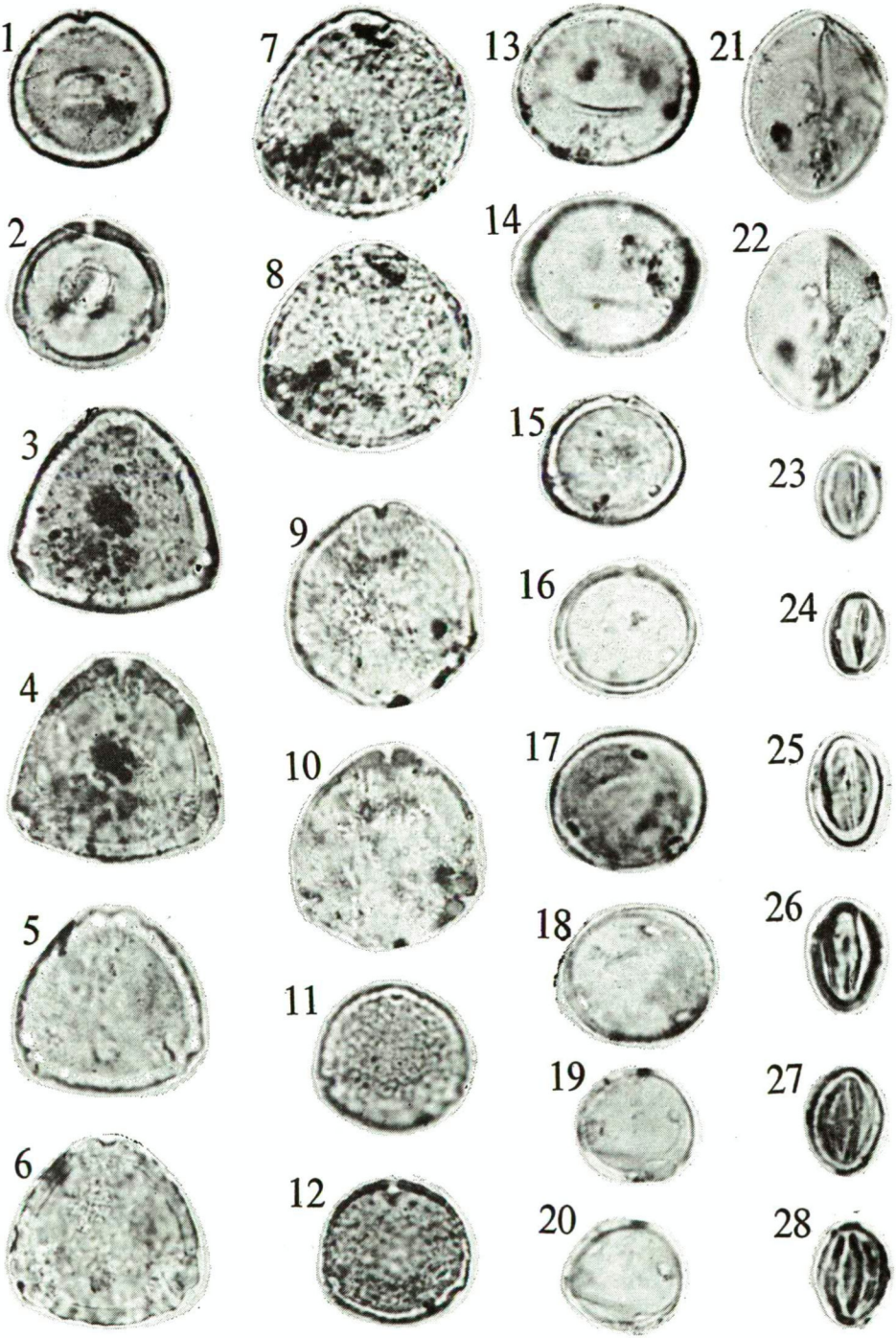
1
2
3
4
5
6
7
8
9
10
11
12
13
14
15
16
17
18
19
20
21
22
23
24
25
26
27
28

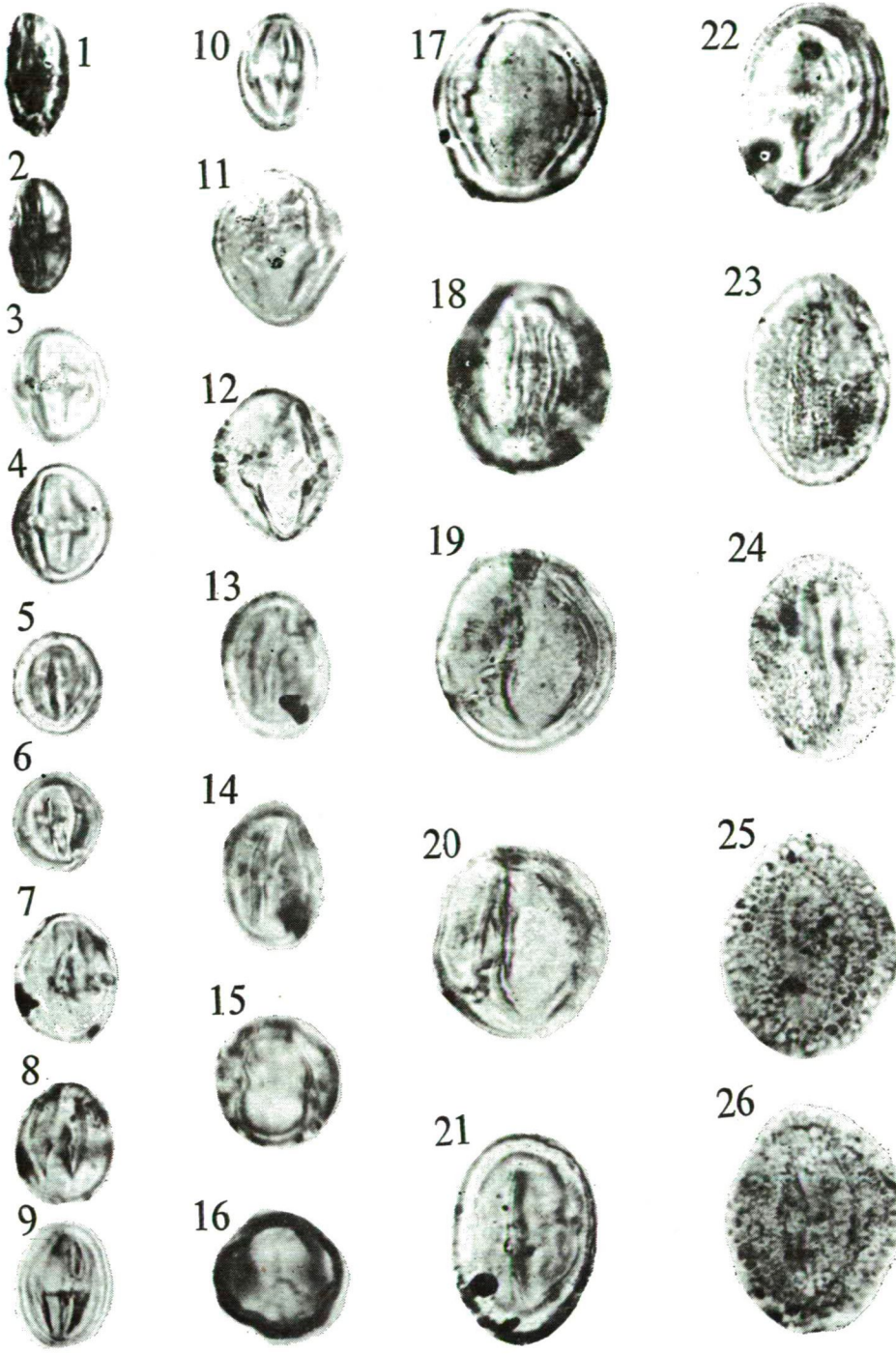
1
2
3
4
5
6
7
8
9
10
11
12
13
14
15
16
17
18
19
20
21
22
23
24
25
26

Acta Mineralogica—Petrographica, Szeged, XXIV/1, 187—188, 1979

BOOK REVIEW

BÁRDOSSY GY.: **Karsztbauxitok. Bauxittelepek karbonátos kőzeteken.** (Karstbauxites. Bauxite deposits on carbonate rocks.) Akadémiai Kiadó (The Publishing House of the Hungarian Academy of Sciences), Budapest, 1977, 413 p, 178 figures, 23 colour-photos and coloured figures, 49 tables, 3 supplements. (In Hungarian)

The bauxite ranks among those exploitable rocks which are connected with numerous branches of geology by means of their special mode of genesis and their usability for indicating facies and climate. On the basis of a profound examination of the bauxite deposits a lot of genetic theories arose, but neither of them was applicable unrestricted to other types of deposit. With progress of the investigations more and more occurrences were discovered of which constitution did not perfectly keep to the patterns of the former theories.

The author properly recognized that only an objective investigation and classification, as manysided as possible, could show the way out of this chaos. In the focus of his investigation the karstbauxites are placed to which also the Hungarian bauxites belong. But in connection with any question of importance, also the laterite-bauxites are drawn into comparison. Till now nobody in the world has undertaken a similar synthesis having so great pretensions and more detailed analyses supported both qualitatively and quantitatively, being in spite of that concise and easy to survey. Of course, a study like this contains many compilative data, too. However, this matter is not simply taken over by the author, but it is — often passed through the filter of his proper investigations — critically summarized. At the same times —if necessary — attention is called to questions unsolved and thus left open.

This book is an excellent example to show how the dispersity of the genesis has to be picked out of the initially analytic, subsequently comprehensive view of the formal and material features of a geologic formation. Starting from the geographic frames of the karstbauxite belts and the periods of the bauxite deposition, a qualitative and quantitative analysis firstly of the modes of genesis, then the same of the petrographic features (bauxite-varieties, their textural, structural and physical properties), further the mineralogic composition — including also the relationships between texture and mineralogy — are given. Description of the bauxite-minerals is succeeded by the outlining of their condition of formation and their genetic system, then the analysis of the relations between karstbauxites and terra rossa. Examining the connection of the bauxite deposits with the local and major tectonics, the author establishes — so to say — a transition to the last, genetic chapter of his book, that comprises a discussion and criticism of the theories on bauxite genesis, the questions regarding the source rock and transport, the environmental conditions and the factors of transformation into bauxite, the characteristics of the depositional areas,

finally the geochronology of bauxite-formation and the relevant paleogeographic conclusions.

Beside the many-sidedness perhaps the greatest merit of the book consists in its never being satisfied with only qualitative distinctions, but — by means of the simple though laboursome methods of mathematical statistics (that under the present circumstances are alone applicable to materials of this kind) — the author always endeavours to asses the quantitative distribution or frequency of the recognized types, components or minerals, too. Because of the rarity of similar calculations, the given numbers are perhaps not always of absolute value. Nevertheless they — as properly grounded estimations — augment the veracity of the conclusions drawn these from.

The statements of the book are based on self-mad field-observations and samplings taken over the major share of the bauxite occurrences of the Earth by the author himself. Beside the profound knowledge of the methods and the world literature, this "personal connection" with his object made possible the creation of this outstanding synthesis clothed by zealous efforts of the Publishing House of the Hungarian Academy of Sciences into a worthy guise. It is a great pleasure to hear that this book — comprising the products of 25 years of tireless labour, for which its author was awarded the Joseph Szabó Medal by the Hungarian Geological Society — will soon be issued by foreign publishers both in English and Russian.

Prof. Dr. K. Balogh